Non-Invasive Assessment of Right Ventricular Function in Health and in Acute and Chronic Pulmonary Arterial Hypertension

Shareen Jaijee

A thesis submitted in fulfilment of the requirements for the degree of

Doctor of Philosophy

Sydney Medical School

University of Sydney

Australia

2017

Declaration

This is to certify that to the best of my knowledge, the content of this thesis is my own work. This thesis has not been submitted for any degree or other purposes. Two semesters of this work were done at The University of Sydney, as well as much of the preparatory work for the results of all of the chapters.

I certify that the intellectual content of this thesis is the project of my own work and that all the assistance received in preparing this thesis and sources have been acknowledged.

Signature:

Name: Shareen Jaijee

Abstract

This thesis investigates the utility of cardiac magnetic resonance imaging (CMR) to assess right ventricular function and dynamic right ventricular (RV) reserve, in health and in acute and chronic pulmonary hypertension.

Right ventricular function is a strong predictor of prognosis, in patients with pulmonary arterial hypertension (PAH), but there are currently no available clinical tests that can predict which right ventricle is destined to fail, despite medical therapy. RV reserve, or the ability of the RV to augment during exercise, has recently gained more attention as a potential marker vascular-ventricular uncoupling, and CMR potentially offers a novel, accurate and reproducible method to assess this.

Exercise CMR is in its developmental stages, and while several groups have used it in healthy volunteers and patients to study dynamic biventricular function, approaches have varied. We set out to develop a novel and robust exercise CMR methodology and demonstrate its accuracy and reproducibility. Furthermore, we aimed to show how timing of acquisition and respiratory variation, are important considerations, potentially affect key pathophysiological changes. In Chapter 3, we outline the developmental considerations and demonstrate intra-observer, inter-observer, inter-study and inter-test reproducibility.

In Chapter 4, we show how the RV remodels after pulmonary thromboendarterectomy in patients with chronic thromboembolic pulmonary hypertension, in a retrospective analysis of CMRs acquired before and after surgery. Importantly, we demonstrate how biventricular interactions, expressed as a composite measure of RV end diastolic volume to left ventricular (LV) end diastolic volume ratio, correlates with change in 6MWD, but parameters of each

ventricular alone do not. Furthermore, we demonstrate a correlation between left atrial size and left ventricular end diastolic index, showing that under-filling is likely to be an important pathophysiological explanation of a reduction in LV size, in these patients. LV under-filling from increased RV pressure, and biventricular interactions, continue to remain key themes throughout the following experiments.

While exercise CMR is a new technique, so is assessment of RV reserve and there are no normal values available. Furthermore, there is conflicting evidence in the literature, as to normal cardiovascular changes that occur during exercise in normal hearts. We demonstrate in Chapter 5 that an increase in RV forward flow is due to a decrease in RV end systolic volume and an increase in RV ejection fraction, leading to an increase in LV end diastolic volume. LV ejection fraction increases as a result of an increase in left ventricular end diastolic volume and a decrease in left ventricular end systolic volume. Understanding normal exercise physiology, during continuous steady state exercise, is key to interpreting pathophysiological changes.

Acute normobaric hypoxia causes hypoxic pulmonary vasoconstriction and an increase in pulmonary vascular resistance and pulmonary pressures. It offers a model in which RV reserve in healthy controls can be studied. It has been hypothesised that the reduction in VO2 max in acute hypoxic exercise is a consequence of a reduction in RV forward flow, however this has never been definitively documented in an imaging study. We show, for the first time using exercise CMR in Chapter 6, that exercise during acute hypoxia leads to a reduction in RV forward flow, a blunting of the rise in RV ejection fraction and LV under-filling with a reduction in LV forward flow. We also show that there is a blunting of the rise in MPA average blood velocity on exercise during acute hypoxia, and hypothesise that this could be a novel CMR parameter to assess pulmonary vascular distensibility.

Identifying patients whose RV will continue to fail despite medical therapy has remained elusive. We go on to demonstrate in Chapter 7 that our approach to exercise CMR is not only feasible in patients with pulmonary arterial hypertensoin, but that exercise in these patients, considered stable on medical therapy with normal resting RV ejection fraction, unmasks impaired right ventricular reserve. Furthermore, we demonstrate that there is heterogeneity of response that cannot be predicted by routine clinical tests and resting biventricular function. This information could potentially be clinically valuable, and we outline where this research will take us to next in Chapter 8, where we hope to demonstrate change in right ventricular reserve before and after medical therapy, in patients with inoperable chronic thromboembolic pulmonary hypertension, predicts long term clinical outcomes on follow up.

Together, these studies demonstrate how CMR can accurately and non-invasively assess RV remodeling and RV reserve, its impact on the LV, and unmask right ventricular − vascular uncoupling which is otherwise not present at rest, in patients with acute and/or chronic pulmonary arterial hypertension.

Acknowledgements

Presentations Arising from this Thesis

Right Ventricular Function in Acute and Chronic Pulmonary Hypertension using Exercise Cardiac Magnetic Resonance Imaging – European Society of Cardiology, August 2016

Deterioration of Right Ventricular Function on Exercise detected by Exercise Cardiac Magnetic Resonance Imaging in Patients with Pulmonary Arterial Hypertension – British Cardiovascular Society Meeting, June 2016

Cardiac Magnetic Resonance Imaging in Healthy Volunteers in Normoxic and Hypoxic Exercise – Society of Cardiovascular Magnetic Resonance Imaging Meeting, January 2016

Exercise Cardiac Magnetic Resonance Imaging – Medical Research Council 'University of the Third Age' event London, United Kingdom, January 2016

'Exercise Cardiac Magnetic Resonance Imaging' Pulmonary Hypertension Physicians Research Forum, London, United Kingdom, November 2015

Manuscripts in Preparation Arising from this Thesis to Date

Shareen Jaijee, Marina Quinlan, Pawel Tokarczuk, Matthew Clemence, Luke Howard, Simon R Gibbs, Declan P O'Regan, Right Ventricular Reserve in Acute and Chronic Pulmonary Hypertension (Submitted)

Shareen Jaijee, Marina Quinlan, Ben Statton, Pawel Tokarczuk, Matthew Clemence, Luke Howard, Simon R Gibbsm Declan O'Regan, Exercise Cardiovascular Magnetic Resonance imaging and the Timing of Image Acquisition: A Key Player in Detecting Pathophysiological Changes

Shareen Jaijee, Marina Quinlan, Ben Statton, Pawel Tokarczuk, Matthew Clemence, Luke Howard, Simon R Gibbsm Declan O'Regan, Recreational exercise and the effect of Resting and Dynamic Biventricular Structure and Function

Awards and Grants Arising from this Thesis

Table of Contents

List of Figures

Chapter 1

Chapter 2

Chapter 3

Chapter 7

List of Tables

Abbreviations

6MWD	Six Minute Walk Distance Test
ANOVA	Analysis of variance
Ao	Aorta
AT	Acceleration time
BMI	Body mass index
BNP	B-type natriuretic peptide
BSA	Body surface area
CI	Cardiac Index
CMR	Cardiac magnetic resonance imaging
CO	Cardiac Output
CPET	Cardiopulmonary Exercise Test
CTEPH	Chronic thromboembolic pulmonary hypertension
CTPA	Computed Tomography Pulmonary Angiogram
dPAP	Diastolic pulmonary arterial pressure
E:A	Early to late diastolic filling ratio
E_a	Arterial elastance
ECG	Electrocardiogram
EDV	End Diastolic Volume
EDVI	Indexed end diastolic volume
EF	Ejection Fraction
E_{max}	Maximal elastance
ESV	End Systolic Volume
ESVI	Indexed end systolic volume
Ex	Exercise

FAC	Fractional area change
FEV1	Forced expiratory value in 1 second
FOV	Field of view
FVC	Forced vital capacity
GOSH	Great Ormond Street
HLA	Horizontal long axis
HR	Heart rate
IPAVA	Intrapulmonary arteriovenous anastomoses
IVRT	Isovolumic relaxation time
LA	Left atrial
LV	Left Ventricle
LVOT	Left ventricular outflow tract
LVSA	Left ventricular short axis
MPA	Main Pulmonary Artery
mPAP	Mean Pulmonary Arterial Pressure
MPI	Myocardial performance index
MRI	Magnetic resonance imaging
NYHA	New York Heart Association classification
PA	Pulmonary arterial
PAH	Pulmonary arterial hypertension
PCWP	Pulmonary capillary wedge pressure
PEA	Pulmonary thromboarterectomy
PRV	Pulmonary regurgitant velocity
PVR	Pulmonary Vascular Resistance
RAA	Right atrial area

RAP	Right atrial pressure
RHC	Right heart catheterisation
RIMP	RV index of myocardial performance
ROI	Region of Interest
RV	Right Ventricle
RVLA	Right ventricular long axis
RVOT	Right ventricular outflow tract
SD	Standard deviation
SENSE	Sensitivity Encoding
sPAP	Systolic pulmonary arterial pressure
SV	Stroke Volume
SVI	Stroke Volume Index
T	Tesla
TAPSE	Tricuspid annular plane systolic excursion
TCPH	The Prince Charles Hospital
TR	Repetition time
TR	Tricuspid regurgitation
TRV	Tricuspid regurgitant velocity
V/Q	Ventilation perfusion scan
VCO_2	Output of carbon dioxide
V_E	Minute ventilation
V_E/VCO_2	The ratio of minute ventilation to carbon dioxide output
VENC	Velocity encoding value
VO_2	Maximal oxygen uptake
W	Watts

Chapter 1 - Introduction

1.1 Right Ventricular Structure and Function

1.1.1 Right Ventricular Anatomy

The right ventricle (RV), the most anterior chamber of the heart, lies immediately behind the sternum. It has a complex shape, crescenteric in cross section, triangular when viewed from the side and in general, can be divided in to three parts. These consist of 1) An inlet which consists of the tricuspid valve, the chordae tendinae and the papillary muscles; 2) A trabeculated apical myocardium and; 3) The infundibulum or conus which is the smooth outflow region, leading to the pulmonary orifice and pulmonary trunk (1, 2) (Figure 1A and B). Furthermore, the RV can be divided in to anterior, lateral and inferior sections, as well as basal, mid and apical (2, 3).

The crista supraventricularis separates the tricuspid and pulmonary valves and has 3 components; the parietal band, infundibular septum and septal band. The infundibular septum separates the two ventricular outflow tracts, the parietal band is a free wall structure and the septal band forms a Y shaped muscle that cradles the infundibular septum. The septal band extends inferiorly and becomes continuous with the moderator band, an intracavitary muscle which attaches to the anterior tricuspid papillary muscle (2, 3) (Figure 1C).

The tricuspid valve is made up of the annulus, leaflets, commissures, chordae tendinae and papillary muscles. The anterior tricuspid leaflet is the largest and most mobile and forms a curtain that partially separates the inflow and outflow tracts of the RV. The posterior leaflet is the smallest and the septal leaflet is the least mobile due to its direct chordal attachments to the

ventricular septum. The annulus is uniquely fibroadipose in nature(3). The pulmonary valve is composed of the annulus, cusps and commissures. The semilunar valves have no chordae tendinae and are equal in size (3).

The RV has several unique features which distinguishes it from the left ventricle (LV): 1) The septal leaflet has a more apical hinge relative to the anterior leaflet of the mitral valve 2) The presence of the moderator band 3) The presence of 3 papillary muscles 4) The trileaflet configuration of the tricuspid valve with septal papillary attachments 5) The presence of coarse trabeculations (2).

The blood supply of the RV varies according to whether the coronary system is left or right-sided dominant. 80% of the population has a right dominant system, where the right coronary artery supplies the majority of the RV. The marginal branches of the right coronary artery supply the lateral wall and the posterior descending artery supplies the posterior and inferoseptal regions. The left anterior descending artery supplies two thirds of the septum and the anterior wall of the RV. The conal artery supplies the infundibulum. Flow is equal in diastole and systole, however, beyond the right ventricular marginal branches, diastolic coronary blood flow predominates (2-4).
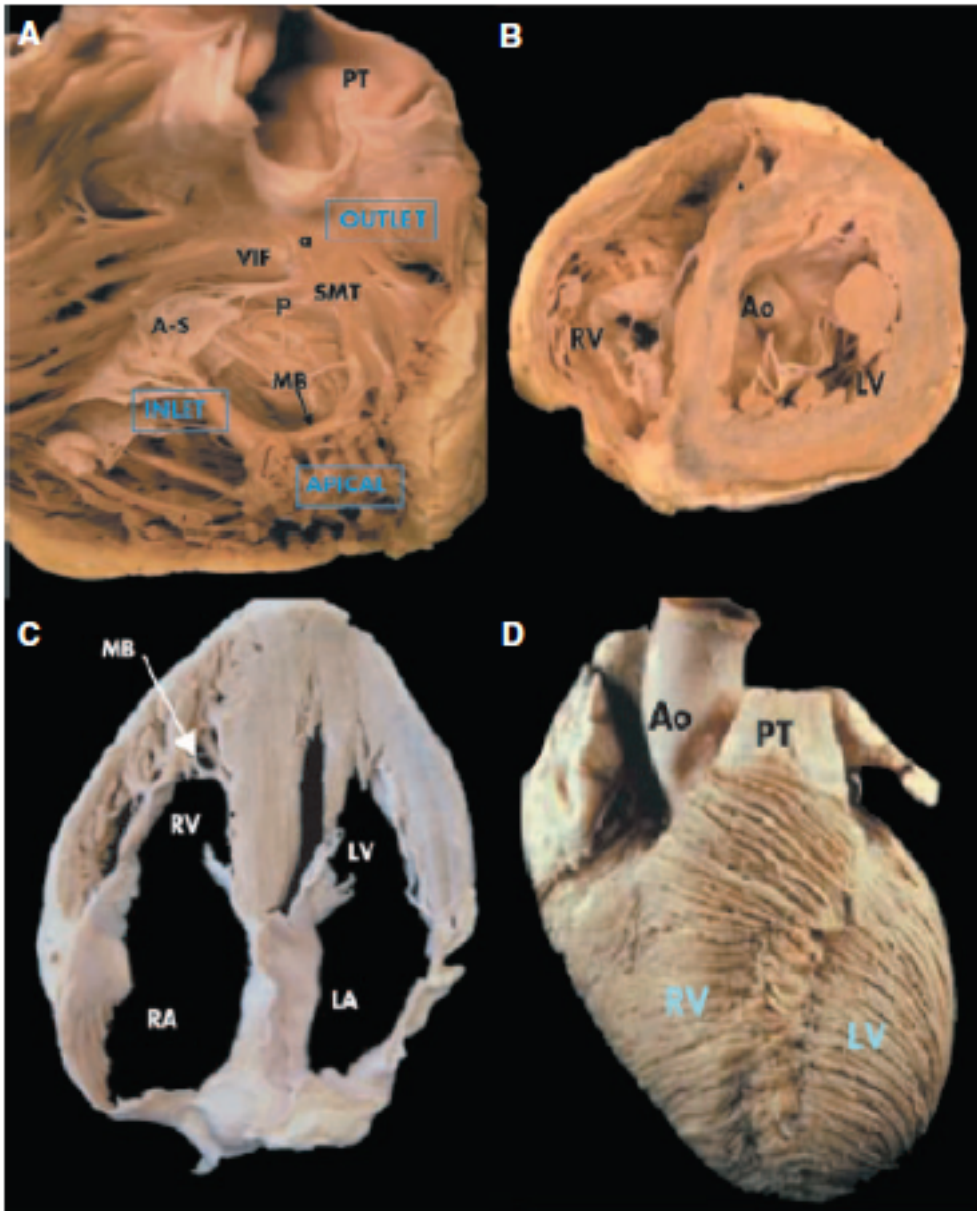
(2)2)(2)(2)(2)(2)(2)(2)(2))

Figure 1.1 Anatomy of the RV: A: The inlet, trabeculated apical myocardium and infundibulum of the RV. The tricuspid and pulmonary valves are separated by the ventriculoinfundibular fold (VIF). B: Short-axis plane of the RV demonstrating its crescenteric shape C: The 4 chamber anatomic plane of the heart showing the moderater band (MB), D: Superficial muscle layer of the RV. SMT indicates septomarginal trabeculation with its anterior (a) and posterior (p) arm. A-S: anterosuperior leaflet of the tricuspid valve; PT, pulmonary trunk; Ao, aorta; RA, right atrium and LA, left atrium. (From Haddad, et al. Right Ventricular Function in Cardiovascular Disease, Part 1: Anatomy, Physiology, Aging and Functional Assessment of the Right Ventricle. Circulation, 2008)

1.1.2 Myofibres and RV Contraction

The myocardial architecture and fibre direction are different between the LV and RV. The RV myocardial fibres are constructed of two layers, whereas the LV is a three-layered structure. The muscle fibres in the superficial layer of the RV are circumferential, parallel to the atrioventricular groove (Figure 1D). They turn obliquely towards the cardiac apex and are continuous with the superficial fibres of the LV. The deep muscle fibres are aligned longitudinally from base to apex (1, 2).

Longitudinal contraction accounts for around 80% of RV stroke volume (SV) and is a more accurate reflection of global RV function and acute afterload increase (5, 6). This contrasts with the LV, which has oblique, longitudinal and circular orientated fibres that contribute to the more complex movements of torsion, translation, rotation and thickening.

Contraction of the RV starts with the inlet and myocardium and ends with the infundibulum, which is of a longer duration than the inflow region. Inlet and infundibular contraction are approximately 25-50ms apart, and peak systolic longitudinal and circumferential shortening occurs earliest at the apex (7). Three separate mechanisms contribute 1) Inward movement of the free wall; 2) Contraction of the longitudinal fibres and; 3) Transmission of tension to the RV free wall secondary to LV contraction (2, 8).

1.1.3 Ventricular Interaction

The mutually encircling circumferential epicardial fibres and the shared interventricular septum and pericardial space are also important determinants of RV function. Ventricular

interdependence is a term used to explain how the size, shape and compliance of one ventricle, affects the size, shape and function of the other, during systole and diastole, independent of neural, humoral or circulatory effects (2, 4, 9, 10). For example, during diastole, competition for space within the limits of the pericardium may lead to impaired LV filling due to a dilated RV (11, 12), or during systole, enhanced LV contraction improves RV function (13) due to shared epicardial fibres.

1.1.4 Physiology of the Right Ventricle

The RV is coupled to the pulmonary circulation, which is a low pressure, high flow circuit. The low pressure allows the RV to function at minimal energy costs, and the low pressure prevents fluid extravasation in to the interstitial space. When pulmonary vascular resistance (PVR) and metabolic demands are low, RV function contributes little to the flow of blood through the lungs and to the left heart, with filling pressures of 10mmHg. However, exercise and activation of the autonomic nervous system can increase cardiac output (CO) up to 6 fold, increase oxygen uptake and carbon dioxide output up to 20 fold, with RV filling pressures increasing to 35-40mmHg. Hence the RV is key in enabling exercise, quality of life and survival (1).

Changes in CO involve both changes in heart rate (HR) and stroke volume (SV). SV is influenced by diastolic stretch, contractility that in turn is regulated by the autonomic nervous system, and arterial pressure that opposes ejection. In healthy hearts, increasing diastolic stretch of the myocardium, referred to as the Frank-Starling mechanism, augments the energy of contraction. However, this relationship is curvilinear, and SV declines in the over-distended heart. Working in opposition to the Frank-Starling law is the LaPlace relationship that states

that for a hollow sphere, the internal pressure is proportional to the wall tension and is inversely proportional to the internal radius. Hence as the radius increases and wall curvature decreases, the ventricle is less able to convert wall tension in to intraventricular pressure (14, 15).

Contractility can also be increased at a given initial fibre length, i.e. without chamber dilatation by internally circulating positive inotropes, of which noradrenaline is the most important. Others include adrenaline, angiotension II and extracellular calcium ions. Sympathetic nervous system activation leads to a more rapid rise in ventricular pressure, an increase in ejection fraction (EF), a fall in diastolic volume, an increase in SV and a shortening of the duration of systole (14, 15).

An increase in arterial pressure, often referred to as afterload, produces less muscle shortening and impairs SV. The heart compensates by distention and increasing diastolic stretch to increase contractile energy through the Frank Starling mechanisms, and also through the Anrep response. The Anrep response is an adaptation that occurs in response to an increase in afterload, whereby myocardial contraction increases at a lower end diastolic volume (EDV), due to local release of inotropic agents such as myocardial angiotensin II and endothelin 1.(14, 15)

1.2 Normal exercise physiology

During exercise, there is an increase in HR, CO and SV. The key mechanisms behind LVSV augmentation during exercise are divided between two theories. 1) That Frank-Starling mechanism and an increase in LVEDV is the most important adaptation and 2) Enhanced contractility as manifested by a decrease in LV end systolic volume (ESV) without an increase

in LVEDV predominates. However, posture, the intensity of exercise and the type of exercise are all-important considerations when describing the physiological changes that occur in normal hearts during exercise.

An increase in LVEDV during upright exercise has been uniformly reported in numerous studies, including males and females, and sedentary, recreationally active and professional athletes (16-24). Where this has been refuted, has been in studies where supine (25, 26) or resistance (27-30) exercise has been studied. There is overall agreement in the literature that there is a greater percentage increase in LVEDV during upright exercise than during supine exercise (23, 25, 31). This can be explained by augmented preload in the supine state due to increased venous return.

Additionally, the intensity of exercise has been recognized as an influential factor on change in LVEDV. At low and moderate levels of exercise, Frank Starling mechanisms and an increase in LVEDV predominate, with a plateau (17, 23, 32) or even decrease (20) reported at peak exercise, with increasing contractility predominating at higher intensities. However, it has also been shown that change in LVEDV on exercise (22, 32), rather than a decrease in LVESV, correlates with increase in LVSV. Furthermore, higher levels of fitness and exercise training lead to greater increases in LVEDV on exercise and greater utilization of Frank-Starling mechanisms, rather than enhancing contractility (19, 33, 34).

Age has been reported to influence (16, 19, 27) and not influence (32) exercise physiology, with greater reliance on Frank-Starling mechanisms than contractility, demonstrated by a greater increase in LVEDVI and an increase in LVESVI on exercise (16, 19). Reports on whether maximal cardiac output is limited by age, is mixed. Also, it has been reported than

women have a greater increase in LVEDVI on exercise while men have a greater increase in ejection fraction (24, 35), while others have reported no differences between genders (21).

While there are numerous reports on LV function during exercise, reports on normal RV exercise physiology are more limited. This is probably due to the fact that radionuclide angiography that was largely used in the 1980s and echocardiography and invasive haemodynamics that was utilized more in the 1990 and 2000s, are limited in their assessment of RV function. However, similar to the LV, some report an increase in RVSV driven by a decrease in RVESV with no increase in RVEDV on exercise (36-40), while others have demonstrated an increase in RVEDV and a decrease in RVESV during upright bicycle exercise (25, 41) and supine bicycle exercise (42).

During exercise, PVR remains unchanged or decreases, due to vascular distention of compliant small vessels and recruitment of additional vessels of the upper portions of the lungs in upright exercise. Mean pulmonary arterial pressure (mPAP) increases, doubling or tripling in heavy exercise, with a rapid return to baseline immediately post exercise (43, 44). This can impose a significant load, on top of an increased preload from venous return, on the thin walled RV. It also has to be remembered that RV function is a reflection of afterload, preload, contractility and ventricular interdependence. Pulmonary vascular resistance (PVR) has been used to represent the afterload of an ejecting RV. However, capacitance and impedance measuring pulsatile flow, are also key contributors, with independent relationships with RV adaptation and prognostic importance.

1.3 Assessment of the Right Ventricle

An ideal measure of RV function should be safe, easy, reliable, independent of afterload, preload, heart size and mass and sensitive to changes in inotropy. The gold standard of measuring contractility in vivo, is considered to be the maximal elastance (E_{max}), or the maximum slope of the pressure-volume relationships measured continuously during the cardiac cycle, and is measured in the upper left corner of the pressure-volume loop. Accurate E_{max} can only be obtained by generating multiple pressure-volume loops at various levels of venous return (Figure 2), by progressive inferior vena cava occlusion (45), although the Valsalva manoeuvre has also been used. Single beat methods which rely on the calculation of maximum pressure (P_{max}) have been reported (Figure 1.2). P_{max} is calculated from a nonlinear extrapolation of the early and late portion of a RV pressure curve, an integration of pulmonary flow or direct measurement of RV volume curve, with synchronization of the signals. (46-49). MRI guided catheterisation has also been reported (50).
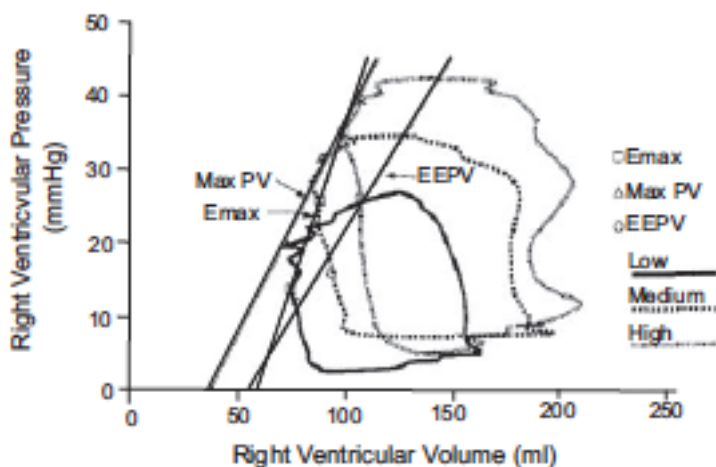
Figure 1.2: Pressure volume loops of the RV under different loading conditions. The slope of the maximum elastance (Emax) and maximum pressure-volume ratio (P_{max} or Max PV) are displayed on the graph. EEPV, end ejection pressure/volume (From Haddad, et al. Right Ventricular Function in Cardiovascular Disease, Part 1: Anatomy, Physiology, Aging and Functional Assessment of the Right Ventricle. Circulation, 2008)

Measurements of systolic function are ideally load independent as contractility or E_{max}, adapts to afterload after several heart beats. Afterload can be measured as arterial elastance (E_a) that is defined by the ratio between pressure at E_{max} and SV, and it can be measured with Emax on the pressure-volume loop. Ideal E_{max}/E_a representing optimal energy transfer from the ventricle to the arterial system is 1.5-2. Other measurements of afterload such as RC-time (51), preload recruitable stroke work (52) and wave intensity analysis (53) have been reported. RV systolic function can also be estimated from measurements during clinical right heart catheterisation (RHC), which is a regular part of practice. From pulmonary pressures, right atrial pressure (RAP) and CO, SV and stroke work can be calculated.

Studies using E_{max}/E_a have been reported in patients with pulmonary arterial hypertension (PAH) and chronic thromboembolic pulmonary hypertensive (CTEPH) disease, as well as other various models of pulmonary hypertension(50, 54). Together these have demonstrated that at rest, RV adaptation to an increased afterload is predominantly systolic, with no increase in RVEDV. RV-arterial uncoupling is characterized by increasing RV volumes.

However, these approaches are invasive, time consuming, require radiation exposure and are ethically problematic in the setting of manipulating venous return, hence difficult to apply clinically and in serial follow up studies. Brewis et al assessed 140 PAH patients using the gold standard measure of RV-PA coupling with Emax/Ea and measured RV function at rest using cardiac magnetic resonance imaging (CMR). They found that the simple ratio of RVSV to ESV and RVEF were the only independent predictors of outcome, and that there was no added value of the invasive measurements. Survival was poorer in patients with a fall in RVEF or SV:ESV during follow up (55). This was also found by Vanderpool et al, who demonstrated SV:ESV as measured by CMR was the only independent predictor of transplantation free

survival, over gold standard invasive measures of RV function (56). Sanz et al found that SV/ESV correlated with E_{max}/E_a calculations (57). These studies add weight to the notion that finding a non-invasive measure of ventricular-vascular coupling is not only desirable but potentially more clinically and prognostically relevant.

In clinical practice, RVEF is the most commonly used index of RV contractility. Echocardiography has remained the mainstay due to its availability and versatility, despite its significant limitations in the assessment of RV volume and RVEF. The best correlations with CMR derived RV volume measurements have been with RV fractional area change (FAC) which expresses the % change in RV area between end diastole and end systole (58, 59), however, there is significant overlap between normal, mild and moderate enlargement of the RV, with reported r values between 0.32 to 0.88 when comparing 2D echo to CMR (60). Indirect measures of RV dysfunction have been developed, including tricuspid annular plane systolic excursion (TAPSE) (61), isovolumic contraction velocity at the tricuspid annulus (62, 63), RV index of myocardial performance (RIMP) or Tei index (64), longitudinal strain and strain rate (65-67) and RA size (68). However, reports vary as to the accuracy, reproducibility and prognostic utility of these measures in the assessment of the RV. While 3D echo is promising and correlates with CMR volumes better than 2D echo (60, 69), CMR remains the gold standard and considered the most reliable method for measuring RV volumes and RVEF.

CMR provides highly reproducible and accurate assessment of the RV that does not rely on consistent acoustic windows nor operator-dependent (70, 71). The reduction in sample size required by CMR interventional studies has been clearly demonstrated (72) and it provides prognostic value over echocardiographic measurements (57, 73-75) in PAH studies. Although

RVEF can be assessed accurately using CMR, it is a single beat derived measurement, dependent on loading conditions and hence may not adequately reflect contractility.

RV contractile reserve, or the ability of the RV to increase contractility at a given level of exercise or pharmacological stress test, can be used to test systolic function adaptation to afterload dynamically. It has been demonstrated that exercise RV function and CO is not related to resting (41, 76-78) or changes (79-81) in resting haemodynamics , nor is exercise capacity related to resting RV function (82-84). The assessment of RV reserve has been carried out in numerous ways thus far. Stress echocardiography using exercise (85) and dobutamine (86), invasively measured haemodynamics on exercise (87-89) and exercise CMR have been utilized, all demonstrating reduced RV contractile reserve on exercise in patients with PAH and other pathologies (41, 76, 90). Furthermore, exercise induced RV dysfunction demonstrated on exercise radionuclide ventriculography, echocardiography and invasively measured haemodynamics have been shown to be a strong predictor of prognosis in heart failure (91, 92), moderate to severe mitral regurgitation (93), PAH and inoperable CTEPH (94, 95).

It has been demonstrated that dobutamine stress and true physiological stress with exercise cannot be used interchangeably and produce different results. Peak CO has been shown to be lower using dobutamine stress, produce a lower SV increment, but increase EF and reduce cardiac chamber volumes hence leading to increased indices of contractility in healthy volunteers (96, 97). In particular, in patients with atrially corrected transposition of the great arteries, exercise led to a decrease in EF on exercise, but it increased with dobutamine stress (96). Exercise is a true physiological stress, and hence is preferable over dobutamine.

One method of assessing both exercise biventricular function and the pulmonary circulation is through exercise echocardiography. Claessen et al have demonstrated that exercise RVEF as assessed by exercise CMR correlates strongly with exercise echocardiography RV FAC and moderately with exercise TAPSE (98). An advantage of echocardiography is that it can provide noninvasive haemodynamic evaluation of pulmonary arterial (PA) pressures which are comparable to invasively derived measurements (43) and has been shown to demonstrate the reactivity of the pulmonary circulation to exercise in relatives carrying the BMPR2 mutation (99). However, it is indisputable that echocardiography is limited by its operator and acoustic windows, with reported inaccuracies of systolic pulmonary arterial pressure (sPAP) in up to 50% of cases (100, 101). Furthermore, up to 30-40% of subjects are not suitable, with no visualization of the RV inflow tract (101, 102) and there is a poor understanding of what the normal upper limit of increases in sPAP during exercise is. SPAP is influenced by age, gender, body mass index (BMI), ventricular function and physical fitness, which makes it difficult to define normal ranges. Currently, there are no indices which are validated during exercise and because of a lack of clarity as to which echocardiographic parameter is the most useful in the assessment of exercise RV function (103), there is a high heterogeneity of study methods, protocols and estimations of haemodynamic parameters (104). Even for the LV, exercise echocardiography has been shown to be unreliable for estimation of LVEDV and dependent considerably on the practical skills of the operator (105). The utility of exercise CMR to assess RV reserve will be discussed in more detail later on.

Given ventricular interdependence and the impact of the function of one ventricle on the other, it's important to consider the impact of RV dysfunction on the LV. A reduction in LV stroke volume and LVEDV has been proposed to be due to LV compression from RV enlargement and left ventricular septal bowing (12) and LV under filling (11, 106, 107), or a combination

of both. Furthermore, LV systolic strain is reduced and associated with early mortality in PAH (108) and electrophysiological remodeling of the LV in RV pressure overload has been demonstrated (109).

1.4 Acute Hypoxia

Hypoxia induces pulmonary vasoconstriction, which has marked interindividual and interspecies variation (110). In humans, hypoxic vasoconstriction may be absent in 20% of people, but strongly present in 1-2% of cases (111, 112). Inhibition of voltage gated potassium channels localized in smooth muscle cells is responsible for the initial hypoxic vasoconstriction, leading to a rapid increase in PVR in the first 5 minutes (113), then a lower increase over 2 hours, with maximal response at 24 hours accompanied by early signs of remodeling, such as medial hypertrophy. During hypoxic exercise, the mean pulmonary arterial pressure (mPAP)- flow relationship is further shifted, imposing higher pressures on the RV (112, 114).

At rest, it is well accepted that acute hypoxia leads to an increase in mPAP, HR and CO (114-116). Other reported findings are an alteration of RV outflow tract flow with a decrease in acceleration time (AT) (115, 117), a reduction in the early to late diastolic filling (E:A) ratio with a decrease in early diastolic filling and an increase in late diastolic filling of both the LV and RV (118-121), an increase in RV dimensions, (122), no change in RV dimensions (123) and preserved RV and LV contractility.

During acute hypoxic exercise, the maximal oxygen uptake (VO_2) max and CO are lower than during normoxic exercise (124, 125). At high altitudes and after a period of acclimatization,

this could be explained by a number of different mechanisms including hypovolaemia, hypocapnia, increased blood viscosity, autonomic nervous system changes and depressed myocardial function. However, in the acute setting, the mechanisms are less clear and exercise capacity may be limited by RV flow output secondary to hypoxic pulmonary vasoconstriction. Studies examining RV function during exercise in acute hypoxia, have largely used echocardiography, which as discussed previously, has important limitations when assessing the RV. Hence indirect methods of assessing RV contractility such as the RIMP (115), strain, strain rate as assessed by speckle tracking (118), isovolumic acceleration and TAPSE (117, 121, 126) and assessment of diastolic function using the E:A ratio have been used. Overall, these studies support the notion that HR increases, LV contractility increases (119, 127), and there are signs of RV strain and functional limitation but overall RV systolic function is preserved. An altered LV diastolic filling pattern is also consistently reported, which has been hypothesised is due to diastolic dysfunction, tachycardia, altered interventricular interactions or hypercontractile atria.

Fukada et al used a novel thoracic impedance model to continuously measure stroke volume and analysed healthy volunteers during acute hypoxic exercise, and they found that VO_2 max, SV and CO at maximal exercise decreased. They also found that SV was lower at identical work rates during hypoxic exercise, compared to normoxic exercise (128). However, whether the attenuation of VO_2 max during acute hypoxia is due to reduced forward flow from the RV has not been definitively documented and to date, there have been no imaging studies during acute hypoxic exercise, which have been able to identify changes in RV stroke volume.

1.5 Pulmonary Hypertension

Pulmonary Hypertension (PH) is defined as an increase in mPAP ≥ at rest. It can be clinically classified in to 5 categories which include 1) Pulmonary Arterial Hypertension 2) Pulmonary Hypertension due to left heart disease 3) Pulmonary Hypertension due to lung diseases and/or hypoxia 4) Chronic thromboembolic pulmonary hypertension and other pulmonary artery obstructions and 5) Pulmonary hypertension with unclear and/or multifactorial mechanisms. (129)

1.5.1 Chronic Pulmonary Arterial Hypertension

PAH refers to patients who have pre-capillary PH, defined by a pulmonary capillary wedge pressure (PCWP) ≤ 15mmHg and a PVR > 3 Wood units, and can be further divided in to idiopathic, heritable, induced by drugs and toxins, or associated with connective tissue disease, human immunodeficiency virus, portal hypertension, congenital heart disease and schistosomiasis (129). In all of these settings, it is a progressive disease of the pulmonary vasculature, which is associated with elevated PVR, progressive RV dysfunction, RV failure and eventually death (130). Drug therapies, which are licensed for PAH, slow disease progression and prolong life (131). There are currently four classes of drugs, which may be combined if response is inadequate to monotherapy, however, the optimal timing to combine or switch agents is unknown and assessment of adequate response to monotherapy has to be individualized. Current guidelines recommend a number of follow up investigations, however, none of them of been validated (132).

1.5.2 Chronic Thromboembolic Pulmonary Hypertension

CTEPH, defined as a mean pulmonary artery pressure (mPAP) ≥25mmHg with a PCWP ≤15mmHg and at least one segmental perfusion defect following three months of adequate anticoagulation, is an important, treatable cause of persistent pulmonary hypertension.(133, 134). Predominant mechanisms include recurrent pulmonary emboli, obliteration of central pulmonary arteries, pulmonary vascular remodeling and progressive small vessel arteriopathy. In selected cases with centrally located anatomic obstruction in one or both branch pulmonary arteries, surgical pulmonary thromboendarterectomy (PEA) can be performed often, but not always, with excellent clinical outcomes. Subsets of patients have predominantly small vessel arteriopathy and are not surgical candidates with medical therapy being the standard of care for these patients. This disease is often progressive with poor outcomes.

1.5.3 Consequences of Pulmonary Arterial Hypertension to the Right Ventricle

In both PAH and CTEPH, consequences may include progressive RV hypertrophy, dilatation and failure with clinical decline (133-135). In response to pressure overload the RV initially adapts with sarcomere synthesis and myocardial hypertrophy. This is followed by progressive contractile dysfunction and chamber dilatation, which is compounded by the volume overload of increasing tricuspid regurgitation (130). Dilatation, pressure and volume overload and failure of the RV impairs LV function through interventricular interactions (136).

The rate and pattern of deterioration is variable and while some RVs will adapt, others fail. Genetic differences, variations in RV chamber geometry, myocardial ischaemia and biochemical factors affecting contractility and hypertrophic growth have been hypothesized as potential determinant factors (136-138). RV function is a reflection of afterload, preload, contractility and ventricular interdependence. Traditionally, PVR has been used to represent

the afterload of an ejecting RV. However, capacitance and impedance measuring pulsatile flow, are also key contributors, with independent relationships with RV adaptation and prognostic importance (139-142).

1.5.4 Exercise in the Assessment of Pulmonary Arterial Hypertension

In patients with PAH, the progressive remodeling of the pulmonary arteries eventually restricts blood flow from the RV to the lungs, leading to an increase in physiological dead space due to underperfusion of well-ventilated lungs. This reduction in blood flow to the LV, means that a rise in SV is limited and an increase in CO is largely reliant on HR. The lack of oxygen delivery to muscles leads to an increase oxygen extraction, uptake and an increase in hydrogen ion concentration at lower workloads during exercise, which stimulates ergoreceptors and chemoreceptors, inducing a hyperventilatory response and exercise induced hypoxia if PAH is severe.

A systematic review in 2010 found that 107 factors have been associated with mortality in PAH, however, only 10 factors were found to have a reproducible predictive association. These include the New York Heart Association functional class (NYHA), HR, six minute walk distance test (6MWD), pericardial effusion, mPAP, mean RAP, cardiac index (CI), stroke volume index (SVI), PVR and mixed venous saturations. However, for mPAP, half as many studies that evaluated the variable did not find an associated with mortality and only mean RAP and PVR have more supporting evidence than non-supporting evidence(143). PH patient registries have shown that poor prognosis is associated with RV haemodynamic function and exercise limitation at the time of diagnosis (144, 145) and the REVEAL study demonstrated that PVR, NYHA class 4, a 6MWD threshold below 165m and RAP, but not mPAP were

associated with survival (131). Humbert at al showed that a greater 6MWD, lower RAP and higher CO were associated with improved survival (146). Similarly in CTEPH, Condliffe et al showed that 6MWD and gas transfer independently predicted perioperative mortality in operable CTEPH, while 6MWD and CI independently predicted outcome in non-operable disease(147). Together these studies demonstrate that exercise capacity reflected in functional class and 6MWD, and variables associated with RV function such as RAP are the key prognostic indictors. These papers have not included CMR assessment of RV function.

RV function is a strong predictor of mortality, outperforming PVR (148-150). On systematic review of CMR measurements only, RVEF as assessed by CMR is the best established and best predictor of mortality (151) and survival is associated with change in RVEF, and not change in PVR or CO. Correlations between change in PVR and change in RVEF are reported to be poor (152). Courand et al have shown that improvement in RVEF at 3-6 month follow up has been shown to be the best predictor of subsequent overall survival, and that 53% of patients with improved PVR, had decreased RVEF on follow up, once again showing a discrepancy between PVR and deterioration in RVEF. Echocardiographic parameters, e.g. TAPSE, lost significance in multivariable analyses (153). Also of key interest, is that at baseline, there are differences between 6MWD and functional class, in those whose RVEF deteriorate or not (75, 153). In patients with stable disease for 5 years, subtle increases in RVEDVI and RVESVI herald the onset of progressive RV dysfunction, so potentially monitoring RV volumes can help anticipate RV decline, even at a time of apparent clinical stability (154).

Despite this, the submaximal 6MWD has been used as the standard of care for serial follow up of PAH patients but while baseline values are prognostic, change in 6MWD does not

provide additional prognostic information beyond that obtained at baseline levels (155-157) and importantly does not reveal the mechanisms of RV dysfunction at increasing cardiovascular workload. Exercise capacity as assessed by functional class and 6MWD is associated with prognosis, but change in 6MWD does not correlate with prognosis (74, 158) and cardio-pulmonary exercise testing (CPET) only adds either marginal prognostic value (159), or no additional prognostic information in larger trials (160) to the 6MWD.

This highlights the point that despite the fact that deterioration in RVEF is a key prognostic indicator, there is currently no way to determine which RV is destined to fail despite medical therapy. Clinical characteristics, the 6MWD and PVR response to therapy as a traditional method of measuring afterload are not sensitive or adequate measures to predict this. Hence assessing RV reserve on exercise as a marker of subclinical RV-PA uncoupling prior to deterioration of resting RV function has gained attention over recent years.

Claessen et al studied 14 inoperable CTEPH patients with exercise CMR with concurrent invasive haemodynamic monitoring, before and after acute administration of Sildenafil. They demonstrated that Sildenafil decreased RVESVi during resting and exercise, increased LVEF and RVEF at rest and exercise and increased SVI, which was greater during peak exercise than at rest. Furthermore, resting RV and LV parameters did not correlate with CPET but RVEF reserve correlated moderately with peak VO_2 and the ratio of minute ventilation to carbon dioxide output (VE/VCO_2). They also found that the reduction in total PVR during peak exercise correlated highly with the increase in peak exercise SVI and RVEF after Sildenafil (161). Surie et al similarly studied 18 operable CTEPH patients and demonstrated, using exercise CMR, an improvement in exercise SVI post PEA in 14 patients while resting SVI, HR and CI were unchanged (162). These studies, together, demonstrate how assessment of the RV

and LV function during exercise post a therapeutic intervention is feasible, with changes in exercise RV and LV function apparent. However, Surie et al did not assess volumes, and Claessen et al did not assess flow parameters.

Exercise echocardiography has been used to assess the response of the RV in PAH, demonstrating that a drop in SV during exercise is associated with significantly worse outcomes (95). Blumberg et al demonstrated that peak VO_2 was the strongest predictor of survival and that exercise CI and the slope of pressure/flow relationship were the only independent prognostic indicators(94). Transplant free survival has been shown to be associated with RV load adaptation at diagnosis, with no other differences in resting RV size and EF at baseline(163). SPAP increase during exercise and peak VO_2 per kilogram remained independent prognostic markers(164). Chaout et al have demonstrated that while change in 6MWD correlates with change in exercise CI, the most significant baseline covariates associated with survival are change in SPAP from rest to exercise and exercise CI measured invasively (165). However, interpretation of sPAP increase on exercise needs to be interpreted with caution, as LV diastolic dysfunction has also been shown to be common and associated with greater elevations of sPAP on exercise(104) in patients diagnosed with scleroderma associated PAH.

Developing non-invasive assessments of RV function is an ongoing challenge in clinical research. The ability to accurately and reproducibly assess RV and LV adaptation to pulmonary hypertensive states, and hence potentially to targeted therapies, would be invaluable. As CMR provides accurate assessment of RV volumes and EF, is not limited by acoustic windows or operator dependent, and does not make use of ionizing radiation, it

potentially provides a novel and exciting method to analyse dynamic RV function and is the ideal modality for assessing serial differences between small groups

1.6 Cardiovascular Magnetic Resonance Imaging

1.6.1 Cardiovascular Magnetic Resonance Imaging Physics

CMR has evolved in the last few decades in to a sophisticated and robust method for studying the cardiovascular system, and is the gold standard for the quantification of RV function (166, 167). It has been built on a century of scientific achievements in mathematics, physics, chemistry and medicine. Six Nobel Prizes have been awarded for breakthroughs related to this technique.

MRI is based on the resonance of the protons in response to radiofrequency waves. Hydrogen is used because it is the simplest and most abundant element in human tissue, water, and lipid molecules. Protons have a magnetic axis, termed magnetic moment, which is normally randomly orientated. When spins are placed in a magnetic field, they align and spin around an axis in line with the direction of the field.

A MRI system is made up of three main electromagnetic components; a set of main magnet coils, three gradient coils and a radiofrequency transmitter coil (Figure 3). Each generates a magnetic field in different directions and times, which when applied in combination, produce MRI signals during the readout that are used to form images. The main magnet coils produces a constant, strong magnetic field, B_0 and defines the operating field strength of the MRI system, measured in units of Tesla (T).

The magnetic field direction is described using three orthogonal axes, x, y and z. When the patient lies supine within the centre of the bore of the magnet, the overall proton alignment is in the direction of the main magnetic field, B_0, which is also denoted by the z axis, and at equilibrium has net longitudinal magnetization (Figure 3). Applied radiofrequency pulses then disrupt this equilibrium, and the net magnetization moves away from its alignment with B_0, in the plane of the x and y axes, or Mxy, or the transverse component. For example, a 90° radiofrequency pulse will move all the net magnetisation from the longitudinal (z axis) through to the transverse (xy) plane. These radiofrequency pulses are classified by their flip angle and their effect, and are known as excitation pulses. This rotating Mxy component generates the detectable signal.
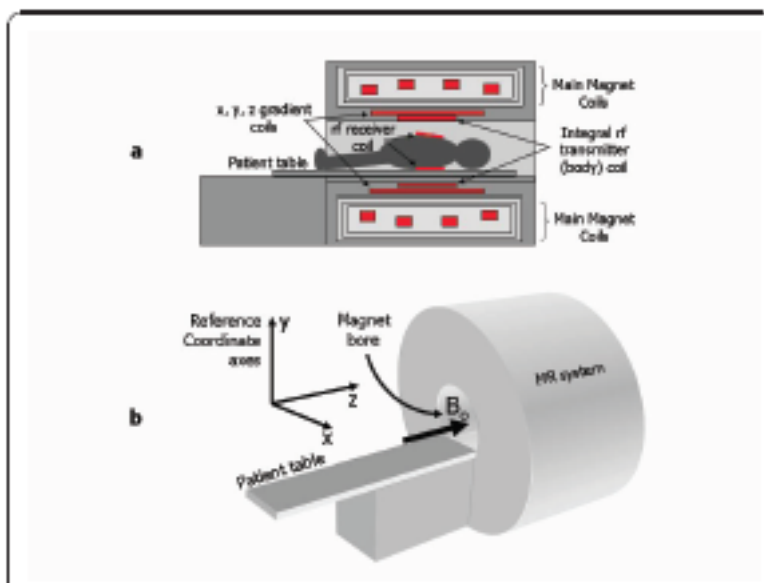
Figure 1.3: MR System components a) Relative locations of main magnet coils, x, y and z gradient coils, and radiofrequency transmitter and receiver coils b) Typical arrangement for a cylindrical bore MR system showing the magnet bore and the reference coordinate axes with the static B_0 field direction along the horizontal z axis (From: Ridgway, J.P. Cardiovascular magnetic resonance physics for clinicians: part 1, Journal of Cardiovascular Magnetic Resonance, 2010)

Immediately after the radiofrequency pulse, the spins start to relax as the energy is dissipated and is defined by two parameters known as T1 and T2. T1 relaxation refers to the recovery along the longitudinal axis, while T2 refers to relaxation of the transverse component. Different tissues have varying relaxation parameters, and hence this can be used for tissue characterization.

Localisation of anatomical position within a selected imaging slice is done with the application of frequency and phase encoding gradients. Reception of the radiofrequency energy is via aerials known as coils, and these MR signals produced can be localized and encoded to produce an image, using a Fourier transformation. However, the Fourier transform can only analyse a signal that changes over time. Hence each phase encoding gradient is applied at an increasing strength, repetitively, by equal increments. For each phase encoding step, the frequency or signal echo is measured and stored in a raw data matrix. Once all the signals for a prescribed number of phase encoding steps have been acquired and stored, they are then analysed together by a 2D Fourier transform to decode both the frequency and phase information (168, 169).

K space has a central role in MRI. MRI scanners collect data on the spatial frequencies on the imaged object. They are stored in a regular grid of values forming a data matrix known as k-space. Each point in k space represents how much of a particular spatial frequency is contained within the image. To make an image, a whole range of spatial frequencies is acquired. Usual standard imaging is acquired by filling k space with equally spaced parallel lines of signal data, known as a Cartesian acquisition.

The repetition time (TR) is an important parameter that determines how fast MR images can be acquired, but also affects image contrast. The spatial resolution, or the ability to

discriminate between two points in space and time, depends on the field of view, and the number of phase and frequency encoding steps, and as a result is often limited by the image acquisition time. A greater spatial resolution requires a greater number of repetitions, and therefore a longer image acquisition time. It is specified by selecting the field of view (FOV) and the number of frequency and phase encoding points, which determines the degree of sampling of the MR signal, which hence specifies the extent of k space that is acquired. Sampling is performed long enough such that all the necessary spatial frequencies to reconstruct an image are collected. Displayed resolution can be improved and is performed routinely with clinical MR, using zero padding and zero filling. The more zeros appended, the better the reconstructed images look. A zero padding factor of 2 is used more commonly to improve the displayed resolution (170).

Temporal resolution is often described as the smallest increment of time over which a change in an imaged dynamic process can be observed. However, this needs to be distinguished from the period of time for data acquisition for a given image. Interpolation methods to improve reconstructed temporal resolution such as view sharing can also used, and display cine images at less than the acquired temporal resolution and do not actually add further information but merely improve the visualization of the images. For routine CMR, the MR signal are acquired over multiple heart beats, synchronized by 'gating' the images by detecting the R wave on the ECG. This is then used to synchronise the MR data acquisition. Hence the resultant image is an average of a heart beat, with the data acquired and averaged over multiple heart beats, synchronized using the ECG (171). Limitations of CMR include claustrophobia, artefacts caused by arrhythmia and motion, metal implants/devices contraindicating CMR and patient size.

1.6.2 Two dimensional phase-contrast imaging

Cine-imaging can also be used to quantify flowing blood through a vascular lumen. Usually, the magnitude of a signal coming from a voxel is used for image reconstruction. However, this signal is a vector, and also possesses a direction or phase, and this is used to quantify the velocity of that voxel. To do this, an additional velocity-encoding gradient switching is introduced, causing phase shifts proportional to blood and tissue velocities in the gradient direction. Then to extract these phase shifts, the signals are acquired with and without switching of the velocity encoding gradient and subtracts the resulting phases. In stationary tissues, this results in a net phase of zero. However, in moving tissue, the effects of these gradients will not cancel each other out and a net phase difference can be detected. Where there is no phase shift, this becomes a gray scale image, and where there is velocity change, this will be displayed as either brighter or darker, depending on the direction. The sequence used is typically a spoiled gradient echo sequence (172, 173).

The plane of the image must be set that it is perpendicular to the path of the flowing blood, and this is achieved by planning on two orthogonal views. Hence it provides cine images of the velocities across the total cross sectional area of flow of interest, and then time courses, maximal velocities, peak velocity and mean velocities can be calculated across that cross sectional area (172, 173).

The proportion of the phase shift in each voxel or tissue is determined by the velocity-encoding (VENC) value, which is pre-set by the operator. Phase shifts are measured in degrees, and their values should be in the range of +/- 180 degrees. Hence the pre-set VENC is set at what the user predicts is the expected peak velocity within the vessel, before starting the

measurement, and the peak velocity corresponds to a phase shift of 180 degrees. If the VENC chosen is too low, then aliasing will occur in the opposite direction, however, when set too high may be insensitive to slower velocities, and hence potentially causing inaccuracies (172, 173).

1.6.3 Real time MRI

Until recently, the relatively low imaging speed of cardiac MRI compared to physiological processes such as blood flow, a heart beat and a respiratory cycle, made dynamic MRI challenging. As discussed, in order to reconstruct an image, as many points in k space are usually sampled over multiple heart beats, which sets the limit as to the speed of acquisition. Various techniques such as parallel imaging, sampling data using alternative trajectories, k-t acceleration, compressed sensing and extra dimensional reconstruction, have been developed to overcome these limitation. Central to these techniques is k space under sampling. This technique reduces the amount of k space acquired and uses prior information to reconstruct the image. However, it can lead to artifacts and the choice of under sampling influences the degree and type of artifact (Figure 4).
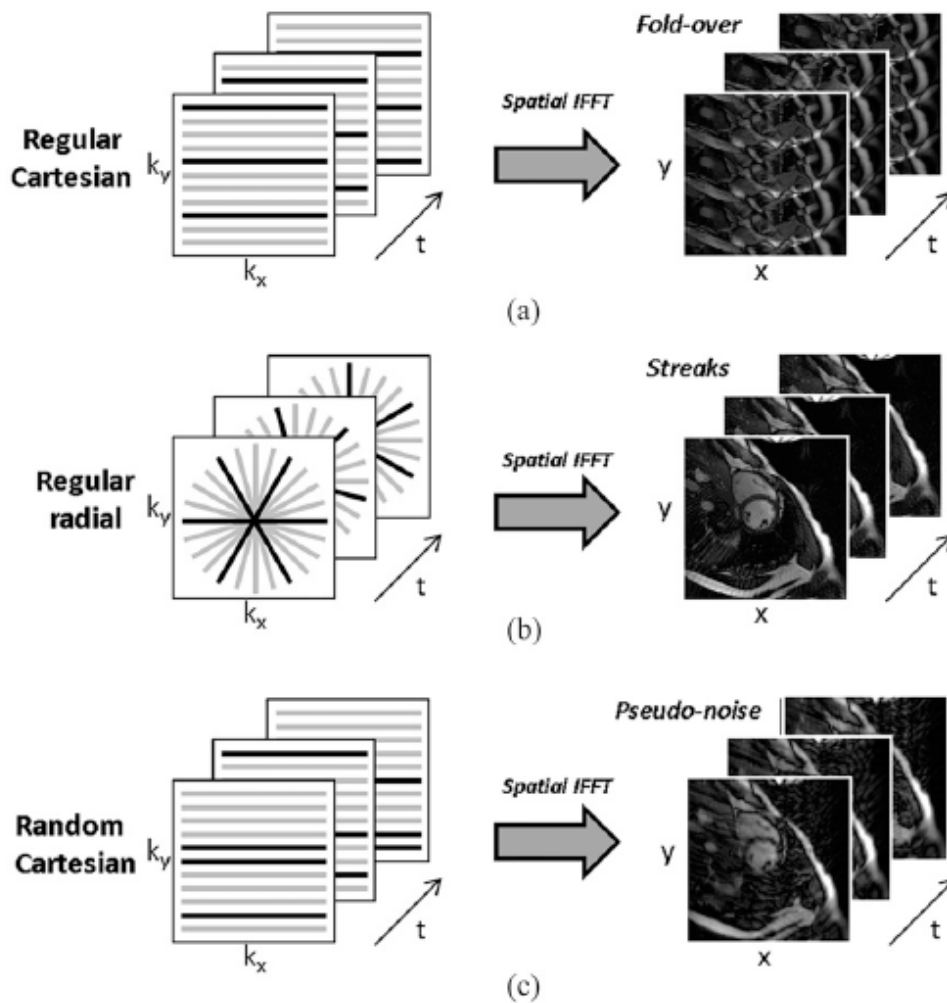
Figure 1.4: Undersampling techniques used for imaging of cardiac function a) Regular Cartesian undersampling e.g. for parallel imaging, which involves (for example) acquiring one out of every four lines and can result in foldover artefacts in the reconstructed image. B) Shows uniform radial undersampling which leads to low-value streaking artefacts c) Random Cartesian undersampling which leads to noise-like artefacts. (From Axel and Otazo, Accelerated MRI for the assessment of cardiac function, British Journal of Radiology, 2016)

There are two main approaches to parallel imaging – SENSE and GRAPPA. SENSE imaging makes use of detecting multiple simultaneous acquisitions with different coils to remove regular aliasing and the images are reconstructed from the signals detected with the different coil elements. GRAPPA uses the varying spatial response patterns of the coil elements to estimate the missing data points from the k-space data.

Each coil had different spatial sensitivity patterns, and hence can provide additional effective spatial information that can produce images without aliasing, even in the setting of under-sampling, as each coil element will have different relative intensities of the aliased component of the images. Theoretically, this should mean that the acceleration factor of a parallel-imaging scan is equal to the number of coils used. However, this is actually limited by the change in signal to noise ratio. Saying this, however, the greater the number of coils, the less likely there will be aliasing in an under sampled acquisition and the maximum acceleration factor in parallel imaging is limited to the number of independent coils along the phase-encoding dimension (174-176). Figure 5 shows a 32 elements cardiac coil used in the Philips Achieva 1.5T, at the Robert-Steiner Unit, Hammersmith Hospital.
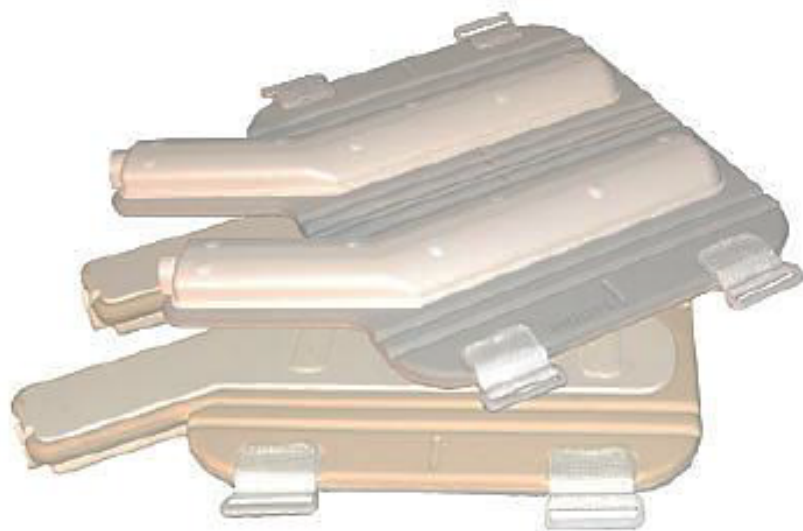
Figure 1.5: A 32- element cardiac-coil used to obtain high resolution imaging with high acceleration factors (Philips sensitivity encoding (SENSE) Cardiac coil for Achieva 1.5T.

1.6.4 Exercise MRI

Thus far, accelerated Cartesian (26, 37-40, 42) and non Cartesian imaging (177-180) approaches have been used by several authors, with some being conventional, retrospectively acquired gated images (29, 30) or triggered real time (26, 40, 42), while others have used 'true' real time imaging with no triggering (37). There has been little published in regards to comparison between the different techniques.

Lurz et al reported their radial k-t imaging against 'standard' (accelerated Cartesian acquisition) real time. Their standard real time approach had a voxel size of 3.1 x 3.9 x 10mm and a temporal resolution of 80ms, while their radial k-t SENSE sequence had a voxel size of 3 x 3 x 10 and a temporal resolution of 35.5. They reported that their radial k-t SENSE sequence was more accurate and reproducible than the standard real time sequence, with accuracy defined as RVSV = LVSV. However, the spatial resolution of their standard sequence was poor, and they only allowed 30 seconds to achieve 'steady state' exercise. In other words, SV may have been steadily increasing throughout acquisition, leading to inaccuracies in SV calculation. Furthermore, simultaneous aorta (Ao) and main pulmonary arterial (MPA) SV has not been reported. Reproducibility was also only reported for CO, and not cardiac volumes or SV (178).

Pflugi et al compared radial vs. Cartesian acquisitions during exercise CMR perfusion studies. They compared radially acquired data reconstructed using several techniques to Cartesian data reconstructed using SENSE. There was no statistical difference in image quality in the radially

acquired data compared to the Cartesian. Temporal resolution was 93ms for the Cartesian acquisition and 62ms for the radial acquisition.(180)

La Gerche et al compared ungated, standard real time to gated sequence during 3 levels of exercise, as well as comparing MRI derived CO to simultaneously invasively derived CO from the Fick method. Their ungated real time sequence had a reconstructed voxel size of 2.3 x 2.3 x 8 (though actual voxel size has not been reported) and they have reported their temporal resolution to be 35-38ms. This research team, however, have given our research team a copy of their exam card, and their TFE duration acquisition is 47ms. They reported that due to considerable ECG artifact, analyzable images from only 6 subjects out of 15 were acquired during the gated sequence, however, all the images were acquired during the real time acquisition. They also reported considerable artifact in the gated images, in those that were acquired. There was excellent correlation between CO derived by the Fick method to that from real time exercise CMR calculated CO, and excellent inter and intra observer reproducibility. However inter-study reproducibility was not reported and similar to Lurz et al, simultaneous Ao and MPA flow was not reported.(37)

Exercise CMR has now been used by several research groups in healthy volunteers (18, 26-30, 37, 177, 178, 181-183) and a number of different pathologies including chronic obstructive pulmonary disease (42), PAH(40), BMPR2 gene positive subjects (184), heart failure (37), CTEPH (161, 162), congenital heart disease (38, 179), pulmonary regurgitation (39), coronary artery disease (180), bicuspid aortic valve disease (185) and athlete's cardiomyopathy (102). However, there are a number of issues. Firstly, each research group has used different MRI acquisition protocols with differing temporal resolutions and spatial resolutions. Secondly, while most report consistent inter and intra observer reproducibility, none have reported inter-

test or inter-study reproducibility, and the majority have acquired volume or flow, rather than acquiring both. This is an important consideration when discussing the accuracy of the test. Furthermore, exercise protocols have varied greatly, with some groups acquiring images after during exercise, during intermittent breaks or immediately after exercise. This will be discussed in further detail in Chapter 3. Fourthly, some groups have not taken in to account respiratory variation on exercise, which is an important consideration, which will also be discussed further in Chapter 3. While change in dynamic biventricular function and RV reserve is clearly demonstrable with exercise CMR, a consistent, accurate and reproducible methodology needs to be developed. Otherwise, it will threaten to become 'just a research tool', utilized in inconsistent, heterogeneous ways so that data becomes difficult to interpret.

1.7 Summary, Hypotheses and Specific Aims

The gold standard of measuring RV function has traditionally thought to be best done with invasive haemodynamics, however, developments in non-invasive imaging techniques are potentially safer and more clinically and prognostically relevant. Conventional indices of resting RV function have prognostic significance in PAH but do not take in to account exercise capacity, and conventional cardio-pulmonary exercise tests do not directly assess RV dysfunction at increasing workload. Imaging cardiac function at rest, has also been shown consistently not to correlate with exercise capacity. RV reserve has been gaining interest recently, as a way to detect subclinical ventricular-vascular uncoupling. While exercise echocardiography is feasible and available, it cannot directly measure RV volumes and EF accurately, so surrogate methods of RV function have been developed with mixed results in terms of reproducibility. CMR is a highly reproducible and accurate method of evaluating biventricular function at rest and during exercise, and can be used to assess RV remodeling

after interventions. However, there is already a high heterogeneity of approaches developing to this technique, with no reports of inter-study and inter-test reproducibility, nor has there been any model tested to demonstrate the sensitivity of CMR to detect subtle changes in RV and LV function, say as in the setting of acute pulmonary hypertension in the healthy heart.

Specific Aims

1. Develop and demonstrate an exercise CMR protocol which is feasible, accurate and reproducible

2. Study the ability of CMR to detect physiological LV and RV changes at rest and on exercise in normal subjects in a model of acute pulmonary hypertension, induced by hypoxia

3. Study the ability of CMR to detect changes in right ventricular reserve on exercise in patients with pulmonary arterial hypertension, and the impact on LV preload

4. Describe the spectrum of ventricular volume and flow in normal hearts, normal hearts in acute pulmonary hypertension and in patients with chronic pulmonary arterial hypertension

5. Study the pathophysiology of exercise cardiac function in patients with PAH and correlate with cardiopulmonary exercise testing and 6MWD

6. Study the impact of RV obstruction from acute pulmonary vasoconstriction and chronic pulmonary remodeling on LV geometry and filling

7. Study the ability of the RV to remodel post pulmonary thromboarterectomy, the relationship with the left ventricle and MRI correlations with functional capacity, in particular, improvements in exercise capacity

Specific Hypotheses:

1. During exercise in healthy volunteers, LV and RV SV will increase driven by a decrease in ESV and an increase in EDV

2. In acute pulmonary hypertension, RV-PA coupling will be maintained in healthy subjects demonstrated by a preservation in right ventricular reserve on exercise

3. In patients with PAH and normal resting RV function, RV-PA uncoupling will occur, with deterioration of RVEF only apparent on exercise

4. Left ventricular size will decrease during acute hypoxia, will be smaller in patients with chronic pulmonary hypertension and will become more apparent on exercise, due to under filling.

5. On relief of RV obstruction, LV size will increase due to improvements in filling

6. Resting parameters of cardiac function on MRI will not correlate with exercise capacity in patients

Chapter 2 – General Methodology

2.1 Ethics Approval

For the studies described in Chapters 5-7, informed written consent was obtained from all subjects and each study was approved by the Health Research Authority, Research Ethics Committee South East Coast, Surrey, Research Ethics Committee reference number 13/LO/1398, the Joint Research Compliance Office (13HH0838) and sponsored by Imperial College London. The study was included on the National Institute for Health Research Clinical Research Network Portfolio. Chapter 4 was a retrospective analysis with the knowledge of The Prince Charles Hospital Ethics Committee in Queensland, Australia.

2.2 Funding

The studies described in Chapters 5-7 were funded by the British Heart Foundation, Project Grant number PG/13/44/30321 for the sum of £232,551 and peer reviewed by three independent reviewers.

2.3 Study population and Recruitment for the Exercise CMR study

Two groups were recruited:

    1) Healthy volunteers

    2) Patients with Class 1 PAH

2.3.1 Healthy Volunteers

Healthy volunteers were screened initially via email using a simple health questionnaire. On the day of attendance, a more detailed screening questionnaire was carried out, with height, weight, heart rate, blood pressure, electrocardiogram (ECG) and cardiovascular examination.

Inclusion criteria

1   Male or female

2   Age ≥18

3   Able and willing to give consent

4   Able to participate for the planned duration of the study

5   No clinically important abnormal clinical findings at the screening examination

6   Normal ECG

7   Normal blood pressure

8   Able to perform all the test procedures in the study

Exclusion criteria

1   Known to be pregnant

2   Have medical conditions that precludes his or her ability to participate

3   Have history of high-altitude pulmonary oedema or mountain sickness

4   Inability to perform or have contraindications to the test procedures

5   Currently enrolled in other interventional study

6   Have impairment in communication (learning disability or impaired cerebral function)

7   History of recent drug dependence and alcohol abuse (<2 years)

8   Have BMI >35kg/m^2 or weigh >120kg

2.3.2 Pulmonary Arterial Hypertension Subjects

Inclusion criteria

1   Male or female

2   Age ≥18 years old

3   Have pulmonary arterial hypertension: idiopathic, hereditary, anorexigen-induced or connective tissue related pulmonary hypertension.

4   Resting RVEF ≥ 45%

Exclusion criteria

1   Known to be pregnant

2   Have lung disease-related and left heart disease related pulmonary hypertension

3   FEV_1 <50% predicted

4   Have medical conditions that precludes his or her ability to participate

5   Inability to perform or have contraindications to the test procedures

6   Currently enrolled in other interventional study

7   Have impairment in communication (learning disability or impaired cerebral function)

8   History of recent drug dependence and alcohol abuse (<2 years)

2.4 Recruitment

2.4.1 Healthy volunteers

The healthy volunteers were recruited via advertisement to the general public.

2.4.2 Participants with Pulmonary Arterial Hypertension

The participants were recruited from referrals from the staff in the Pulmonary Hypertension service and then directly approached and invited to participate.

2.5 Follow up

10 Healthy volunteers were asked to return within three months to repeat the above procedure for validation during normoxia. Exercise CMR was separated from other routine tests, such as CPET and 6MWD, by at least 4 hours.

2.6 Our Services

The Pulmonary Hypertension service at Hammersmith hospital is part of the designated national pulmonary hypertension service for England. We have a programme of clinical and basic science research in pulmonary hypertension and exercise physiology. Diagnosis is made according to current European guidelines. (186). In 2012 the service saw 1162 patients; 361 were new referrals of whom 95 had PAH.

2.7 Statistical Analysis:

Data was analysed using IBM SPSS statistics Version 22. Descriptive data for continuous variables was expressed as medians and the interquartile range, or as mean ± standard deviation where appropriate. Comparisons between groups for continuous variables were performed where normally distributed using unpaired two sample t tests or the Mann-Whitney U test as appropriate. Comparisons within groups for continuous variables were performed where normally distributed using the paired samples t test or the Wilcoxon signed rank test. A two way repeated measures analysis of variance (ANOVA) was used to compare cardiac response from rest, exercise to immediately post exercise in healthy volunteers during normoxia and hypoxia. A mixed ANOVA was used to compare biventricular response from rest, exercise to immediately post exercise in healthy volunteers and patients. Pearsons correlation coefficients were used to evaluate the bivariate relationship between resting and exercise measures of biventricular function and relevant demographic and clinical factors. The Bland Altman test was used to compare between tests and alpha coefficient to compare intra and inter-observer reproducibility and inter-study reproducibility. A Bonferroni correction was applied to adjust for multiple comparisons where appropriate. A two tailed p-value <0.05 was considered statistically significant with a bonferroni correction used where appropriate.

2.8 Clinical Data

2.8.1 6MWD

The 6MWD was carried out as part of the patient's usual clinical work up. It was carried out by the Pulmonary Hypertension Specialist Nurse according to the American Thoracic Society

Guidelines (187). The following data was captured 1) Distance walked 2) O_2 saturations at the beginning 3) O_2 saturations at the end

2.8.2 Cardiopulmonary Exercise Testing

CPET comprised a ramp-protocol cycle test on an electronically braked bicycle ergometer (Bike, VIASprint 200; Equipment, Jaeger Masterscreen CPX; Software, JLAB LABManager 5.3.0.4) (188). The value for the bicycle ergometer increase (watts/min) was estimated so that the subject's peak workload would be achieved in around 10 minutes, and was based on the subject's reported level of fitness. Subjects were encouraged to exercise until exhaustion and 3 minutes of rest and recovery data were also recorded. Each participant breathed through a calibrated mass flow sensor with expired gas sampled on a breath by breath basis enabling measurement of VO_2, VCO_2, minute ventilation (V_E), and respiratory rate. Oxygen saturation was monitored with a finger probe attached to a pulse oximeter. Subjects were monitored throughout testing with a 12 lead ECG.

The CPET operator recorded the peak VO_2 as the highest peak VO_2 over a 30 second period. V_E/VCO_2 was calculated by fitting a first order polynomial to the $V_E/VCO2$ data where the relationship becomes linear, near the start of incremental exercise until the respiratory compensation point using the metabolic cart software. The following data were captured 1) Peak VO_2 2) Peak work rate and 3) V_E/VCO_2 slope

2.8.3 Lung Function Testing

Spirometry was carried out according to American Thoracic Society/European Respiratory Society standards. The following data was captured: 1) Forced expiratory value in 1 second (FEV$_1$) and 2) Forced vital capacity (FVC)

2.8.4 Echocardiogram

The following data was captured where possible from the patient's most recent echocardiogram.

Parasternal Long Axis View

LV end diastolic diameters (cm)	Posterior wall (cm)
LV end systolic diameter (cm)	Aortic root diameter (cm)
Interventricular septum (cm)	

Parasternal Short Axis view of Right ventricular outflow tract (ROVT)

Doppler
RVOT acceleration time (m/sec)
Pulmonary regurgitant velocity (PRV), beginning of diastole (m/sec)
PRV end diastole (m/sec)

Short Axis View at the Level of the Papillary Muscles

LV eccentricity index systole	LV eccentricity index diastole

Apical Four Chamber View

2D	Doppler	Tissue Doppler Imaging
Basal diameter of RV (cm)	TRV (m/sec)	LV septal E'
RAA (end systole) (cm2)	Mitral inflow (m/sec) (E and A waves)	LV septal A'
RA volume index (ml/m^2)	DT (mitral inflow, m/sec)	LV lateral wall E'
RV FAC (%)	LVOT tract velocity (m/sec)	LV lateral wall A'
LVEF (Simpsons)	Aortic flow (m/sec)	RV free wall E'
	AR velocity (cm/sec)	RV free wall A'
	Tricuspid inflow (m/sec) (E and A waves)	RV free wall S wave
	DT (tricuspid inflow, m/sec)	RV MPI
	TAPSE (mm)	RV IVRT

RV: Right ventricle, ED: End diastolic, ES: End systolic, RAA: right atrial area, FAC: fractional area change, TRV: tricuspid regurgitant velocity, DT: deceleration time, LVOT: left ventricular outflow tract, MPI: myocardial performance index, IVRT: isovolumic relaxation time

Subcostal view

- Inferior vena cava size

- RA pressure estimation from % collapsing

2.8.5 Ventilation Perfusion scan

The results of the patient's ventilation perfusion (V/Q) scan were documented.

2.8.6 Computed Tomography Pulmonary Angiogram

The results of the patient's computed tomography pulmonary angiogram (CTPA) scan were documented.

2.8.7 Cardiac catheterisation

Right heart catheterisation at was carried out as a routine clinical test for the patients at diagnosis. The following data was collected from patient files: 1) Blood pressure and heart rate 2) Right atrial pressure 3) Pulmonary artery systolic pressure 4) Pulmonary artery diastolic pressure 5) Mean pulmonary arterial pressure 6) Pulmonary capillary wedge pressure 7) Cardiac output 8) Pulmonary vascular resistance

2.8.8 Plasma Assays

Data from the following blood test was captured.

- Full blood count

- Electrolytes, urea and creatinine

- Liver function tests

- B-type natriuretic peptide (BNP)

2.9 Subject Preparation

All subjects were instructed to avoid alcohol in the preceding 24 hours, and to avoid caffeine intake 6-8 hours before attending for the research tests. They were also instructed, depending on the time of day of the test, to keep meals light. Patients were instructed to continue their regular medications as usual.

2.10 Imaging Protocol

2.10.1 Cardiac Magnetic Resonance Imaging

CMR was performed on a 1.5T Philips Achieva system (Best, Netherlands). A 32-element cardiac phased-array coil was used for signal reception. Continuous heart rate and oxygen saturations were monitored (Nonin 7500FO MRI Compatible Pulse Oximeter).

The subject's height was used to determine the optimal positioning on the MRI couch. Care was taken to ensure that the subject was positioned such that they could pedal within the scanner with no restriction, and that their heart was no more than 10cm from isocentre. Once the subject was optimally positioned, the feet were taken out of the pedals to rest on the couch during rest scanning and placed in to the pedals just prior to the commencement of exercise.

A resting and exercise protocol was used to acquire the data. 20 minutes of rest or the period of time it took for heart rate returned to baseline was given to healthy volunteers before the administration of the 12% oxygen. Participants breathed 12% oxygen for 10 minutes before resting acquisitions commenced and the same exercise protocol was used in the hypoxic study.

After all the images were acquired, participants were taken out of the CMR bore, the hypoxic gas removed and they were monitored supine until saturations and heart rate returned to normal.

2.10.2 Breath hold Ventricular Volumes and Function

In accordance with the international guidelines on tomographic imaging, the standardized approach to MRI image acquisition and display was used (189). The heart is orientated and displayed using the long axis of the left ventricle. Other selected planes are orientated at 90° angles relative to this long axis, and are described as short axis, vertical long axis and horizontal axis.

Scout images were obtained and used to plan standard, retrospectively gated, breath hold, 2D cine balanced steady-state free precession (B-SSFP) images in the left ventricular short axis (LVSA) plane from base to apex using the following parameters: Field-of-view=370mm x 370mm; Repetition time/Echo time = 3.0/1.5msec; Flip angle 60˚; Bandwidth = 1250Mz/pixel; Acquired pixel size = 2.0 x 2.2mm; Section thickness = 8mm with a 2mm gap; Reconstructed voxel size = 1.2 x 1.2 x 8mm; Number of sections = 10-12; Cardiac phases = 30

2.10.3 Breath hold Aortic and Main Pulmonary Arterial Flow Quantification

MPA and aortic flow data were acquired using a retrospectively gated flow sensitive gradient-echo sequence acquired during a breath hold. Image planes were located at the midpoint of the main pulmonary artery and ascending aorta (sino-tubular junction). The parameters were: Field-of-view = 350 x 302; Repetition time/Echo time = 4.2/2.6 msec; Flip angle 20 ˚;

Bandwidth = 1724Hz; Acquired pixel size = 3.0 x 3.0 x 10mm; Section thickness = 10mm;

Reconstructed voxel size = 1.37 x 1.37 x 10mm;

2.10.4 Real time, Free Breathing Ventricular Volumes and Function at Rest and Exercise

Free breathing, real time LVSA images were acquired using the following parameters: Field-of-view = 305mm x 305mm; Repetition time/echo time = 2.5/1.26msec; Flip angle 50˚; Bandwidth = 87.9 Hz; Acquired voxel size 2.73 x 2.73 x 10mm; Section thickness = 10mm with no gap; Reconstructed voxel size = 1.19 x 1.19 x 10; Number of sections = 14; Slice scan order = base to apex; Dynamic scan time = 66 seconds, with 50 dynamics per slice; Temporal resolution 74ms;

Real time images were acquired using LVSA stack geometry by specifying a number of frames acquired at each section before moving the imaging plane to the next contiguous slice position. Furthermore, the number of slices was adjusted according to the individual's cardiac size and also anticipating downward cardiac translation, in order not to inadvertently miss acquisition of the apex.

2.10.5 Real time, Free Breathing Aortic and Main Pulmonary Arterial Flow Quantification at Rest and Exercise

Free breathing, real time MPA and aortic phase contrast images were acquired using the following parameters: Field-of-view = 300 x 300; Repetition time/Echo time = 11/3.7 msec; Flip angle 20 ˚; Bandwidth = ; Acquired pixel size = 3.0 x 3.0 x 10mm; Section thickness =

10mm; Reconstructed voxel size = 1.17 x 1.17 x 10mm; Dynamic scan time = 4.5 seconds with

100 dynamics; Temporal resolution = 44ms

Phase contrast velocity was set at 200cm/s for the aorta and 150cm/s for the MPA at rest, and

at 200cm/s for both the aorta and MPA during exercise and immediately post exercise

acquisition.

During exercise, the slice locator was re-positioned in the expiratory phase on the exercise

RVOT and LVOT images to acquire optimal MPA and aortic flow data respectively. Prior to

cessation of exercise, the position of the aortic and MPA acquisitions was checked for accurate

placement and aliasing. It was repeated if these were considered to be less than ideal. This

was repeated immediately post exercise.

2.11 Ventricular Volumes and Mass Analysis

Volume and mass analysis was carried out on Osirix (available at The Royal Prince Alfred

Hospital, Sydney) and CVI cmr42 (available at Imperial College, London). To carry out

volumetric analysis of the heart from a cine image, two frames must be identified: end systole

and end diastole. The end-diastolic frame is usually acquired immediately after the R wave

and the end systolic frame is identified visually as that with the smallest left and right

ventricular cavity.

Segmentation of the breath hold and real time short axis cine stacks was performed by semi-

automated left ventricular and right ventricular endocardial and epicardial surface contour

detection, with manual adjustment, at end diastole and endocardial surfaces only in end systole

(cvi42) (Figure 2.1a and b). Semi automated techniques have been demonstrated to have better inter-observer agreement, and detailed contouring shown to have less variability that simplified contouring (190). For the real-time, free breathing cines, care was taken to choose a heart beat that occurred during end expiration, by visually tracking the position of the diaphragm.

In both the breath hold and real time, rest and exercise cines, the papillary muscles and trabeculae were included as part of the blood pool to maintain consistency and reduce the chance of bias (191). The mitral and tricuspid valve planes were tracked manually using the breath hold LVOT, RVOT and right ventricular long axis (RVLA) images for the rest cine analysis, and were tracked using exercise LVOT and RVOT images for the exercise cines. Care needs to be taken in identifying the basal slice, as this is a potential source of error (192).

End diastolic and end-systolic volumes were calculated using measurements from each slice and were summed using the method of the disks. Stroke volume was calculated as EDV – ESV. Cardiac output was calculated as SV x HR and ejection fraction was calculated as (EDV – ESV) / ESV (193). Left and right ventricular mass was calculated from the total myocardial volume multiplied by the specific gravity of myocardium (1.05 g/mL). Values were indexed to body surface area e.g. LVEDV index = LVEDV / BSA. Right ventricular reserve was calculated as Exercise RVEF – Rest RVEF. Septal curvature was measured in the short axis plane at the level of the LV papillary muscles. Segmentation was carried out by drawing 3 point arcs on the epicardial surface of the LV septal and lateral walls. The curvature was calculated as the ratio of the septal and lateral wall curvatures.
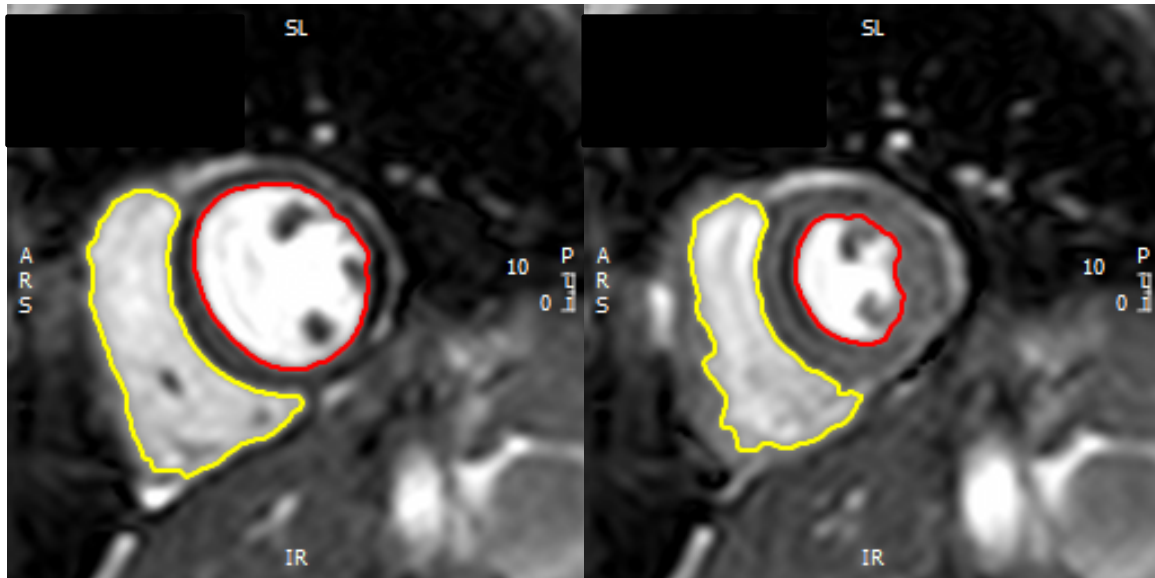
A
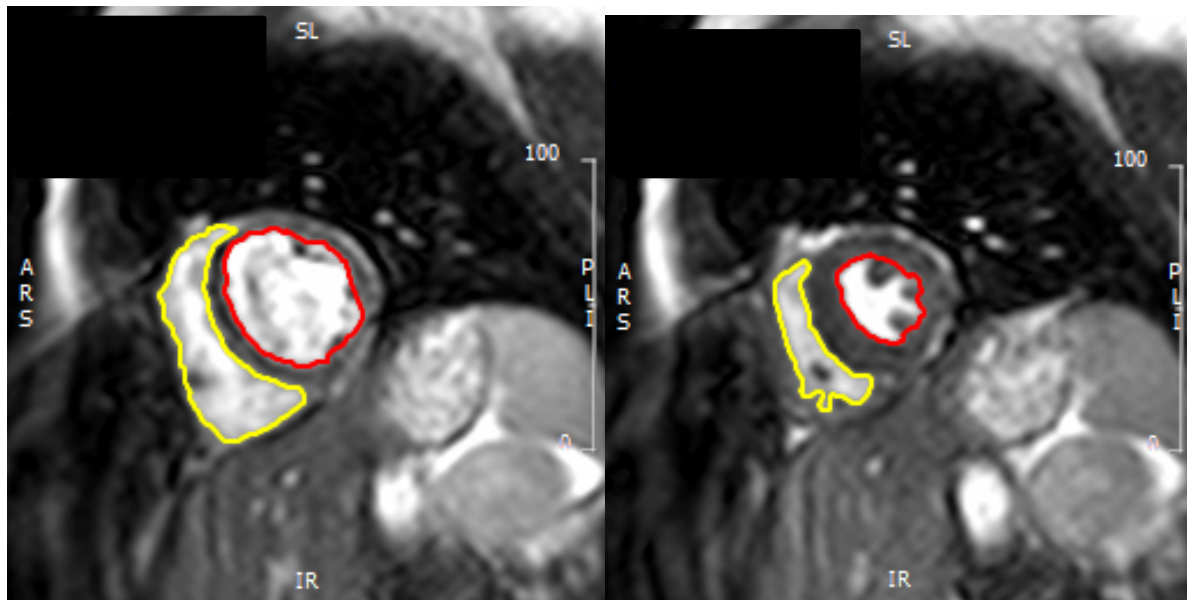
B

Figure 2.1: Segmentation of real time LVSA cines at rest and exercise A) Rest end diastole and end systole, B) Exercise end diastole and end systole. Papillary muscles and trabeulcations were included as part of the bloodpool and measurements were made during expiration

2.12 Aortic and MPA Flow Analysis

Assessment of the breath hold aortic and MPA flow images was performed by semi automated vessel edge detection with manual operator correction (ArtFun, Paris)

Assessment of the breath hold and real time, free breathing aortic and MPA flow images were performed by semi-automated vessel edge detection with manual operator correction (ArtFun, Paris). ROIs were created around the aorta and MPA using a semi automated method with manual correction (Figure 2.2.) This created time-volume and time-velocity curves from which SV and mean and average velocity could be calculated.
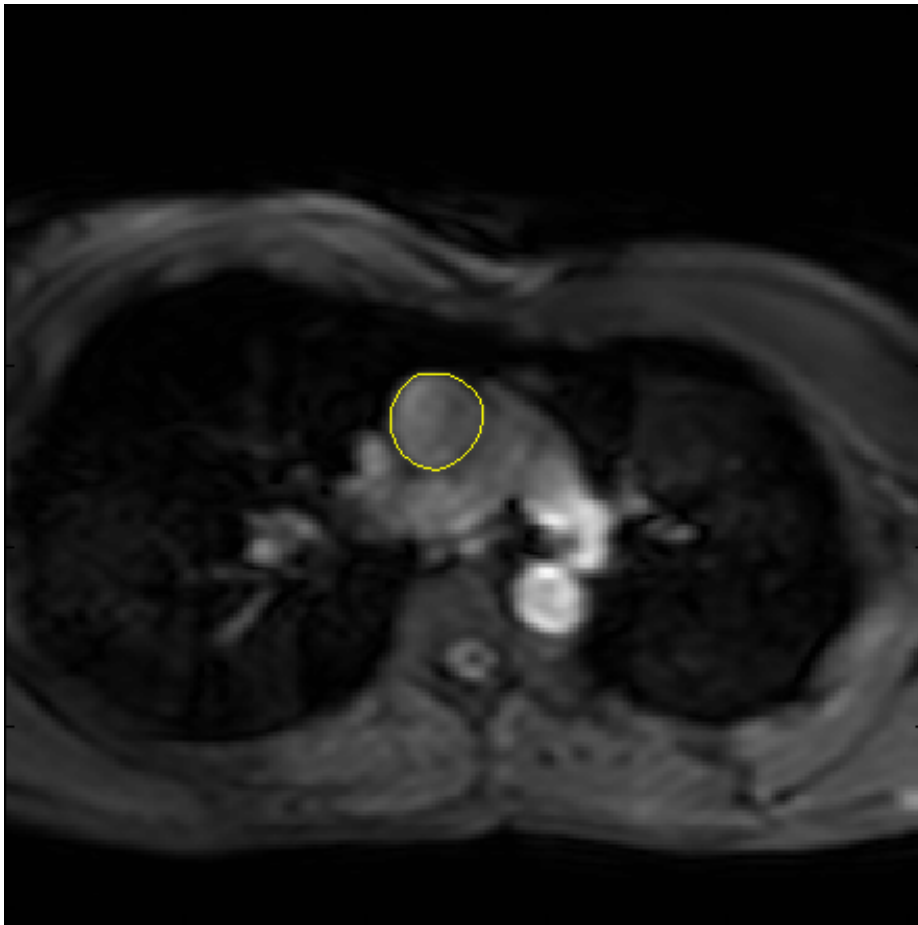
Figure 2.2. : Real time aortic flow with region of interest. This was created using ArtFun.

SV was calculated as the area under the curve of the time-volume curve, and calculated as the total forward flow minus any backward flow, for both the aorta and MPA (Figure 2.3). Peak

velocity was taken as the peak velocity occurring during systole (Figure 2.4), and mean velocity as the mean of the velocities through systole (Figure 2.5).   For the real time analysis, an average of the first 5 consecutive heartbeats was taken. Pulsatility was calculated as Maximum area – Minimum area/Minimum area x 100. Cardiac output was calculated as SV x HR and indexed to body surface area.

Flow data was checked for aliasing and phase offsets >0.6cm/second prior to analysis and unwrapped or adjusted prior to analysis using software developed in-house by our physicist, Pawel Tokarczuk.
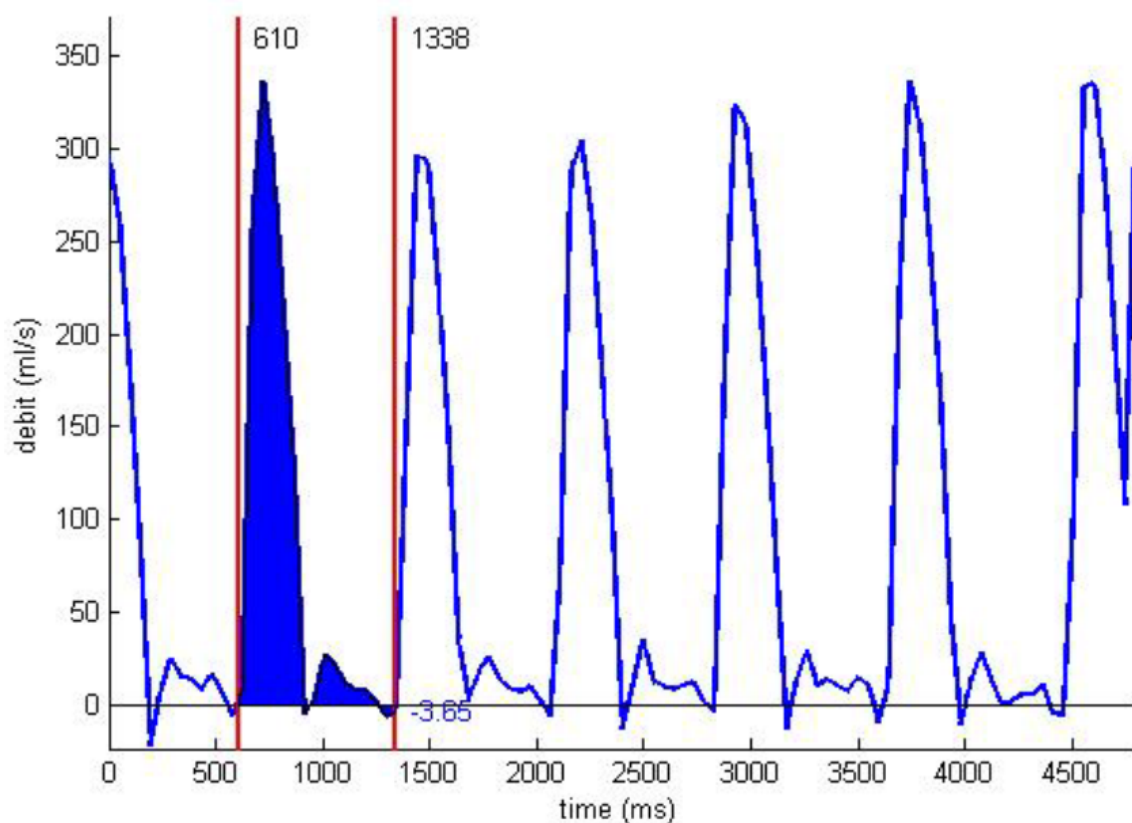
Figure 2.3: Time-flow curve: Stroke volume was calculated as the area under time-flow curve, and then averaged over 5 heartbeats
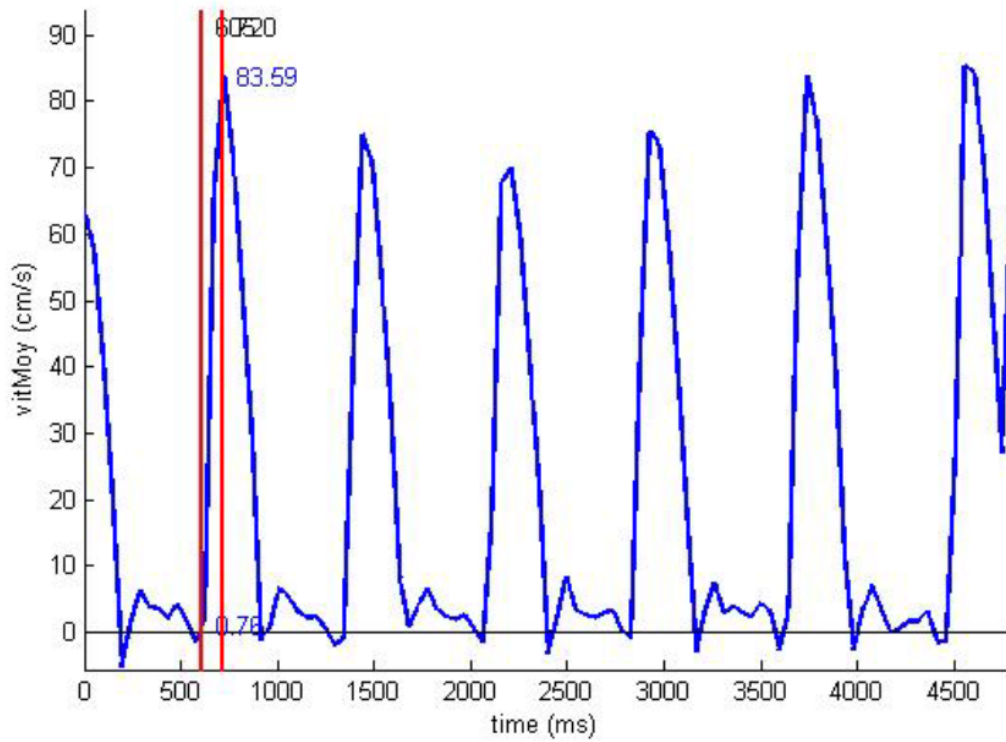
Figure 2.4: Time-velocity curve and peak velocity: Peak velocity was taken as the peak velocity per beat, and then averaged over 5 heartbeats.
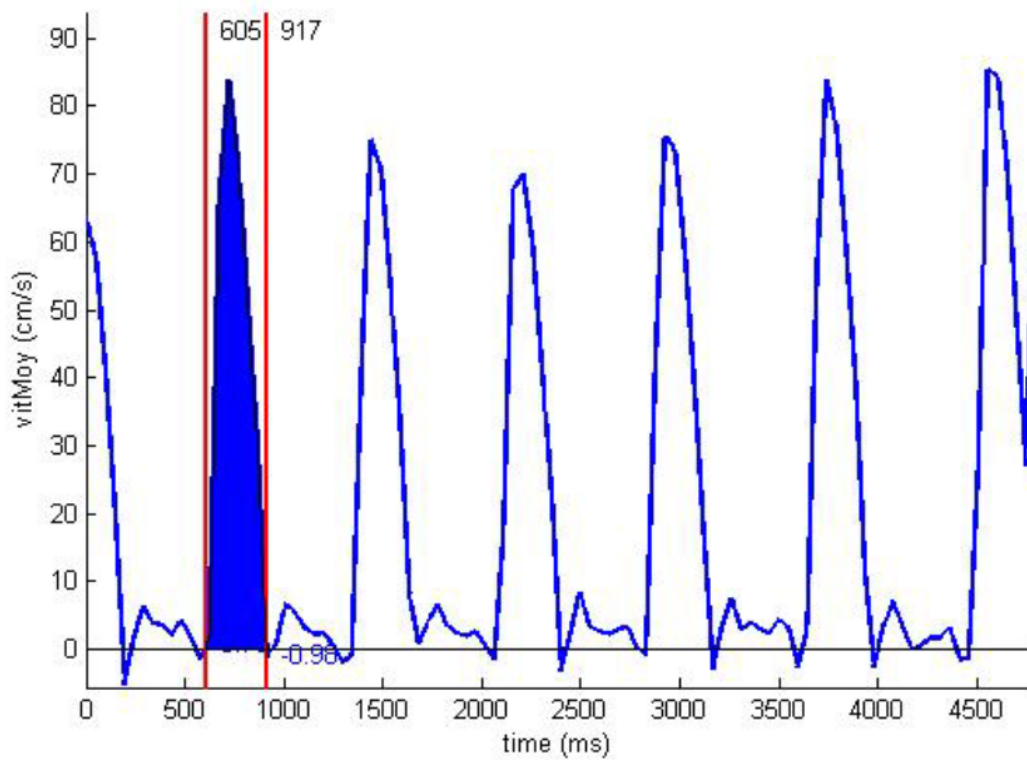
Figure 2.5: Time-velocity curve and mean velocity: Mean velocity was taken as the mean velocity throughout systole

2.13 Exercise protocol

Exercise was performed supine, inside the scanner, using an MRI compatible circular ergometer (Lode MRI Circular Ergometer, Netherlands). An exercise protocol was tailored for each subject according to his or her CPET result.

Subjects performed 3 minutes of warm up which included 1 minute of cycling while the load was gradually increased to the pre-determined power set at 40% of the watts achieved during CPET. Subjects then exercised at this load for 2 minutes, until steady state was achieved which was confirmed by stabilisation of heart rate. Images were acquired during continuous exercise.

Once the exercise images were acquired, subjects were instructed to stop cycling, at which time, the imaging protocol for immediately after exercise imaging commenced. Imaging commenced within 2 seconds of the subject ceasing exercise. MPA and then aortic flow were acquired first, taking 9 seconds, and then the LVSA stack commenced. Hence the LVSA cine commenced around 10 seconds after the subject ceased exercise and took 66 seconds to acquire.

Subjects were encouraged during the exercise protocol, and were able to listen to the music of their choice. The exercise was terminated at the end of the protocol, or if any concerns were raised by the staff or subject.

2.14 Acute Hypoxia Protocol

Hypoxia was induced by using 12% oxygen, with continuous oxygen saturation and heart rate monitoring. Each subject was fitted with an extra small, small, medium or large mask, as

appropriate, to ensure the correct fit and reduce the chance of gas leakage. The inspirate was supplied from a medical gas mixture containing 12% oxygen in nitrogen administered from a commercially prepared cylinder (British Oxygen Company) and was kept in the outside MRI room. A 1000L Douglas bag was filled from the cylinder that could be taken inside the MRI room. A 35mm breathing tube connected to a 3 way T shaped stopcock, ran from the Douglas bag, and connected to a mask adaptor 7400/7450 which in turn was connected to a T shaped, non-rebreather valve on the 7450 V2 Blue Silicone Rubber Mask, which is airtight, fitted on the subject's face. All the equipment was supplied from Cranlea Human Performance Ltd, Birmingham and manufactured by Carefusion Corporation, USA. Subjects were instructed to breath the 12% oxygen at rest, for 10 minutes, until saturations dropped and had plateaued. Images were then acquired at rest, with alteration to breath hold duration according to the subject's perception of breathlessness. Exercise and immediately post exercise imaging was then performed as per protocol. The total duration of hypoxia was around 35 minutes.

Chapter 3 – Exercise CMR Methodology Development

3.1 Introduction

Exercise CMR is a new, innovative method that is being developed by several research groups to assess dynamic biventricular function. However, there are several important methodological considerations that may significantly alter the quality and accuracy of the results, and research groups have varied in their approaches thus far. These include the exercise protocol and the timing of imaging, respiratory variation, how aliasing and phase offset errors are accounted for, and the correct balance between spatial and temporal resolution. We aimed to develop a methodological approach that was feasible for both healthy volunteers and patients, gathered data during steady state exercise, contained accurate and analyzable data, and could demonstrate accuracy and inter-test, intra-observer, inter-observer and inter-study reproducibility.

3.2 Exercise protocol

Exercise protocols have varied widely amongst groups using exercise CMR as well as exercise haemodynamic studies. Incremental increases in watts to exhaustion (177-179), exercise fixed at 2 levels of 0.5 and 1 watt per kilogram (194), fixed heart rate aims (181, 185, 195), the Bruce protocol (196, 197), fixed levels of exercise (182) and static exercises including handgrip (27), bicep curls (28) and one legged raises (30) have been used. Other groups have performed CPET in subjects prior to the exercise CMR and then tailored an exercise protocol according to these parameters. These protocols have also been mixed. Medium intensity exercise defined as 40% of maximal watts (42, 198), a graded protocol of low, medium and high intensity

exercise defined as 25%, 50% and 66% watts(193) and a fixed level of exercise at 60% maximal VO$_2$ uptake have been used (38, 39, 199).

Most groups have utilized supine, cycle ergometers (38, 39, 42, 193, 198, 199). This form of exercise has been able to achieve a higher levels of watts, reaching 218 +/- 52W in an athlete, contrasting with a straight leg, kicking motion which was able to achieve a maximum of only 22.5W in a healthy volunteer (178), limited by small muscle exhaustion. However, the group who used this form of exercise felt that this helps reduce motion artifact. Upright exercise has been used within the scanner, however, this is not widely available (195). Exercise on an external bike or treadmill has also been utilised, with scanning occurring during recovery (196, 197). Scanning during continuous exercise (37, 40, 102), intermittent breaks during exercise (18) and immediately after exercise (182, 183) has also been carried out, with and without breath holds.

When developing the exercise protocol, there were several considerations: 1) Data is collected during continuous steady state exercise when heart rate and stroke volume are stable and hence reproducible 2) Patients who are likely to have symptoms such as shortness of breath, are able to complete the exercise protocol and all the relevant data collected 3) The exercise level is set high enough to achieve clinically significant physiological changes 4) Image quality is preserved.

We aimed to determine:

1. The optimal timing at which to collect exercise data

2. Examine the rate of change in physiology immediately post exercise on CPET in order to justify imaging during continuous exercise

3. The optimal positioning for the subject within the scanner, to ensure that exercise and imaging could be carried out simultaneously

3.2.1 Methods

In order to ensure that the exercise level would be aerobic as opposed to static and achieve high enough levels of wattage in order to demonstrate clinically relevant physiological changes, a MRI compatible supine cycle ergometer (Lode, Netherlands) was purchased. (Figure 3.1) Modifications to the tabletop were made, to ensure that the cycle ergometer was able to sit low as low as possible on the tabletop.

Figure 3.1: Set up of cycle ergometer with a subject inside the scanner.

Two healthy volunteers underwent upright CPET with a ramp protocol, and then supine CPET at a fixed level of exercise, set at 40% of the watts achieved on the upright CPET.

These healthy volunteers were then positioned inside the scanner. Height was measured, and once the subject was in the optimal position for cycling and scanning, the distance from the sole of the foot extended, to the centre of the posterior coil was measured.

They were exercise at multiple levels of exercise, including 20%, 40% and 66% of the watts achieved on CPET.

3.2.2 Observations

During the progressive ramp protocol, VO_2, VCO_2 and HR steadily increased throughout exercise. Oxygen pulse, which is used as a surrogate for SV, increased steadily and plateaued after approximately 7 minutes of exercise (Figure 3.2a and b). However, as HR continued to rise, CO would also continue to rise as, given it is a product of SV and HR. Also of note, CPET clearly demonstrated that immediately after cessation of exercise, VO_2, VCO_2, HR, SV and hence CO (Figure 3.2a and b), immediately begins to decrease hence as the CMR protocol takes 66 seconds to acquire, post exercise imaging would not accurately image the cardiac responses that had occurred during exercise.

During supine CPET at 40% of the watts achieved, wattage was increased to the target load over the first minute of exercise. As demonstrated in Figures 3.3 a and b, VO_2 and VCO_2 plateaued after 3 minutes of warm up, and similarly, so did HR. SV plateaued slightly earlier. This showed that in order to acquire images at steady state exercise, a warm up of 3 minutes – 1 minute to increase the load to target and 2 minutes at that load, is required to ensure steady SV, HR and CO calculations. Also of note, the VO_2 at 40% of the watts achieved on upright exercise did not correspond to the same VO_2 on supine exercise. While peak cardiac output

may be marginally higher during upright exercise, cardiac output, blood volume distribution and efficacy of the muscle pump and oxygen supply differ during upright and supine cycle exercise due to differeing kinetics. Cardiac output is higher during supine exercise at mild to moderate exercise intensities. Hence using the watts at a certain VO_2 on upright exercise as your target for supine exercise cannot be used interchangeably (200).
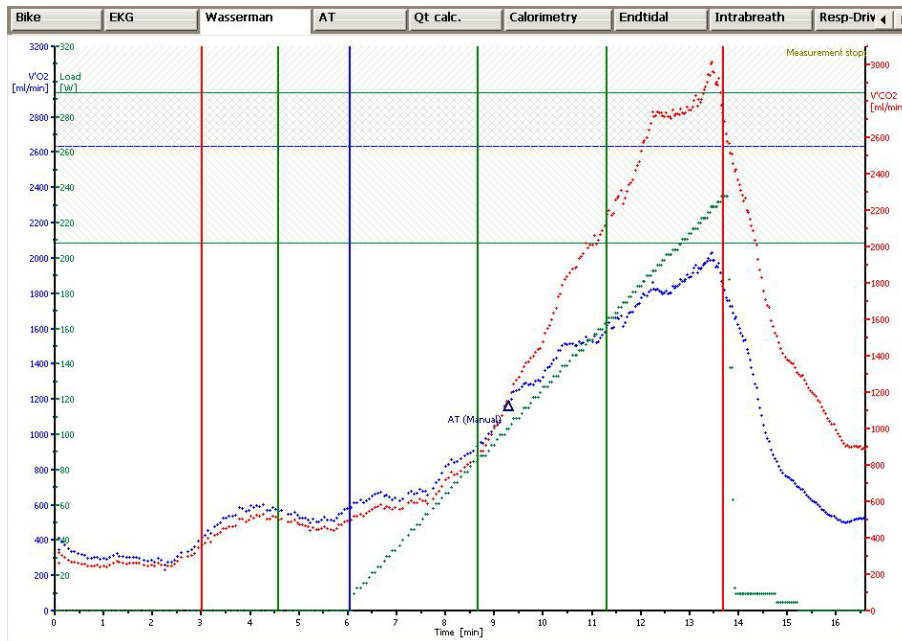
a

VCO2 **VO2**
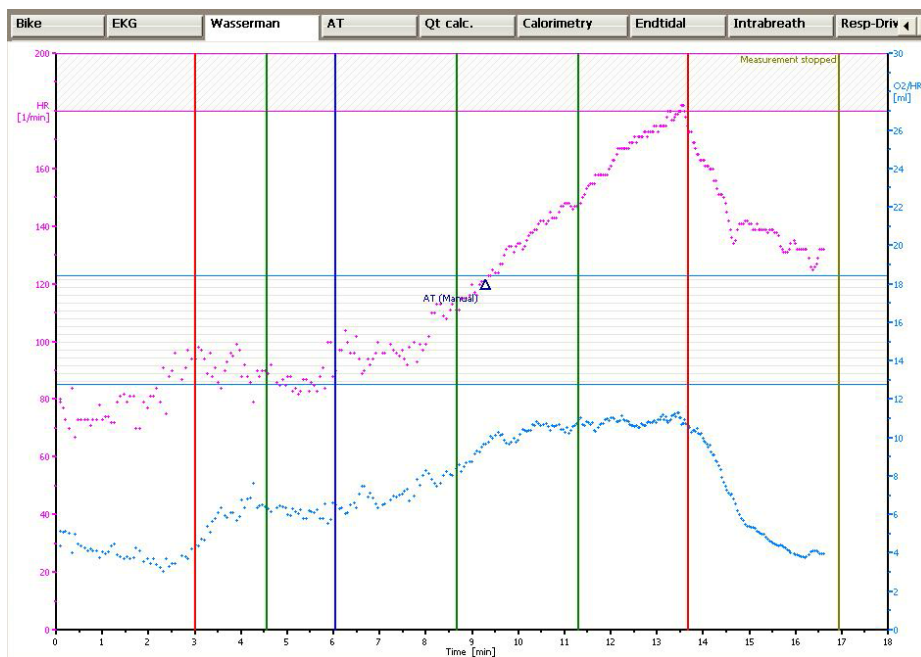
b

HR **Oxygen pulse**

Figure 3.2 CPET results from a healthy volunteers on a ramp protocol. The vertical red lines indicate the beginning and end of exercise: a) VO2 in blue and VCO2 in red increase consistently throughout exercise with the ramp protocol, with immediate fall after cessation of exercise. b) Heart rate in pink and oxygen pulse in blue also steadily increase, and immediately fall after exercise. Oxygen pulse reaches a plateau after around 7 minutes
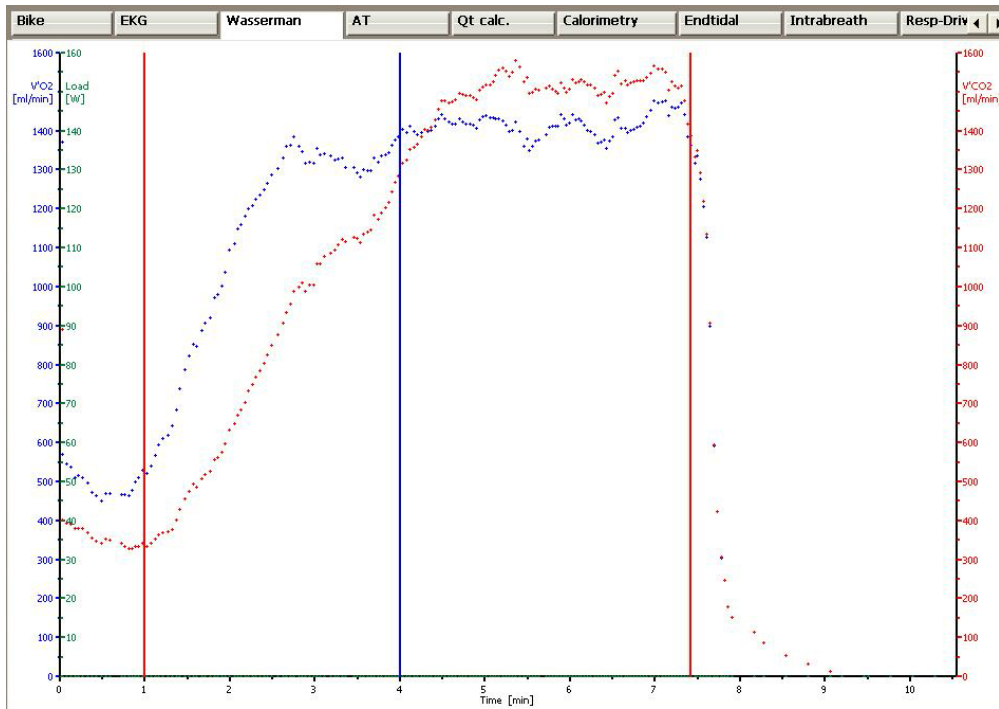
a
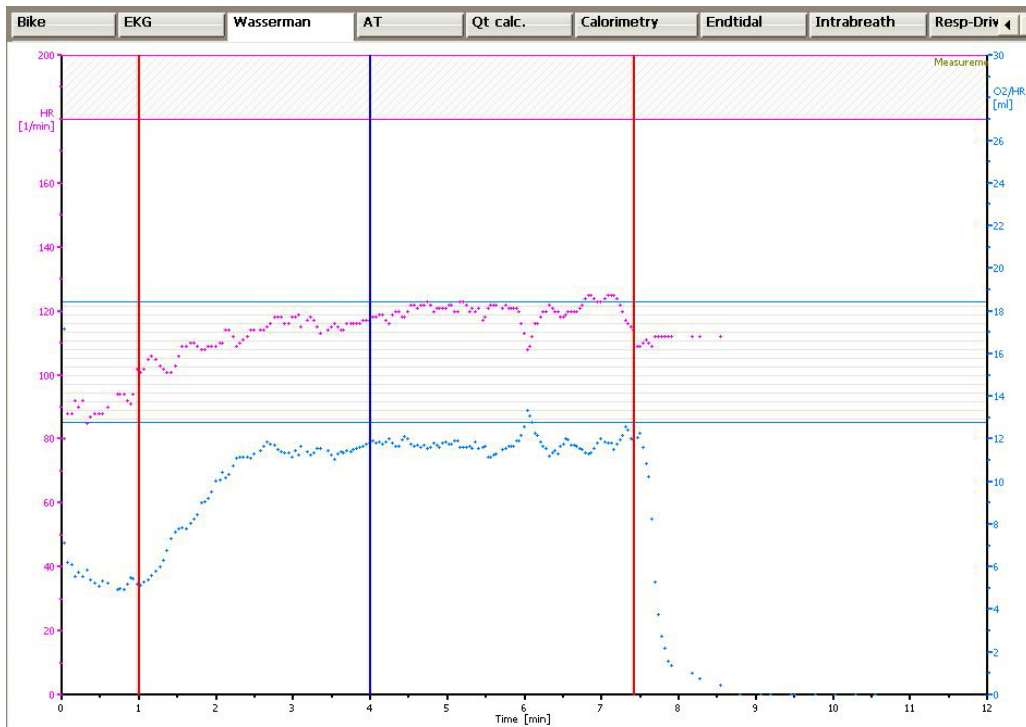
b

Figure 3.3: CPET at 40% of the watts on upright exercise a) VO_2 in blue and VCO_2 in red, b) Heart rate in pink and oxygen pulse in blue; all parameters plateau at 3 minutes of warm up.

3.2.3 Outcomes

It was noted that the ideal point to place the centre of the posterior coil was at 0.7 x subject's height (cm), with the subject lying on the MRI couch with their feet fully extended in to the pedals. This simple calculation avoided taking the subject on and off the couch to make adjustments and streamlined the set up. All subjects were able to be positioned such that they were able to perform continuous exercise during image acquisition, however, due to space restriction, some subjects had to be scanned off isocentre to enable this. This did not cause any significant issues with data acquisition or analysis

We demonstrated that it takes 3 minutes to achieve steady state and approximately 2-3 minutes to acquire images. Hence we decided that imaging at two levels of exercise would not be feasible for patients, as that would entail at least 12 minutes of exercise, and due to subject exhaustion, may end up with immediately post exercise imaging as opposed to imaging during continuous exercise. In addition, as 66% of the watts achieved on upright exercise corresponds with high intensity supine exercise (37), 40% of the watts achieved, to correspond with moderate intensity exercise was set as our pre-determined load. Furthermore, it was noted when we exercised healthy volunteers at 3 levels of supine exercise during protocol development, image quality deteriorated significantly at high intensity exercise due to sideways movements of the subject.

Hence we decided that exercising at one fixed level of moderate intensity exercise, set at the level of watts achieved on upright CPET, would achieve satisfactory physiological changes, but ensure that all subjects, particularly patients, could sustain exercise and complete the protocol. In particular, data collection would occur during steady state exercise, which was of utmost importance. The comparison between continuous steady state exercise and immediately post exercise imaging in both health and disease will be discussed in detail, in Chapters 5, 6 and 7.

3.3 Respiratory Variation

Inspiratory fluctuations of LV and RV SV have been well documented over many years, with an increase in RV SV and a decrease in LV SV on inspiration (201-205). Claessen et al documented with real time CMR LVSA cines a fluctuation of 21 mL ± 10% between inspiratory and expiratory RVSV, but no difference for LVSV fluctuations (4mL ± 10%) at rest, with a significant decline in both RVSV and LVSV during the Valsalva manoeuver, 36 mL ±14% and -22 mL ± 17% respectively. On exercise, variations in RVSV were maintained, but variations in LVSV became significant, with larger LVSV during expiration, in exercise. Van de Hout et al demonstrated with real time Ao flow acquisitions with CMR that aortic stroke volume ranged around 13.1 ± 2.7mL for normal breathing and 35.3 ± 8.3 with deep breathing, with large drops in SV with the Valsalva Manoeuvre (206).

Some groups have attempted to mitigate this during exercise CMR, by attempting to acquire images during breath holds, either immediately post exercise or during intermittent breaks during exercise, while others have not taken respiratory variation in to account as previously discussed.

We aimed to:

1. Demonstrate that LV and RVSV fluctuates during rest and exercise with respiration

2. Determine the ideal point at which to analyse LV and RV volumes on the real-time cine stacks, as to correlate with conventional analysis at rest

A subject's left and right ventricular volumes were analysed for a slice using the methods outlined in Chapter 2. The results were plotted on a graph for rest and exercise and compared to the volume from the equivalent slice obtained from conventional breath hold cine stacks.

3.3.1 Observations

Fluctuation of RV (Figure 3.4a) and LV (Figure 3.4b) volume at rest, and on exercise (Figure 3.4c) was demonstrated. In this subject, respiratory variation appeared to be more prominent for the RV than for the LV at rest, but then it became apparent for the LV on exercise. Also of note in this subject, the volume for the RV correlated with the volume calculated from the breath hold slice during the expiratory phase. It was approximately 2mL lower for the breath hold acquisitions than the real time, for the end-diastolic volume for the LV.

Respiratory Variation of RV Volume

Respiratory Variation of LV Volume

LV and RV Volumes on Exercise
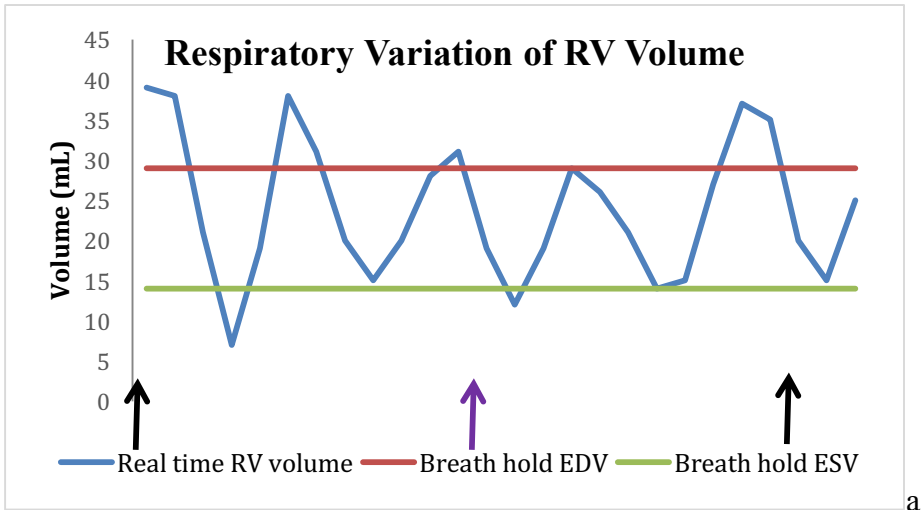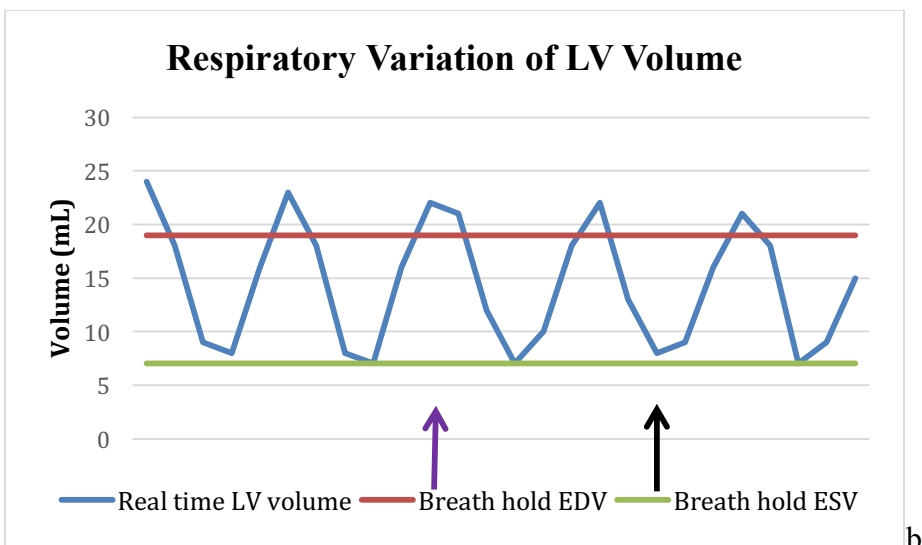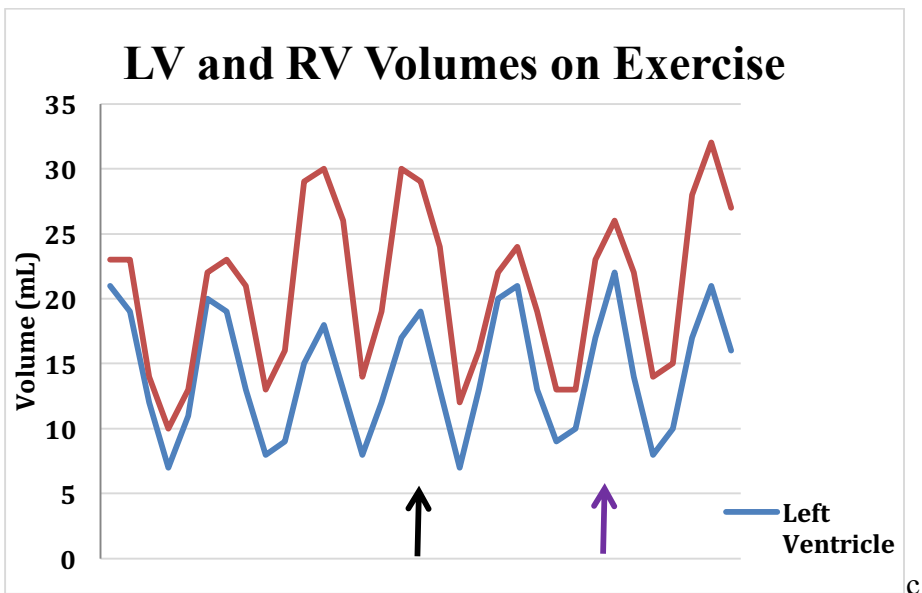
Figure 3.4 Fluctuations in RV and LV volume with respiration: a) Fluctuation in RV volume during inspiration and expiration b) No fluctuation in LV volume during inspiration and

expiration c) Fluctuation in LV and RV volume during exercise. For the LV, it became apparent: EDV, End diastolic volume; ESV, End systolic volume, The black arrow represents inspiration and the purple arrow represents expiration

3.3.2 Outcomes

This demonstrated that respiratory fluctuations in SV need to be accounted for particularly for the RV, to ensure accuracy and reproducibility, but furthermore, if we wanted to show that conventional breath hold imaging correlated with real time free breathing imaging, volumetric analysis should be carried out during the expiratory phase.

The respiratory bellows was applied to subjects during scanning, at rest and during exercise. Unfortunately, the trace was occasionally lost due to unknown reasons and not necessarily due to interference from exercise. This was raised with Philips, the MRI manufacturer, but a resolution could not be found. However, respiratory traces for all subjects were collected and filed where possible.

Ideally, the ability to input this data in to the software to assist in analyses would have been desirable. Unfortunately, the software did not allow for this, and the technology to develop our own software was not available, as it had been to the Leuven group. Funding for software development or collaboration with software developers will be a consideration for our next grant application.

When analysing the cines, the phase of respiration was evident from tracking the diaphragm. For each slice, end diastole and systole were identified at the point or near the point of end

expiration. As there were multiple heartbeats and respiratory cycles for each slice, the best heart beat that, for example, that had less movement artifact, could be chosen and analysed.

As respiratory bellows data could not be used for flow analysis, aortic and MPA flow was calculated as the mean of the first 5 consecutive heartbeats. This decision was made for two main reasons 1) It has been previously demonstrated that mean aortic flow correlates with breath hold Ao flow (207) when averaged over multiple heart beats, and does not correlate if just one free breathing heart beat is compared to one heart beat acquired during a breath hold (208). 2) 5 heartbeats would cover one phase of respiration at rest and during exercise.

In terms of cardiac displacement along the long axis, Hori et al also demonstrated that during free breathing, mean displacement of the heart on the long axis was 2.2mm to 3.7mm (209), which did not cause significant variations in volumetric analysis in CMR, as slices are set at 10mm. We noticed that during exercise, this displacement increased, particularly at high intensity exercise. This was rectified by installing handlebars that the subjects could hold on to during exercise. Subjects were instructed to hold them during exercise, and to keep their upper body still, which was simple but very effective. Furthermore, we used moderate level intensity exercise so that upper body effort was not required to maintain effort.

3.4 Aliasing

Aliasing results when the velocity encoded value (VENC) is set below the peak velocity in the vessel of interest. If the velocity phase shift exceeds ±180°, it cannot be distinguished from one within the ±180° range, and velocity information is 'wrapped' within a voxel, known as velocity aliasing (wraparound). In other words, a physical phase of 190° is interpreted in the

image as -170˚. Aliasing causes errors in flow measurements, however, it is easy to detect this during imaging as inaccuracies in the VENC amount and direction, leads to distorted field gradients and inverted signal intensity of the peak velocities, as compared with that of surrounding voxels (Figure 3.5). VENC, is available as an adjustable sequence parameters. Once the images are acquired, VENC cannot be changed, hence during imaging if aliasing occurs and is excessive, imaging should be repeated with a larger VENC (172, 173, 210).

During exercise, it was noted that the velocity in the aorta and MPA increased and necessary adjustments of the VENC were made, pre-imaging. For the aorta, the VENC was set to 220cm/s, and for the MPA, it was set to 200cm/s.

However, these increases in VENC were inadequate in certain subjects, in particular, in individuals with large CO such as tall men or very physically fit individuals, or patients with significantly turbulent flow in the MPA. While it was noticed during imaging, in the setting of exercise and a limited period of time to acquire the images, repeat imaging was occasionally not carried out, particularly in the early, development stages of the protocol.
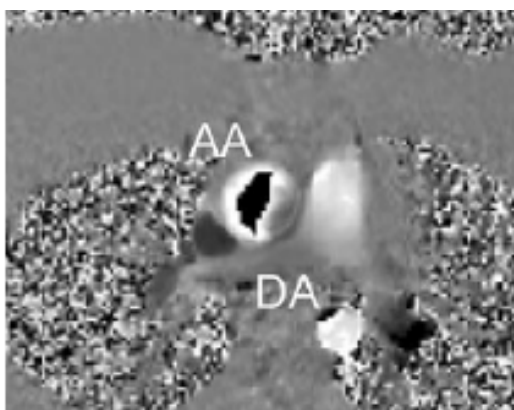
Figure 3.5:   Aliased phase contrast image of the aorta, AA = Ascending aorta, DA = Descending aorta: Black represents wraparound flow, while white represents no wraparound. This diagram shows significant wraparound in the ascending aorta due to high velocity flow

from LV ejection. (From: Gatehouse et al, Applications of phase-contrast flow and velocity imaging in cardiovascular MRI, Eur Radiol, 2005)

In house software was developed by our physicist, Pawel Tokarczuk, to spatially and temporally phase unwrap these datasets. The correction in aliasing was carried out in two stages. Firstly, the phase in each region of interest (ROI), at each epoch, was spatially unwrapped. This was usually enough to lead to a correct result, but occasionally, the choice of the initial seed point within an ROI, introduced an overall shift in the unwrapped phase of $2M\pi$, where M is some random integer. Since each epoch is unwrapped separately, the effect was to introduce uncontrolled jumps in the mean phase between one epoch and the next, leading to an incorrect flow curve even though the spatially unwrapped flow profile within each ROI is smooth. However, it was possible to correct for this by looking at the mean phase in each ROI across the epochs and assuming that this does not step by more than π from one epoch to the next. Once this mean regional phase has been temporally unwrapped, the difference between the two means can be used to correct the phase in each region. An example of this is demonstrated in Figure 3.6.
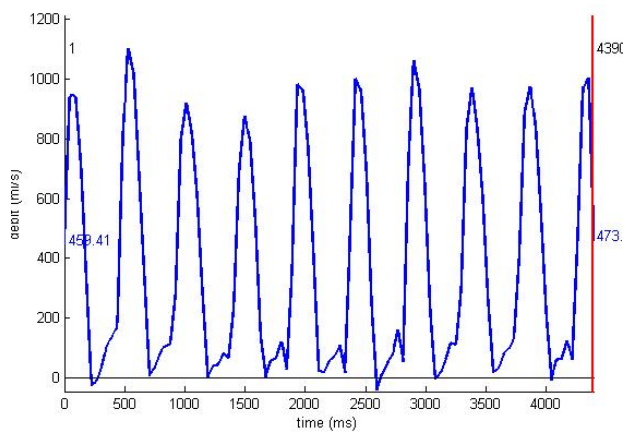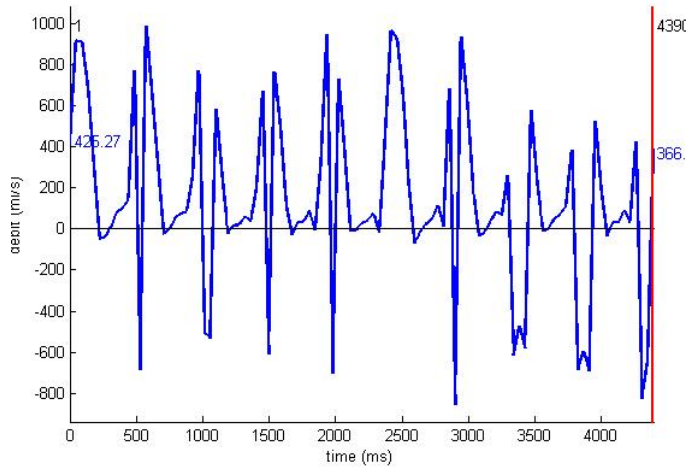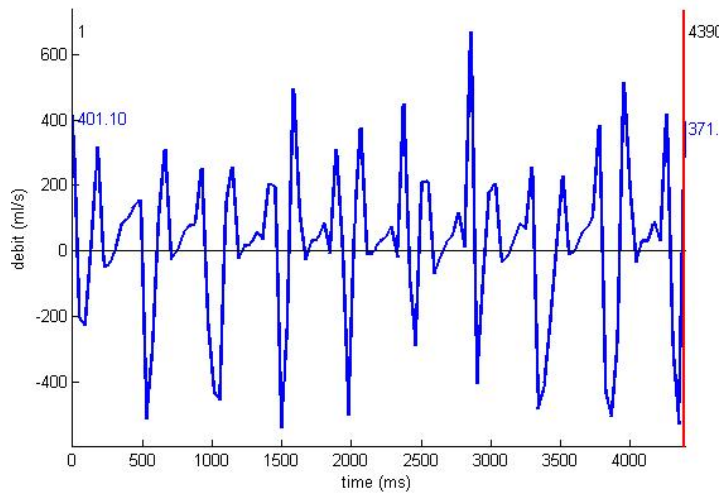
Figure 3.6 Volume-time curves demonstrating aliasing and unwrapping spatially and temporally a) aliased dataset (b) not interpretable after spatial unwrapping (b), but was c) successfully unwrapped after temporal unwrapping

Untenberger et al also developed software to unwrap aliased, real time flow data, both spatially and temporally. They tested the software using phantom, aliased human flow data which was unwrapped and un-aliased flow data and demonstrated that unwrapped flow data allowed for accurate analysis of real-time, aliased flow data, acquired with a reduced velocity encoding (211). Our software similarly, allowed us to analyse aliased flow data, when the VENC settings were not adequately set.

3.5 Phase shift

Cine phase contrast velocity images may contain an artificial, positive or negative, spatially varying velocity offset, which may significantly distort flow volumes. Phase offset error occurs when stationery tissues erroneously show a small velocity. After the subtraction of one gradient velocity from the other to form the phase difference image, residual errors may remain including gradient eddy currents, concomitant field terms and gradient field distortions (212). Whether phase offset causes a significant clinical issue varies in the literature, with some authors concluding that without hardware or software to reduce phase offset errors, significant flow errors occur (213, 214), but other authors concluding that background phase correction makes no difference to flow analysis (215). A phase offset of 0.6cm/second has been published as the limit of acceptability (213). Furthermore, the occurrence of phase offset errors have been reported as similar for both breath hold and non breath hold ascending aorta acquisitions (208) .

Velocity offsets can be reduced by decreasing the distance between the flow of interest and the magnetic isocentre and most current CMR systems have automatic couch positioning for flow imaging, which brings the vessel of interest for flow measurement in to the isocentre plane. However, the degree of phase offset can also vary unpredictably with slice orientation and slice shift so does not occur predictably (212). Several post-processing techniques have been developed to correct phase offset errors. One method is to acquire a stationary phantom phase contrast image after the clinical scan, with the identical imaging parameters. Then the phantom phase offsets are subtracted from the patient phase contrast images to produce background phase correct images. This however, is time consuming and hence clinically limited. Alternatively, some post processing software may allow for the user to place a ROI in stationary tissue near the vessel being measured, and the correction ROI value is subtracted from the vessel velocity. However, with free breathing, exercise imaging, it is difficult to find any stationary tissue.

So far in the exercise CMR literature, Steeden et al reported using Maxwell correction to remove the effects of concomitant gradients originating from the low encoding gradients. This was done automatically by fitting a quadratic surface through the stationary tissue (177). They however, could not see the images during scanning, in order to assess accurate placement, as the images took 5 minutes to reconstruct. Roberts et al stated they accounted for phase shift using static tissue (18), however, we found that there was not any stationary tissue due to free breathing and movement of respiratory and muscle tissue. In order to scan quickly, we did not correct for background phase effects during imaging as with the short echo time and the adequate shimming (a shim is a device in the magnet used to reduce inhomogeneties), the background effects were considered to be small. During analysis, if the phase offset was considered to be >0.6cm/second, the unwrapping software that was developed in house, had

the function of adjusting the x axis (Figure 3.7). However, as small adjustments can cause large changes in flow calculations, these adjustments were kept to a minimum and only 3% of all flow acquisitions including aorta, MPA, rest and exercise in healthy volunteers and patients were adjusted.
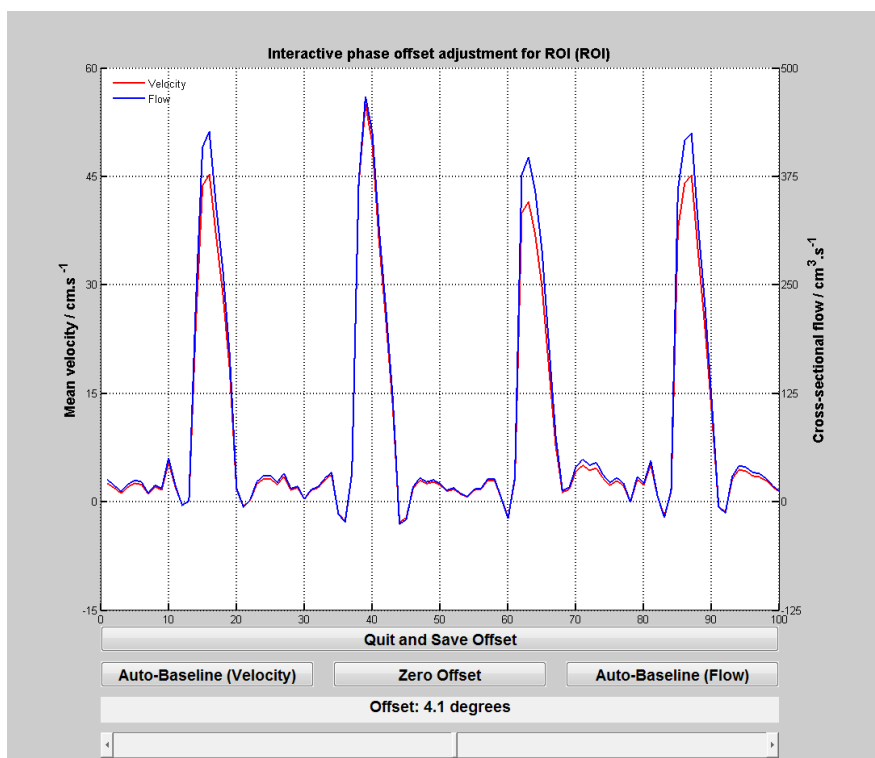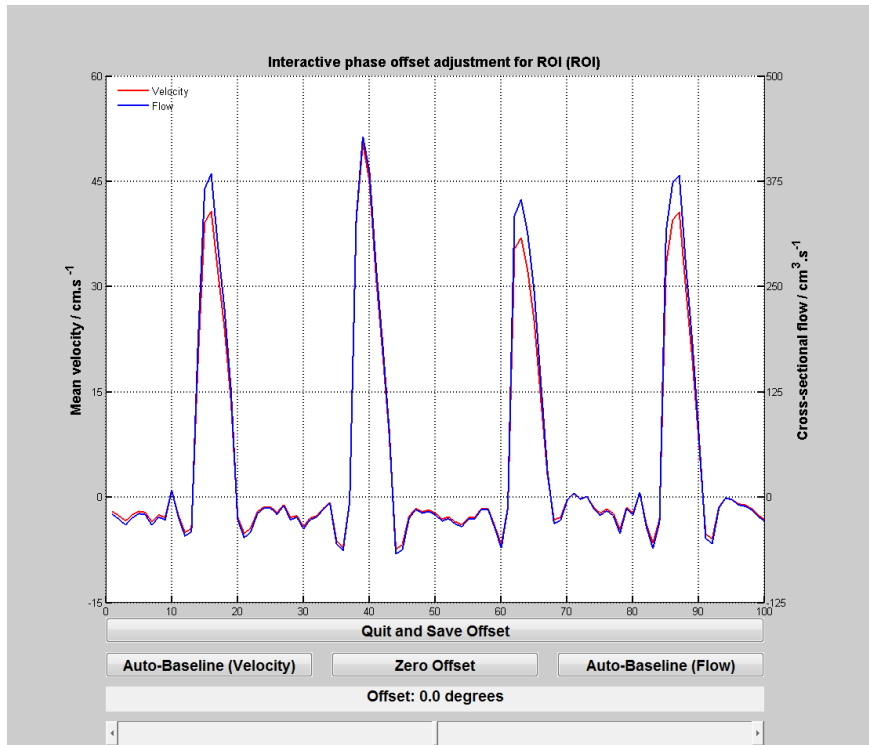
Figure 3.7 Phase offset and correction a) Flow-time curve demonstrating a significant phase offset, with the zero point well below the zero point of the x-axis b) Adjusted baseline, demonstrating a correction of 4.1 cm/s.

3.6 Imaging Protocol Development and Assessment of Accuracy and Reproducibility

3.6.1 Introduction

It has been demonstrated that real time CMR cine and phase contrast imaging of the aorta and MPA is feasible and accurate at rest, and potentially already clinically applicable in the setting of arrhythmias and shortness of breath (207, 216-219). A wide variety of acceleration techniques have been used, including Cartesian and non-Cartesian, and gated and non-gated methods. Furthermore, respiratory variation has been managed by employing short breath holds, shallow breathing, free breathing with respiratory navigation, or with no compensation for respiratory variations in volume.

Systole is known to be shorter than diastole, isovolumic relaxation (or end-systole) time is actually longer, ranging between 85-106ms, with isovolumic contraction (or end diastole) around 36ms. (220-222). While it is recommended that in order to reliably capture end diastole and end systole in conventional LVSA imaging, the temporal resolution of retrospectively gated cine images should be 50ms (171), temporal resolutions of 180ms (218), 164ms (209) and 87ms (219) have been shown to be accurate and reproducible for the LV and RV when compared to a conventional breath hold, retrospectively gated sequence at rest.

It is important to keep in mind the definition of temporal resolution, and how a low temporal resolution is maintained in conventional imaging versus real time imaging. In conventional

imaging, images are constructed over several heartbeats, resulting in an image, which appears to be one heartbeat, but is actually a reconstruction of the average of several heartbeats. So while the increment of time by which a change in the imaged dynamic process can be seen may be in the range of 40-50ms, the actual period of time for data acquisition is actually longer. However, real time imaging, like echocardiography, is capturing true dynamic data, and true temporal resolution is defined as the actual period of time that data is acquired.

In more recent exercise CMR reports, the group from Amsterdam reported a temporal resolution of 100ms for their real time, LVSA in their initial report (223). In subsequent reports, temporal resolution improved to 56ms for LVSA and 43.6ms for flow acquisitions with a spatial resolution of 2.2 x 1.5mm. The sequence was not 'true' real time, in that they were gated, and there were breaks in exercise between cine acquisitions and flow acquisitions, but the images were taken during exercise (40, 42, 162). Parallel SENSE imaging was used. Inter-test and inter-study reproducibility has not been reported, nor how respiratory variation and how valvular plane discrimination was assessed.

The group from Leuven has published several reports using exercise CMR(37, 102, 161, 184, 224). Reported temporal resolution is 35-38ms and the reconstructed but not acquired spatial resolution has been reported as 2.3 x 2.3 x 8mm. They used true real time, un-gated acquisitions using parallel sensitivity encoding (SENSE) imaging, with an acceleration factor of 2. While they demonstrate excellent correlation between Fick derived CO and CMR derived CO, again inter-test and inter-study reproducibility has not been reported, and flow and cine images have not been acquired in each subject. They describe in detail how respiratory variation was carefully taken in to account, and they developed their own software that integrated ECG and respiratory bellow information. Furthermore, they acquired LVSA and

horizontal long axis (HLA) stacks, and the software was able to assist with mitral and tricuspid plane delineation, using both stacks. This was demonstrated to me personally and it was an elegant approach to ensuring accurate basal analysis.

Great Ormond Street Hospital (GOSH) in London has also published several reports (28, 177-179). They use a radial k-t SENSE, a non-Cartesian, sequence which is gated and only captures 2 heart beats per slice, with a temporal resolution of 35.5ms and a voxel size of 3.0 x 3.0 and 10. They also compare this to a standard real time, parallel GRAPPA sequence that has a temporal resolution of 80ms and a spatial resolution of 3.1 x 3.9 x 10. They concluded that their non-Cartesian acquisition is more accurate and reproducible with accuracy defined as LVSV = RVSV, and reproducibility defined as CO, and that this is due to the improved temporal resolution of the non-Cartesian approach. However, the spatial resolution is poor and they only acquire 2 heartbeats per slice, rather than 8-10 heart beats. Furthermore, they have not acquired LVSA and flow sequences simultaneously so there is no inter-test reproducibility reported, and they do not report volumes or ejection fraction reproducibility for their non-Cartesian sequence. They also do not take respiratory variation in to account.

3.6.2 Aims

We aimed to

1. Develop a LVSA cine sequence and imaging protocol that balance spatial and temporal resolution, so that valvular plane delineation was accurate

2. Demonstrate inter-test reproducibility

3. Demonstrate intra and inter-observer and inter-study reproducibility

4. Demonstrate inter-study reproducibility

3.6.3 Methods

3.6.3.1 Sequence Development

Three subjects carried out several sessions of real time LVSA optimisations within the scanner at rest and exercise. Several sequences were trialed, and the approach included 1) Starting with the protocol used by Leuven (37), with attempts to optimize contrast by altering the flip angle 2) Testing k-t blast sequences 3) Acquiring triggered conventional LVSA, while free breathing during exercise. 4) Testing real time sequences with improved spatial resolution. All sequences were Cartesian.

Real time LVSA 1: Flip angle 50, SENSE with an acceleration factor of 2

Field-of-view = 320 x 334mm; Repetition time/echo time = 1.86/0.93msec; Flip angle 50°; Acquired voxel size 3.64 x 4.78 x 8mm; Reconstructed voxel size: 2.58 x 2.61 x 8mm; Section thickness = 8mm with no gap; Number of sections = 18; Dynamic scan time = 59 seconds with 50 dynamics per slice and 12 slices, Temporal resolution 44.6ms;

Real time LVSA 2- Flip angle 60, SENSE with an acceleration factor of 2

Field-of-view = 320 x 334mm; Repetition time/echo time = 1.86/0.93msec; Flip angle 60°; Acquired voxel size 3.64 x 4.78 x 8mm; Reconstructed voxel size: 2.58 x 2.61 x 8mm; Section thickness = 8mm with no gap; Dynamic scan time = 90 seconds with 50 dynamics per slice and 12 slices; Temporal resolution 44.6ms;

Real time LVSA 3 – Flip angle 80, SENSE with an acceleration factor of 2

Field-of-view = 320 x 334mm; Repetition time/echo time = 1.86/0.93msec; Flip angle 80˚; Acquired voxel size 3.65 x 4.87 x 8mm; Reconstructed voxel size: 2.61 x 2.61 x 8mm; Section thickness = 8mm with no gap; Dynamic scan time = 2 minutes with 50 dynamics per slice and 12 slices; Temporal resolution 45.5ms;

Real time LVSA 4 – k-t blast

Field-of-view = 320 x 308mm; Repetition time/echo time = 2.6/1.29msec; Flip angle 80˚; Acquired voxel size 2.96 x 3.21 x 10mm; Reconstructed voxel size: 2.5 x 2.49 x 10mm; Section thickness = 10mm with no gap; Dynamic scan time = 60 seconds with 50 dynamics per slice and 12 slices; Temporal resolution 56.5;

Conventional gated sequence, free breathing LVSA 5 –

Field-of-view=370mm x 370mm; Repetition time/Echo time = 3.0/1.5msec; Flip angle 60˚; Acquired pixel size = 2.0 x 2.2mm; Section thickness = 8mm with a 2mm gap; Reconstructed voxel size = 1.2 x 1.2 x 8mm; Number of sections = 10-12; Cardiac phases = 30

Real time LVSA 6 – Improved spatial resolution

Field-of-view = 305mm x 305mm; Repetition time/echo time = 2.5/1.26msec; Flip angle 50˚; Acquired voxel size 2.73 x 2.73 x 10mm; Section thickness = 10mm with no gap; Reconstructed voxel size = 1.19 x 1.19 x 10; Number of sections = 14; Slice scan order = base to apex; Dynamic scan time = 66 seconds, with 50 dynamics per slice as 12 slices; Temporal resolution 74ms;

Real time phase contrast sequence

The real time phase contrast sequence provided by Philips was trialed for both the aorta and MPA during rest and exercise. The parameters were: Field-of-view = 300 x 300; Repetition time/Echo time = 11/3.7 msec; Flip angle 20 ˚; Acquired pixel size = 3.0 x 3.0 x 10mm; Section thickness = 10mm; Reconstructed voxel size = 1.17 x 1.17 x 10mm; Dynamic scan time = 4.5 seconds with 100 dynamics; Temporal resolution = 44ms

3.6.3.2 Accuracy and Reproducibility study

Subjects

The methodology is described in Chapter 2 and will be briefly described here. Healthy volunteers were recruited to the study via advertisement with pre-screening via email with a simple questionnaire. Inclusion and Exclusion criteria are discussed in Chapter 2. More detailed screening was carried out on the day of attendance with height, weight, heart rate, blood pressure and a cardiovascular examination. Cardiopulmonary exercise testing was carried out to pre-determine the load that the subject would exercise at in the scanner.

Rest Imaging

Imaging was carried out on a 1.5 Tesla Philips Achieva with a 32 cardiac channel coil. Conventional retrospectively gated cine and phase contrast imaging was carried out. Resting free breathing, high temporal resolution, real time LVSA cine and Ao and MPA phase contrast images were taken.

The parameters for the real time, free breathing, rest and exercise LVSA cines were as follows: Field-of-view = 305mm x 305mm; Repetition time/echo time = 2.5/1.26msec; Flip angle 50˚; Acquired voxel size 2.73 x 2.73 x 10mm; Section thickness = 10mm with no gap;

Reconstructed voxel size = 1.19 x 1.19 x 10; Number of sections = 14; Slice scan order = base to apex; Dynamic scan time = 66 seconds, with 50 dynamics per slice and 12-14 slices; Temporal resolution 74ms;

The parameters for the real time, free breathing, rest and exercise phase contrast images were as follows: Field-of-view = 300 x 300; Repetition time/Echo time = 11/3.7 msec; Flip angle 20 °; Bandwidth = ; Acquired pixel size = 3.0 x 3.0 x 10mm; Section thickness = 10mm; Reconstructed voxel size = 1.17 x 1.17 x 10mm; Dynamic scan time = 4.5 seconds with 100 dynamics; Temporal resolution = 44ms

Exercise and immediately post Exercise Imaging

During exercise and immediately after exercise, LVOT, RVOT, LVSA and 4 chamber cines, as well as Ao and MPA phase contrast images were acquired. The slice locator was re-positioned in the expiratory phase on the RVOT and LVOT to determine optimal placement for MPA and Ao flow acquisitions respectively. Prior to cessation of exercise, the position of the Ao and MPA acquisitions was checked for accurate placement and aliasing and repeated if required.

Exercise Protocol

Exercise was carried out on an MRI compatible ergometer (Lode, Netherlands). Each subject's predetermined load was set at 40% of the watts achieved during upright CPET. Warm up consisted of increasing the load to target over one minute, and then maintaining that for 2 minutes. At 3 minutes, heart rate was monitored for stability, and then imaging commenced. Subjects were spoken to continuously during the exercise protocol. Once exercise imaging

was complete, the subject was instructed to cease exercise and remain with their feet in the pedals, while immediately post exercise imaging commenced.

Inter-study reproducibility

10 subjects were asked to return for repeat exercise CMR imaging within three months of the initial scan.

Inter-observer reproducibility

Data from 15 subjects was chosen randomly. One observer with 4 years of CMR experience (A.D.M) analysed the real time LVSA cine acquisitions and an observer with 5 years CMR experience (B.S.) analysed the real time aortic and MPA flow acquisitions.

Image Analysis:

Breath hold and real time LVSA cines were analysed using cvi42. Breath hold and real time phase contrast images were analysed on ArtFun (Paris).

Volume, Stroke volume and Ejection Fraction analysis from LVSA

Endocardial surfaces were traced at end systole and end diastole for each slice using a semi automated method with manual correction (cvi42) and volumes were calculated by the Simpsons summation rule. LV and RVSV were calculated as EDV – ESV and EF was calculated as EDV-ESV/EDV x 100 and expressed as a percentage. Care was taken in the real time images to analyse heartbeats that occurred during or near to the expiratory phase of respiration. All volumes were indexed to body surface area.

Stroke Volume analysis from Phase Contrast Images

ROIs were created around the aorta and MPA using a semi automated method with manual correction. This created time-volume curves from which could be calculated. SV was calculated as the area under the curve of the time-volume curve. For the real time analysis, an average of the first 5 consecutive heartbeats was taken. Cardiac output was calculated as SV x HR and indexed to body surface area.

Unwrapping and Phase offset adjustments

Flow data was checked for aliasing and phase offsets >0.6cm/second prior to analysis and unwrapped or adjusted prior to analysis developed by in house software.

Statistical Analysis:

IBS SPSS Version 22 and Sigma Plot Version 13 were used for data analysis. Continuous data is expressed as mean +/- standard deviation. The Bland-Altman test was used to demonstrate inter-test reproducibility. Intra-class correlations were used for intra and inter observer reproducibility, and inter-study reproducibility. Accuracy was defined as LVSV = RVSV, LVSV = AoSV and RVSV = MPASV

3.6.4 Results

3.6.4.1. Sequence Development

Real time sequence 1

This sequence was the same published by the Leuven group (Figure 3.8)(37). We found that

when used in our scanners, significant SENSE artifact obscured the lateral wall.

Furthermore, the spatial resolution did not lend itself to accurate basal analysis, particularly

as we did not have an integrated system that could track the mitral and tricuspid planes using

the HLA.
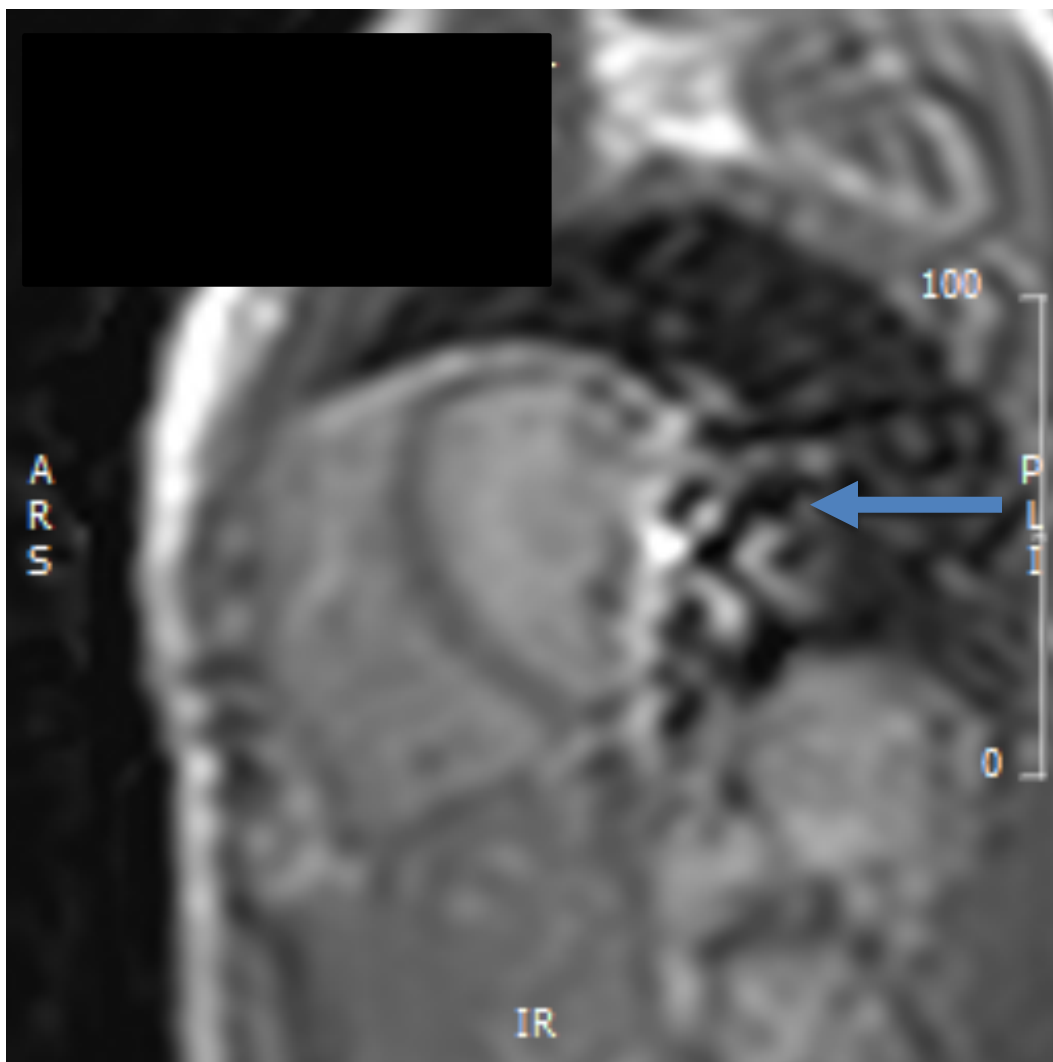
Figure 3.8: Real time LVSA sequence 1: Significant SENSE artifact obscuring the lateral wall
and inadequate spatial resolution indicated by blue arrow

Real time sequence 2

In order to improve the blood-pool contrast and reduce artifact, the flip angle was increased to 60 degrees (Figure 3.9). While this did reduce artifact, the spatial resolution was still deemed inadequate for accurate analysis.
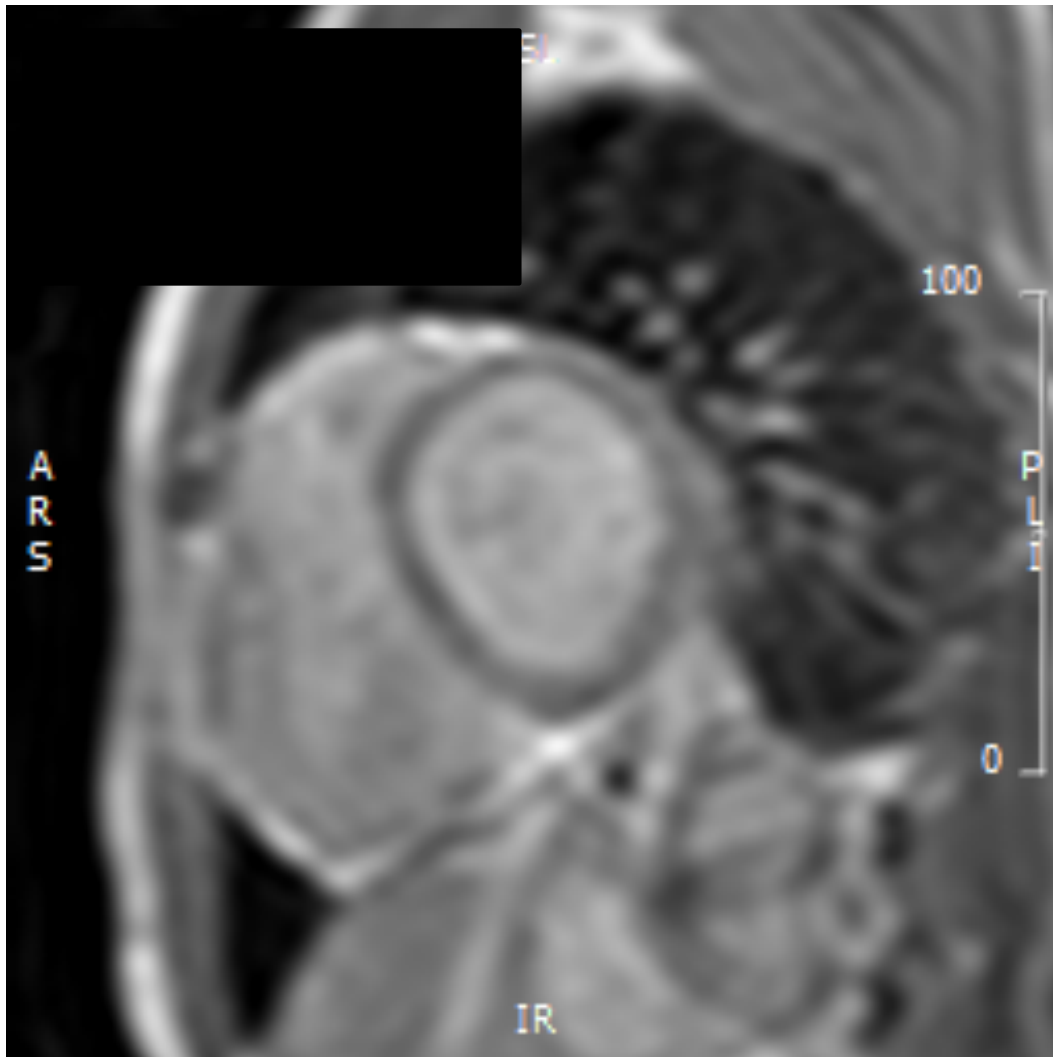
Figure 3.9: Real time LVSA sequence 2: Reduction in SENSE artifact but ongoing inadequate blood-pool contrast

Real time sequence 3

The flip angle was increased to 80 degrees to further improve blood-pool contrast, however, this increased the acquisition time to 2 minutes. Furthermore, we still considered that the spatial resolution was not adequate for basal analysis (Figure 3.10)
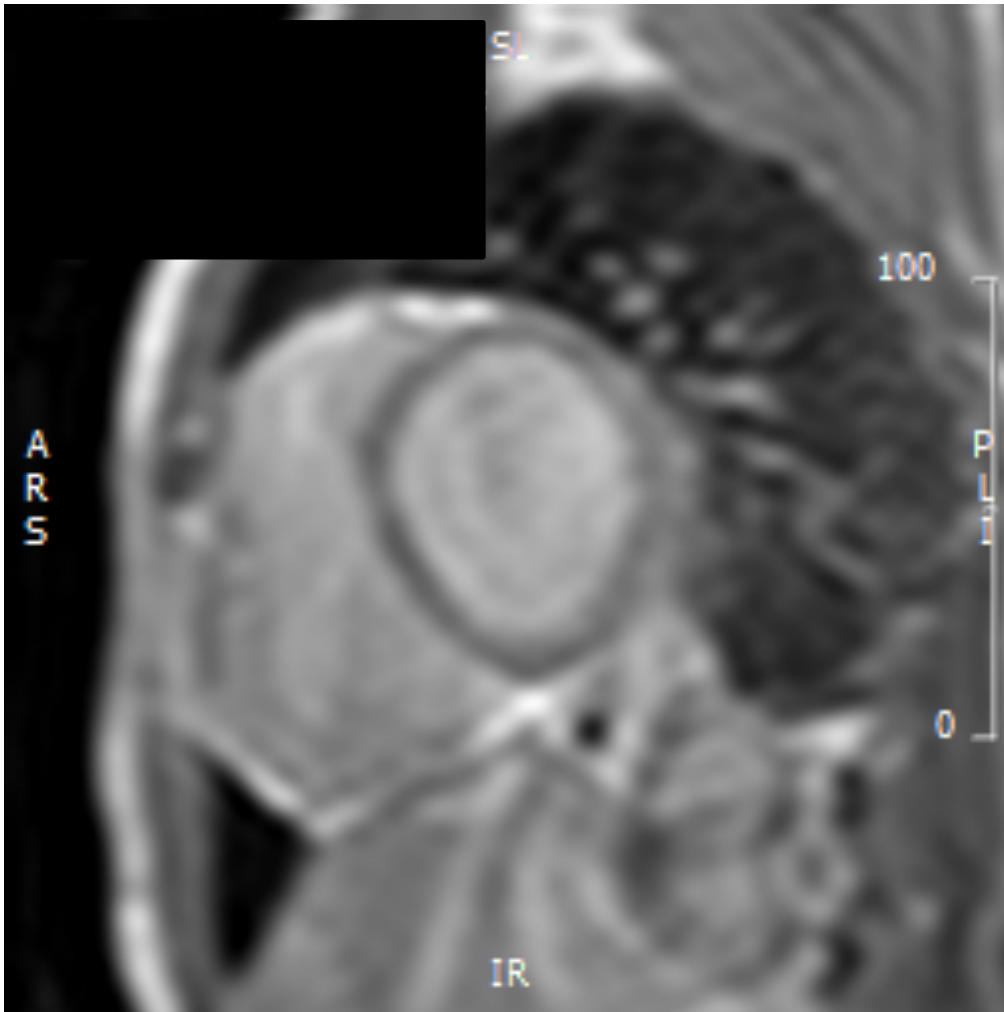
Figure 3.10: Real time LVSA sequence 3: Improved contrast but longer acquisition time

Real time stack 4 – kt blast

The blood-pool contrast significant improved, with excellent temporal resolution using k-t blast. Unfortunately, there were significant issues with SENSE artifact obscuring the lateral and anterior walls (Figure 3.11)
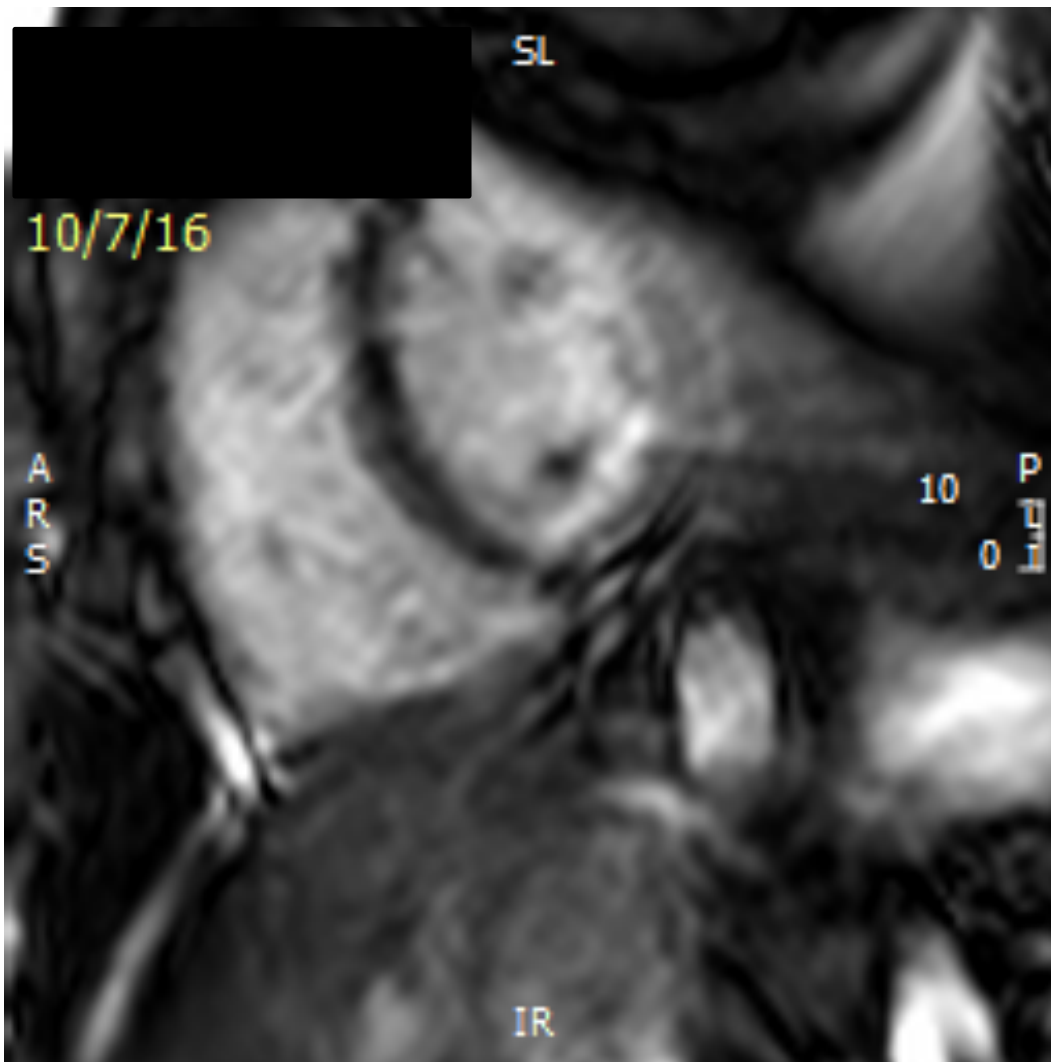
Figure 3.11: Real time LVSA sequence 4: Improved blood pool contrast and excellent temporal resolution, but SENSE artifact obscuring lateral and anterior walls

Triggered free breathing real time stack 5

Conventional triggered LVSA was trialed during exercise. Movement artifact obscured the lateral and inferior walls and it also appeared that end systole was not adequately captured during exercise (Figure 3.12 a and b). Furthermore, as the ECG trigger was occasionally lost during exercise, this would interrupt the acquisitions, occasionally making it impossible to acquire exercise images.
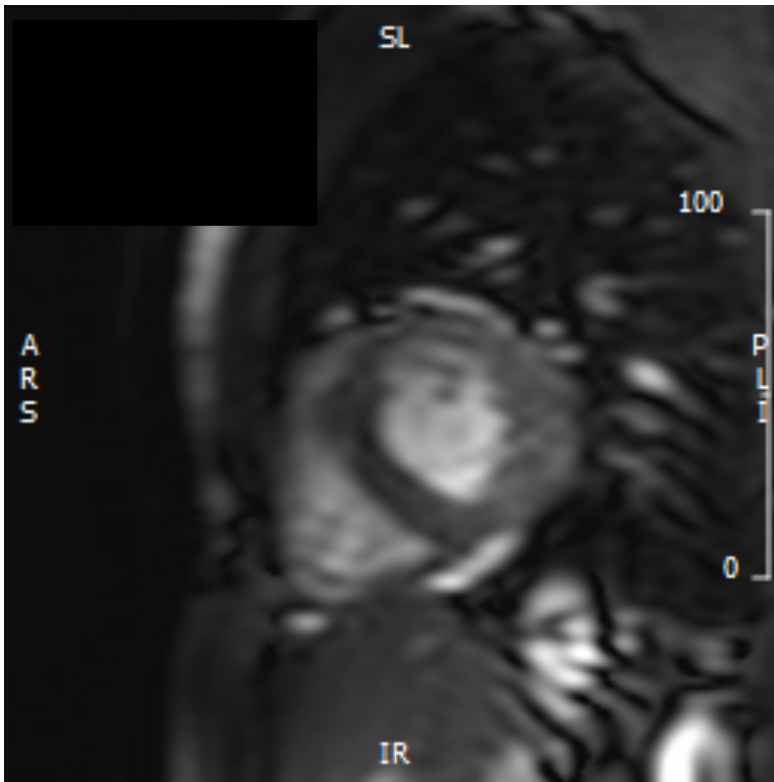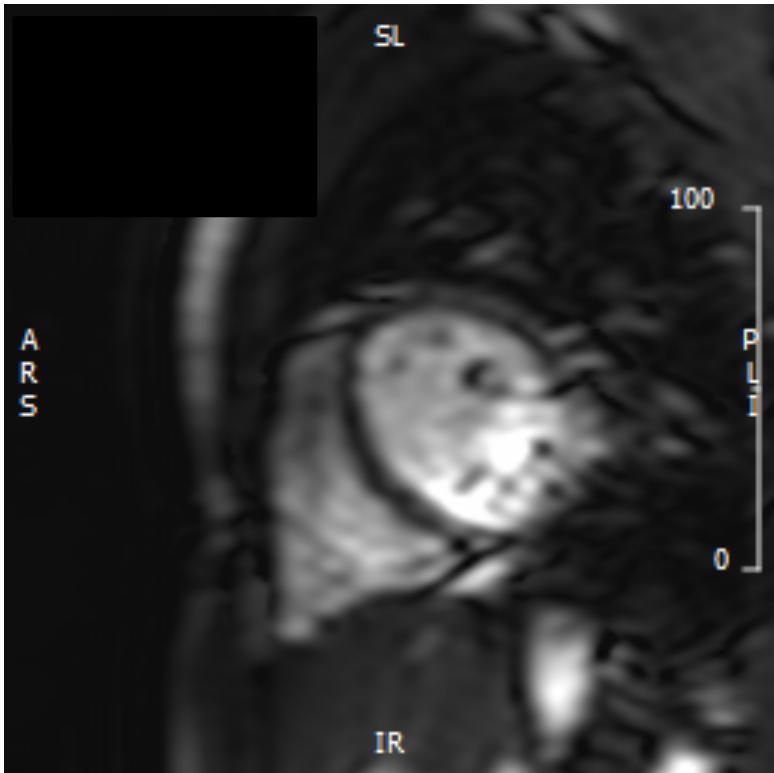
Figure 3.12: Gated conventional LVSA sequence during exercise a) End diastolic volume, significant movement artifact obscuring lateral and inferior walls b) End systolic volume, did not appear to be true end systole (given this was an exercise acquisition)

Real time LVSA – improved spatial resolution

Temporal resolution was compromised marginally (from 47ms to 74ms), however, the spatial resolution improved significantly and the blood-pool contrast was excellent (Figure 3.13). On testing with exercise, we felt that end diastole and end systole were captured, and this sequence lent itself to accurate mitral and tricuspid plane delineation.
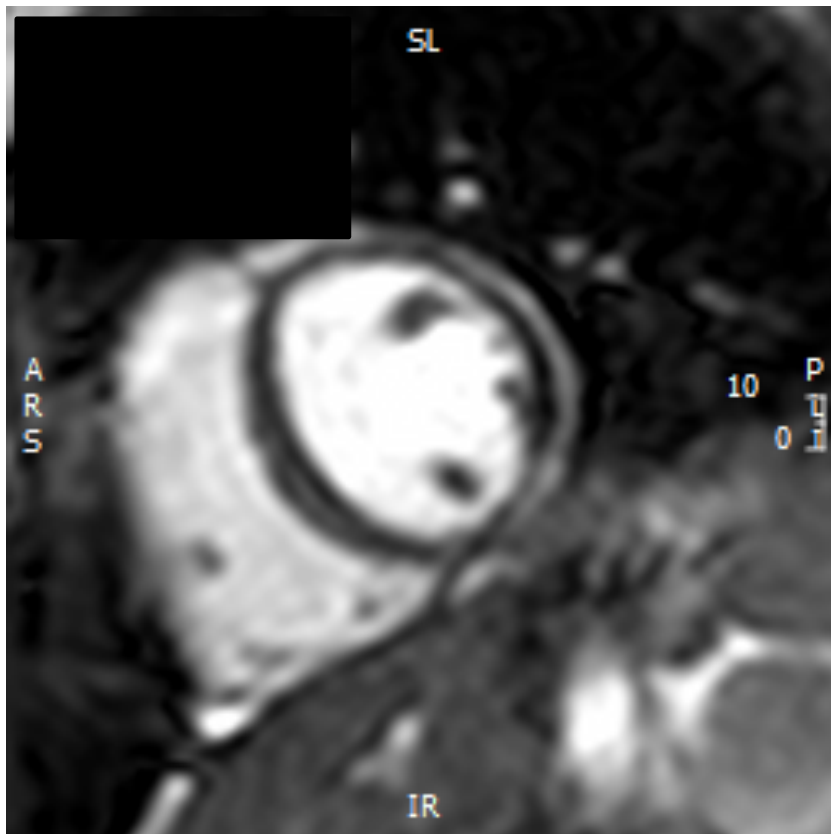
Figure 3.13: Real time LVSA sequence 6: Improved spatial resolution and a reduction in temporal resolution. Excellent blood-pool contrast

Real time MPA and Aorta phase contrast acquisitions:

The sequence provided by Philips was suitable for analysis, and no adjustment to the sequence was required. However, it was noted that during exercise, the cut-plane would shift due to movement of the diaphragm and downward displacement of the heart during exercise, leading to inaccurate flow data (Figure 3.14). By acquiring RVOT and LVOT views at the beginning

of the exercise acquisition protocol, the slice locator could be adjusted. Furthermore, once the data was acquired, as re-construction occurred immediately, the data was reviewed for accurate placement and acquisition before the subject stopped exercising, and repeated if it was deemed inadequate.
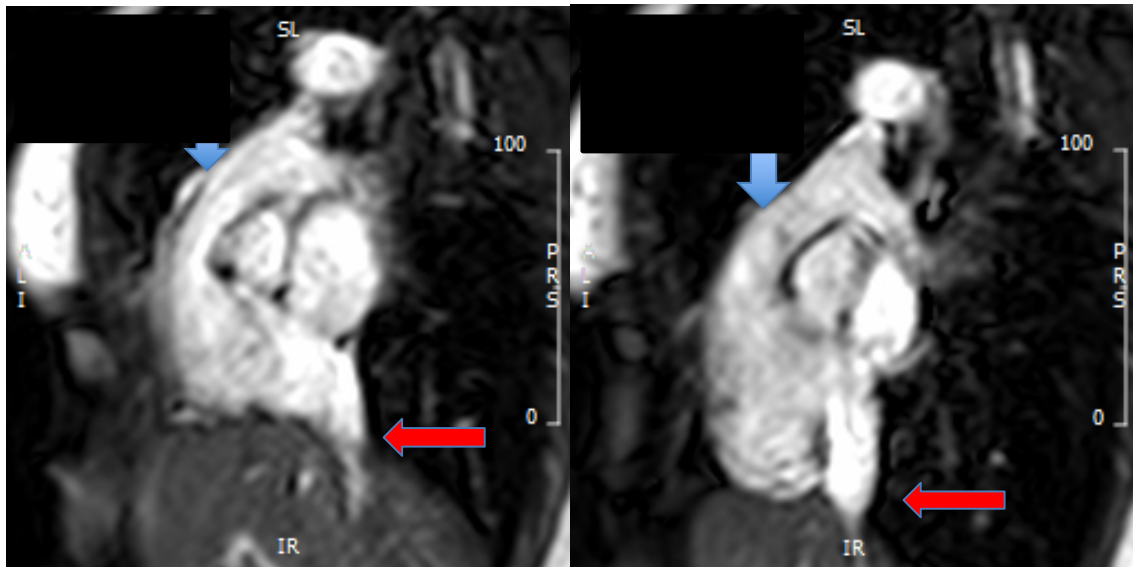
a   b
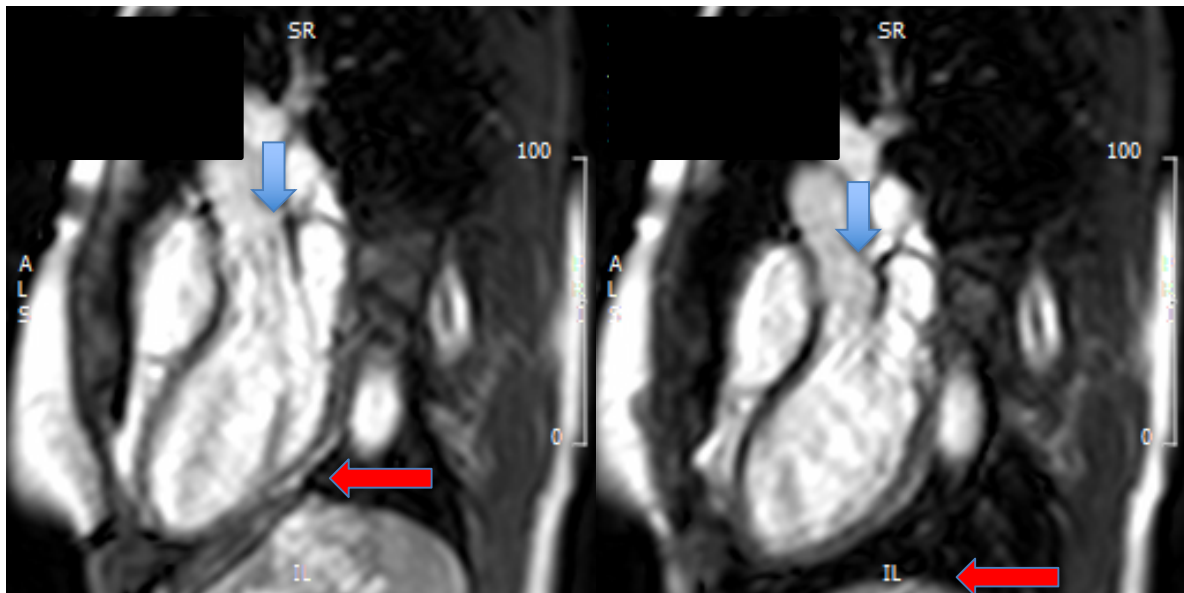
c   d

Figure 3.14:   RVOT and LVOT exercise acquisitions demonstrating movement of the diaphragm during expiration and inspiration and cut-plane location a) RVOT during expiration

b) RVOT during inspiration c) LVOT during expiration d) LVOT during inspiration. Blue arrow indicates cut-plane location and red arrow indicates diaphragm

Furthermore, a real-time rest and exercise 4 chamber (Figure 3.15) was acquired for several reasons 1) To assist with mitral and tricuspid plane delineation 2) Assess for the occurrence of tricuspid regurgitation during exercise, particularly during patients. A phase contrast 4 chamber was also acquired to assist with this.
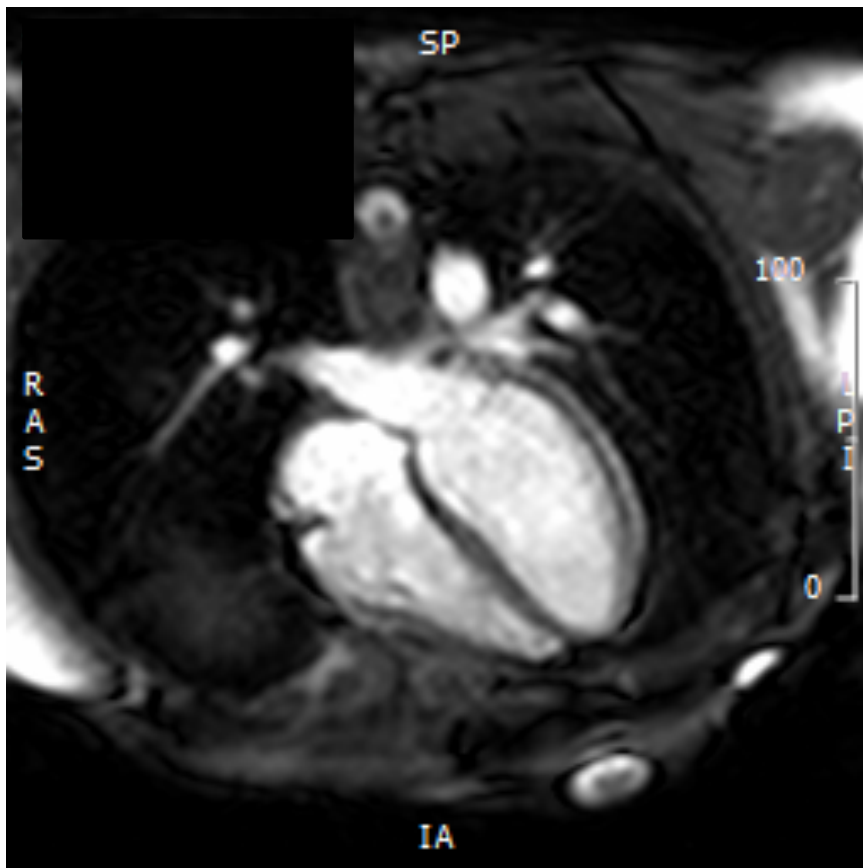
Figure 3.15: Real time, exercise 4 chamber cine

3.6.4.2 Accuracy and Reproducibility study

Subjects

38 subjects participated and completed rest and exercise breathing room air. All resting breath hold and real time data was analyzable. From the exercise data, all phase contrast imaging was well located and analyzable. From the exercise cine acquisitions, the base of the RV was not captured in one subject due to cardiac displacement downwards during exercise, but all LV data was available. Subject demographics will be outlined in detail in Chapter 5.

Intra-observer reproducibility

The inter-observer intra-class correlation coefficients for real time rest and exercise aortic and MPA phase contrast and LVSA cines are summarized in table 3.1.

Table 3.1: Intra-observer reproducibility: Intra-class correlation

	Alpha coefficient	**95% confidence interval**	
		Lower Bound	Upper Bound
Resting Ao SV	1.000	1.000	1.000
Resting MPA SV	0.999	0.997	1.000
Resting LVEDV	0.978	0.935	0.992
Resting LVESV	0.925	0.793	0.974
Resting LVSV	0.960	0.884	0.986
Resting LVEF	0.587	0.127	0.840
Resting RVEDV	0.976	0.931	0.992
Resting RVESV	0.910	0.755	0.969
Resting RVSV	0.955	0.871	0.985
Resting RVEF	0.707	0.323	0.891
Exercise Ao SV	0.999	0.997	1.000
Exercise MPA SV	0.998	0.994	0.999

Exercise LVEDV	0.972	0.919	0.991
Exercise LVESV	0.928	0.8	0.975
Exercise LVSV	0.951	0.862	0.983
Exercise LVEF	0.824	0.554	0.937
Exercise RVEDV	0.972	0.919	0.991
Exercise RVESV	0.871	0.660	0.955
Exercise RVSV	0.966	0.903	0.989
Exercise RVEF	0.625	0.185	0.856

Intra-observer reproducibility was excellent for rest and exercise aortic and MPA phase contrast acquisitions, and excellent for rest and exercise LV and R volumes. It was moderate for rest and exercise LV and RVEF.

Inter-observer reproducibility

Inter-observer intra-class coefficients for real time, rest and exercise, aortic and MPA phase contrast and LVSA cine acquisitions are summarized in Table 3.2.

Table 3.2: Inter-observer reproducibility: Intra class correlation

	Alpha coefficient	**95% confidence interval**	
		Lower Bound	Upper Bound
Resting Ao SV	0.999	0.998	1.0
Resting MPA SV	0.999	0.996	1.0
Resting LVEDV	0.986	0.958	0.996
Resting LVESV	0.893	0.666	0.966
Resting LVSV	0.971	0.909	0.991

Resting LVEF	0.599	-0.248	0.871
Resting RVEDV	0.975	0.921	0.992
Resting RVESV	0.923	0.76	0.975
Resting RVSV	0.957	0.865	0.986
Resting RVEF	0.854	0.546	0.953
Exercise Ao SV	0.998	0.993	0.999
Exercise MPA SV	0.983	0.951	0.994
Exercise LVEDV	0.980	0.937	0.994
Exercise LVESV	0.950	0.844	0.984
Exercise LVSV	0.976	0.924	0.992
Exercise LVEF	0.880	0.626	0.961
Exercise RVEDV	0.984	0.951	0.995
Exercise RVESV	0.939	0.811	0.980
Exercise RVSV	0.975	0.922	0.992
Exercise RVEF	0.744	0.202	0.918

Inter-observer reproducibility was excellent for rest and exercise aortic and MPA phase contrast acquisitions. It was excellent for rest and exercise LV and RV volumes, and resting RVEF and exercise LVEF. It was moderate for resting LVEF and exercise RVEF.

Inter-test correlation

Table 3.3 summarises the Bland Altman Results for the comparisons between resting real time to breath hold LVSA and phase contrast acquisitions. Table 3.4 summarises the Bland-Altman results for the comparisons between resting real time flow and LVSA derived stroke volumes.

Table 3.5 summarises the Bland-Altman results for comparisons between real time exercise flow and LVSA stroke volumes, and left and right stroke volumes.

Table 3.3: Bland Altman comparisons of resting real time to breath hold LVSA and phase contrast acquisitions

Parameter	Bias	Standard Deviation	Limits of Agreement	95% confidence interval	Bias Present
LVEDV	-0.80	9.39	-19.20, 17.59	-3.88 to 2.28	No
LVESV	1.45	7.55	-13.35, 16.25	-1.02 to 3.92	No
LVSV	-2.23	7.10	-16.14, 11.68	-4.56 to 0.09	No
LVEF	-0.96	4.06	-8.92, 6.99	-2.29 to 0.37	No
RVEDV	-1.19	9.13	-19.10, 16.71	-4.19 to 1.80	No
RVESV	-1.11	8.66	-18.90, 15.97	-3.95 to 1.72	No
RVSV	-0.27	7.74	-15.21, 15.15	-0.599 to 2.05	No
RVEF	0.73	10.7	-20.26, 21.73	-2.78 to 4.25	No
MPA SV	7.4	9.2	-10.68, 25.51	4.39 to 10.44	Yes
Ao SV	0.73	10.7	-20.26, 21.73	-2.78 to 4.25	No

Table 3.4: Bland Altman Comparison of Resting Real time Flow and LVSA Stroke Volumes

Parameter	Bias	Standard Deviation	Limits of Agreement	95% confidence interval	Bias Present
Ao to LVSV	5.0	11.5	-17.6, 27.6	1.24 to 8.8	Yes
Ao to MPA SV	-0.59	10.5	-21.2, 20.04	-4.04 to 2.86	No

MPA to RVSV	1.22	11.23	-20.81, 23.24	-2.47 to 4.90	No
LV to RVSV	-4.40	4.62	-13.45, 4.66	-5.91 to -2.88	Yes

Table 3.5: Bland Altman comparison of Real time Exercise Flow and Cine stroke volumes, and Left and Right Stroke Volumes.

	Bias	**Standard Deviation**	**Limits of agreement**	**95% confidence interval**	**Bias present**
Ao to MPA	-3.43	9.49	-22.04, 15.18	-6.54 to -0.32	Yes
Ao to LVSV	5.78	10.62	-15.05, 26.6	2.29 to 9.26	Yes
MPA to RVSV	2.73	8.61	-14.14, 19.61	-0.13 to 5.6	No
LVSV to RVSV	-6.25	8.07	-22.06, 9.56	-8.94 to -3.56	Yes

There was a bias between real time and breath hold MPA phase contrast acquisitions, with a bias of 7.4mL. Otherwise, there no other bias between resting breath hold and real time acquisitions. There was a consistent bias demonstrating that real time LVSA derived stroke volumes were higher than Ao phase contrast derived stroke volumes at rest and exercise, with the bias at rest being 5.0mL and 5.78mL on exercise. There was a consistent bias demonstrating that real time LVSA derived LVSV was higher than RVSV at rest and exercise. At rest the bias was 4.4mL and on exercise, it was 6.25mL. There was a bias between Ao and MPA stroke volumes on exercise, with Ao higher with a bias of 3.4mL.

Inter-study reproducibility

Table 3.6 summarises the exercise inter-study reproducibility.

Table 3.6: Inter-study reproducibility on exercise: Intra-class Correlation

	Alpha coefficient	95% confidence interval	
		Lower Bound	Upper Bound
Ao SV	0.874	0.493	0.969
MPA SV	0.919	0.674	0.980
LVEDV	0.939	0.776	0.985
LVESV	0.920	0.712	0.979
LVSV	0.900	0.651	0.974
LVEF	0.819	0.428	0.952
RVEDV	0.923	0.723	0.980
RVESV	0.750	0.269	0.931
RVSV	0.945	0.795	0.986
RVEF	0.603	0.002	0.884

There was excellent correlation between exercise aortic and MPA phase contrast SV, as well as LV volumes, LVEF and RV volumes and stroke volumes. There was a moderate correlation between exercise RVEF.

3.6.5 Discussion

3.6.5.1 Sequence Development

We found that the spatial resolution of the Leuven protocol (2.3 x 2.3 x 8mm) did not lend itself to accurate delineation of the mitral and tricuspid valve planes, with significant SENSE

artifact with a flip angle of 50° that resolved with an increase in flip angle, but led to an increase in acquisition time. The Leuven had developed their own software to integrate the HLA stack to assist analysis in the setting of poorer spatial resolution, however, we did not have this ability with cvi42. Furthermore, as we were planning on acquiring LVSA, MPA and Ao flow sequences, acquiring a HLA stack would add at least another minute and a half to the protocol, which I felt was not possible in the setting of a patient exercising. As to using gating, we also found similarly to Leuven, that often images could not be acquired due to loss of the ECG trace during exercise, and then the images that were captured were often not of suitable quality to analyse due to artifact. Furthermore, it appeared to us that end systole was not captured during exercise.

While the GOSH group had reported that their standard real time with a temporal resolution of 80ms was not accurate, they only acquired 2 heart beats per slice and their sequence was gated to specifically such that the first R-R interval was used to reach steady state, and the next R-R interval for data acquisition. Hence there was only one heart-beat per slice. Gating was probably possible in their setting, as subjects were not exercising at medium to high workloads, so perhaps there was little ECG interference. Our sequence acquired between 6-8 heartbeats, to allow for at least 2 respiratory cycles and hence respiratory variation to be taken in to account. If several heartbeats are acquired, then instead of just one chance, in one heartbeat, to acquire end diastole and end systole, there are multiple opportunities. Furthermore, our spatial resolution was much better than GOSH reported standard real time sequence, and better than any other research groups thus far.

Hence to improve the spatial resolution, we compromised marginally on temporal resolution. We found that this allowed for accurate mitral and tricuspid plane delineation, but also captured

end diastole and end systole. Furthermore, our exercise protocol was during submaximal exercise, hence the heart rates would not be reaching maximal levels, as compared to the Leuven exercise protocol.

To assist with mitral and tricuspid plane delineation, we acquired exercise LVOT and RVOT views at start of the exercise protocol. This not only helped with repositioning of the slice locater, but it also assisted with tracking the location of the valvular planes during downward cardiac translation through respiration, and for endocardial surface tracing in analysis. Furthermore, we acquired a 4 chamber cine and a 4 chamber phase contrast cine, to assist with analysis and to document qualitatively when tricuspid regurgitation occurred during exercise.

For the real time flow sequence an echo planar imaging sequence was used with a temporal resolution of 44ms and a reconstructed voxel size of 1.17 x 1.17 x 10mm. This was comparable to the other groups previously mentioned. The Amsterdam group has a temporal resolution of 47ms and the GOSH group's was 40.4ms. The Leuven group have not yet reported exercise flow data. 100 dynamics were acquired and this took a total of 4.5 seconds.

Acquiring the flow data in the correct location was of utmost importance, particularly during exercise. The imaging plane for both the MPA and Aorta must be prescribed perpendicular to the course of the vessel. For the pulmonary artery, the cutplane is defined in a systolic phase, as to ensure optimal image angulation during the majority of blood flow. For the MPA Hori et al have demonstrated that up and down displacement is 4.6 – 6mm during free breathing at rest (209). Thus far, only one group has reported that MPA flow acquisition was compromised by motion artifact and shifted acquisition plane due to downward cardiac translation during

exercise (183). The sequence used by Steeden et al required 5 minutes to reconstruct(177). However, I felt that to ensure accuracy, a sequence was required that could reconstruct in real time.

Overall, our emphasis was on a balance between an adequate temporal resolution that captured end systole and end diastole, but also to have adequate spatial resolution to delineate the tricuspid and mitral valve planes. We also developed a sequence that allowed for flow and cine acquisitions during exercise, and acquired RVOT, LVOT and 4 chamber and phase contrast cines to assist with analysis and account for the development of tricuspid regurgitation.

3.6.5.2 Accuracy and Reproducibility study

We have shown that at rest, there is a bias between real time aortic SV and LVSV with LVSV a mean of 5mL higher, and real time MPA SV and breath hold MPA SV acquisitions with breath hold acquisitions a mean of 7mL higher. There was no bias at rest between real time and breath hold LVSA acquisitions.

On exercise, there was a bias between real time aortic SV and MPA SV, with MPA SV a mean of 3mL lower, aortic SV and LVSV with LVSV a mean of 5.8mL higher and LVSV and RVSV with RVSV a mean of 6mL lower. Taken together, these suggest that left sided SV calculations on exercise are higher than right sided, but that also LVSV calculations tend to be higher than aortic and RVSV.

There are several explanations for this. Aortic and MPA stroke volumes were calculated as an average over 5 consecutive heartbeats, while LVSA cines were analysed during expiration.

Hence, it may be expected that the flow acquisitions may be lower than the LVSA generated stroke volumes. Additionally, we were conservative with our approach to the correction of phase offsets, hence real time flow acquisitions with phase offsets, could contribute to this bias. Furthermore, we know that there is an increase in left side flow during expiration, which could explain the bias between left and right-sided stroke volumes, as well as aortic and MPA stroke volumes.

Furthermore, it has been shown that there are differences between stroke volume analyses between the aorta and MPA. Using phase contrast measurement, Evans et al found a 5% difference between flow in the ascending aorta and flow in the pulmonary artery in health volunteers. A deviation from the true flow of 3.5% - 4.5% was estimated as the inborn technical error of phase contrast measurement when a non-breath hold cine gradient-echo sequence with prospective gating is used (225). Kondo et al (226) found similar deviations between flow in the aorta and flow in the pulmonary trunk.

However, the difference found between breath hold and real time MPA stroke volume acquisitions could also be because real time acquisitions are actually more physiologically representative than inspiratory or expiratory acquisitions (227). Johansson et al demonstrated that expiratory held acquisitions reduced the pulmonary regurgitant fraction compared to help inspiratory and non-breath hold, and was different to volumetric derived stroke volumes. The non breath hold calculation was the same as the stroke volume difference calculation, so potentially more accurate (228).

The difference between left and right-sided stroke volumes on exercise could also have a physiological explanation. Pulmonary vascular distensibility and shunting through

intrapulmonary arteriovenous anastomoses, and not intra-cardiac shunts, has been hypothesized and demonstrated to occur in humans, as well as be present anatomically (229). It is thought to occur, as a mechanism to decrease afterload on the right ventricle, during episodes of elevated pulmonary pressures, such as during exercise or hypoxia, and occur in more than 95% of healthy humans on exercise, starting during submaximal exercise and increasing with exercise intensity (229-231) and has been shown to be proportional to increases in pulmonary capillary pressure and capillary blood volume (232). Mechanisms and causes of intra-pulmonary shunting are shown in Figure 3.16.
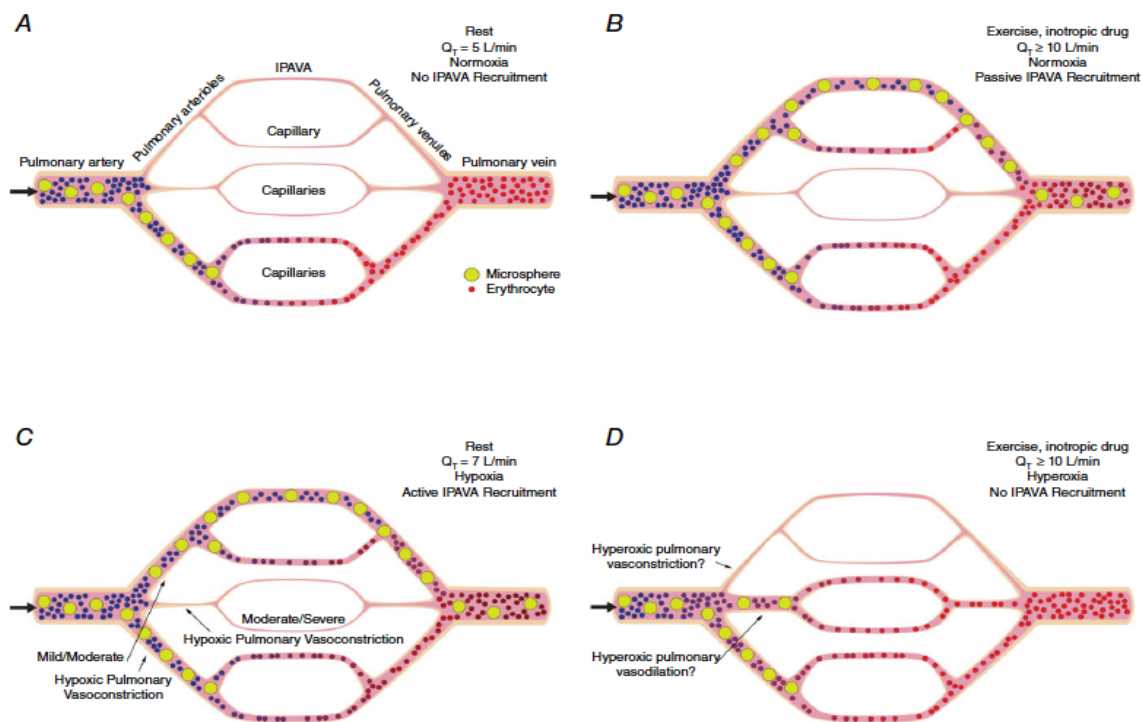
Figure 3. Intrapulmonary arteriovenous anastomoses: Summary of the model of how active and passive regulation of the pulmonary circulation could determine the recruitment and perfusion of intrapulmonary arteriovenous anastomoses (IPAVA) under various conditions. Small/thin vessels with a pink background with no erythrocytes or microspheres represent no pulmonary perfusion but the potential for recruitment. Yellow spheres represent intravenously injected microspheres. A) At rest, breathing room air – there is only recruitment of a small portion of the pulmonary vasculature with no shunting, and no appearance of microspheres in the left ventricle. B) Increased blood flow during exercise or due to an intravenous inotropic drug and breathing room air – this causes passive recruitment of a larger proportion of the pulmonary vasculature which contains IPAVA. Hence microspheres appear in the left ventricle. The volume of flow through the IPAVA increases as the intensity of exercise increases. C) At rest breathing hypoxic gas – Flow is increased slightly. Hypoxia causes an active redistribution of pulmonary blood flow towards those areas of the lung with IPAVA and consequently, IPAVA are passively recruited. Hence microspheres appear in the left ventricle. D) Increased flow during exercise or during inotropic infusion breathing 100% oxygen. Hyperoxia causes an active redistribution of pulmonary blood flow through hyperoxic vasoconstriction of IPAVA or hyperoxic vasodilation of areas without IPAVA> Hence IPAVA are not recruited and no microspheres appear in the left ventricle. (Adapted from Lovering et al, Intrapulmonary arteriovenous anastomoses in humans – response to exercise and the environment, J Physiol)

Hence these biases could represent a true bias, or could be due to intra-pulmonary arteriovenous anastomoses. However, it was important to ensure that the LVSA cines were analysed at the same point in the respiratory cycle, so that rest and exercise comparisons could be made, given the known fluctuations in stroke volume and these differences are small and unlikely to have clinical impact. Furthermore, the fact that LVSA derived SV were consistently higher, demonstrates that temporal resolution was infact adequate to capture end diastole and end systole – the concern with a lower temporal resolution would be that EDV would be underestimated and ESV overestimated, hence a lower stroke volume, however, we did not have that problem. Future work could include developing software that can integrate respiratory bellow tracing with time-volume curves, so that stroke volume from phase contrast acquisitions can be analysed only during expiration. Designing a study to see if these differences are reduced with hyperoxia may clarify whether shunting is present.

Our intra and inter-observer reproducibility is also excellent for all parameters, and moderate for RVEF. We feel that the acquisition of RVOT, LVOT and 4 chamber cines were instrumental, to allow for accurate analysis between observers for the LVSA cines.

We have demonstrated that there is excellent inter-study reproducibility of exercise CMR for aortic and MPA stroke volumes, LV volumes and ejection fraction and RV volumes, and moderate reproducibility for RVEF. This has not been published by other groups, and demonstrates the reproducibility of steady state, continuous exercise acquisitions on follow up.

3.6.6. Summary:

1. On exercise, left sided stroke volumes from aortic phase contrast and LVSA cines to be higher than right-sided MPA and RV stroke volumes.

2. Stroke volume calculated from LV volumes is consistently 5mL higher than stroke volumes calculated from aortic phase contrast images. This is likely a result of analysis of the LVSA during expiration

3. There is excellent intra-observer reproducibility for real time resting and exercise aortic and MPA stroke volumes, resting and exercise LV volumes and ejection fraction and resting and exercise RV volumes. There is moderate reproducibility for resting and exercise RVEF

4. There is excellent inter-observer reproducibility for real time resting and exercise aortic and MPA stroke volumes, resting and exercise LV and RV volumes and RVEF and moderate reproducibility for resting LVEF and exercise RVEF.

5. There is excellent inter-study reproducibility for exercise aortic and MPA stroke volumes, LV volumes and ejection fraction and RV volumes, and moderate reproducibility for RVEF

3.7 Overall Conclusions

We developed a methodology that accounted for several important factors:

1. The exercise protocol allowed for:
    a. An adequate warm up

b.   Data acquisition during continuous steady state exercise

   c.   Patients could realistically complete the exercise protocol and all data could be collected

2. The LVSA and flow sequences had adequate temporal resolution

3. Mitral and tricuspid valve planes could be adequately delineated in analysis through adequate spatial resolution and tracking from exercise LVOT and RVOT planes

4. That aortic and MPA exercise data was collected accurately

5. That respiratory variation, which has a significant impact on volumes, stroke volume and hence cardiac output calculation was taken in to account

6. That aliasing and phase offset errors were accounted for

Overall, we believe we have developed a protocol that allows for accurate data acquisition and analysis, and that we have robustly assessed reproducibility. From this, we felt that we could set out to use it to demonstrate pathophysiological changes in biventricular function in acute and chronic pulmonary hypertension.

Chapter 5 – Exercise and Immediately Post Exercise CMR in healthy volunteers

5.1 Introduction

Exercise CMR is a novel, innovative approach to assessing dynamic biventricular function. Several research groups have used it so far, to assess biventricular function in healthy adults, as well as in a number of pathologies. However, approaches have varied, particularly the timing of imaging that may affect the interpretation of exercise physiology, in health and disease.

5.2 Aims and Hypotheses

We aimed to demonstrate that our approach to carrying out and analyzing exercise CMR was feasible, accurate and reproducible as well as demonstrate and describe normal biventricular function and flow during steady state exercise and immediately post exercise, generate normal values in healthy adults, and correlate resting and exercise biventricular function with VO_2 peak. We hypothesized that a moderate level of exercise in healthy volunteers would produce a decrease in LVESV and RVESV, an increase in LVEDV, an increase in LVSV and RVSV and an increase in LVEF and RVEF. Immediately post exercise, we hypothesized that there would be an immediate decrease in CO and a decrease in LV and RVEF.

5.3 Methodology

The methodology is described in Chapter 2 and will be briefly described here. Healthy volunteers were recruited to the study via advertisement with pre-screening via email with a simple questionnaire. Inclusion and Exclusion criteria are discussed in Chapter 2. More

detailed screening was carried out on the day of attendance with height, weight, heart rate, blood pressure and a cardiovascular examination. Cardiopulmonary exercise testing was carried out to pre-determine the load that the subject would exercise at in the scanner.

5.3.1 Preparation

Care was taken to ensure that the subject was positioned such that they could pedal within the scanner with no restriction, and that the heart was no more than 10cm from isocentre. Continuous heart rate and oxygen saturation monitoring was carried out throughout the study.

5.3.2 Imaging

5.3.2.1 Rest Imaging

Imaging was carried out on a 1.5 Tesla Philips Achieva with a 32 cardiac channel coil. Conventional retrospectively gated cine and phase contrast imaging was carried out. Resting free breathing, high temporal resolution, real time LVSA cine and aortic and MPA phase contrast images were taken.

5.3.2.2 Exercise and Immediately Post Exercise Imaging

During exercise and immediately after exercise, free breathing, high temporal resolution, real time LVOT, RVOT, LVSA and 4 chamber cines, and Ao and MPA phase contrast images were acquired.

5.3.3 Exercise Protocol

Exercise was carried out on an MRI compatible ergometer (Lode, Netherlands). Each subject's predetermined load was set at 40% of the watts achieved during upright CPET. Warm up consisted of increasing the load to target over one minute, and then maintaining that for 2 minutes. At 3 minutes, heart rate was monitored for stability, and then imaging commenced. Subjects were spoken to continuously during the exercise protocol. Once exercise imaging was complete, the subject was instructed to cease exercise and remain with their feet in the pedals, while immediately post exercise imaging commenced. Immediately post exercise imaging commenced within 1 second of the subject ceasing exercise and the full protocol took a minimum of 86 seconds to acquire.

5.3.4 Image Analysis:

Breath hold and real time LVSA cines were analysed using cvi42 (Circle, Cardiovascular Imaging, Canada). Breath hold and real time phase contrast images were analysed on ArtFun (UPMC, Paris).

5.3.4.1 Volume, Stroke volume and Ejection Fraction analysis from LVSA

Endocardial surfaces were traced at end systole and end diastole in the expiratory phase of respiration, for each slice using a semi automated method with manual correction and volumes were calculated by the Simpsons summation rule. LV and RVSV were calculated as EDV – ESV and EF was calculated as EDV-ESV/EDV x 100 and expressed as a percentage. All volumes were indexed to body surface area.

5.3.4.2 Stroke Volume, Mean and Average Velocity and Pulsatility analysis from Phase Contrast Images

ROIs were created around the aorta and MPA using a semi automated method with manual correction. This created time-volume and time-velocity curves from which SV and mean and average velocity could be calculated. SV was calculated as the area under the curve of the time-volume curve. Peak velocity was taken as the peak velocity occurring during systole, and mean velocity as the mean of the velocities through systole (Figure). For the real time analysis, an average of the first 5 consecutive heartbeats was taken. Pulsatility was calculated as Maximum area – Minimum area/Minimum area x 100. Cardiac output was calculated as SV x HR and indexed to body surface area.

5.3.4.3 Unwrapping and Phase offset adjustments

Flow data was checked for aliasing and phase offsets >0.6cm/second prior to analysis and unwrapped or adjusted prior to analysis using software developed in-house by our physicist, Pawel Tokarczuk.

5.3.5 Statistical Analysis

IBM SPSS Version 22 was used for data analysis. Data was checked for normality. Continuous data is expressed as mean ± standard deviation. Paired t-tests were used to compare differences between measurements. Pearson's correlation was used to test the associations

between CPET parameters and biventricular function. A Bonferroni correction was applied to adjust for multiple comparisons.

5.4 Results

38 subjects participated and completed rest and exercise breathing room air. All resting breath hold and real time data was analyzable.

From the exercise data, all phase contrast imaging was well located and analyzable. From the exercise cine acquisitions, the base of the right ventricle was not captured in one subject due to cardiac displacement downwards during exercise, but all left ventricular data was available.

From the immediately post exercise data, 37 aortic and MPA phase contrast data was available. 1 subject's immediately post exercise flow data was too aliased and could not be unwrapped by the software. Out of the cine acquisitions, 31 real time LVSA were analyzable. 6 cine stacks could not be analysed as due to deep breathing immediately post exercise, the base of the left and right ventricle were not captured during expiration, and in one case, the table moved spontaneously during acquisition.

Reproducibility and accuracy data have been presented and discussed in Chapter 3.

5.4.1 Subject characteristics:

The gender distribution was equal with 19 men and 19 women. Relevant characteristics are summarized in Table 5.1.

Table 5.1: Subject characteristics

	Mean	Standard Deviation	Minimum	Maximum
Age	35.6	9.3	24	66
BMI	24.5	3.2	20.2	35.3
BSA	1.9	0.2	1.6	2.3
Peak VO2 (mL/min)	2690.6	841.2	964	4814
Max Load (W)	240.8	81.1	93	452
Set load in scanner (W)	93.2	30.5	37	180

Values are expressed as Mean +/- SD

Subjects were also asked to classify the amount of exercise they carried out per week, as either less than 1 hour, between 1-3 hours, between 3-5 hours and above 5 hours a week. 6 subjects said less than 1 hour, 10 between 1-3 hours, 7 between 3-5 hours and 14 above 5 hours a week.

5.4.2 Rest, Exercise and Immediately After Exercise Physiology

Rest, exercise and immediately post exercise heart rate, stroke volume index, cardiac index and LV and RV volumes, stroke volumes and ejection fraction are summarized in Table 5.2.

From rest to exercise and from rest to immediately post exercise, heart rate, CI, LVSV, RVSV, Aortic SVI and MPA SVI increased. An increase in LVSV was driven by an increase in LVEDVI and decrease in LVESV. Increase in RVSV was driven by a decrease in RVESV. Both LV and RVEF increased. All changes were significant to p <0.0001. There was no significant difference between rest and exercise RVEDVI, p=0.245. Figure 5.1 demonstrates

change in RVEF from rest to exercise in all subjects. One subject had a slight decrease in RVEF on exercise. There was no issue with scan quality.

Table 5.2: Heart rate, Cardiac Index and Biventricular Parameters at Rest, Exercise and Immediately post Exercise

	Rest	Exercise	Immediately post Exercise
HR	61 ± 11	122 ± 12	91±16
Ao SVI	51.4 ± 11.0	61.7 ± 10.3	64.7 ± 12.3
MPA SVI	51.4 ± 9.9	60.0 ± 9.3	62.1 ± 11.2
CI	3.1 ± 0.6	7.6 ± 1.5	5.9 ± 1.6
LVEDVI	84.3 ± 14.7	90.1 ± 15.5	91.2 ± 16.4
LVESVI	30.4 ± 5.3	25.5 ± 7.0	26.2 ± 5.3
LVSVI	53.8 ± 10.7	64.6 ± 10.7	65.1 ± 13.2
LVEF	63.7 ± 3.6	71.9 ± 4.5	71.1 ± 4.2
RVEDVI	90.4 ± 17.5	88.1 ± 14.5	89.2 ± 18.3
RVESVI	38.9 ± 8.8	27.1 ± 8.4	25.8 ± 8.1
RVSVI	51.5 ± 10.8	60.9 ± 9.5	63.4 ± 12.4
RVEF	57.0 ± 5.1	69.6 ± 6.1	71.4 ± 5.0

All results expressed as mean ± standard deviation. All comparisons from rest to exercise, and rest to immediately post exercise are highly significant, $p < 0.0001$, except for RVEDVI that is not significant for both settings.

Figure 5.1: Change in RVEF from Rest to Exercise
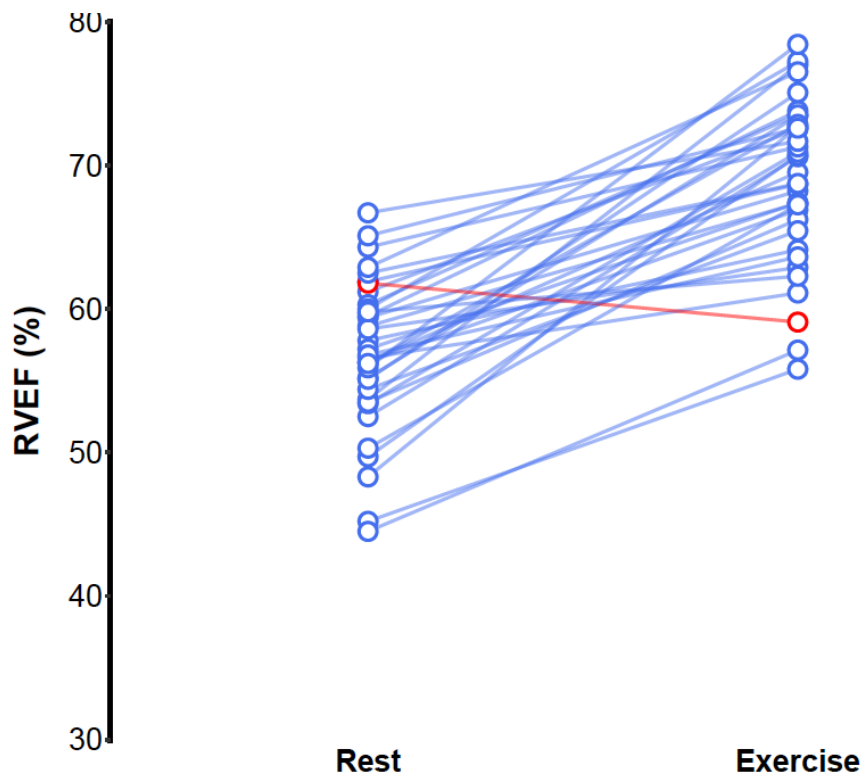
5.4.3 Exercise to Immediately Post Exercise – Comparison of Right Ventricular Parameters and Cardiac Index

When comparing right and left ventricular parameters from exercise to immediately post exercise, there is a significant increase in RVEF ($p=0.022$) with an increase in LVEDVI ($p=0.036$) and an increase in Ao SVI ($p=0.001$). Cardiac Index is significantly lower immediately post exercise, compared to exercise $p < 0.0001$ driven by a decrease in heart rate ($p < 0.0001$). Change in cardiac index from rest, to exercise to immediately post exercise is shown in Figure 5.2

Table 5.3: Comparison of Cardiac Index and Right Ventricular Parameters from Exercise to Immediately Post Exercise

	Exercise	Immediately post Exercise	P value
CI	7.6 ± 1.5	5.9 ± 1.6	<0.0001
HR	122.4 ± 12.3	91.6 ± 16.1	<0.0001
Ao SVI	61.4 ± 10.4	64.7 ± 12.3	0.001
MPA SVI	60.0 ± 9.3	62.1 ± 11.2	<0.0001
RVEDVI	88.6 ± 14.9	91.2 ± 16.4	0.036
RVEF	69.6 ± 6.1	71.4 ± 5.0	0.022

Figure 5.2: Change in Cardiac Index from Rest to Exercise to Immediately post Exercise
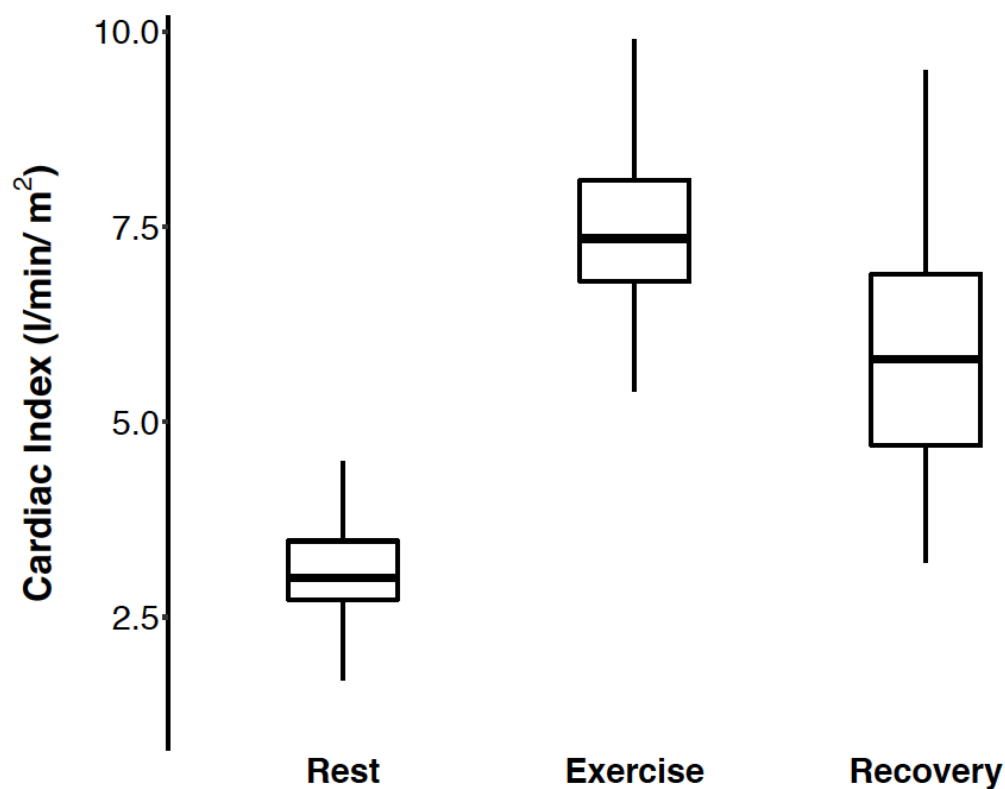
5.4.4 Range of Change of Biventricular Parameters on Sub-Maximal Exercise

The mean, standard deviation and minimum and maximum values for the change in biventricular parameters and cardiac index are summarized in Table 5.3. There was no difference in the change in cardiac index and biventricular parameters between genders, from rest to exercise, summarized in Table 5.4

Table 5.4: Mean, standard deviation and range of the change of Biventricular Parameters and Cardiac Index in the Healthy Volunteers

	Mean	Standard Deviation	Minimum	Maximum
LVEDVI	5.8	7.0	-7.2	22.6
LVESVI	-4.9	5.2	-17.41	8.94
LVSVI	10.8	4.9	0.57	18.8
LVEF	8.1	4.6	-2.7	20.7
RVEDVI	-1.6	8.0	-21.47	14.76
RVESVI	-11.3	7.4	-29.3	6.1
RVSVI	9.7	5.7	-4.6	25.19
RVEF	12.4	6.5	-2.71	24.4
CI	4.5	1.3	2.3	8.0

Table 5.5: Comparison of Change of Biventricular Parameters between Males and Females

Change on Exercise	Female	Male	P value
LVEDVI	4.1 ± 7.2	7.6 ± 6.5	1.0
LVESVI	-4.5 ± 4.5	-5.3 ± 5.8	1.0
LVSVI	8.8 ± 5.1	12.8 ± 3.9	0.09

LVEF	7.2 ± 3.9	9.0 ± 5.2	1.0
RVEDVI	-2.1 ± 7.8	-1.0 ± 8.4	1.0
RVESVI	-10.8 ± 7.0	-11.9 ± 8.0	1.0
RVSVI	8.7 ± 5.3	10.9 ± 6.0	1.0
RVEF	11.5 ± 5.2	13.5 ± 7.6	1.0
CI	4.0 ± 1.3	5.0 ± 1.0	0.18

5.4.5 MPA Area, Pulsatility and Velocity

MPA area, pulsatility and velocity data are summarised in Table 5.6. Maximum and minimum MPA area increased significantly during exercise. Peak and average velocity increased. There was no significant difference in the change in pulsatility from rest to exercise, however, the trend was for pulsatility to decrease on exercise.

Table 5.6: MPA Velocity, Area and Pulsatility from Rest to Exercise

	Rest	**Exercise**	**P value**
Maximum Area	8.2 ± 1.5	9.1 ± 1.9	0.005
Minimum Area	5.0 ± 1.0	6.0 ± 1.3	<0.0001
Pulsatility (%)	65.7 ± 27.9	53.2 ± 25.0	0.22
Peak Velocity	58.4 ± 14.4	91.3 ± 24.2	<0.0001
Average Velocity	12.6 ± 2.8	14.6 ± 3.4	<0.0001

5.4.6 Resting and Exercise Correlations with VO$_2$ peak and Amount of Exercise/week

The correlations of subject characteristics and biventricular parameters are summarized in Table 5.7. Peak VO$_2$ correlated moderately with LV and RVEDVI, LV and RVESVI and LV and RVSVI at rest and exercise, as well as change in LVEDVI on exercise. It also correlated moderately with male gender, higher BSA and with the amount of exercise carried out during the week. There was no correlation with age, resting cardiac index or with resting or exercise LV or RV ejection fraction.

Table 5.7: Peak VO$_2$ Correlations with subject characteristics and Biventricular Parameters

	Pearson's correlation	P value
Male gender	0.533	0.001
BSA	0.570	<0.0005
Amount of exercise/week	0.522	0.001
LVEDVI	0.543	<0.0001
LVESVI	0.407	0.011
LVSVI	0.543	<0.0001
RVEDV	0.593	<0.0001
RVESVI	0.530	0.001
RVSVI	0.523	0.001
Exercise CI	0.666	<0.0001
Ex LVEDV	0.671	<0.0001
Ex LVESVI	0.433	0.007
Ex LVSVI	0.668	<0.0001
Ex RVEDVI	0.522	0.001

Ex RVSVI	0.602	<0.0001
Change in LVEDVI	0.350	0.031

Furthermore, the more exercise carried out per week correlated with resting LV and RVEDVI, resting LV and RVESVI and resting LV and RVSVI. However, it correlated with exercise LV and RVEDVI and exercise LV and RVSVI but not exercise LV or RVESVI.. This is summarized in Table 5.8.

Table 5.8: Correlation of amount of exercise/week with Biventricular Resting and Exercise Parameters

	Pearson's Correlation	**P value**
LVEDVI	0.509	0.001
LVESVI	0.415	0.010
LVSVI	0.494	0.002
RVEDVI	0.551	<0.0001
RVESVI	0.530	0.001
RVSVI	0.455	0.004
Ex LVEDVI	0.531	0.001
Ex LVSVI	0.577	<0.0001
Ex RVEDVI	0.496	0.002
Ex RVSVI	0.556	<0.0001

5.5 Discussion

We have demonstrated that moderate supine exercise is characterized by an increase in LV and RVSVi, an increase in LV and RVEF, a decrease in LV and RVESVi, an increase in LVEDVi and no change in RVEDVi. The exercise LV dynamics is consistent with a large body of evidence over many years, carried out using radionuclide angiography, invasive haemodynamics and exercise echocardiography (17, 20, 21, 23, 31, 34, 102, 233-237) and confirms that LVSV is augmented by Frank Starling mechanisms, as well as an augmentation of contractility.

The mechanisms of augmenting RVSVi on exercise appear to be different to that of the LV. Our results demonstrated that augmentation of RVSVi on exercise was due to an increase in contractility, shown by the decrease in RVESVi with no increase in RVEDVi. Mols et al demonstrated using radionuclide ventriculography that on exercise, RVEDVi remains unchanged, with a decrease in RVESV, concluding that increased contractility and not Frank-Starling mechanisms contribute to an increase in RVSVi on supine exercise (36). Conversely, Mahler et al showed an increase in RVEDVi and LVEDVi on upright exercise, however, did not show a decrease in RV or LVESVi, which is contrary to most of aerobic exercise literature (238). Using exercise CMR, Holverda et al have demonstrated that RVSVi increases due to a decrease in RVESVi with no change in RVEDVi, however, they did not demonstrate an increase in LVEDVi on exercise as we have (42). Lurz et al showed an increase in LV and RVSVi, driven by a decrease in LV and RVESVi. However, they showed a trend for a decrease in LV and RVEDVi (178). La Gerche et al reported no increase in LV or RVEDVi at peak exercise, but a decrease in LV and RVESVi(37). Roest et al also showed no increase in LV or RVEDVi, and a decrease in RV and LV ESVi (26). Hence while these studies agree that

RVEDVI does not increase on exercise, the majority of the more recent exercise CMR studies are contrary to previous research and our findings, in terms of change of LVEDVI on exercise.

It is important to note that both Lurz and La Gerche did not allow a 3 minute warm up and did not scan during steady state exercise, and Lurz et al used a resistive type exercise rather than aerobic. Holverda and Roest scanned during breaks in exercise. Furthermore, these differences may be due to posture, as it is documented that change in LVEDVi is more dramatic on upright, compared to supine exercise, particularly if the subject's legs are left in the pedals during rest scanning (25). We were particular about taking the subject's legs out of the pedals during rest scanning, to ensure the legs were not elevated relative to the chest. This also demonstrates the importance of the type of exercise, exercise protocol and the timing of imaging, and how it can influence exercise physiology and results.

Furthermore, we have demonstrated that healthy subjects who have a higher VO_2 peak, have a larger resting and exercise biventricular size. This is perhaps of little surprise, as we know that athletes have larger cardiac chamber size (20), and it has been demonstrated that in sedentary healthy subjects and patients, exercise training leads to an increase in resting and exercise LVEDVi (233-236, 239) and RVEDVi (240). However, we have also noted that change in LVEDVi correlates with peak VO_2, suggesting that higher VO_2 relies on enhancement of Frank-Starling mechanisms, rather than improvements in contractility. We have also shown that the more exercise the subject does per week correlates with higher resting and exercise LV and RVEDVI, and resting and exercise LV and RVSVI, but not with that exercise LV and RVESVI suggesting that exercise training increases exercise stroke volume by augmenting biventricular preload, rather than changes in the contractile states of both ventricles. This is supported by a study carried out by Wolfe et al, demonstrating that exercise training in

sedentary subjects led to a higher SVi on exercise due to a larger LVEDVi rather than changes in contractile state from studying invasive haemodynamics on exercise (235). Kitzman et al showed that in patients with heart failure with preserved ejection fraction and healthy volunteers, that change in LVEDVi on exercise correlated with LVSVi and CI. In the patient group, abnormalities in diastolic function limiting the patient's ability to augment SV by means of the Frank-Starling mechanism, limited exercise physiology (22). Higginbotham et al have also reported that increases in LVSVi on exercise is augmented by increases in LVEDVi rather than changes in LVESVi, supporting the hypothesis that Frank-Starling mechanisms are key in LVSVi augmentation during exercise (32). Furthermore, Boutcher et al studied 10 trained, 10 active and 10 sedentary men and showed that trained men had greater LV filling and contractility and active men had greater filling, than sedentary men (33). This supports this notion that due to greater LV compliance or increased LV filling from exercise training, Frank Starling mechanisms augment a higher LVSVi and hence CI and higher VO_2 peak, rather than due to improvements in contractility.

However, we showed no correlation of change of cardiac chamber size or VO_2 peak with age. Rodheffer et al demonstrated an age related increase in LVEDVi on exercise, with no blunting of CO response, and concluded that with age, there is a shift from catecholamine mediated increase in heart rate and reduction in ESV, to a greater reliance on the Frank Starling mechanisms (16). However, the fitness of the subjects was not documented, and we have shown that the more exercise subjects carried out in the week, the larger the cardiac chamber size. Conversely, Stratton et al studied 13 older and 11 younger men, before and after exercise training. Both groups increased resting LVEDVi, but also increased exercise LVEDVi further, and hence CO and EF increased as a result of improved Frank-Starling mechanisms, in both

the young and elderly (19), and other studies have also demonstrated no association between change in LVEDVI, SVI or EF and age (32).

Higginbotham et al have demonstrated that exercise EF is lower in women than in men, and women have a higher exercise LVEDV(24). Hanley et al similarly showed that men had a greater increase in LVEF and women had a greater increase in LVEDVI(35). Aksut et al showed no gender differences (21). In our study, while male gender was associated with a higher VO_2 peak, there was no association with change in LVEDVi or change in LVEF. Once again, it is important to document the amount of exercise that individual subjects do a week, as this may influence the results.

Another important finding of our study, is that there are significant differences in heart rate, cardiac index, stroke volume, RVEF and LVEDVI between exercise and immediately post exercise. Immediately post exercise, there is a drop in heart rate leading to a large decrease in CI. However, there is an increase in SVI, with an increase in RVEF and LVEDVI. Horwitz et al noted that in dogs, LVEDVi increased during exercise and remained elevated during recovery, with a prompt recession of contractility, concluding that Frank-Starling mechanisms play an important role after exercise (241). Stein et al demonstrated no increase in LVEDV during exercise, but then an increase in LVEDV during recovery, hence concluded that during recovery, there is a measurable effect of Frank-Starling mechanisms (242). More recently, Takahashi et al demonstrated that on supine exercise, stroke volume increased markedly during recovery, with a decrease in cardiac output due to an immediate, rapid decrease in heart rate (243) which is similarly supported by a number of other studies (244, 245). Together, these studies support our findings, however, no study to date has documented changes in RVEF from continuous exercise to immediately after exercise, and we have shown a significant increase.

This potentially explains the increase in LVEDVI found during recovery, as it can be hypothesized that there is an increase in RV contractility due to a reduction in pulmonary pressures, and a subsequent increase in LV filling. Furthermore, LaFountain et al carried out exercise CMR in 10 fit subjects, but scanned their subjects immediately after exercise to maximum exhaustion. While there was a correlation between SV and VO_2 peak, there was no correlation between CO and VO_2 peak. This could be explained by out data, as we have shown that exercise CI correlates with peak VO_2 and then also clearly demonstrated that CI immediately decreases after exercise, hence carrying out imaging after exercise would not reflect peak exercise physiology.

Identifying these differences in exercise versus immediately post exercise is crucial, as this may have implications when studying patients and how results are interpreted. Plotnick et al have demonstrated using radionuclide angiography, comparing health volunteers and patients with myocardial ischaemia, that at peak exercise, those with ischaemia had a lower LVEF and higher LVESV, however, immediately post exercise, there was no significant difference between these parameters. In the patients, ejection fraction recovery was characterized by a decrease in LVESV, concluding that enhanced contractility played a major role in recovery in the patient group (246). Despite this, several groups who have started using exercise CMR have carried out imaging immediately after exercise or during short breaks in exercise (18, 26, 162, 180-183). Demonstrating these differences in a patient group using exercise CMR, would be vital to highlight methodology flaws that could affect the interpretation of results.

Also of note, is that in all 38 subjects, we were able to gather analyzable data at rest and exercise, which contrasts with exercise echocardiography where analyzable exercise data varies. La Gerche et al have reported that when comparing exercise CMR to exercise

echocardiography, high quality images were available in all subjects using exercise CMR, but only 71% using exercise echocardiography (102). We have also been able to propose a range of normal parameters for change in biventricular function during sub-maximal exercise, which is currently not available in the literature.

A number of studies have been carried out to explore the use of CMR indices to quantify pulmonary pressures including (247) as well as PVR (248) and relative area change or pulsatility has been shown to be a predictor of RV function (84) and predict mortality in patients with PAH (249). Furthermore, stroke volume index, relative area change and PA average blood flow velocity have been shown to be associated with functional class in pulmonary hypertension (82). Garcia-Alvarez et al demonstrated that pulmonary artery velocity was the parameter that had the strongest univariate correlation with PVR (250). On exercise, it is known that in healthy subjects, pulmonary arterial pressure increases while PVR decreases. The distensibility of the pulmonary circulation has been demonstrated by Argiento et al who showed on exercise echocardiography that pulmonary arteries distend by 2% of their initial diameters for each mmHg increase in transmural pressure (43). It is important to note that pulsatility measured on CMR is looking at changes in vessel size, while studies using echocardiography measuring distensibility are linked to pressure.

We have demonstrated on exercise that PA pulsatility does not change on exercise, and that peak and average velocity increase. Farouzan et al demonstrated changes in MPA pulse wave velocity, but similarly no change in pulsatility on exercise in healthy volunteers, concluding that exercise CMR can identify a decrease in proximal pulmonary artery compliance (183). Hence no change or the trend of PA pulsatility to decrease on exercise could be a reflection of increased pulmonary pressures on exercise, while the increase in average blood velocity, given

its association with PVR, could reflect the distensible pulmonary circulation on exercise, and a decrease in PVR. If this is the case, we would expect on hypoxic exercise, that PA pulsatility would decrease, and that average blood velocity on exercise would not rise due to hypoxic pulmonary vasoconstriction.

5.5.1 Limitations

There are several limitations to our study. The analysis of the real time LVSA cines, is manual and can be time consuming. Furthermore, there is reliance on the operator of identifying the correct phase of respiration, as well as end diastole and end systole. The temporal resolution of our LVSA cines is 74ms, and could be improved. However, we have demonstrated excellent intra and inter-observer reproducibility, inter-study reproducibility and inter-test reproducibility, as discussed in Chapter 3.

We have shown an increase in LVEDVI on exercise, and while our findings are consistent with older studies, they are not consistent with the more recent exercise CMR studies. This could be explained by the position of the subject's legs during exercise, the type of exercise, the intensity of exercise, but also the phase in the respiratory cycle that the images are analysed. We have analysed our images during end expiration, which could explain why we have demonstrated an increase in LVEDVI, as we know there is an increase in LV filling on expiration. However, this further highlights the importance of the methodology, and how the exercise protocol, respiration and method of analysis, may affect the interpretation of results. While not necessarily a limitation, these results also have to be interpreted in the knowledge that the subjects are supine and not erect. These physiological differences are described in

Chapter 1.2. Also, we are comparing peak VO_2 recorded on erect CPET to cardiac parameters acquired during supine steady state exercise.

There is also a relatively small sample size, which limits the ability to set normal ranges, particularly when comparing gender, age or ethnicity groups. Furthermore, our group was a relatively active and fit group, which may introduce bias, as there was no difference in resting LV and RV size between genders, which has otherwise been shown in the literature (251).

5.6 Conclusions

We have demonstrated several key points:

1. Supine moderate level intensity exercise is characterized by an increase in LVSV, RVSV, LVEF and RVEF, a decrease in LVESV and RVESV, an increase in LVEDV and no change in RVEDV. We have proposed a range of normal values for biventricular volumes and function, in men and women, between 25-65 years old, during sub-maximal exercise.

2. Immediately post exercise, there is a decrease in CO, a decrease in HR, an increase in SV, an increase in LVEDVI and an increase in RVEF. This could have implications in the assessment of patient pathophysiology.

3. On exercise, there is no change in MPA pulsatility on exercise, but an increase in MPA average blood flow velocity, which could reflect pulmonary vascular distensibility. Whether this can detect subtle changes in the pulmonary vasculature, such as in a model

of acute pulmonary hypertension driven by hypoxic pulmonary vasoconstriction, would be interesting to study.

4. Peak VO_2 correlates with male gender, larger BSA, amount of exercise you do in a week, larger resting and exercise LV and RV volumes, larger exercise MPA area, exercise CI and an increase in LVEDVI on exercise. The amount of exercise carried out per week correlates with biventricular size, but not biventricular end systolic volume, suggesting that exercise training augments preload rather than contractility

Chapter 6 – Cardiovascular Changes at Rest and Exercise in Healthy Volunteers During Acute Normobaric Hypoxia

6.1 Introduction

The effects of hypoxia on RV and LV volumes and function have not been well characterized in humans during exercise stress. It is known that acute hypoxic exercise is characterized by an attenuation of VO_2 peak, pulmonary vasoconstriction, and signs of RV strain. The attenuation of VO_2 peak is thought to be secondary to reduced RV forward flow, however, no imaging studies thus far have been able to definitively document changes in RVSV or RVEF. Hence real-time, free breathing MRI afford the opportunity to study the consequences of these changes in detail.

6.2 Aims and Hypotheses

We hypothesized that acute hypoxia would have adverse effects on the RV, particularly during exercise – and that reduced forward flow from the RV during acute hypoxic exercise might lead to reduced LV volumes, from reduced pre-load. In this MRI study, therefore, we examined detailed parameters of RV and LV volumes and function, as well as flows in the PA and aorta, to examine this hypothesis.

6.3 Methodology

The methodology is described in Chapter 2, 3 and 5 and will be briefly described here. Healthy volunteers were recruited to the study via advertisement with pre-screening via email with a simple questionnaire. More detailed screening was carried out on the day of attendance with height, weight, heart rate, blood pressure and a cardiovascular examination. Cardiopulmonary exercise testing was carried out to pre-determine the load that the subject would exercise at in the scanner.

6.3.1 Preparation

Care was taken to ensure that the subject was positioned such that they could pedal within the scanner with no restriction, and that there heart was no more than 10cm from isocentre. Continuous heart rate and oxygen saturation monitoring was carried out throughout the study.

6.3.2 Imaging

Rest Imaging

Imaging was carried out on a 1.5 Tesla Philips Achieva with a 32 cardiac channel coil. Conventional retrospectively gated cine and phase contrast imaging was carried out. Resting free breathing, high temporal resolution, real time LVSA cine and Ao and MPA phase contrast images were taken.

Exercise and immediately post Exercise Imaging

During exercise and immediately after exercise, free breathing, high temporal resolution, real time LVOT, RVOT, LVSA and 4 chamber cines, and Ao and MPA phase contrast images were acquired.

6.3.3 Exercise Protocol

Exercise was carried out on an MRI compatible ergometer (Lode, Netherlands). Each subject's predetermined load was set at 40% of the watts achieved during upright CPET. Warm up consisted of increasing the load to target over one minute, and then maintaining that for 2 minutes. At 3 minutes, heart rate was monitored for stability, and then imaging commenced. Subjects were spoken to continuously during the exercise protocol. Once exercise imaging was complete, the subject was instructed to cease exercise and remain with their feet in the pedals, while immediately post exercise imaging commenced.

6.3.4 Hypoxic Protocol

Hypoxia was induced by using 12% oxygen with continuous oxygen saturation and heart rate monitoring (Nonin MRI Compatible Oximeter, 7500). Each subject was fitted with an extra small, small, medium or large mask, as appropriate, to ensure the correct fit and reduce the chance of gas leakage. The inspirate was supplied from a medical gas mixture containing 12% oxygen in nitrogen administered from a commercially prepared cylinder (British Oxygen Company) and was kept in the outside MRI room. A 1000L Douglas bag was filled from the cylinder that could be taken inside the MRI room. A 35mm breathing tube connected to a 3 way T shaped stopcock, ran from the Douglas bag, and connected to a mask adaptor 7400/7450 which in turn was connected to a T shaped, non-rebreather valve on the 7450 V2 Blue Silicone Rubber Mask fitted on the subject's face. All the equipment was supplied from Cranlea Human Performance Ltd, Birmingham. Subjects were instructed to breath the 12% oxygen at rest, for 10 minutes, until saturations dropped and had plateaued. Images were then acquired at rest, with alteration to breath hold duration according to the subject's perception of breathlessness.

Exercise and immediately post exercise imaging was then performed as per protocol. The total

duration of hypoxia was around 35 minutes. This is summarized in figure 6.a.
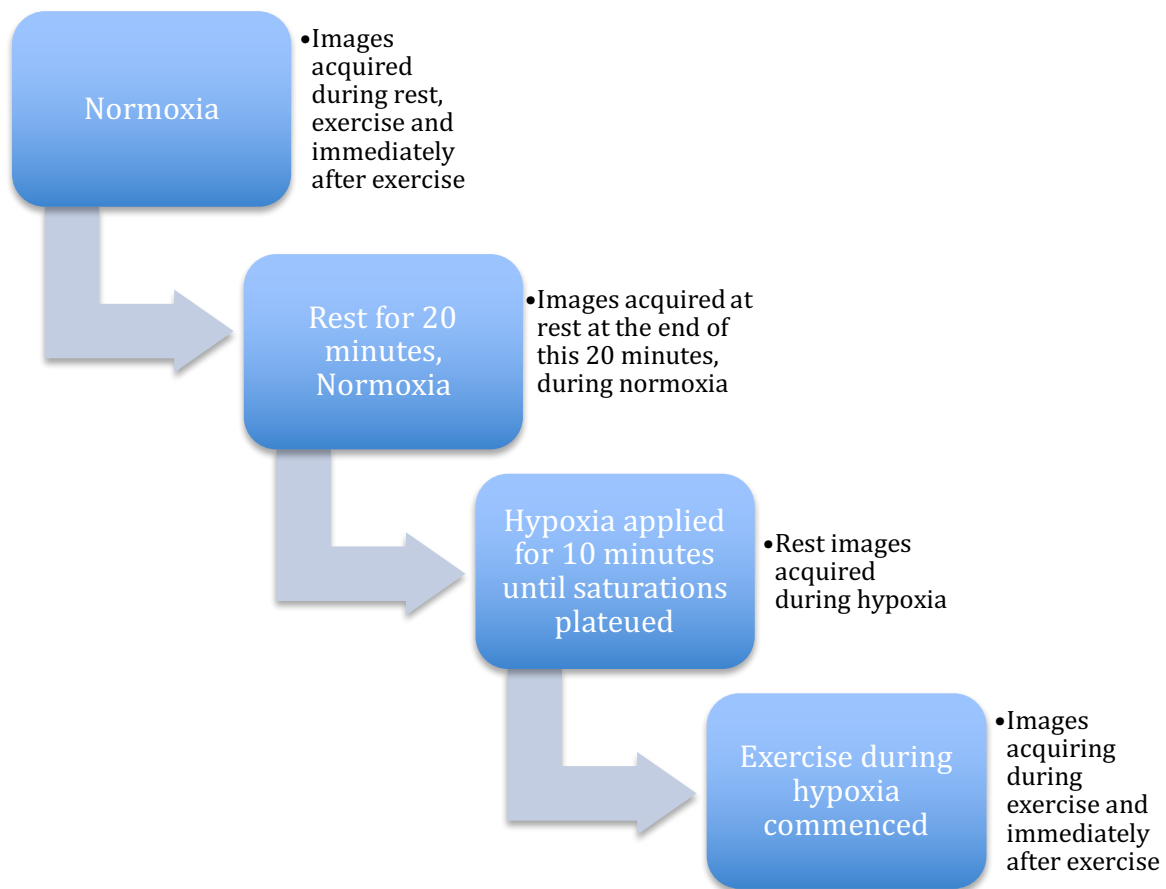
Figure 6.a: Flow diagram showing steps of image acquisition, during rest, exercise and

immediately after exercise, during normoxia, rest after normoxia and hypoxia.

6.3.5 Image Analysis:

Breath hold and real time LVSA cines were analysed using cvi42 (Circle, Cardiovascular

Imaging, Canada). Breath hold and real time phase contrast images were analysed on ArtFun

(UPMC, Paris).

6.3.5.1 Volume, Stroke volume and Ejection Fraction analysis from LVSA

Endocardial surfaces were traced at end systole and end diastole in the expiratory phase of respiration for each slice, using a semi-automated method with manual correction and volumes were calculated by the Simpsons summation rule. LV and RVSV were calculated as EDV – ESV and EF was calculated as EDV-ESV/EDV x 100. All volumes were indexed to body surface area.

6.3.5.2 Stroke Volume, Mean and Average Velocity and Pulsatility analysis from Phase Contrast Images

ROIs were created around the aorta and MPA using a semi-automated method with manual correction. This created time-volume and time-velocity curves from which SV and mean and average velocity could be calculated. SV was calculated as the area under the curve of the time-volume curve. Peak velocity was taken as the peak velocity occurring during systole, and mean velocity as the mean of the velocities through systole. For the real time analysis, an average of the first 5 consecutive heartbeats was taken. Pulsatility was calculated as Maximum area – Minimum area/Minimum area x 100 and expressed as a percentage. Cardiac output was calculated as SV x HR and indexed to BSA.

6.3.5.3 Unwrapping and Phase offset adjustments

Flow data was checked for aliasing and phase offsets >0.6cm/second prior to analysis and unwrapped or adjusted prior to analysis (Omnibus Velocity Unwrapping With Phase Offset Correction, MATLAB wrapper, Pawel Tokarczuk).

6.3.6 Statistical Analysis:

IBM SPSS Version 22 was used for data analysis. Data was checked for normality. Continuous data is expressed as mean ± standard deviation. Paired t-tests were used to compare differences between measurements. A two way repeated measures ANOVA was used to test the interaction between the effect of oxygen level and exercise on right and left ventricular cardiovascular parameters with main and simple main effects analysis. A Bonferroni correction was applied to adjust for multiple comparisons for all simple main effects and pairwise comparisons.

6.4 Results

38 subjects were recruited. 37 subjects completed resting hypoxia and 34 subjects completed exercise hypoxia. Saturations fell to 84±4% at rest and 77±5% during exercise.

From the data, all images acquired at rest could be analysed. From the exercise images, all 34 phase contrast and LV volumes could be analysed. 2 exercise LVSA cines missed the RV base.

Immediately after exercise, 32 from 34 phase contrast images were analyzable. 2 were not correctly positioned. 24 LVSA cines could be analysed. The 10 cines that could not be analysed was due to an increase in the depth of subject respiration immediately after exercise, causing incomplete acquisition of the base of the RV and LV and hence were excluded from the analysis.

17 subjects had LVSA cines acquired at the start of the study and then after the period of rest, before commencing the hypoxia protocol.

6.4.1 Biventricular volumes at the start of the study vs. after the period of rest

Table 6.1 summarises the results of biventricular volumes at the start of the study and the normoxia protocol, and then after the period of rest before commencing the hypoxia protocol. There was no significant difference in LV volumes, SV or LVEF. There was no difference in RVEDVI, RVSVI or RVEF. However, RVESVI was significantly smaller, p=0.032, which could be as a result of the exercise carried out prior to the hypoxia study.

Table 6.1: Comparison of biventricular volumes pre-normoxia and pre-hypoxia, n = 17

	Pre Normoxia Protocol	Pre Hypoxia Protocol	p value
LVEDVI	83.7 ± 14.6	79.0 ± 14.6	1.0
LVESVI	30.2 ± 5.2	28.2 ± 7.7	0.32
LVSVI	53.5 ± 10.7	51.0 ± 8.3	1.0
LVEF	63.8 ± 3.6	65 ± 4.5	0.488
RVEDVI	90.0 ± 17.8	81.8 ± 15.2	0.136
RVESVI	38.6 ± 8.9	32.1 ± 8.0	0.032
RVSVI	51.3 ± 11.1	49.7 ± 8.3	1.0
RVEF	57.1 ± 5.2	60 ± 5	0.352

LV = Left ventricular; RV = Right ventricular; EDVi = Indexed end diastolic volume; ESVi = Indexed end systolic volume; SVi = Indexed stroke volume; EF = Ejection fraction;

6.4.2 Effects of Hypoxia at Rest

The comparisons of heart rate, cardiac index and biventricular volumes between normoxia and hypoxia are summarized in Table 6.2.

Table 6.2: Rest Normoxia vs. Rest Hypoxia Biventricular Volumes, n = 37

	Rest Normoxia	Rest Hypoxia	p value
HR	61.6 ± 10.6	74.5 ± 12.2	<0.001
Ao SVI	51.3 ± 10.9	50.4 ± 12.3	1.0
MPA SVI	51.3 ± 9.9	51.6 ± 9.8	1.0
CI	3.1 ± 0.6	3.6 ± 0.7	<0.001
LVEDVI	83.7 ± 14.6	79.9±13.8	<0.001
LVESVI	30.2 ± 5.2	26.7 ± 5.6	<0.001
LVSVI	53.5 ± 10.7	53.0 ± 10.1	1.0
LVEF	63.8 ± 3.6	66.6 ± 4.7	0.036
RVEDVI	90.0 ± 17.8	87.6 ± 16.7	0.828
RVESVI	38.6 ± 8.9	26.9 ± 8.7	0.024
RVSVI	51.3 ± 11.1	51.7 ± 9.4	1.0
RVEF	57.1 ± 5.2	59.4 ± 5.1	0.12

Ao = Aortic, MPA = Main Pulmonary Artery, CI = Cardiac Index, LV = Left ventricular; RV = Right ventricular; EDVi = Indexed end diastolic volume; ESVi = Indexed end systolic volume; SVi = Indexed stroke volume; EF = Ejection fraction;

Cardiac Index, heart rate and SVI

Cardiac index was higher at rest during hypoxia, driven by a higher heart rate, with no change in Ao, MPA, LV or RV SVI.

Right Ventricle

There was no difference in RVEDVI or RVEF during hypoxia at rest compared to normoxia. RVESVI was significantly smaller (p <0.024), however, there was a significant difference in RVESVI post exercise but pre hypoxia that may influence this result.

Left Ventricle

LVEDVI and LVESVI were significantly smaller at rest during hypoxia, compared to normoxia (p <0.001 for both comparisons). LVEF was significantly higher at rest during hypoxia (p = 0.036)

6.4.3 Effects of Hypoxia on Atrial size

Table 6.3: Comparison of Left and Right Atrial size from Normoxia to Hypoxia

	Normoxia	**Hypoxia**	**P value**
Left Atrial Area	24.1 ± 5.4	21.0 ± 9.3	0.032
Right Atrial Area	24.8 ± 5.9	25.0 ± 5.4	0.621

There was a significant decrease in left atrial size at rest, p=0.032

6.4.4 Effects of Hypoxia on Interventricular septum

Table 6.4: Effect of Hypoxia on the Interventricular Septum

	Normoxia	Hypoxia	P value
Rest	0.91 ± 0.2	0.81 ± 0.2	<0.0001

There was a significant flattening of the interventricular septum, p <0.0001

6.5.5 Biventricular Response from Rest to Exercise during Hypoxia

The response of heart rate, cardiac index and biventricular function is summarized in Table 6.5.

Table 6.5: Comparison of Heart rate, Cardiac Index and Biventricular Parameters from Rest to Exercise, during Hypoxia

Outcome Variable	Hypoxia Rest	Hypoxia Exercise	P value
HR (bpm)	74.5 ± 12.2	142.8± 12.2	<0.0001
Ao SVi (ml/m^2)	50.4 ± 12.3	58.3 ± 11.4	<0.0001
MPA SVi (ml/m^2)	51.6 ± 9.8	56.2 ± 10.9	0.05
CI (l/min/m^2)	3.6 ± 0.7	8.3 ± 1.8	<0.0001
LV EDVi (ml/m^2)	79.9±13.8	81.5±13.6	1.0
LV ESVi (ml/m^2)	26.7 ± 5.6	20.6 ± 5.2	<0.0001
LV SVi (ml/m^2)	53.0 ± 10.1	60.7 ± 10.3	<0.0001
LV EF (%)	66.6 ± 4.7	74.7 ± 4.3	0<0.0001
RV EDVi (ml/m^2)	87.6 ± 16.7	82.5 ± 15.4	0.132
RV ESVi (ml/m^2)	35.8 ± 9.4	25.6 ± 8.9	<0.0001
RV SVi (ml/m^2)	51.7 ± 9.4	56.7 ± 10.0	<0.0001
RVEF (%)	59.4 ± 5.1	69.9 ± 6.3	<0.0001

6.5.5.1 Cardiac Index, Heart Rate and Stroke Volume Index

There is a significant increase in heart rate (p<0.0001), cardiac index (p < 0.0001), Ao stroke volume (p < 0.0001) and MPA stroke volume (p = 0.05) during hypoxic exercise.

6.5.5.2 Right Ventricular Volumes and Ejection Fraction

There is an increase in RVSVI on exercise (p < 0.0001) that is driven by a decrease in RVESVI (p < 0.0001), with no change in RVEDVI (p=0.132).

6.5.5.3 Left Ventricular Volumes and Ejection Fraction

There is an increase in LVSVI on exercise (p < 0.0001) that is driven by a decrease in LVESVi (p < 0.0001) with no change in LVEDVI (p = 1.0).

6.5.6 Biventricular Response from Rest to Exercise: Comparison of Normoxia to Hypoxia

The interaction of exercise and oxygen level, on the change of heart rate, cardiac index and biventricular function is summarized in Table 6.6. Simple main effects analysis comparing exercise parameters during normoxia to hypoxia is summarized in Table 6.7.

Table 6.6: Interaction between Oxygen level and the effect on Exercise: Comparison of Heart rate, Cardiac Index and Biventricular Function from Rest to Exercise, during Normoxia and Hypoxia

Outcome Variable	Normoxia		Hypoxia		Interaction of effect of oxygen
	Rest	Exercise	Rest	Exercise	

					level on exercise: p value
HR (bpm)	61.6 ± 10.6	123.0± 10.5	74.5 ± 12.2	142.8± 12.2	0.004
Ao SVi (ml/m^2)	51.3 ± 10.9	62.0 ± 10.3	50.4 ± 12.3	58.3 ± 11.4	0.048
MPA SVi (ml/m^2)	51.3 ± 9.9	60.2 ± 9.3	51.6 ± 9.8	56.2 ± 10.9	0.014
CI (l/min/m^2)	3.1 ± 0.6	7.6 ± 1.5	3.6 ± 0.7	8.3 ± 1.8	0.328
LV EDVi (ml/m^2)	83.7 ± 14.6	89.6 ± 15.1	79.9±13.8	81.5±13.6	<0.0001
LV ESVi	30.2 ± 5.2	25.0 ± 6.7	26.7 ± 5.6	20.6 ± 5.2	0.375
LV SVi (ml/m^2)	53.5 ± 10.7	64.6 ± 10.7	53.0 ± 10.1	60.7 ± 10.3	0.001
LV EF (%)	63.8 ± 3.6	72.2 ± 4.5	66.6 ± 4.7	74.7 ± 4.3	0.958
RV EDVi (ml/m^2)	90.0 ± 17.8	88.3 ± 15.2	87.6 ± 16.7	82.5 ± 15.4	0.036
RV ESVi	38.6 ± 8.9	26.9 ± 8.7	35.8 ± 9.4	25.6 ± 8.9	0.322
RV SVi (ml/m^2)	51.3 ± 11.1	61.3 ± 10.0	51.7 ± 9.4	56.7 ± 10.0	<0.0001
RVEF (%)	57.1 ± 5.2	69.9 ± 6.3	59.4 ± 5.1	69.1 ± 6.6	0.017

Ao = Aortic, MPA = Main Pulmonary Artery, CI = Cardiac Index, LV = Left ventricular; RV = Right ventricular; EDVi = Indexed end diastolic volume; ESVi = Indexed end systolic volume; SVi = Indexed stroke volume; EF = Ejection fraction;

Table 6.7: Simple main effects analysis: Comparison of Heart rate, Cardiac Index and Biventricular Parameters on Exercise, during Normoxia vs. Hypoxia

Outcome Variable	Normoxia Exercise	Hypoxia Exercise	P value
HR (bpm)	123.0± 10.5	142.8± 12.2	<0.0001

Ao SVi (ml/m^2)	62.0 ± 10.3	58.3 ± 11.4	0.012
MPA SVi (ml/m^2)	60.2 ± 9.3	56.2 ± 10.9	0.012
CI (l/min/m^2)	7.6 ± 1.5	8.3 ± 1.8	<0.0001
LV EDVi (ml/m^2)	89.6 ± 15.1	81.5±13.6	<0.0001
LV ESVi (ml/m^2)	25.0 ± 6.7	20.6 ± 5.2	<0.0001
LV SVi (ml/m^2)	64.6 ± 10.7	60.7 ± 10.3	<0.0001
LV EF (%)	72.2 ± 4.5	74.7 ± 4.3	0.036
RV EDVi (ml/m^2)	88.3 ± 15.2	82.5 ± 15.4	<0.0001
RV ESVi (ml/m^2)	26.9 ± 8.9	25.6 ± 8.9	1.0
RV SVi (ml/m^2)	61.3 ± 10.0	56.7 ± 10.0	<0.0001
RVEF (%)	69.9 ± 6.3	69.9 ± 6.3	1.0

6.5.6.1 Heart Rate

There was significant interaction between the effects of oxygen level and exercise on heart rate (p=0.004) with a more pronounced increase of heart rate during hypoxia. (Figure 6.1). Simple main effects analysis showed that heart rate was higher at rest and also on exercise, p < 0.0001

Figure 6.1 – Change in Heart Rate from Rest to Exercise, during Normoxia and Hypoxia

Change in Heart Rate from Rest to Exercise, during Normoxia and Hypoxia
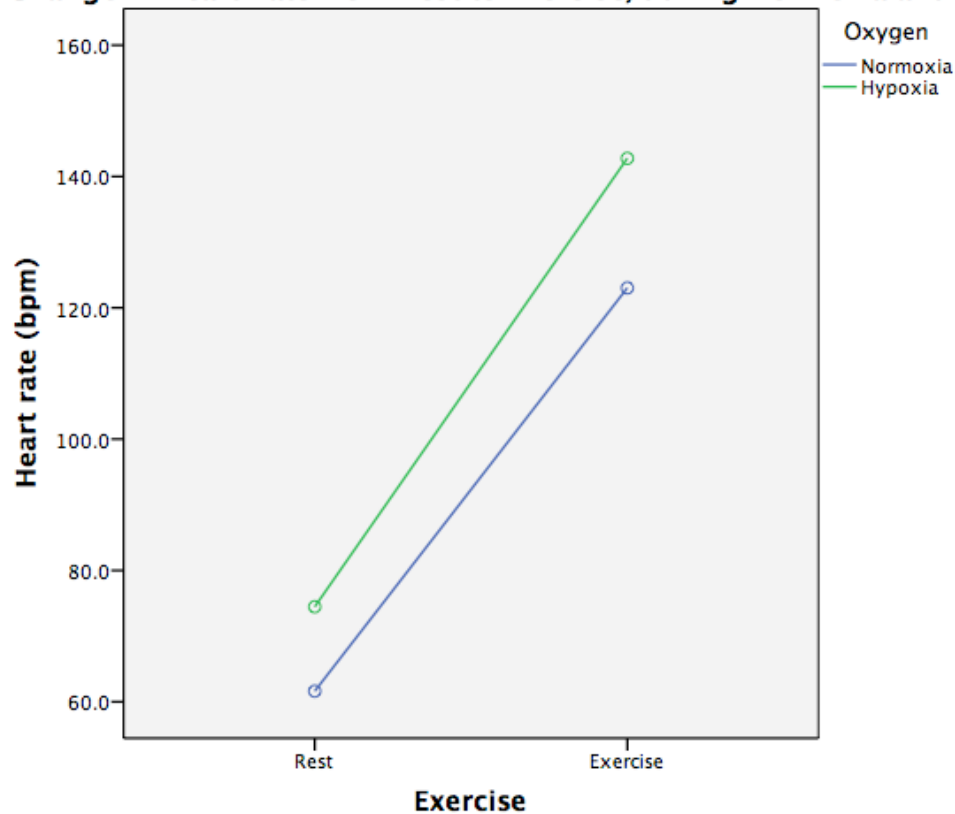
6.5.6.2 Cardiac Index

There was no significant interaction between the effects of hypoxia on the change of CI on exercise (p=0.328). Simple main effects analysis showed that CI was significantly higher at rest (p<0.001) and exercise (p<0.0001)

6.5.6.3 Aortic and MPA Stroke Volume

There was a significant interaction between the effects of hypoxia on the change of aortic and MPA SVI on exercise (Ao SVI, p=0.048, Figure 6.2 and MPA SVI, p=0.014, Figure 6.3). Simple main effects analysis showed that this was driven by a significant difference between aortic and MPA SVI during hypoxic exercise (p=0.012 for both comparisons), and that there was no difference at rest (p = 1.0 for both comparisons).

Figure 6.2 – Change in Ao SVI from Rest to Exercise during Normoxia and Hypoxia

Change in Ao SVI from Rest to Exercise, during Normoxia and Hypoxia
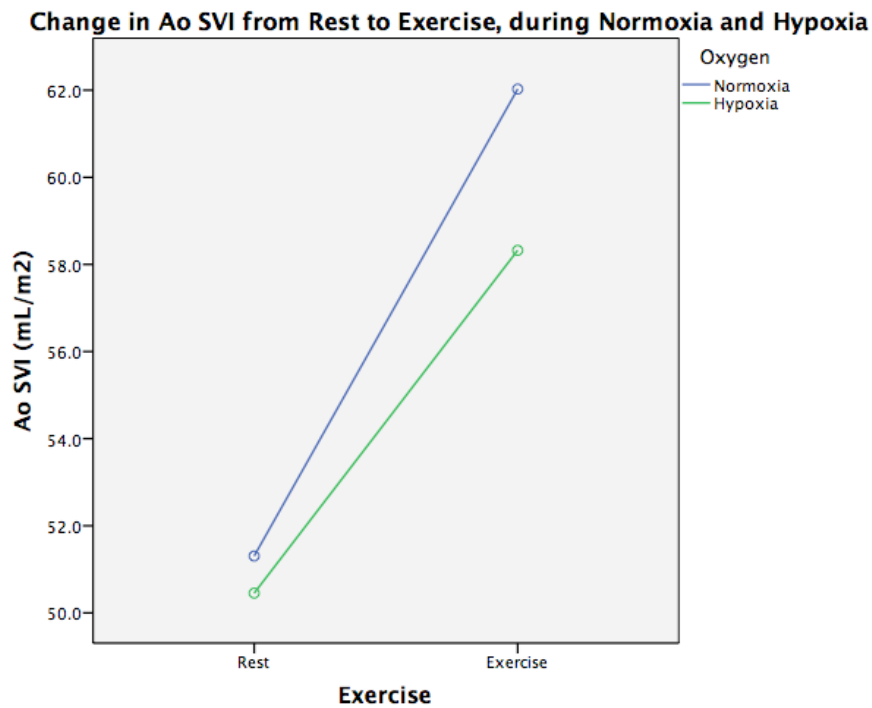
Figure 6.3 – Change in MPA SVI from Rest to Exercise during Normoxia and Hypoxia

Change in MPA SVI from Rest to Exercise, during Normoxia and Hypoxia
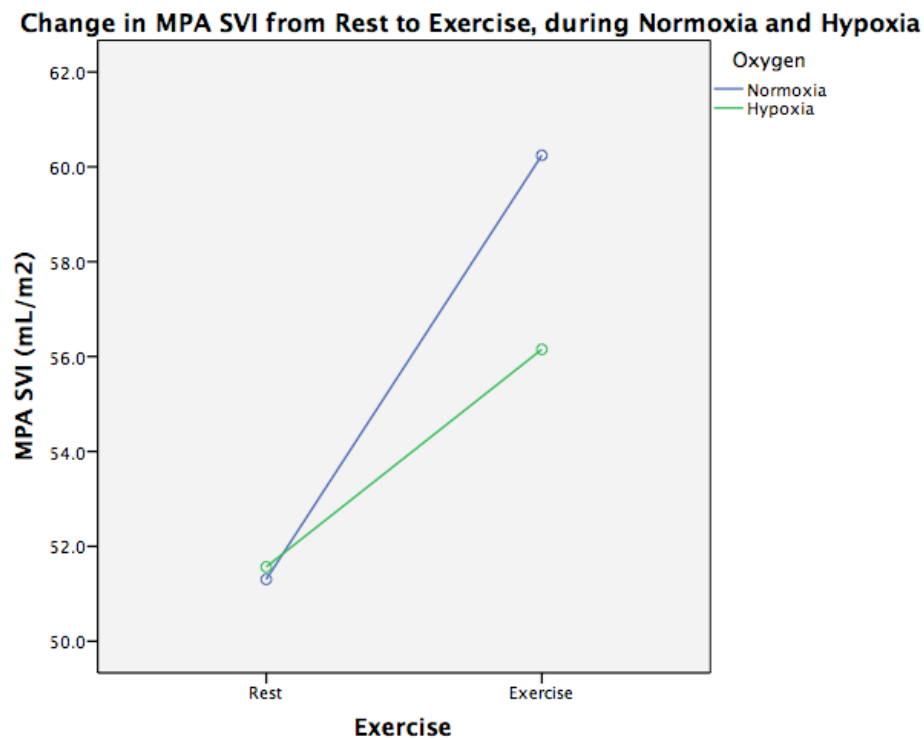
6.5.6.4 Left and Right Ventricular Stroke Volume

There was a significant interaction of hypoxia on the change of LVSVI (p=0.001) and RVSVI (p<0.0001) on exercise (Figure 6.4 and 6.5 respectively). Simple main effects analysis showed that was driven by a lower RVSVI and LVSVI during hypoxic exercise compared to normoxic exercise on simple main effects analysis (p<0.0001 for both comparisons). There was no difference at rest (p = 1.0 for both comparisons).

Figure 6.4: Change in LVSVI from Rest to Exercise, during Normoxia and Hypoxia
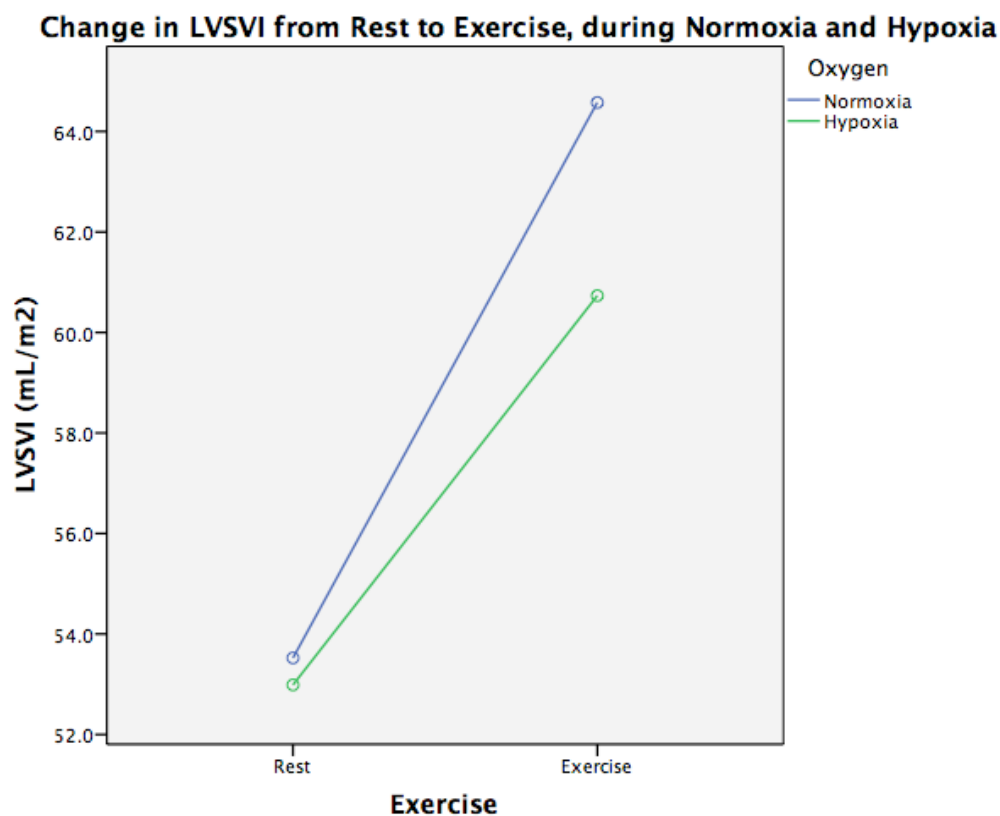
Figure 6.5: Change in RVSVI from Rest to Exercise, during Normoxia and Hypoxia

Change in RVSVI from Rest to Exercise, during Normoxia and Hypoxia
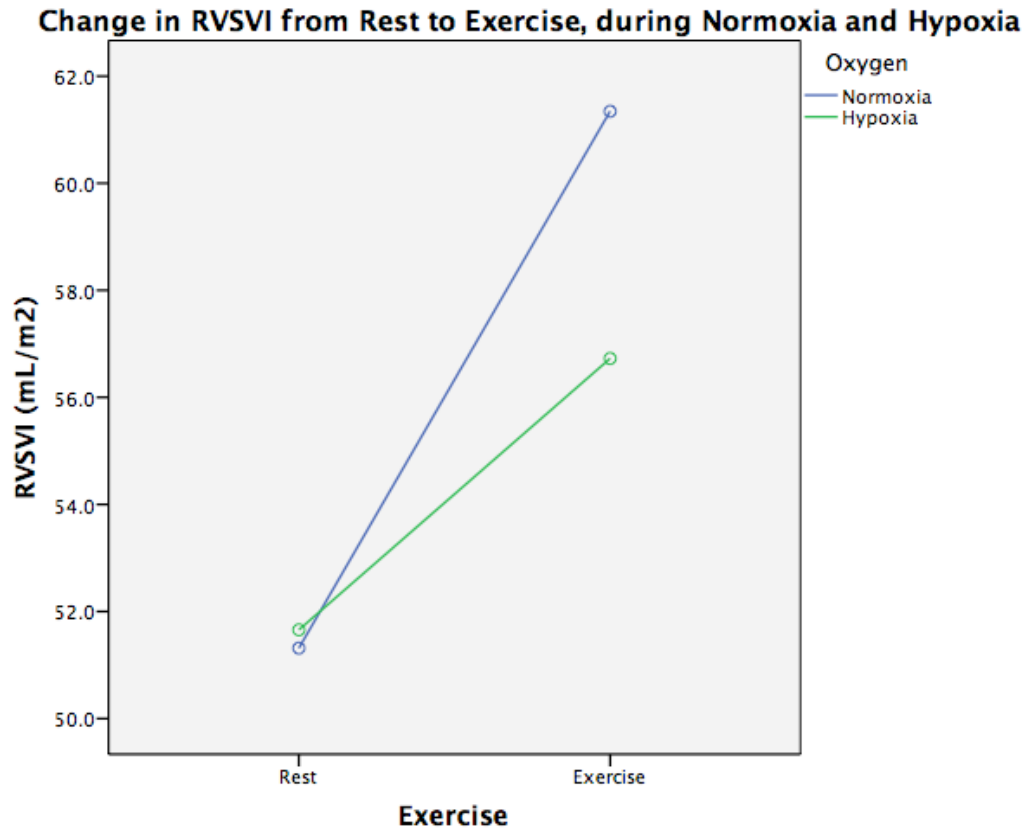
6.5.6.5 Left Ventricular Volumes and Ejection Fraction

There was a significant interaction between the effects hypoxia on change of LVEDVI on exercise (p <0.0001, Figure 6.6). Simple main effects showed that LVEDVI increased during normoxic exercise (p <0.0001), but did not increase during hypoxic exercise (p=0.112) and that LVEDVI was lower at rest and exercise, during normoxia and hypoxia (p<0.0001).

There was no interaction with the change in LVESVI, p = 0.375 or LVEF p=0.958. Simple main effects analysis showed that LVESVi was smaller and LVEF higher at rest and exercise during hypoxia, compared to normoxia (p<0.0001 for all comparisons except LVEF at exercise, p=0.036)

Figure 6.6: Change in LVEDVI from Rest to Exercise, during Normoxia and Hypoxia

Change in LVEDVI from Rest to Exercise, during Normoxia and Hypoxia
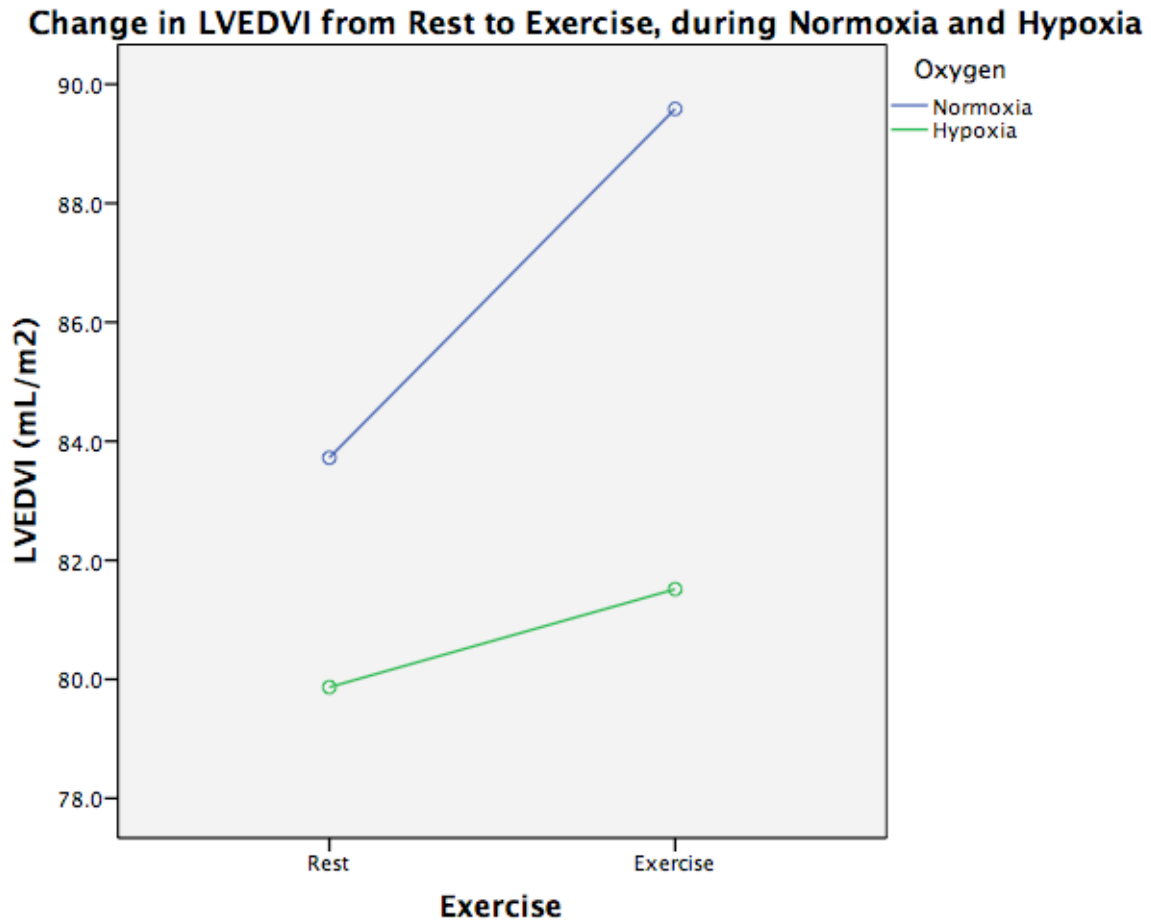
6.5.6.6 Right Ventricular Volumes and Ejection Fraction

There was a significant interaction between hypoxia and change of RVEDVI on exercise (p=0.036, Figure 6.7). This was driven by a significantly smaller RVEDVI was during hypoxic exercise than normoxic exercise (p < 0.0002), with no significant difference at rest (p = 0.828)

There was no interaction between the effects of oxygen level and exercise on RVESVi, p = 0.322. However, while RVESVI was significant lower at rest (p = 0.024), RVESVi was not significantly different on hypoxic exercise (p=0.294).

There was a significant interaction of hypoxia on the change RVEF on exercise (p=0.017, Figure 6.8). There was no difference between rest and exercise RVEF during normoxia or hypoxia (p=0.12 and 1.0 respectively), hence the rise in RVEF on exercise during hypoxia was less than during normoxic exercise.

Figure 6.7: Change in RVEDVI from Rest to Exercise, during Normoxia and Hypoxia
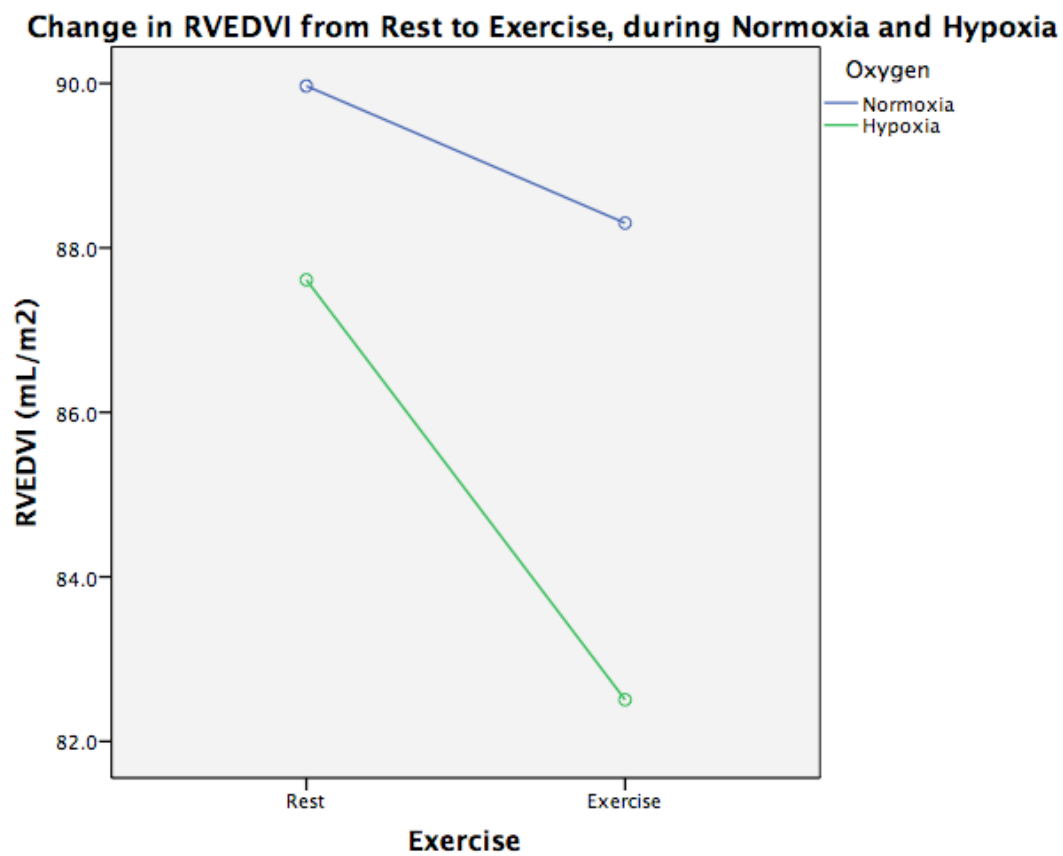
Figure 6.8: Change in RVEF from Rest to Exercise, during Normoxia and Hypoxia

Change in RVEF from Rest to Exercise, during Normoxia and Hypoxia
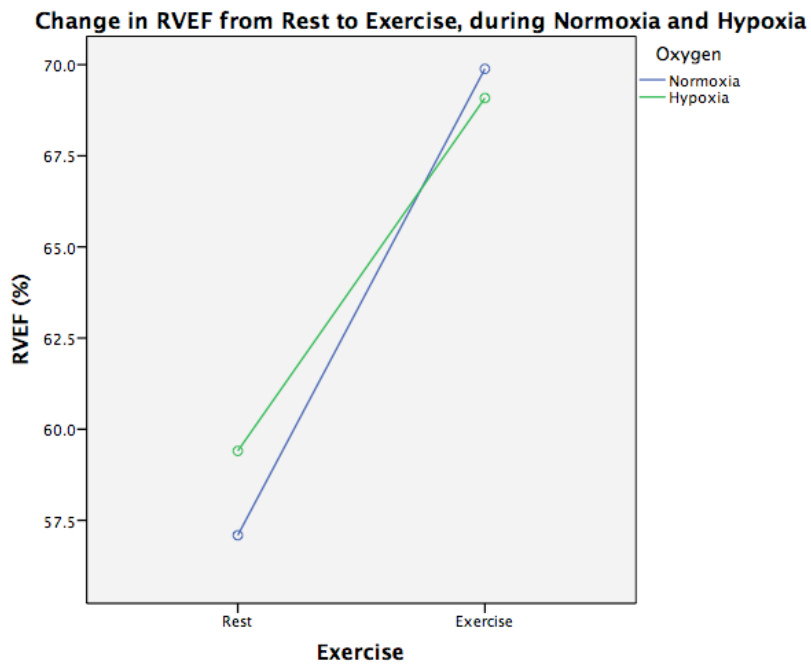
Figure 6.8a – Change in RVEF from Rest to Exercise during Hypoxia for each Individual
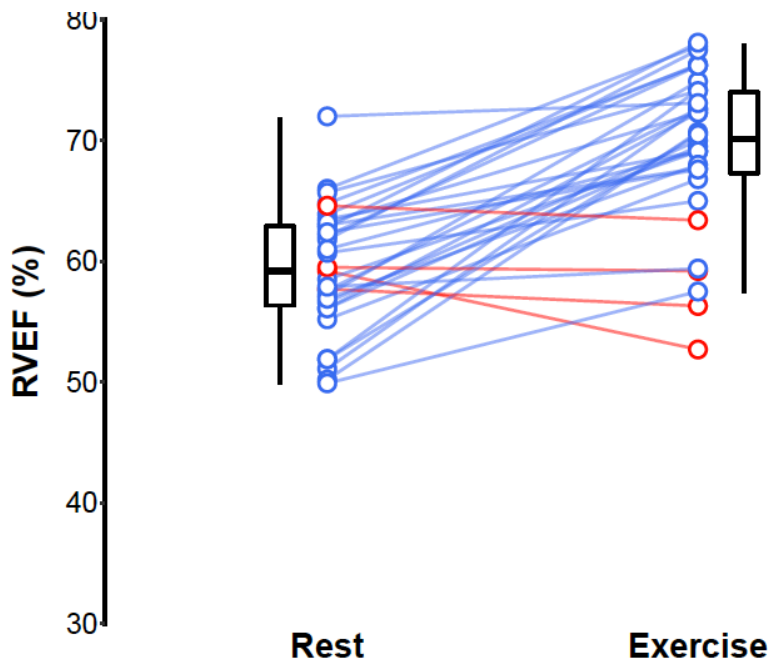
6.5.7 Biventricular Response from Rest to Immediately after Exercise

The response of heart rate, cardiac index and biventricular parameters as assessed from immediately after exercise during hypoxia are summarized in Table 6.8.

Table 6.8: Comparison of Heart rate, Cardiac Index and Biventricular Parameters from Rest to Immediately after Exercise, during Hypoxia

Outcome Variable	Hypoxia Rest	Hypoxia IAE	P value
HR (bpm)	73.9 ± 11.9	110.0 ± 25.1	<0.0001
Ao SVi (ml/m^2)	50.5 ± 12.4	61.7 ± 13.1	<0.0001
MPA SVi (ml/m^2)	51.2 ± 9.6	57.5 ± 11.6	<0.0001
CI (l/min/m^2)	3.6 ± 0.7	6.7 ± 2.0	<0.0001
LV EDVi (ml/m^2)	78.5 ± 13.0	84.9 ± 13.7	<0.0001
LV ESVi (ml/m^2)	25.8 ± 4.9	20.0 ± 3.9	<0.0001
LV SVi (ml/m^2)	52.5 ± 9.9	65.0 ± 11.3	<0.0001
LV EF (%)	67.0 ± 4.5	76.4 ± 3.1	<0.0001
RV EDVi (ml/m^2)	85.8 ± 15.8	87.4 ± 15.0	0.369
RV ESVi (ml/m^2)	35.0 ± 8.4	23.4 ± 7.3	<0.0001
RV SVi (ml/m^2)	50.8 ± 9.4	64.1 ± 10.3	<0.0001
RVEF (%)	59.3 ± 4.8	73.6 ± 5.1	<0.0001

Heart Rate, Cardiac Index and Stroke Volume

There is a significant increase in heart rate, cardiac index and aortic and MPA stroke volume, $p < 0.0001$ for all comparisons.

Right Ventricular Volumes and Function

There is an increase of RVSVI, which is driven by a decrease in RVESVI ($p < 0.0001$ for both comparisons.) There is no change in RVEDVI.

Left Ventricular Volumes and Function

There is an increase in LVSVI, which is driven by an increase in LVEDVI and a decrease in LVESVI (p < 0.0001).

6.5.8: Biventricular Response from Rest to Immediately after Exercise: Comparison of Normoxia and Hypoxia

The interaction between normoxia and hypoxia and changes in biventricular parameters from rest to immediately after exercise is summarized in Table 6.9. The simple main effects comparing normoxia to hypoxia biventricular parameters immediately after exercise are summarized in Table 6.10.

Table 6.9: Comparison of the interaction between Normoxia and Hypoxia on Heart rate, Cardiac Index and Biventricular Function from Rest to Immediately After Exercise, during Normoxia and Hypoxia

Outcome Variable	Normoxia		Hypoxia		Exercise*Oxygen
	Rest	IAE	Rest	IAE	
HR (bpm)	61.6 ± 10.8	92.1 ± 15.9	74.1 ± 12.1	110.0 ± 25.1	0.127
Ao SVi (ml/m^2)	51.3 ± 11.2	65.1 ± 12.8	50.3 ± 12.6	61.7 ± 13.1	0.08
MPA SVi (ml/m^2)	50.9 ± 10.2	62.1 ± 11.6	51.1 ± 9.7	57.5 ± 11.6	0.014
CI (l/min/m^2)	3.1 ± 0.6	6.0 ± 1.5	3.6 ± 0.7	6.7 ± 2.0	0.198
LV EDVi (ml/m^2)	82.3 ± 13.8	90.9 ± 16.0	78.5 ± 13.0	84.9 ± 13.7	0.025
LV ESVi	29.9 ± 5.3	26.0 ± 4.7	25.8 ± 4.9	20.0 ± 3.9	0.023
LV SVi (ml/m^2)	52.3 ± 9.7	64.9 ± 13.7	52.5 ± 9.9	65.0 ± 11.3	0.905

Outcome Variable					P value
LV EF (%)	63.8 ± 3.6	71.1 ± 4.2	66.6 ± 4.7	76.4 ± 3.1	0.047
RV EDVi (ml/m^2)	90.0 ± 17.8	89.2 ± 18.3	87.6 ± 16.7	87.4 ± 15.0	0.955
RV ESVi	38.9 ± 8.8	25.8 ± 8.1	35.0 ± 8.4	23.4 ± 7.3	0.766
RV SVi (ml/m^2)	51.3 ± 11.1	63.4 ± 12.4	51.7 ± 9.4	64.1 ± 10.3	0.810
RVEF (%)	57.1 ± 5.2	71.4 ± 5.0	59.4 ± 5.1	73.6 ± 5.1	0.714

Table 6.10: Simple main effects analysis: Heart Rate, Cardiac Index and Biventricular Parameters Immediately After Exercise during Normoxia and Hypoxia

Outcome Variable	Normoxia Immediately After Exercise	Hypoxia Immediately After Exercise	P value
HR (bpm)	91±16	110.0 ± 25.1	<0.0001
Ao SVi (ml/m^2)	64.7 ± 12.3	61.7 ± 13.1	0.048
MPA SVi (ml/m^2)	62.1 ± 11.2	57.5 ± 11.6	0.012
CI (l/min/m^2)	5.9 ± 1.6	6.7 ± 2.0	0.012
LV EDVi (ml/m^2)	91.2 ± 16.4	84.9 ± 13.7	<0.0001
LV ESVi (ml/m^2)	26.2 ± 5.3	20.0 ± 3.9	<0.0001
LV SVi (ml/m^2)	65.1 ± 13.2	65.0 ± 11.3	1.0
LV EF (%)	71.1 ± 4.2	76.4 ± 3.1	<0.0001
RV EDVi (ml/m^2)	89.2 ± 18.3	87.4 ± 15.0	1.0
RV ESVi (ml/m^2)	25.8 ± 8.1	23.4 ± 7.3	0.564
RV SVi (ml/m^2)	63.4 ± 12.4	64.1 ± 10.3	1.0
RVEF (%)	71.4 ± 5.0	73.6 ± 5.1	0.228

Heart Rate

There is no significant interaction between hypoxia and normoxia and the change of heart rate when comparing rest to immediately after exercise. (p = 0.127). However, heart rate is higher during hypoxia than normoxia immediately aft exercise (p < 0.0001)

Cardiac Index

There is no significant interaction between hypoxia and the change of cardiac index. Cardiac index is significantly higher immediately after exercise during hypoxia, than normoxia, p = 0.012.

Aortic and MPA Stroke Volume Index

There is no significant interaction between hypoxia and the change of aortic SVI (p = 0.08) although on simple main effects analysis, aortic SVI is slightly lower immediately after hypoxic exercise, than normoxic exercise, p = 0.048. There is a significant interaction between hypoxia and the change of MPA SVI (p = 0.014). Simple main effects shows that MPA SVI is significantly lower immediately after hypoxic exercise, than normoxic exercise, p = 0.012.

Left Ventricular Volumes and Function

There is a significant interaction between normoxia and hypoxia, and change in LVEDVI from rest to immediately after exercise in both conditions, normoxia and hypoxia (Figure 6.9). However, simple main effects analysis shows there is a significant increase in LVEDVI from rest to immediately after exercise, p < 0.0001, which contrasts to no increase in LVEDVI during continuous exercise, suggesting an improvement in LV filling immediately after.

There was a significant interaction between changes in LVESVI from rest to immediately after exercise, p = 0.025 (Figure 6.10), with a bigger decrease in LVESVI during hypoxia

immediately after exercise compared to normoxia, p <0.0001. There was no interaction and

no significant difference between resting or exercise values of LVSVI.

Figure 6.9: Change in LVEDVI from Rest to Immediately after Exercise

Change in LVEDVi from Rest to Immediately after Exercise, Normoxia vs Hypoxia
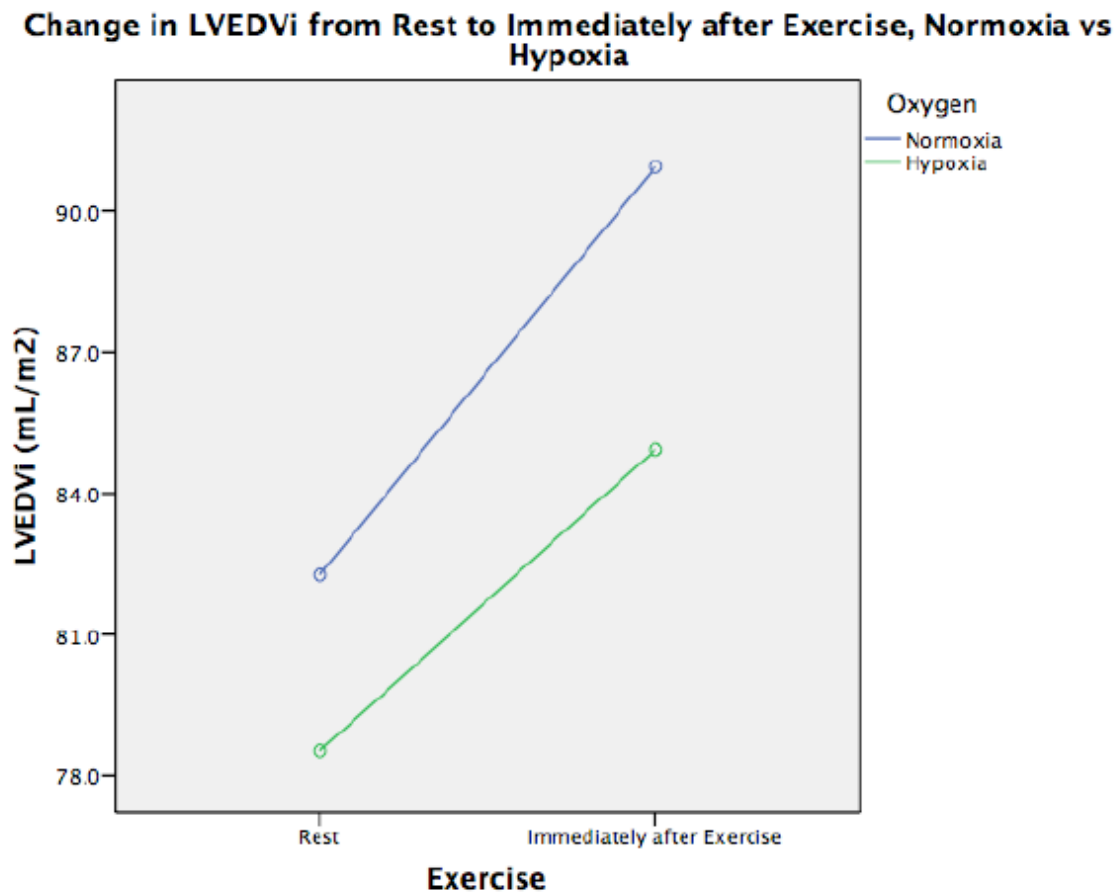
Figure 6.10: Change in LVESVi from Rest to Immediately after Exercise

Change in LVESVi from Rest to Immediately after Exercise, in Normoxia vs Hypoxia
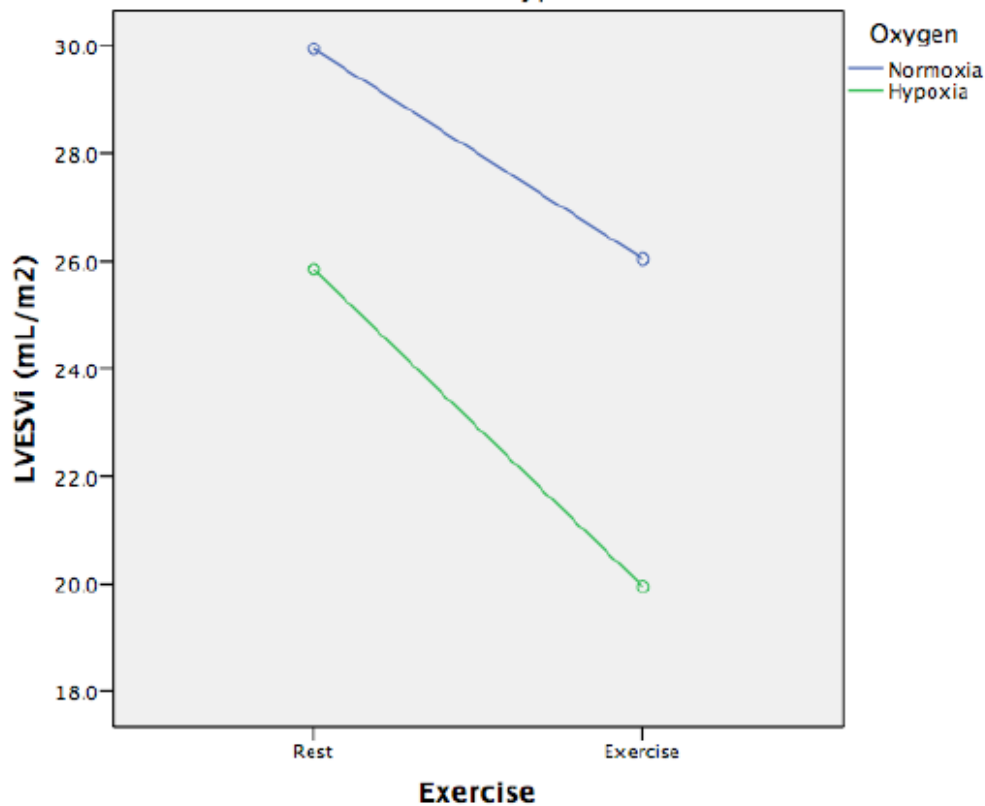
Right Ventricular Volumes and Function

There was no significant interaction of change in RVEDVI, RVESVI, RVSVI or RVEF between hypoxia and normoxia, rest to immediately after exercise, with no significant difference between these parameters immediately after exercise on simple main effects analysis.

6.5.9 MPA Area, Pulsatility and Velocities

Table 6.11: Comparison of MPA Area, Pulsatility and Velocities from Rest to Exercise during Hypoxia

MPA Parameter	Hypoxia Rest	Hypoxia Exercise	P value
Maximum Area	8.4 ± 1.3	9.1 ± 1.6	0.01
Minimum Area	5.8 ± 1.1	6.3 ± 1.1	0.06
Pulsatility	48.3 ± 23.5	45.2 ± 14.6	1.0
Peak Velocity	62.4 ± 14.1	91.6 ± 26.1	<0.0001
Average Velocity	12.1 ± 2.5	13.1 ± 3.3	0.065

MPA Area

Maximum MPA area increased in size on hypoxic exercise, p=0.01, however, there was no significant increase in MPA minimum area p = 0.06. There was no significant change in MPA pulsatility, p=1.0.

MPA Velocities

There was a significant increase in MPA Peak velocity, p < 0.0001, however, the increase in MPA average velocity was not significant, p=0.065.

When analyzing the interaction between hypoxia and normoxia on the change of MPA size, pulsatility and velocities, there were no significant interactions. However, the change of average MPA velocity on hypoxic exercise trended towards significance, p = 0.059, with a trend for the rise of MPA average velocity during hypoxic exercise to be lower, than that of normoxic exercise (Figure 6.9)

Figure 6.11: Change of MPA Average Velocity from Rest to Exercise, during Normoxia and Hypoxia

Change of MPA Average Velocity from Rest to Exercise during Normoxia and Hypoxia
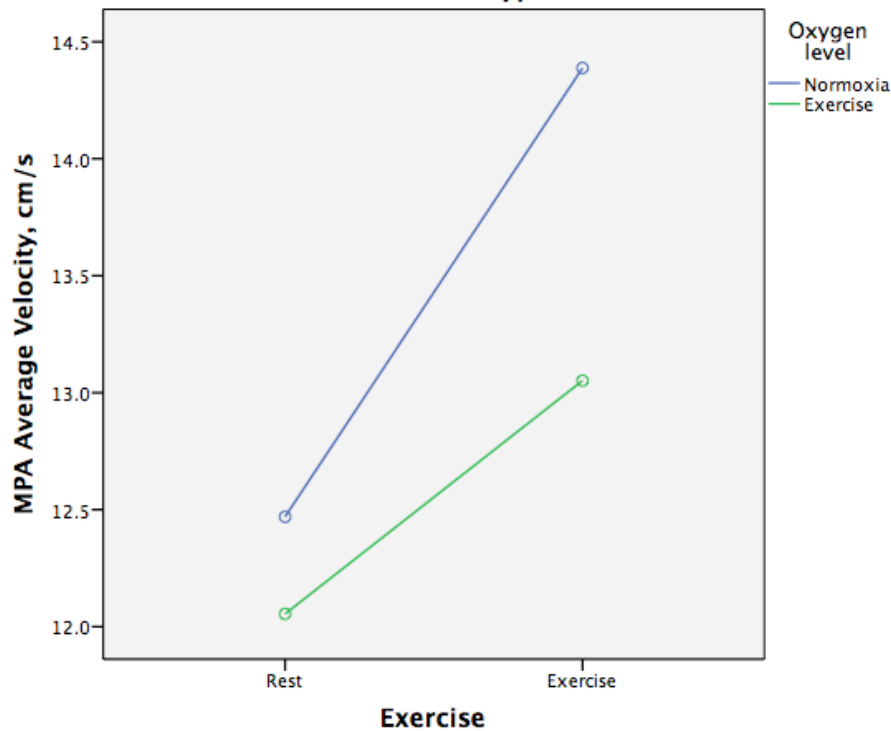
p = 0.065

n=34

6.6 Discussion

6.6.1 Changes at Rest with Hypoxia

We have shown that during acute hypoxia at rest, there is a decrease in LV volumes, an increase in LV contractility reflected in a marginally higher LVEF, with no change in RV volumes or RVEF. There was no change in right or left sided stroke volume, but an increase in cardiac index driven by a higher heart rate. This is likely to be the consequence of sympathetic nervous system activation. Furthermore, we have shown a shift in the interventricular septum, as well as a decrease in left atrial area.

It is well accepted acute hypoxia leads to an increase in heart rate and cardiac output, with no change in resting stroke volume at rest and our results are consistent with that(114-116). At rest, acute hypoxia increases heart rate and cardiac output, with no change in SV. During submaximal exercise during acute hypoxia, it is recognized that initially CO at any workload is higher, but VO_2 peak is blunted by a decrease in maximum heart rate. It is believed that SV is also blunted, but never demonstrated on an imaging study. We also showed that LVEDVI and LVESVI were smaller at rest with a higher LVEF. A resting LVSA was performed, after the a period of rest and before inducing hypoxia, to ensure that exercise was not a confounder, and it was shown that LV volumes and ejection fraction had returned to baseline. Hence we can conclude that these findings are a true consequence of acute hypoxia.

A reduction in LV volumes has also been demonstrated, on echocardiography, in other studies, however most have allowed a degree of acclimatization. Stembridge et al demonstrated that after 10 days of high altitude exposure in lowlanders, LVEDVI was 19% lower at rest and did not increase in size during exercise, despite evidence of enhanced diastolic relaxation on speckle tracking analysis (252). This is supported by Boussuges et al, who demonstrated that aortic and LV diameters fell regularly on simulated ascent to altitude, with a change in LV diastolic filling parameters, and no elevation of LV end diastolic pressure(120). Allemann et al similarly demonstrated an increased LVEF with changes in LV diastolic filling parameters in children and adolescents on rapid ascent to high altitude(253). However, it could be argued that the mechanisms leading to a change in LV size after acclimatization, could be due to reduced plasma volume, which would not contribute during acute hypoxic exposure, and Reciehnberger at al reported no change in LV systolic or diastolic parameters on acute hypoxic exposure, using echocardiography (115). However, we hypothesize that the cause of the

decrease in LVEDV at rest could be due to sympathetic nervous system activation and LV under-filling,

Acute hypoxic exposure has been shown to markedly elevate noradrenaline levels(254-256). Furthermore, sympathetic nervous system activation has been shown to decrease LVEDV, LVESV and increase LVEF in dogs (257). LV under-filling could also contribute given that other studies have demonstrated changes in diastolic filling patterns at rest, however, there is no demonstrable change in RV forward flow or RVSV so this may be less likely.

We also showed no change in RV function at rest in acute hypoxia. Stembridge et al showed no change in RVEDVI at rest in lowlanders after 10 days of acclimatization. Oliver et al showed during acute hypoxic exposure, that there was no change in RV volumes, stroke volume or ejection fraction at rest(123), and Reichenberger et al demonstrated that while sPAP increases during acute hypoxia, indices of RV contractility do not change at rest (115). Pavelescu et al also demonstrated that while acute hypoxia increases PVR, indices of RV systolic function remain the same. They noted a change in RV filling, with a decrease in the tricuspid E:A ratio(121). Conversely, Netzer et al found that acute hypoxia increased RV dimensions as measured on echo (122), and Allemann et al found that RVEDVi area decreased in children and adolescents at high altitude (253). This could be a reflection of the limitation of echocardiography to accurately assess RV size and dimensions, and hence, only indirect signs of RV function such as TAPSE or the TEI index can be reliably reported. For both the LV and RV volume changes, it could be argued that as MRI is a more accurate method of assessing biventricular volumes and this is the first study to assess biventricular volumes at rest during acute hypoxia using MRI, that our findings are likely to be more sensitive and accurate to detecting subtle changes, than previous studies that used echocardiography or radionuclide

ventriculography. Hence changes in diastolic filling pattesr would appear to be less likely based on our data.

6.6.2 Changes on Exercise with Hypoxia

During hypoxic exercise, we have demonstrated a reduction in RV forward flow with blunting of the rise in MPA SVI and RVSVI, with a decrease in RVEDVI and blunting of the rise in RVEF. Furthermore, LVEDVI does not increase on exercise, with a blunting of the rise in LVSVI and Ao SVI, despite a decrease in LVESVI and a higher LVEF. These changes are suggestive of increased pulmonary vascular resistance leading to a reduction in RV forward flow and blunting of the rise of RVEF, with the decrease in RVEDVI as an adaptive mechanism to cope with the increased afterload. This leads to LV under-filling, a reduction in LV preload and diastolic stretch, and hence a reduction in LVSVI and Ao SVI, despite an increase in LV contractility from sympathetic nervous system activation.

A number of studies have demonstrated evidence of RV strain on acute hypoxic exercise. Kjaergaard et al showed that RV contractility as measured by isovolumic acceleration on echocardiography is impaired during hypoxic exercise, and is restored to normal values when sildenafil is given (126). Evidence of RV strain during acute hypoxia, which is restored or partially restored with pulmonary vasodilators, has been reported in several studies using echocardiography. Reichenberger et al shown that Sildenafil administration reduced sPAP and the TEI index during acute hypoxia, as compared to placebo (115) . Naeije et al showed that Sitaxsentan decreased PVR and restored VO2 max on CPET by 30% during acute hypoxic exercise, and by 10% after chronic hypoxic exposure, suggesting that by reducing hypoxic pulmonary vasoconstriction, RV forward flow improved (125). Similarly, Faoro et al showed

that Bosentan restored VO2 max by 30% during acute hypoxic exercise (258) and Ghofrani et al showed that Sildenafil decreased sPAP at rest and exercise at high altitude, and improved exercise capacity (259). Furthermore, Hsu et al have shown a reduction in stroke volume using a thoracic impedance method during acute hypoxic exercise, which was restored with sildenafil (260). Together, these studies support the hypothesis that acute hypoxic pulmonary vasoconstriction leads to signs of RV strain on exercise and a reduction of VO2 peak, which is partially restored with pulmonary vasodilators. However, ours is the first imaging study to our knowledge, to directly document a reduction in RVSVI and MPA SVI, with evidence of blunting of the rise of RVEF. Previously studies using echocardiography have only been able to provide indirect evidence, and hence this demonstrates the ability of exercise MRI, to assess exercise RV reserve in detail.

We have also shown a reduction in RVEDVI on acute hypoxic exercise. This has never been shown before, however, there have been now acute hypoxic exercise MRI studies to date. Our study in healthy volunteers, showed that normal exercise is characterized by no significant change in RVEDVI. Exercise imposes a large increase in RV wall stress, documented to be up to 125% compared to a 14% increase in LV wall stress (261). During hypoxic exercise, the mPAP-flow relationship is further shifted, posing higher pressures on the RV (112, 114). The RV is known to adapt to chronic exposure to this higher stress, by evidence of RV remodeling by way of an increase in RVEDVI and mass in athletes and recreationally fit subjects (262-264). We have also demonstrated in our healthy volunteers, than an increase in biventricular volumes at rest and exercise correlate with a higher VO2 peak. However, those exposed to chronic hypoxia, have demonstrated lower RV and LVSV, reduced early diastolic filling of both the LV and RV, and decreased RV and LV volumes, which are likely to reflect an impact

of chronically elevated pulmonary pressures, ventricular under-filling, as well as hypovolaemia(265, 266).

However no study to date, has demonstrated how the healthy RV adapts to an acute increase in load in humans. The reduction in RVEDVI may be a consequence of sympathetic nervous system activation. It has been shown in the LV on echocardiography, that a reduction in LVEDVI from sympathetic nervous system activation and an increase in systemic blood pressure, reduces the load on the LV (257), and according to the LaPlace relationship, a reduction in diameter reduces wall stress. Furthermore, changes in RV filling with a decrease in early diastolic filling in acute hypoxia at rest has been demonstrated, which may become accentuated at rest (121).

In animal studies, it has been shown in an acute model of pulmonary hypertension using pulmonary artery balloon inflation and a respiratory distress syndrome, that the RV adapts and increases cardiac output, not by increasing RVEDVI, but by improving contractile performance through homeometric autoregulation.(267, 268). Dobutamine stress was performed in rats, after 6 weeks of RV pressure overload induced by pulmonary artery banding, demonstrating that there was an increase in RV contractility in the banded rats in response to dobutamine stress, with no change in RVEDVI (269). These studies together with ours, suggests that the initial adaptation of the RV to an increased load, is by homeometric augmentation and an increase in contractility, rather than by an increase in RVEDVI and enhancement of Frank-Starling mechanisms, to maintain stroke volume. Furthermore, the degree of pulmonary pressure elevation and time of exposure to this is an important factor. In pigs, it has been shown that acute moderate levels of RV pressure overload leads to maintenance of end-diastolic and end-systolic RV segment length, implying that there is an increase in RV

contractility. With severe acute pressure overload, there was a significant increase in both end diastolic and end systolic lengths (270). Furthermore, that has been shown in pigs, with a step-by-step embolic increase in afterload, that the initial RV adjustment required pure homeometric regulation. Dilatation occurred subsequently as a consequence of the limitation of contractile reserve, which then led to vascular-ventricular uncoupling and a decrease in pulmonary blood flow. Hence RV contractile recruitment represents a compensatory mechanism, whereas RV enlargement heralds the onset of regulatory failure (271)

We have shown in our first study in healthy volunteers, that an increase in LVEDVI is a normal manifestation of exercise. However, during acute hypoxia, there is no increase in LVEDVI suggesting relative under-filling and a reduction in preload. As RVEDVI decreases in size, there is no restriction of LV filling from RV compression. As described earlier, there is evidence of LV under-filling despite enhanced diastolic indices on speckle tracking analysis, during acute hypoxia (127, 265), with evidence of a reduction in SV on acute hypoxic exercise (128). We have demonstrated for the first time, that the reduction in Ao SVI and LVSVI, can be explained a blunting in LV preload on exercise shown by no rise in LVEDVI, despite an increase in LV contractility shown by a decrease in LVESV and an increase in LVEF. A previous study by Kullmer et al using echocardiography, showed no change in LVEDV or LVESV on exercise (119) and Ricart et al showed no change in LVEF between hypoxic and normoxic exercise (272), however, this could be due to the lack of sensitivity of echocardiography to detect biventricular volume change.

6.6.3 Hypoxia-related changes Immediately After Exercise

We have shown that if imaging is performed immediately after exercise, there are no detectable differences in changes RV function and stroke volume between normoxic and hypoxia. Furthermore, while LV volumes remain lower immediately after exercise during hypoxia compared to normoxia, there is an increase in LVEDVI immediately after exercise suggesting an improvement in LV-filling, and a larger decrease LVESVI and hence increase in LVEF, suggesting an increase in contractility which could be related to the improvements in filling and utilization of Frank-Starling mechanisms. There is also no difference in LVSVI, RVSVI and Ao SVI detectable when imaging is performed immediately after exercise, between hypoxia and normoxia, which contrasts to when imaging is performed during steady state exercise. However, there is a significant reduction in MPA SVI during hypoxia as compared to normoxia. While cardiac index and heart rate are higher, there is no difference in interaction on hypoxia on the change of these parameters.

In Chapter 5, we demonstrated that immediately after exercise there is increase in stroke volumes, an increase in LVEDVI and an increase in RVEF, and we suggested that this may be important when assessing exercise pathophysiology in disease. We have shown that there are subtle but highly significant differences in biventricular function in the healthy heart during exercise in acute pulmonary hypertension, which are not detected if imaging is carried out immediately after exercise. In fact, imaging immediately after exercise was characterized by improvements in LV filling and contractility.

We did find that MPA SVI was significantly lower immediately after exercise during hypoxia compared to normoxia, and there was a significant interaction. This is likely due to the fact that MPA SVI acquisition was the first image acquired in the sequence. Ao SVI was next, with the LVSA cine immediately after. As outlined in Chapter 2, the full protocol acquisition time

is 86 seconds. Hence within that time frame RV recovery was able to take place, further emphasizing our point that continuous steady state acquisition in exercise CMR is important.

MPA Area, Pulsatility and Velocities

We have found that average MPA velocity does not increase significantly during hypoxic exercise, and that there is a trend, though non-significant, for blunting of the rise in MPA average velocity during hypoxic exercise versus normoxic exercise It is difficult to know, however, whether this is a reflection of the increase in pulmonary vascular resistance, and a reduction in pulmonary vascular distensibility during hypoxia and hypoxic exercise, and could the subject of further research. It also raises an interesting clinical question whether a blunting of a rise in average MPA blood velocity, has the potential to non-invasively detect subclinical pulmonary vascular disease that is otherwise not present at rest, and warrants further investigation.

6.6.4 Limitations

We have demonstrated a reduction in RV forward flow, with indirect evidence of elevated pulmonary pressures and pulmonary vascular resistance, with interventricular septal flattening. However, it could be argued that acute hypoxia as a model of pulmonary hypertension, could cause myocardial ischaemia, acidosis and hypocapnia, leading to myocardial impairment as a cause of reduced RV and LV stroke volume.

Acute hypoxia leads to pulmonary vasoconstriction, systemic vasodilatation, and an increase in ventilator drive and sympathetic nervous system activity via peripheral chemoreceptors.

Blood pressure remains unchanged or slightly decreased in the first few hours of hypoxic exposure, as hypoxic vasodilatation tends to override sympathetic vasoconstriction, with a rise in blood pressure occurring after 3-4 weeks of hypoxic exposure due to increasing sympathetic activity (110-112, 114, 273). It has been used in numerous studies in healthy volunteers at rest and exercise, to study how the respiratory and cardiovascular systems respond. Clearly, while the use of balloon catheters in the pulmonary circulation has been used to induce pulmonary hypertension in humans in the 1960s (274), this would not be ethically acceptable in healthy volunteers in now.

The response to acute hypoxia is rapid, with an increase in PVR within the first 5 minutes, a lower increase over 2 hours and a maximal response at 24 hours at which early signs of remodeling such as medial hypertrophy, start to occur (113).   However, one concern of using hypoxia as a model of acute pulmonary hypertension, would be the effect of hypoxia directly on the myocardium. Silverman et al demonstrated that isolated rat myocytes, when exposed to 1% oxygen, had reduced myocyte contractility and slower relaxation and it has been long thought that the myocardium may self limit its pump function because of decreased oxygen availability thereby preventing potentially fatal hypoxia induced arrhythmia or failure.

However, myocardial blood flow has been shown to be preserved at rest, with an increase during exercise despite a lower workload at an altitude of 4500m (275).   Furthermore, Malconian et al showed there is no demonstrable cardiac ischaemia on exercise in healthy young men at extreme altitude, up to 8,848m on exercise, despite severe hypoxaemia and alkalosis, suggesting that oxygen delivery to the myocardium was maintained even at oxygen saturations as low as 49% (276). Dilatation of epicardial coronary arteries and an increase in resting myocardial blood flow, compensates for the reduced oxygen content of the blood.

Healthy young men subject to hypoxia at rest and during submaximal and maximal workloads showed that reduction in arterial content was compensated by increased oxygen extraction while at exercise with an increase coronary blood flow. At a reduction of 20-25% in arterial oxygen content, increase in flow was sufficient to supply the heart with enough oxygen during submaximal exercise. Hence normal heart has a 'coronary flow reserve' of above 33% (277). Furthermore, comparable lactate steady states at relatively the same VO2 levels in normoxia and hypoxia in arterial blood has been demonstrated in healthy adults(278) although alkalosis and a decrease in CO_2 has been reported (254).

Also, we hypothesized that the lack of increase of LVEDVI on exercise is due to a reduction in preload and under-filling. We do not have direct evidence of that, as the temporal resolution on real time imaging on CMR, does not allow for diastolic evaluation. Furthermore, preload is dependent on multiple factors other than filling, such as heart rate, contractility and ventricular compliance and we are unable to measure all of these directly. However, we have shown that normoxic exercise is characterized by an increase in LVEDVI, hence the lack of rise in LVEDVI on hypoxic exercise, may be a consequence of the reduction in RV forward flow.

For the immediately post exercise acquisition, we were only able to analyse 24 LVSA due to incomplete acquisition of the basal part of the heart. This was due to vigorous respiration of the subject's post exercise, and malpositioning of the imaging window.

6.7 Conclusions

1. Acute normobaric hypoxia leads to an increase in cardiac index driven by an increase in heart rate, with no change in stroke volume. LV volumes decrease and LVEF increases could be the result of sympathetic nervous system activation. There is no change in RVEDVI or RVEF.

2. Exercise during acute normobaric hypoxia leads to a reduction in RV forward flow, a blunting of a rise in RVEF, LV underfilling and a reduction in LV forward flow. This is likely to a consequence of increased pulmonary pressures.

3. These changes are not detected if imaging is performed immediately after exercise

4. There is a non-significant blunting of the rise in MPA average blood velocity which warrants further investigation, as to its significance and potential clinical meaning.

5. Exercise CMR during acute normobaric hypoxia has the ability to detect subtle changes in RV and LV function, in the healthy heart

Chapter 7 – Cardiovascular Changes at Rest and Exercise in Patients with Pulmonary Arterial Hypertension and Normal Resting Right Ventricular Function

7.1 Introduction

Deterioration of RV function is a strong predictor of mortality in patients with PAH, however, baseline clinical characteristics and traditional tests such as 6MWD, serial 6MWD, indirect determinants of RV function using echocardiography and invasive haemodynamics, cannot determine which RV is destined to fail despite medical therapy (148-151). Assessing RV reserve as a marker of subclinical RV-PA uncoupling prior to deterioration of resting RV function has gained attention over recent years. Exercise CMR is a promising new technique, and is potentially an accurate, reproducible and non-invasive method for measuring dynamic RV function, that could be an ideal modality for assessing serial differences between small groups.

7.2 Aims and Hypotheses

Aims:

1. To assess dynamic biventricular function in patients with PAH and normal resting RV function

2. To correlate RV reserve with clinical characteristics, baseline haemodynamics at diagnosis, 6MWD, CPET and echocardiography parameters

Hypotheses

1. We hypothesize that patients will demonstrate reduced RV reserve, despite normal resting RV function

2. That RV reserve will not correlate with traditional clinical measures used for follow up, nor baseline haemodynamics

3. That there will be heterogeneity of dynamic RV response amongst patients

7.3 Methodology

The methodology is described in Chapter 2, 3, 5 and 6 and will be briefly described here. Healthy volunteers were recruited to the study via advertisement with pre-screening via email with a simple questionnaire. More detailed screening was carried out on the day of attendance with height, weight, heart rate, blood pressure and a cardiovascular examination. Cardiopulmonary exercise testing was carried out to pre-determine the load that the subject would exercise at in the scanner.

Patients were recruited from referrals from the staff in the Pulmonary Hypertension service and then directly approached and invited to participate. Patients underwent 6MWD, CPET, lung function testing, echocardiography, plasma assays, CTPA, V/Q scanning and right heart catherisation as part of their routine clinical work up and their most recent relevant clinical data was collected. RVEF was assessed by resting CMR. Exercise CMR was separated from other routine tests, such as CPET and 6MWD, by at least 4 hours. The inclusion criteria and exclusion criteria are outlined in Chapter 2.

7.3.1 Preparation

Care was taken to ensure that the subject was positioned such that they could pedal within the scanner with no restriction, and that their heart was no more than 10cm from isocentre. Continuous heart rate and oxygen saturation monitoring was carried out throughout the study.

7.3.2 Imaging

Rest Imaging

Imaging was carried out on a 1.5 Tesla Philips Achieva with a 32 cardiac channel coil. Conventional retrospectively gated cine and phase contrast imaging was carried out. Resting free breathing, high temporal resolution, real time LVSA cine and Ao and MPA phase contrast images were taken.

Exercise and immediately post Exercise Imaging

During exercise and immediately after exercise, free breathing, high temporal resolution, real time LVOT, RVOT, LVSA and 4 chamber cines, and Ao and MPA phase contrast images were acquired.

7.3.3 Exercise Protocol

Exercise was carried out on an MRI compatible ergometer (Lode, Netherlands). Each subject's predetermined load was set at 40% of the watts achieved during upright CPET. Warm up consisted of increasing the load to target over one minute, and then maintaining that for 2 minutes. At 3 minutes, heart rate was monitored for stability, and then imaging commenced. Subjects were spoken to continuously during the exercise protocol. Once exercise imaging

was complete, the subject was instructed to cease exercise and remain with their feet in the pedals, while immediately post exercise imaging commenced.

7.3.4 Image Analysis:

Breath hold and real time LVSA cines were analysed using cvi42 (Circle, Cardiovascular Imaging, Canada). Breath hold and real time phase contrast images were analysed on ArtFun (UPMC, Paris).

7.3.4.1 Volume, Stroke volume and Ejection Fraction analysis from LVSA

Endocardial surfaces were traced at end systole and end diastole in the expiratory phase of respiration for each slice, using a semi-automated method with manual correction and volumes were calculated by the Simpsons summation rule. LV and RVSV were calculated as EDV – ESV and EF was calculated as EDV-ESV/EDV x 100. All volumes were indexed to body surface area. RV reserve was calculated as RVEF Exercise – RVEF Rest.

7.3.4.2 Stroke Volume, Mean and Average Velocity and Pulsatility analysis from Phase Contrast Images

ROIs were created around the aorta and MPA using a semi-automated method with manual correction. This created time-volume and time-velocity curves from which SV and mean and average velocity could be calculated. SV was calculated as the area under the curve of the time-volume curve. Peak velocity was taken as the peak velocity occurring during systole, and

mean velocity as the mean of the velocities through systole.   For the real time analysis, an average of the first 5 consecutive heartbeats was taken. Pulsatility was calculated as Maximum area – Minimum area/Minimum area x 100 and expressed as a percentage. Cardiac output was calculated as SV x HR and indexed to BSA.

7.3.4.3 Unwrapping and Phase offset adjustments

Flow data was checked for aliasing and phase offsets >0.6cm/second prior to analysis and unwrapped or adjusted prior to analysis (Omnibus Velocity Unwrapping With Phase Offset Correction, MATLAB wrapper, Pawel Tokarczuk).

7.3.5 Statistical Analysis:

IBM SPSS Version 22 was used for data analysis.   Data was checked for normality. Continuous data is expressed as mean ± standard deviation. Paired t-tests were used to compare differences between measurements. A repeated ANOVA was used to test the interaction on right and left ventricular cardiovascular parameters between healthy volunteers and patients with main and simple main effects analysis.   Pearson's correlation was used to test the associations between clinical haemodynamic and CPET parameters and resting and exercise biventricular function. A Bonferroni correction was applied to adjust for multiple comparisons for all simple main effects and pairwise comparisons.

7.4 Results

7.4.1 Study Population and Baseline Characteristics

14 patients with idiopathic (n=12) or hereditary PAH (n=2) were enrolled in the study. All subjects completed the study and all data was analyzable at rest, exercise and immediately after exercise. They were compared to the 38 controls recruited in the first study, described in Chapter 5.

Baseline characteristics, clinical and haemodynamic data are summarised in Table 7.1. Baseline resting biventricular function is summarised in Table 7.2. A summary of the treatments the patients were on at the time of the study are summarised in Table 7.3.

Table 7.1. Demographic, clinical and haemodynamic characteristics of patients

Age	39.1 ± 9.4
Gender (M/F)	4/10
BSA	1.8 ± 0.2
BMI	25.6 ± 4.3
NYHA	
1	2
2	8
3	4
6MWD	446.9 ± 75.4
BNP	$30.1 \pm 1\ 9.6$ (normal < 100)
VO$_2$ peak	1424.9 ± 362.0
V$_E$/VCO$_2$	35.4 ± 5.2
Max Load	118.9 ± 30.1

Level of watts in scanner	47.4 ± 13.1
TAPSE	1.7 ± 0.46
sPAP	79.8 ± 27.0
dPAP	31.7 ± 13.6
mPAP	50.6 ± 17.6
PVR	10.5 ± 6.3
Years since Diagnosis	3.9 ± 3.3
Months between Echo and Exercise CMR	3 ± 4.2
Months between CPET and Exercise CMR	1.7 ± 2.2

Values are expressed as mean ± standard deviation

Table 7.2. Resting LV and RV CMR parameters of patients

Parameter	Value
LVEDVI	70.3 ± 14.6
LVESVI	25.7 ± 9.3
LVSVI	44.6 ± 6.7
LVEF	64.3 ± 6.2
RVEDVI	88.1 ± 2.5
RVESVI	40.1 ± 9.5
RVSVI	45.3 ± 2.6
RVEF	53.6 ± 4.3
LV mass index	52.2±11.5
RV mass index	26.4±7.1

Ventricular mass index	0.53 ± 0.19

Values are expressed as mean ± standard deviation

Table 7.3: Summary of treatments

Type of therapy	Number of patients	Specific treatments
Anticoagulation	6	Warfarin
Monotherapy	2	Sildenafil Bosentan
Dual therapy	8	Sildenafil and Ambrisentan Sildenafil and Bosentan Sidenafil and Macitentan Ambrisentan and Tadalafil
Calcium channel blocker only	3	Diltiazem Nifedipine
Triple therapy	1	Ambrisentan, Tadalafil and Amlodipine

7.4.2. Baseline Resting Biventricular Function Compared to Controls

There was no difference in RV volumes or ejection fraction between patients and controls as summarized in Table 7.4. There was a significant difference between LVSVI (p=0.048), MPA SVI (p=0.012), and LVEDVI (p=0.048).

Table 7.4: Heart rate, Cardiac output and Biventricular Function at Rest: Healthy Controls vs. Patients

Outcome Variable	Controls	Patients	P value
HR	61.2 ± 10.8	63.4 ± 11.5	1.0
CI	3.1 ± 0.6	2.9 ± 0.6	1.0
Ao SVI	51.4 ± 11.0	45.7 ± 8.6	1.0
MPA SVI	51.4 ± 9.9	40.0 ± 8.0	0.012
LVEDVI	84.3 ± 14.7	70.3 ± 14.6	0.048
LVESVI	30.4 ± 5.3	25.7 ± 9.3	0.312
LVSVI	53.8 ± 10.7	44.6 ± 6.7	0.048
LVEF	63.7 ± 3.6	64.3 ± 6.2	1.0
RVEDVI	89.6 ± 2.7	85.8 ± 14	1.0
RVESVI	38.4 ± 8.5	40.1 ± 9.5	1.0
RVSVI	51.2 ± 1.6	45.3 ± 2.6	0.612
RVEF	57.1 ± 5.2	53.6 ± 4.3	0.36

7.4.3 Biventricular Response to Exercise in Patients

The biventricular response to exercise in patients is summarized in Table 7.5. There was no increase in stroke volume, as measured by flow or volumes. RVEDVI increased (p=0.048), with no change in RVESVI or RVEF. LVEF increased (p <0.001), driven by a decrease in LVSVI (p=0.012). There was no increase in LVEDVI which started at a significantly lower volume in the patient group.

However, if RV function is assessed from rest to immediately after exercise, there is no increase in RVEDVI and an increase in RVESVI, leading to an increase in mean RVEF and a rise in RVSVI. Hence, the changes seen during continuous steady state exercise acquisition are lost. This is summarized in Table 7.6.

Table 7.5: Heart rate, Cardiac Index and Biventricular Function from Rest to Exercise in Patients

Outcome Variable	Rest	Exercise	P value
HR	63.4 ± 11.5	114 ± 15.6	<0.001
CI	2.9 ± 0.6	5.2 ± 1.2	<0.001
Ao SVI	45.7 ± 8.6	46.2 ± 12.1	1.0
MPA SVI	40.0 ± 8.0	40.0 ± 13.3	1.0
LVEDVI	70.3 ± 14.6	67.2 ± 16.3	1.0
LVESVI	25.7 ± 9.3	18.4 ± 8.8	0.012
LVSVI	44.6 ± 6.7	48.9 ± 9.1	0.192
LVEF	64.3 ± 6.2	73.7 ± 6.7	<0.001
RVEDVI	85.8 ± 14	93.2 ± 16	0.048
RVESVI	40.1 ± 9.5	45.8± 15.9	1.0
RVSVI	45.3 ± 6.8	47.4 ± 10.1	1.0
RVEF	53.6 ± 4.3	51.4 ± 10.7	1.0

Table 7.6: Right Ventricular Function from Rest to Immediately after Exercise in Patients

	Rest	Immediately after Exercise	P value

RVEDVI	85.8 ± 14	88.0 ± 15.5	0.317
RVESVI	40.1 ± 9.5	36.4 ± 10.7	0.031
RVSVI	45.3 ± 6.8	51.6 ± 10.9	0.012
RVEF	53.6 ± 4.3	58.8 ± 7.6	0.01

7.4.4 Biventricular Response to Exercise: Patients vs. Controls

The comparison between patients and healthy volunteers is summarized in Table 7 and Table 8.

Table 7.7: Simple main effects analysis: Heart Rate, Cardiac Index and Biventricular Parameters on Exercise, Healthy Controls vs Patients

Outcome Variable	Exercise in Healthy Controls	Exercise in Patients	p value
HR (bpm)	122 ± 12.1	114.1 ± 15.6	0.564
Ao SVi (ml/m^2)	61.7 ± 10.3	46.2 ± 12.1	<0.0001
MPA SVi (ml/m^2)	60.0 ± 9.3	40.0 ± 13.3	<0.0001
CI (l/min/m^2)	7.6 ± 1.5	5.2 ± 1.2	<0.0001
LV EDVi (ml/m^2)	90.1 ± 15.5	67.2 ± 16.3	<0.001
LV ESVi (ml/m^2)	25.5 ± 7.0	18.4 ± 8.8	0.156
LV SVi (ml/m^2)	64.6 ± 10.7	48.9 ± 9.1	<0.0001
LV EF (%)	71.9 ± 4.5	73.7 ± 6.7	1.0
RV EDVi (ml/m^2)	88.1 ± 14.5	93.2±4.0	1.0
RV ESVi (ml/m^2)	27.1 ± 8.4	45.8 ± 15.9	0.012

RV SVi (ml/m^2)	60.9 ± 9.5	47.4 ± 2.6	<0.0001
RVEF (%)	69.6 ± 6.1	51.4 ± 10.7	<0.0001

Table 7.8: Heart Rate, Cardiac Index and Biventricular Function from Rest to Exercise: Controls vs. Patients

Outcome Variable	Controls		PAH patients		Effects, p value	
	Rest	Exercise	Rest	Exercise	Interaction	Between-subjects effect
HR	61.2 ± 10.8	122.4 ± 12.1	63.4 ± 11.5	114.1 ± 15.6	0.022	0.321
CI	3.1 ± 0.6	7.6 ± 1.5	2.9 ± 0.6	5.2 ± 1.2	<0.0001	<0.0001
Ao SVI	51.4 ± 11.0	61.7 ± 10.4	45.7 ± 8.6	46.2 ± 12.1	<0.0001	0.001
MPA SVI	51.4 ± 9.9	60.0 ± 9.3	40.0 ± 8.0	40.0 ± 13.3	<0.0001	<0.0001
LVEDVI	84.3 ± 14.7	90.1 ± 15.5	70.3 ± 14.6	67.2 ± 16.3	0.001	<0.0001
LVESVI	30.4 ± 5.3	25.5 ± 7.0	25.7 ± 9.3	18.4 ± 8.8	0.169	0.005
LVSVI	53.8 ± 10.7	64.6 ± 10.7	44.6 ± 6.7	48.9 ± 9.1	<0.0001	<0.0001
LVEF	63.7 ± 3.6	71.9 ± 4.5	64.3 ± 6.2	73.7 ± 6.7	0.405	0.363
RVEDVI	89.6 ± 2.7	85.8 ± 4.4	88.1 ± 2.5	93.2±4.0	0.001	0.890
RVESVI	38.4 ± 8.5	27.1 ± 8.4	40.1 ± 9.5	45.8 ± 15.9	<0.0001	0.001
RVSVI	51.2 ± 1.6	60.9 ± 1.6	45.3 ± 2.6	47.4 ± 2.6	<0.0001	0.002
RVEF	57.1 ± 5.2	69.6 ± 6.1	53.6 ± 4.3	51.4 ± 10.7	<0.0001	<0.0001

7.4.4.1 Heart Rate

There was significant interaction between the rise in heart rate between patients and controls, with an attenuated rise in patients (p=0.02) (Figure 7.1). However simple main effects did not show any significant difference p = 0.321 between resting or exercise values.
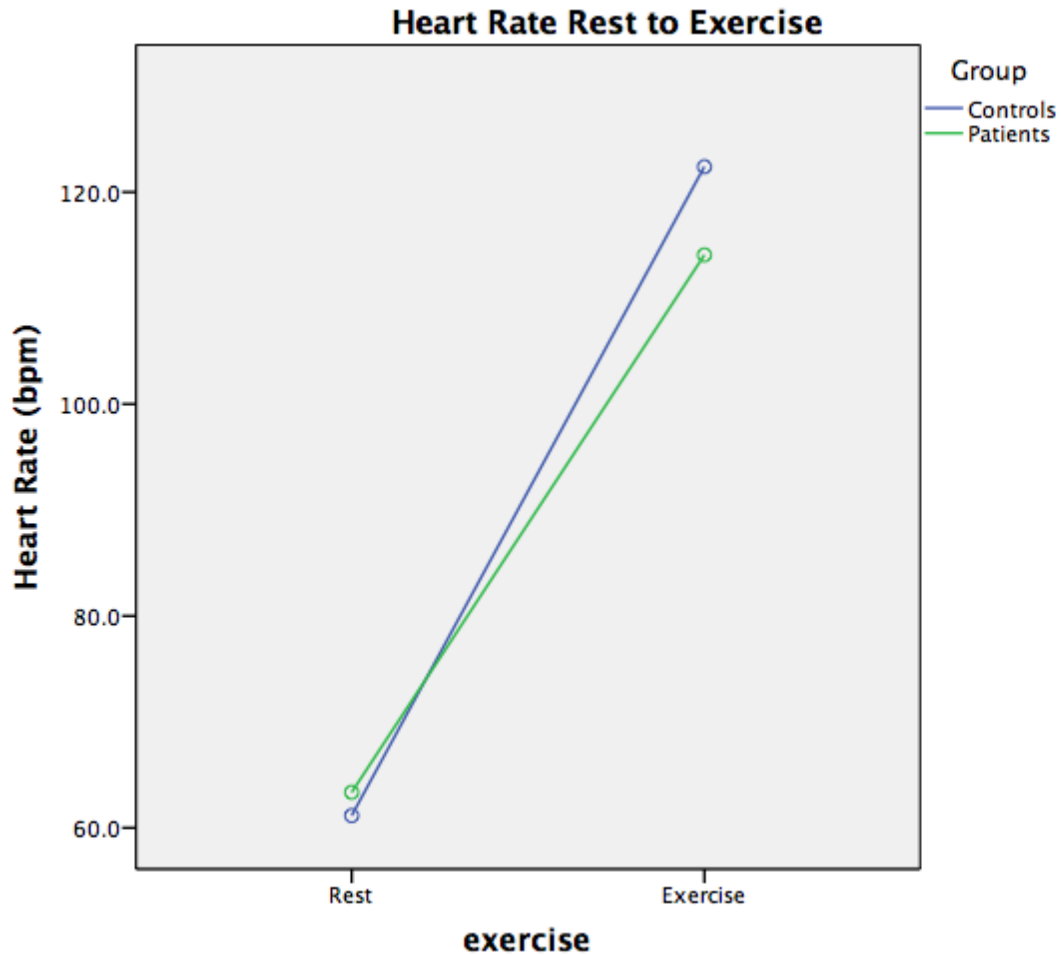
Figure 7.1: Change in heart rate from rest to exercise, in healthy controls and patients

7.4.4.2 Cardiac Index

There was a significant interaction between rise in CI between patients and controls (p <0.0001), with the rise in CI in patients being less than controls (Figure 7.2). There was a significant between subject's effect (p<0.0001). Simple main effects analysis showed that this was driven by a lower CI in patients than in controls on exercise (p<0.0001). There was no significant difference at rest (p = 1.0).
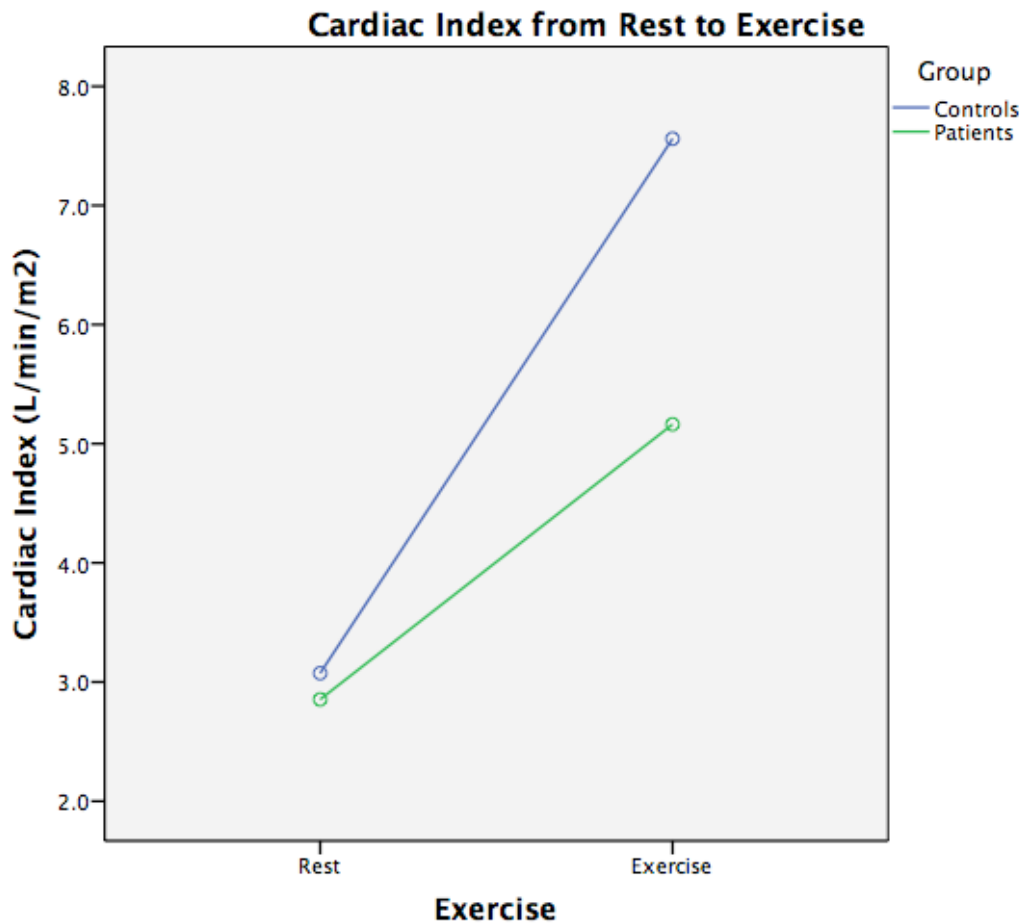
Figure 7.2: Change in cardiac index from rest to exercise, in healthy controls and patients

7.4.4.3 Aortic and MPA Stroke Volumes

There was a significant interaction between rise in aortic and MPA SVI between patients and controls ($p < 0.0001$), with no rise in both aortic and MPA SVI as compared to controls (Figure 7.3 and 7.4). There was a significant between subject's effect ($p < 0.0001$). Simple main effects analysis showed that for aortic SVI, there was no difference between patients and controls at rest, and this only became apparent on exercise ($p<0.0001$). For MPA SVI, there was a significant difference at rest ($p=0.012$) which become more apparent on exercise ($p < 0.0001$).
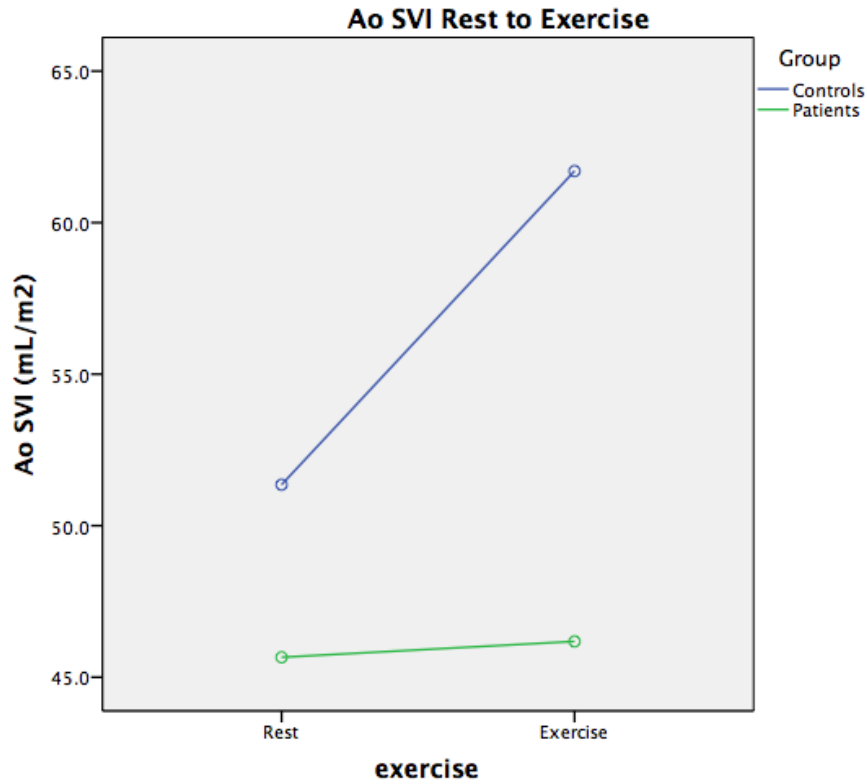
Figure 7.3: Change in aortic SVI from rest to exercise, in healthy controls and patients
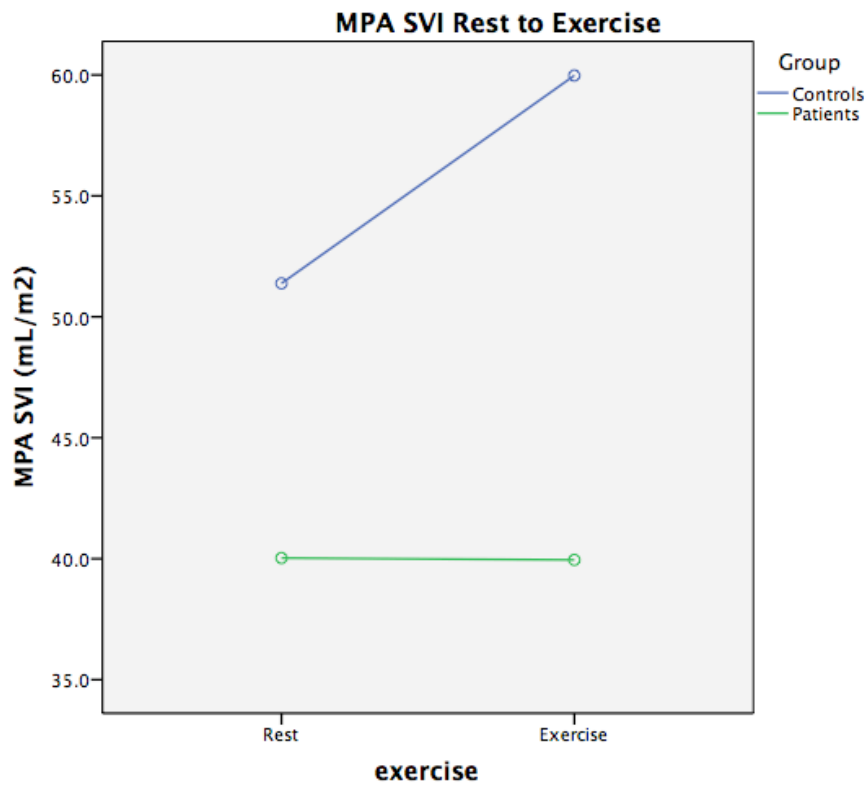
Figure 7.4: Change in MPA SVI from rest to exercise, in healthy controls and patients

7.4.4.4 Right Ventricular Function

RVEDVI

There was a significant interaction of exercise on the change of RVEDVI (p=0.001). Patients increased RVEDVI while controls decreased RVEDVI (Figure 7.5). However, between subject's effect was not significant (p=0.890) and simple main effects analysis showed no difference between resting and exercise RVEDVI (p = 1.0 for both comparisons).
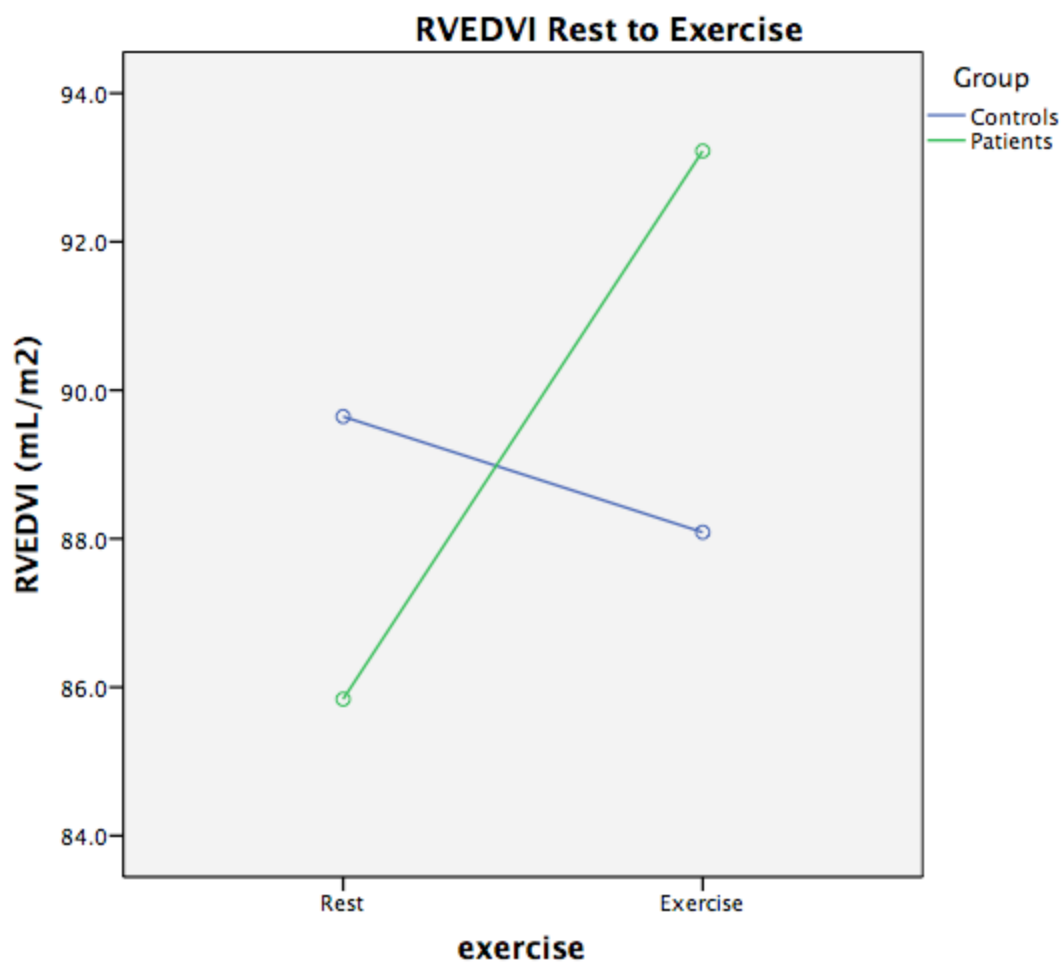
Figure 7.5: Change in RVEDVI from rest to exercise, in healthy controls and patients

RVESVI

There was significant interaction of exercise on the change of RVESVI ($p = $ <0.0001). RVESVI decrease in controls and increased in patients (Figure 7.6). Between subject's effect analysis was significant ($p = 0.001$) and simple main effects analysis showed this was driven by a significant difference on exercise ($p = 0.012$) and not at rest ($p = 1.0$).
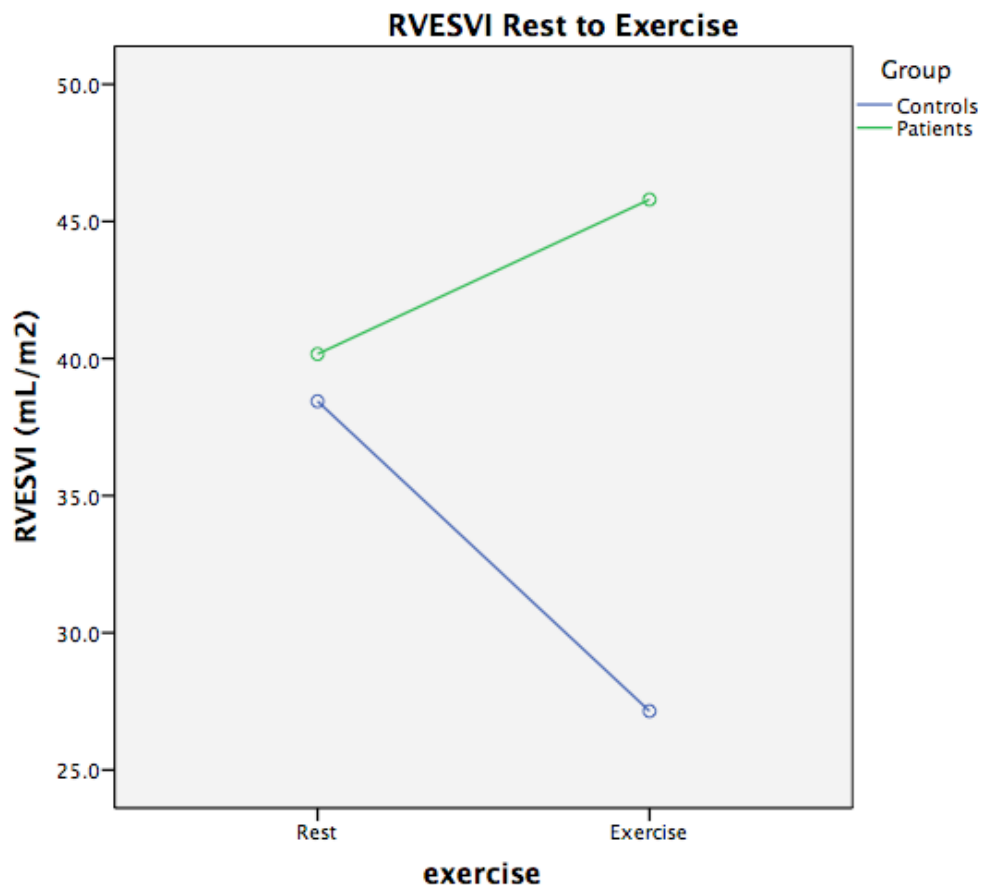
Figure 7.6: Change in RVESVI from rest to exercise, in healthy controls and patients

RVSVI

There was significant interaction of exercise on the change of RVSVI ($p = $ <0.0001) (Figure 7.7). Between subject's effect analysis was significant ($p = 0.002$) and simple main effects analysis showed this was driven by a significant difference on exercise ($p = $ <0.0001) and not at rest ($p = 0.612$).
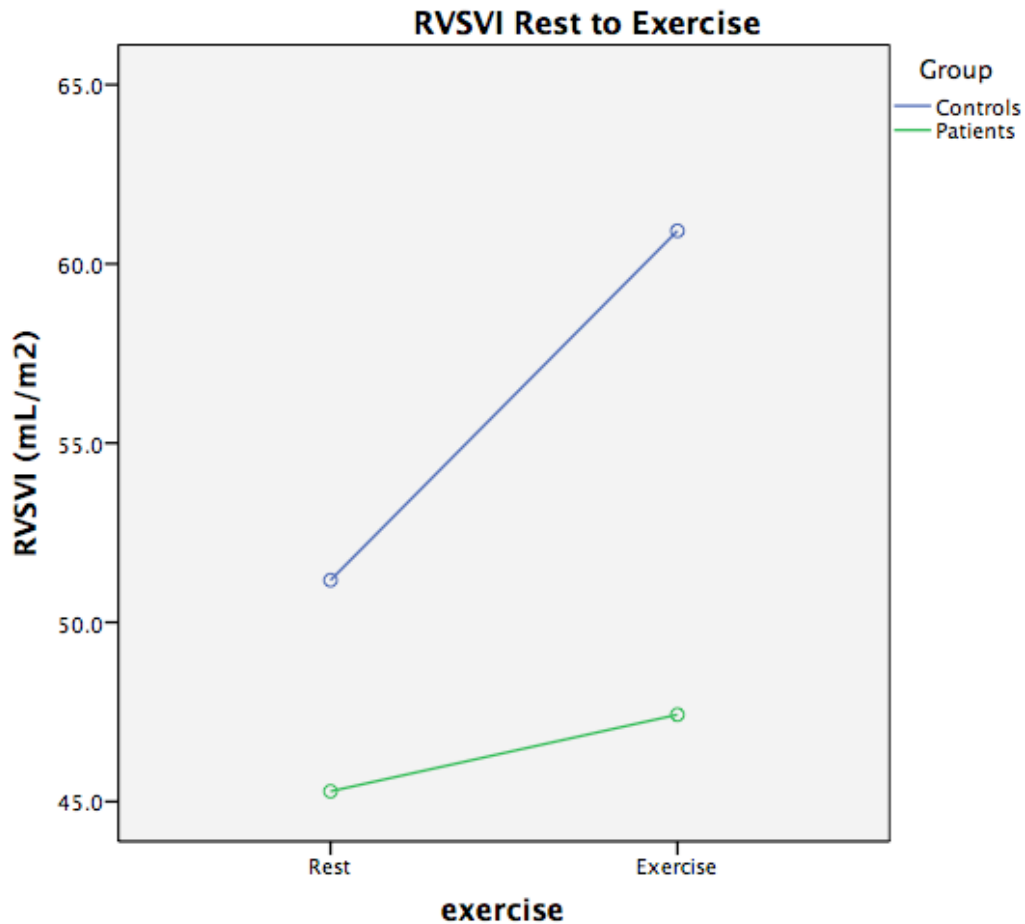
Figure 7.7: Change in RVSVI from rest to exercise, in healthy controls and patients

RVEF

There was significant interaction of exercise on the change of RVEF (p = <0.0001) (Figure 7.8). Between subject's effect analysis was significant (p < 0.0001) and simple main effects analysis showed this was driven by a significant difference on exercise (p < 0.0001) and not at rest (p = 0.36).
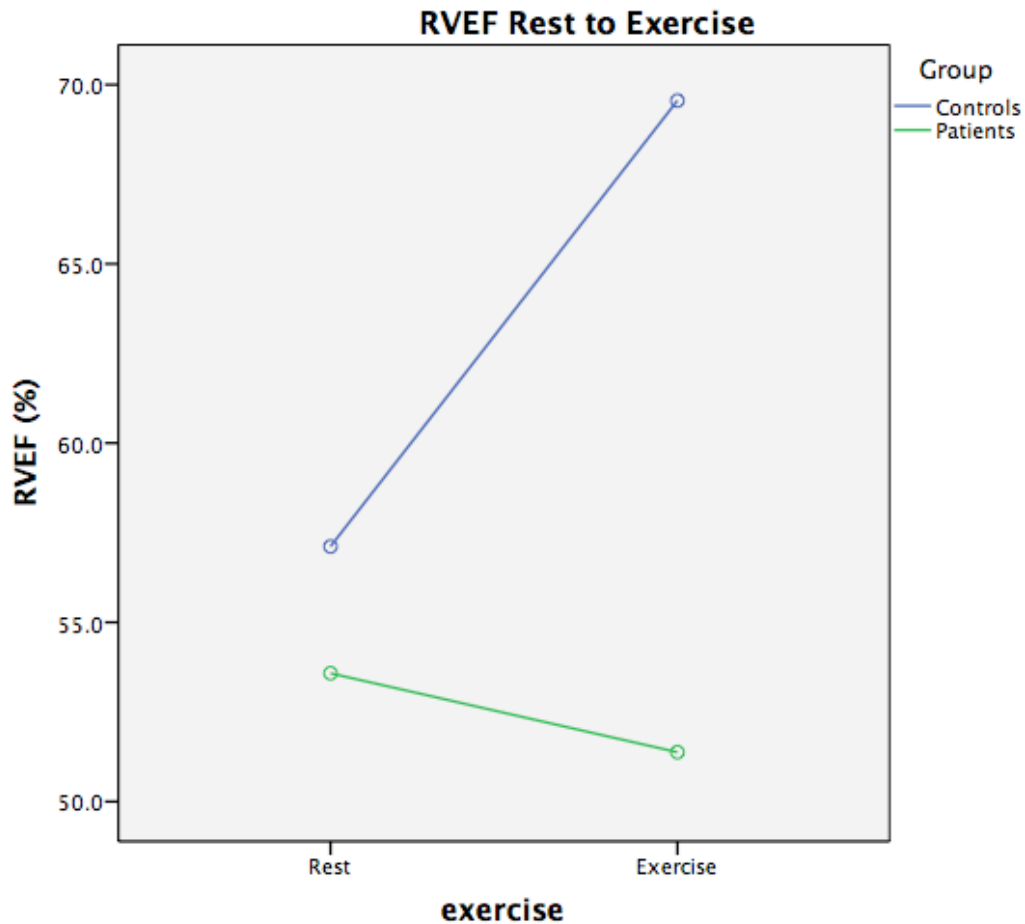
Figure 7.8: Change in RVEF from rest to exercise, in healthy controls and patients

7.4.4.5 Left Ventricular Function

LVEDVI

There was significant interaction of exercise on the change of LVEDVI ($p = 0.001$) (Figure 7.9). Between subject's effect analysis was significant ($p < 0.0001$) and simple main effects analysis showed this was driven by largely by a significant difference on exercise ($p < 0.001$), however, there was also a significant difference in LVEDVI at rest ($p=0.048$).
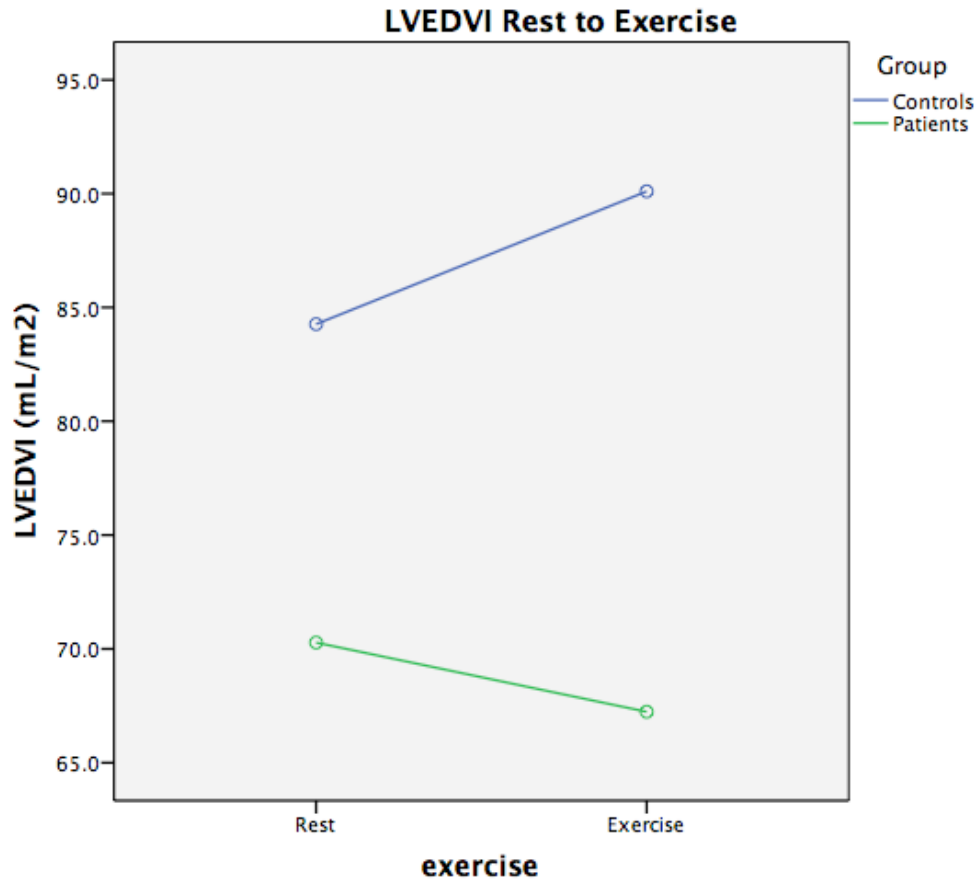
Figure 7.9: Change in LVEDVI from rest to exercise, in healthy controls and patients

LVESVI

There was no interaction of exercise on the change of LVESVI ($p = 0.169$) (Figure 7.10).

Between subject's effect analysis was significant ($p < 0.005$) suggesting that LVESVI was

smaller in patients than controls at rest and exercise, however, simple main effects analysis was

not significant for either rest or exercise ($p = 0.312$ and 0.156).
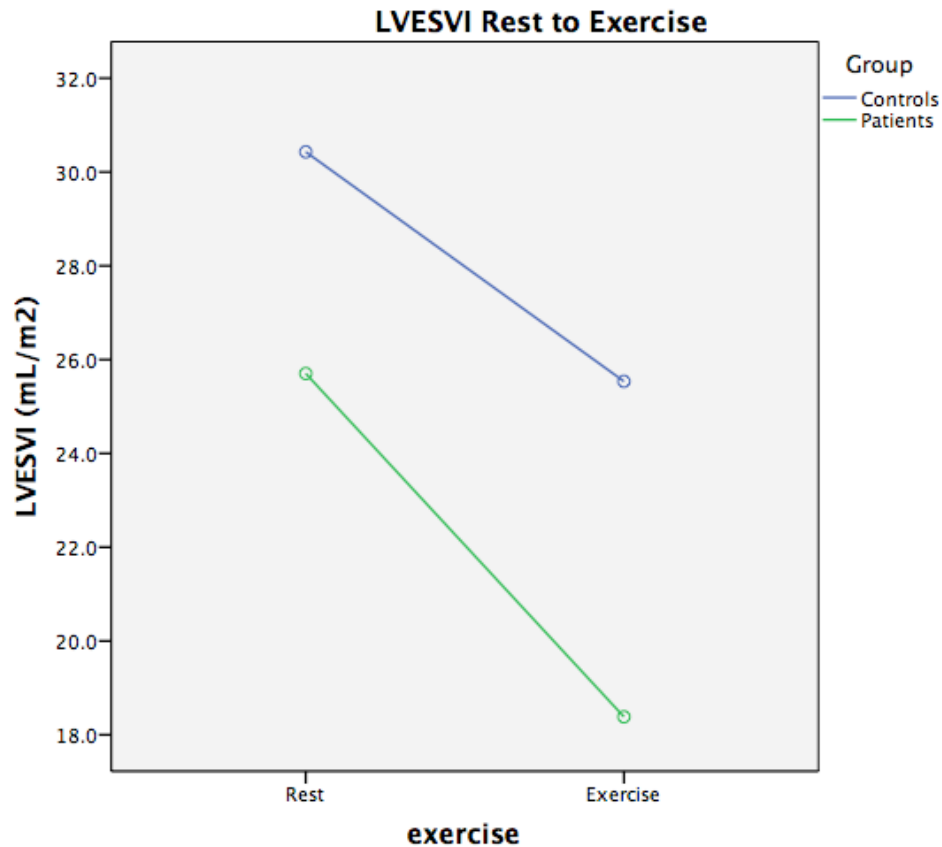
Figure 7.10: Change in LVESVI from rest to exercise, in healthy controls and patients

LVSVI

There was significant interaction of exercise on the change of LVSVI (p = <0.0001). Between subject's effect analysis was significant (p < 0.0001) and simple main effects analysis showed this was driven largely by a significant difference on exercise (p < 0.0001), however, there was a significant difference at rest between patients and controls (p = 0.048).
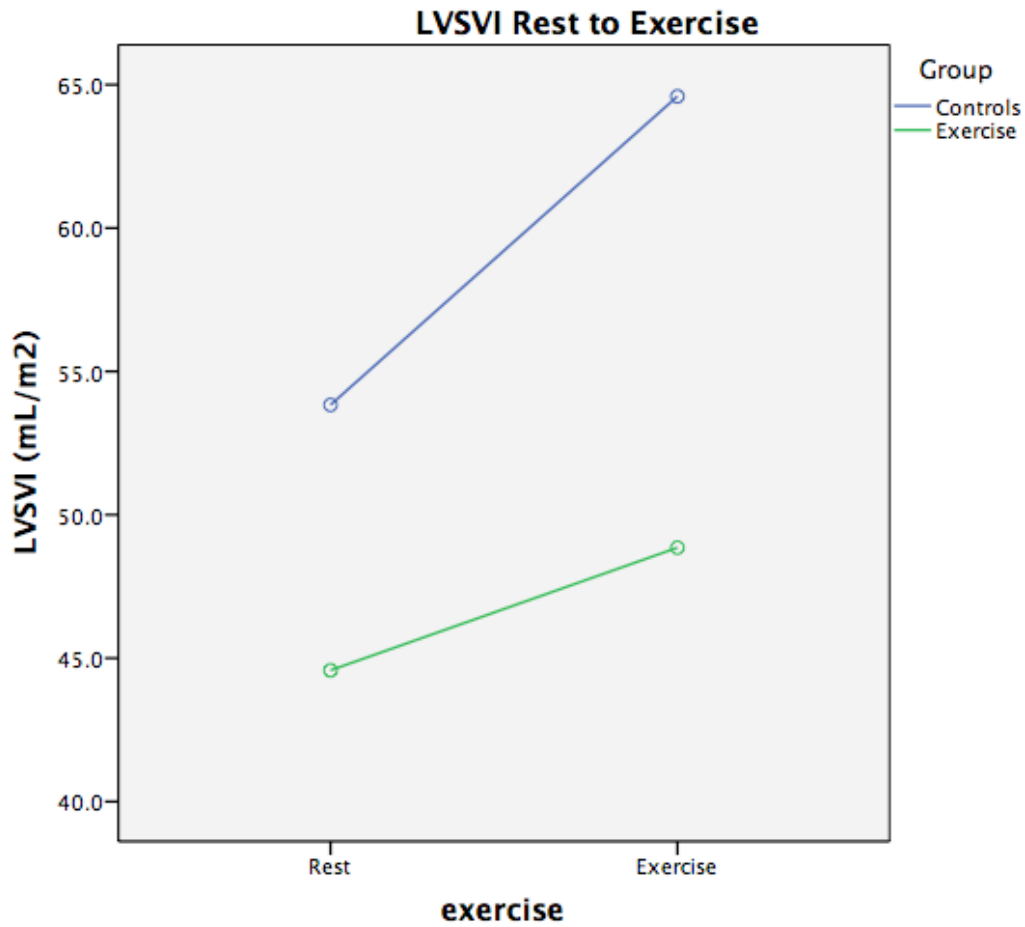
Figure 7.11: Change in LVSVI from rest to exercise, in healthy controls and patients

LVEF

There no significant interaction of exercise on the change of LVEF (p = 405) (Figure 7.12).

Between subjects effect analysis was not significant (p = 0.363).
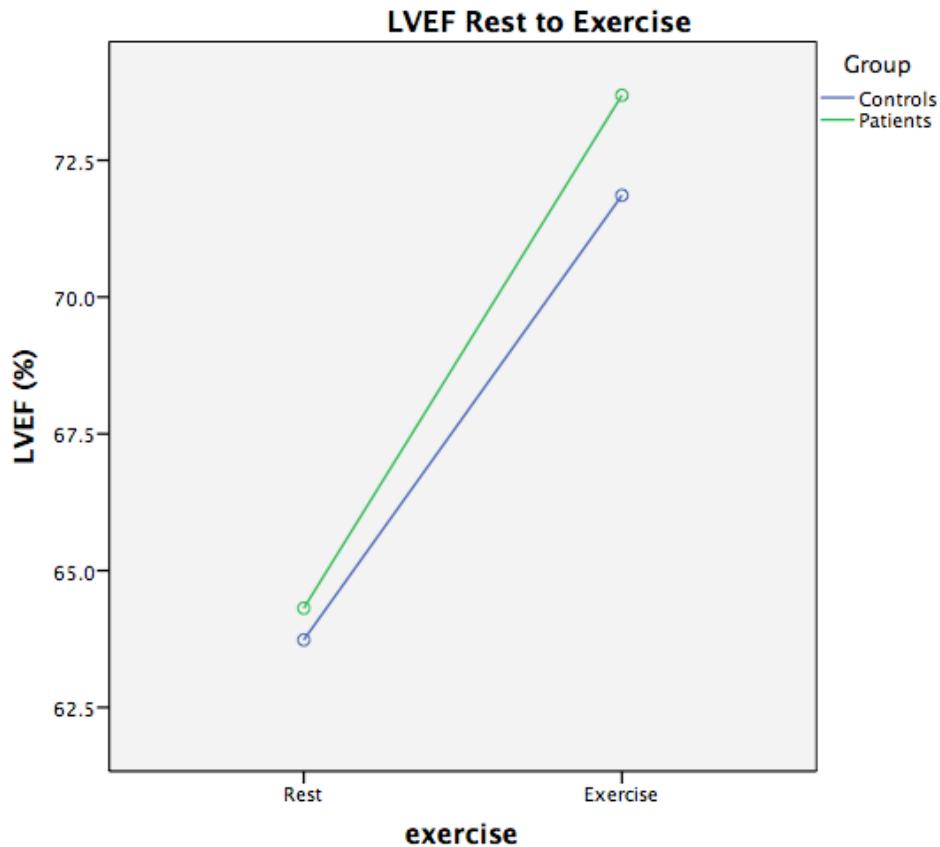
Figure 7.12: Change in LVEF from rest to exercise, in healthy controls and patients

7.4.5 Comparison of patients who increase RVEF to those who decrease RVEF on exercise

Within the patient group, 7 patients increased RVEF on exercise, while 7 decreased RVEF on exercise (Figure 7.13). There were no differences in resting biventricular parameters, years since diagnosis, 6MWD, BNP level and haemodynamic parameters at diagnosis. These are summarised in Table 8.
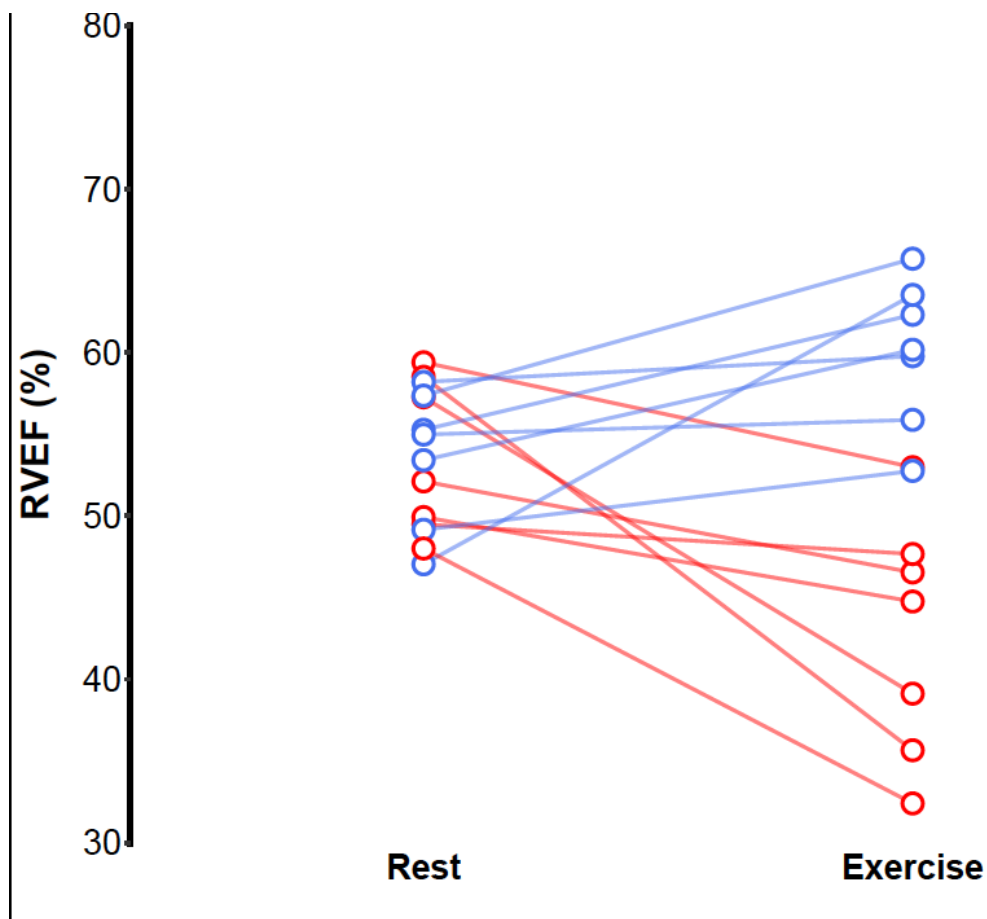
Figure 7.13: Graph of every patients' RVEF from Rest to Exercise. 7 patients increased while 7 patients decreased RVEF on exercise

Table 7.9: Baseline clinical, haemodynamic and resting biventricular parameters

	Increase RVEF n=7	Decrease RVEF n=7	p value
Years since diagnosis	2.0 (6)	3.0 (5)	1.0
BMI	27.5 (5.1)	22.8 (4)	1.0
6MWD	456 (120)	432.0 (82)	1.0
VO2 peak	1600 (293)	1260 (205)	0.52
VE/VCO2	33.3 (12.4)	36.7 (5.6)	1.0
BNP	18.1 (14)	35.5 (40.9)	1.0
PVR	6.3 (2.9)	17.0 (12.1)	0.612

mPAP	42 (15)	69.0 (23)	0.612
LVEDVI	72.8 (25.5)	61.3 (23.1)	1.0
LVESVI	24.3 (8.8)	21.5 (13.3)	1.0
LVSVI	48.5 (11.0)	41.2 (9.6)	1.0
LVEF	66.2 (2.5)	63.2 (11.4)	1.0
RVEVDI	81.1 (19.8)	80.0 (26.2)	1.0
RVESVI	37.8 (5.3)	34.2 (18.7)	1.0
RVSVI	45.6 (4.)	46.4 (10.5)	1.0
RVEF	55.0 (8.2)	53.5 (9.0)	1.0
RV mass index	20.9 (11.1)	32.0 (9.2)	1.0
LV mass index	54.8 (25.8)	45.3 (15.2)	1.0
CI	3.2 (0.4)	2.7 (0.7)	1.0

Values reported as median (interquartile range)

Change of RVEDVI, RVESVI and LVEDVI

The interaction of exercise on the change on RVEDVI, RVESVI and LVEDVI between these two subgroups was analysed.

RVEDVI

There was no significant difference in the change in RVEDVI from rest to exercise, between those who increase or decrease RVEF on exercise (86.7 ± 10.8mL/m2 to 90.5 ± 9.1mL/m2 vs. 85.0 ± 18.1mL/m2 to 95.9 ± 21.6mL/m2), interaction $p = 0.095$ and between subjects effect was also not significant $p = 0.825$. (Figure 7.14)

Change in RVEDI on Exercise
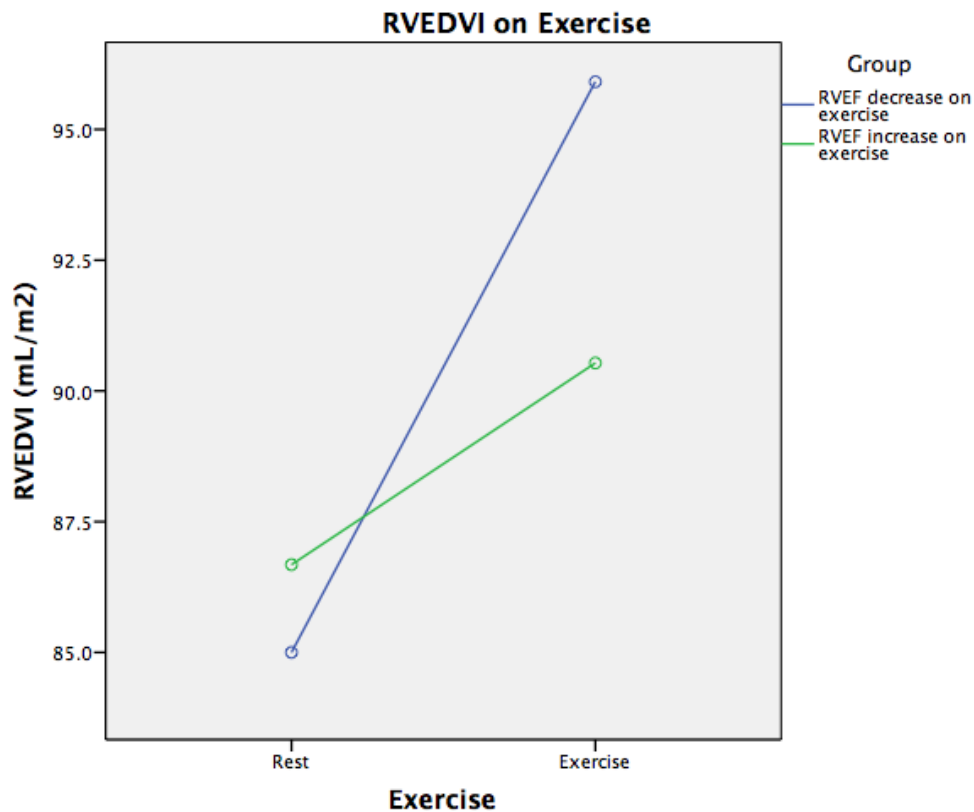
Figure 7.14: Change in RVEDVI from rest to exercise, in patients who increase vs those who decrease RVEF on exercise

RVESVI

There was a significant difference in the change of RVESVI from rest to exercise, between those who increase and decrease RVEF on exercise (40.2±6.9mL/m2 to 36.2±5.9mL/m2 vs. 40.1±12.2mL/m2 to 55.3±17.3mL/m2, p=0.001) (Figure 7.15). Between subject's effects, however, was not significant p = 0.124.

Change in RVESVI on Exercise
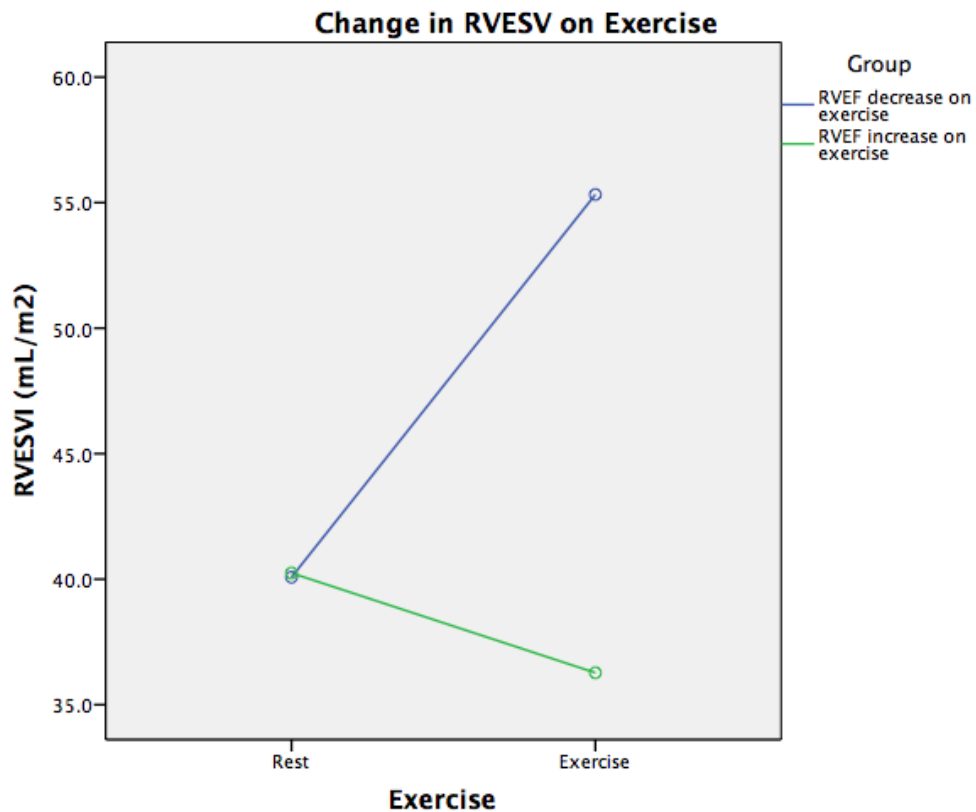
Figure 7.15: Change in RVESVI from rest to exercise, in patients who increase vs those who decrease RVEF on exercise

LVEDVI

There was a significant difference in the change of LVEDVI from rest to exercise, between those who increase and decrease RVEF on exercise (74.7±13.0 to 76.9±13.9 vs. 65.9 ±15.7 to 57.5±12.7, p=0.043), but between subject's effect was not significant, p=0.069. (Figure 7.16)
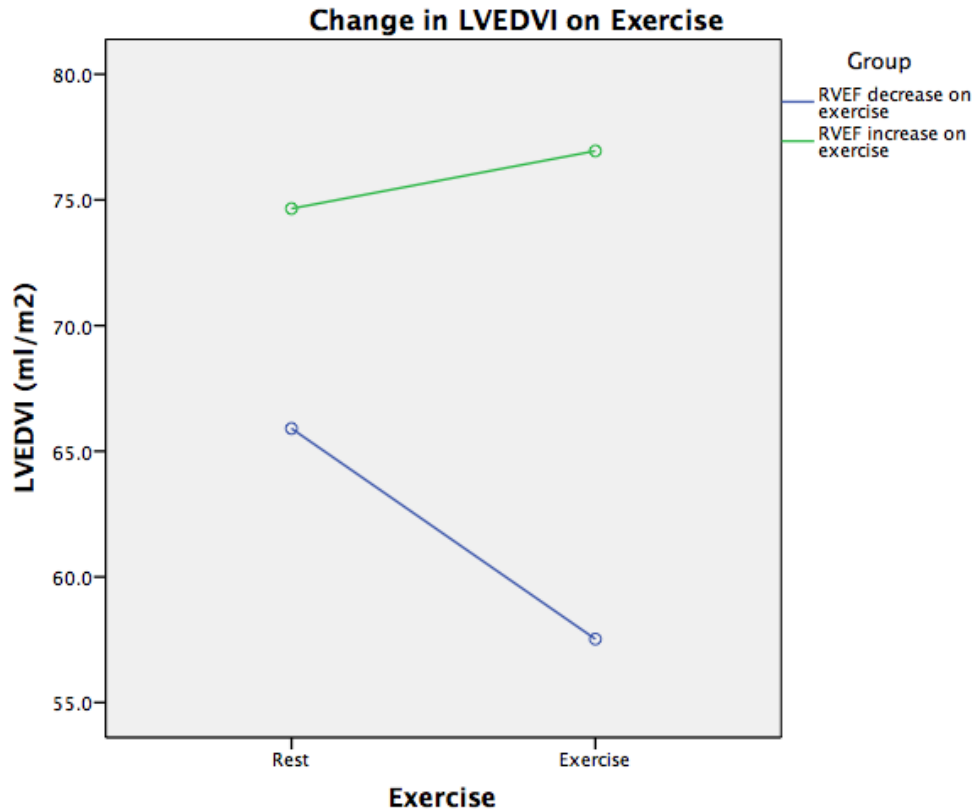
Figure 7.16: Change in LVEDVI from rest to exercise, in patients who increase vs those who decrease RVEF on exercise

7.5.6 Correlations with Exercise Capacity and Right Ventricular Reserve

There was no correlation between right ventricular reserve and age, years since diagnosis, recent 6MWD, TAPSE or BNP and haemodynamics and pulmonary vascular resistance at diagnosis.

There was a strong, negative correlation between right ventricular reserve and ventricular mass index (-0.710, p=0.004). Right ventricular reserve correlated weakly with resting LV volume (LVEDVI 0.263, p=0.016, LVESVI 0.247, p=0.024) but not with resting RV function.

VO$_2$ peak correlated moderately with right ventricular reserve (0.517, p <0.0001), an increase in LVEDVI (0.513, p<0.0001), and exercise RVEF (0.548, p<0.0001), and strongly with RVSVI and LVSVI (0.722, p<0.0001, 0.770 P<0.0001, respectively. It did not correlate with resting LVEF or RVEF, or exercise LVEF.

7.5.7 MPA Area, Pulsatility and Velocity

7.5.7.1 MPA Maximum Area

There was no significant interaction between exercise and change in MPA maximum area between controls and patients (Controls 8.2±1.5cm2 to 9.1±1.9, Patients 12.7 ± 3.1 to 13.9 ± 3.6, p = 0.380). However, there was a significant between subjects effect (p < 0.0001)

7.5.7.2 MPA Minimum Area

There was no significant interaction between exercise and change in MPA minimum area between controls and patients (Controls 5.0 ± 1.0 to 6.0 ± 1.3, Patients 9.2 ± 2.9 to 10.8 ± 3.1, p = 0.099). However, there was a significant between subjects effect (p < 0.0001)

7.5.7.3 MPA Pulsatility

There was no significant interaction between exercise and change in MPA Pulsatility between controls and patients (Controls, 65.7 ± 27.9 to 40.7 ± 17.5, Patients 40.7 ± 17.5 to 32.4 to 11.0, p = 0.704).

7.5.7.4 MPA Peak Velocity

There was a significant interaction between exercise and change in MPA peak velocity (Controls 58.4 ± 14.3 to 91.3 ± 24.2, Patients 37.1 ± 10.8 to 40.3 ± 15.2, p < 0.0001) with a

blunting of the rise in MPA peak velocity in patients. Between subjects effects was also highly significant ($p < 0.0001$) (Figure 7.17)
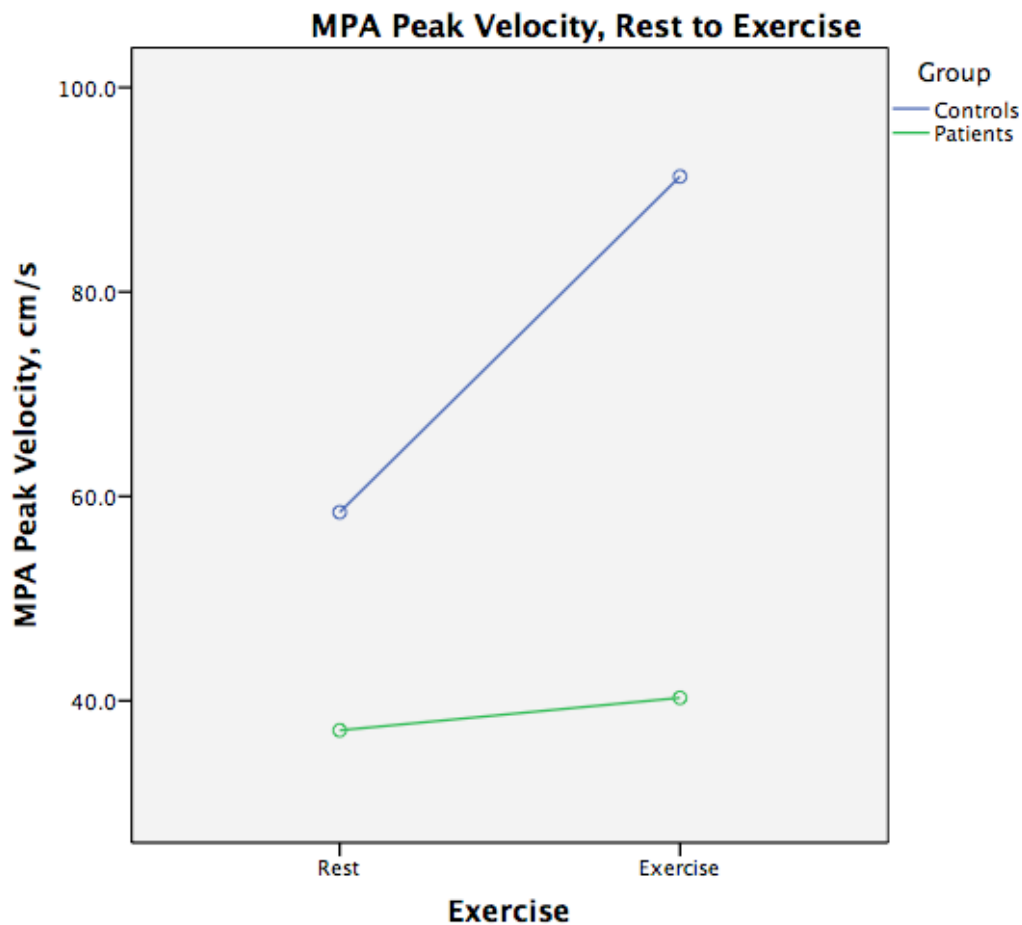
Figure 7.17: Change in MPA Peak Velocity from rest to exercise, in controls and patients

7.5.7.5 MPA Average Velocity

There was a significant interaction between exercise and change in MPA average velocity (Controls 12.6 ± 2.8 to 14.6 ± 3.4, Patients 6.5 ± 2.2 to 6.2 ± 2.8, $p < 0.0001$) with no rise in MPA average velocity in patients compared to a significant rise in controls. Between subjects effects was also highly significant ($p < 0.0001$) (Figure 7.18)
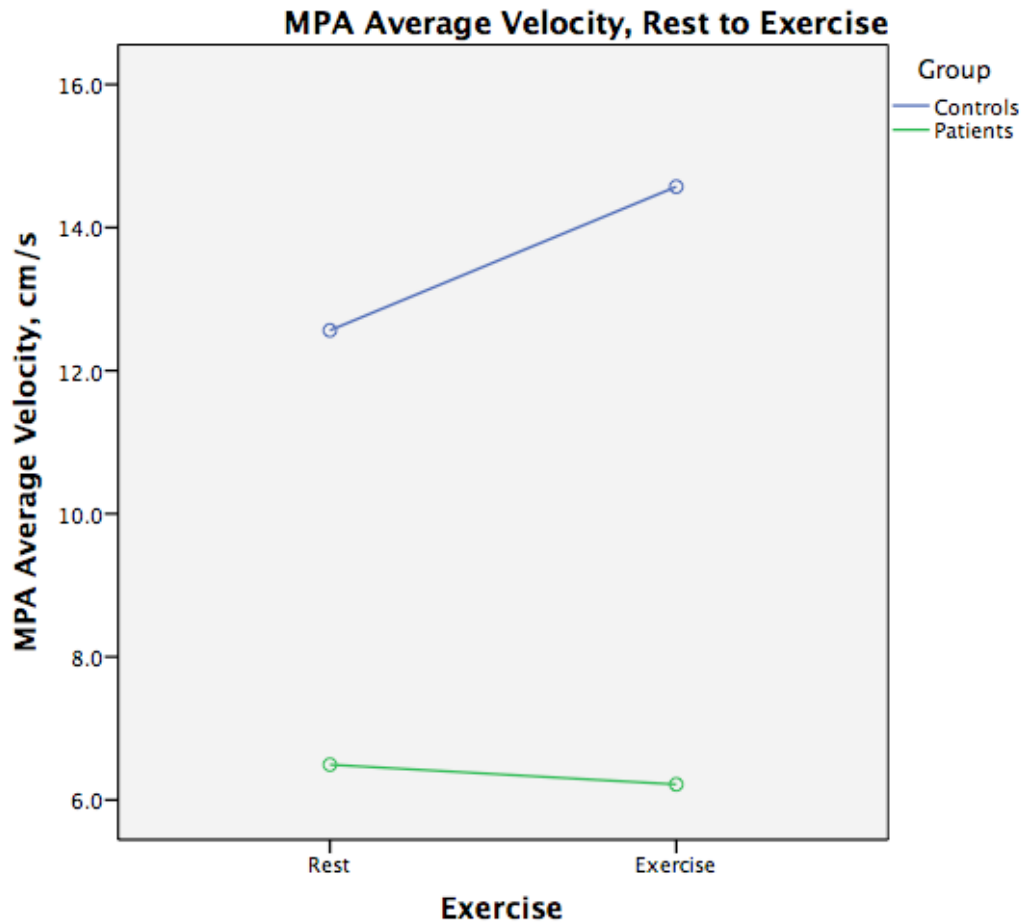
Figure 7.18: Change in MPA Average Velocity from rest to exercise, in controls and patients

7.5 Discussion

7.5.1 RV Reserve and Biventricular Remodeling in patients with normal resting RVEF

As described in Chapter 5, normal exercise is characterized by an increase in RV contractility, and an increase in LVEDVI and decrease in LVESV, with a rise in RV and LV stroke volumes. We know that in normal subjects, exercise is characterized by a reduction or no rise in PVR, due to pulmonary vascular reserve, however in patients with PAH, pulmonary vascular

resistance does not fall, and may even rise during exercise. This puts an even increased load on the RV.

Furthermore, we have shown in Chapter 6, that the healthy RV compensates homeometrically or by increasing systolic contraction rather than heterometrically or through RV dilatation and Frank Starling mechanisms, to cope with an increased load in a model of acute pulmonary hypertension. However, there remains a reduction in RV forward flow and a blunting of the rise in RVEF, leading to LV under-filling.

We have then proceeded to demonstrate that in patients with preserved resting RVEF, exercise is characterized by an increase in mean RVEDVI, with no change in mean RVESVI or RVEF. Cardiac index increases due to an increase in heart rate, with no changes in stroke volume measured by volumes or flow. When comparing change in biventricular parameters to healthy controls, while there was significant interaction, there was no between subjects' difference in rest or exercise RVEVDI, but it was highly significant for RVESVI driven by a between subject's difference in exercise parameters, and hence RVEF. This suggests that in patients with normal resting RVEF, homeometric compensation lacks reserve that is only apparent on exercise, and mechanisms to cope with an increased afterload are blunted. Hence, preload augmentation and RV dilatation, is a secondary consequence, but the degree of increase in RVEDVI is not large enough to be significantly different from healthy controls. There was also a highly significant interaction of the effect of exercise on change in LVEDVI, but LVESVI and LVEF were not, suggesting LV underfilling and maintained LV contractility, supporting our observations in the hypoxia study, that reduced RV forward flow from increased pulmonary vascular resistance, leads to LV under-filling.

When comparing the subgroups that increase or decrease RVEF on exercise, exercise in those who increase RVEF on exercise was characterized by a decrease in RVESVI hence a maintenance of the ability to increase contractility. However, RVESVI and RVEDVI both increased on exercise in those who dropped RVEF. Once again, there was no significant interaction in change in RVEDVI between the two groups. LV under-filling was apparent in those who dropped their RVEF on exercise, with a decrease in LVEDVI.

Furthermore, we have shown that ventricular mass index, and no other resting indices on CMR, correlates with exercise RV function and right ventricular reserve. This suggests that RV hypertrophy from an increase in afterload, combined with LV atrophy from underfilling, is reflected in the dynamic response of the RV to exercise. To our knowledge, we are the first to demonstrate that the ventricular mass index, as a composite index representing RV hypertrophy and LV atrophy, reflects the dynamic response of the RV to exercise, even in patients with normal resting RV function. Hardziyenka et al showed that RVF leads to a reduction in LV mass, altered gene expression and atrophic remodeling. They also demonstrated in CTEPH patients that post PEA, LV free wall mass index increased as RVEF improved(106, 109). Furthermore Gurudevan et al showed that a reduction in LV size is caused largely by a low LV preload and relative underfilling, as opposed to the geometric effects of RV enlargement in CTEPH patients (11).

These studies together demonstrate that RV adaptation to an increased load is initially homeometric, with an increase in contractility and a reduction in RVEDVI. However, in the setting of sustained pressure overload, RV contractility remains intact with RV dilatation and utilization of Frank-Starling mechanisms to increase RVSV and maintain cardiac output. Eventually, RV contractility reserves are depleted, and further RV dilatation to maintain

cardiac output occurs. LV under-filling is a consequence of the reduction in RV forward flow. These changes lead to RV hypertrophy and LV atrophy, which are a consequence of biventricular remodeling to dynamic RV function. Furthermore, we have shown this is demonstrable in patients with normal resting RVEF despite appearing clinically stable on CPET, 6MWD and resting biventricular function assessment.

The response of biventricular function in patients with PAH has been described previously. Nootens et al using CT, demonstrated in PAH patients with impaired resting RV function and dilated RVs, that exercise was characterized by an increase in RVESV, a decrease in RVEF and a decrease in LV volumes, concluding that there is evidence of reduced RV systolic function leading to LV under-filling (279). They did not show evidence of an increase in RVEDV. Similarly, Holverda et al studied 10 patients with exercise MRI, and demonstrated a trend for an increase in RVEDVI on exercise, no change in RVESVI, and a significant decrease in LVEDVI (40). However, it is important to note that both these studies included patients with resting RV impairment and dilated RVs, whereas we have shown these changes and in particular, a heterogeneity of dynamic RV response, in those with normal resting RVEF. It would be expected that patients with impaired resting RV function, would lack homeometric reserve, to increase contractility.

Excessive RV dilatation on exercise in patients with normal resting RV function, may have important clinical consequences. Hsu et al studied RV contractile reserve in patients with iPAH and scleroderma invasively and found that invasively measured resting Ees/Ea predicted RV dilatation during exercise (87). Furthermore, van de Veerdonk et at al found that patients considered stable long term, had subtle increases in resting RVEDVI and RVESVI before the onset of progressive RV dysfunction (154). Hence detecting RV dysfunction using exercise

MRI before it manifests as resting RV dilatation and dysfunction, could help detect otherwise sub-clinical ventricular-vascular uncoupling.

7.5.2 Right ventricular reserve correlates with exercise capacity, but resting biventricular function does not

We have demonstrated that resting RVEF, LVEF and exercise LVEF does not correlate with VO2 peak, however, exercise RVEF and right ventricular reserve do. This is consistent with previous studies, which have shown that exercise capacity is not related to resting RV function (82-84). Furthermore, right ventricular reserve does not correlate with haemodynamics at diagnosis, which is supported by other groups (41, 76-81) This supports the notion that there is a heterogeneity of response of the RV to afterload, and may explain why it's been difficult to be able to identify which RV is destined to fail despite medical therapy.

7.5.3 Average MPA Velocity does not increase

We have shown that in healthy volunteers, average MPA velocity increases, and we have hypothesised that this could be a reflection of pulmonary vascular distensibility. We then shown in the acute hypoxia study, that there was a blunting of the rise in average MPA velocity, and when compared to normoxic exercise, there was a trend towards significance (0.059). We have shown in patients, that there is a highly significant interaction between exercise and change in MPA average velocity, with a non-significant decrease in MPA average velocity in patients. This is an interesting observation, and warrants further investigation, as to whether exercise MPA average velocity, could potentially be a tool to non-invasively and accurately assess pulmonary vascular distensibility and early pulmonary vascular disease. As expected

MPA maximum and minimum area were significantly larger and pulsatility was significant lower in patients at both rest and exercise, with no significant interaction observed on exercise. There was a significant interaction in the change of MPA peak velocity in patients compared to controls, which would be expected given a failure of RV contractility and a reduction in RV forward flow in patients.

7.5.4 Exercise CMR as a tool to assess RV reserve

Right ventricular reserve in patients with pulmonary arterial hypertension, has been assessed by other groups using dobutamine or exercise echocardiography and invasive haemodynamics (87, 280) demonstrating a reduction in RV contractile reserve (85, 88, 164, 281). However as outlined in Chapter 1, echocardiography lacks the ability to accurately measure biventricular volumes, with a heterogeneous approach to measure RV function indirectly using TAPSE, strain, fractional area change, isovolumic acceleration time and change in sPAP (103, 104). Claessen et al have recently demonstrated a moderate correlation between exercise TAPSE and RVEF as assessed by exercise CMR, and a strong correlation between RV FAC and RVEF (282). However, even in their study, 13% of subjects did not have adequate acoustic windows, reaching up to 40% of cases in other studies (101, 102), and sPAP was in accurate in up to 50% in other studies (100, 101). Furthermore, exercise provides a true physiological stress, eliminating any bias that dobutamine may introduce, on the response of RV volumes and ejection fraction (96, 97) such as an increase in contractility or a decrease in afterload. While invasive haemodynamics can provide direct assessment of ventricular-vascular coupling, it has been shown that this does not add any further benefit, on top of SV/ESV or RVEF, as a method of assessing response to afterload in the assessment of prognosis (55, 56).

We have also shown that the timing of imaging is important, when assessing key physiological changes to exercise. When imaging was performed immediately after exercise, mean RVESV decreased with an increase in mean RVEF. As discussed in Chapter 1, previous groups using exercise CMR have performed imaging either immediately after exercise, during short breaks, or prior to reaching steady state exercise. This may miss important changes in right ventricular volumes and function.

7.5.4 Limitations

We chose to exercise patients at one level of watts that was submaximal. This was chosen in particular, so we could complete imaging during steady state exercise, and have a protocol that patients were more likely to complete. This means that patients were not imaged at peak VO_2 that may explain why right ventricular reserve correlated moderately, rather than strongly with VO_2. However, as imaging would take 2 minutes to complete, it would be unlikely that patients would be able to sustain the level of watts at peak VO_2 for that period of time.

There was variability in patient treatments, as well as the time from diagnosis and hence time from initial right heart catheterisation. The number of patients in the analysis was also small, and hence particularly in the subgroups who increased vs. decreased RVEF on exercise. Despite that, there were clear and highly significant differences in right ventricular reserve between patients and healthy controls, and delineation of those who increased versus those who decreased RVEF on exercise.

7.6 Conclusions

1. We have demonstrated that continuous, steady state exercise MRI provides an accurate, direct and non-invasive method of assessing, biventricular response to exercise, in patients with pulmonary arterial hypertension. This could add valuable information in the treatment of patients with pulmonary arterial hypertension, and may be the key to identifying those RVs which are at more risk of progressive RV failure, before resting dysfunction becomes manifest.

2. There is a heterogeneous response of right ventricular reserve amongst patients. Clinical tests such as 6MWD, TAPSE, VO2 peak and NYHA class and resting CMR biventricular parameters, as well as resting invasive haemodynamics on diagnosis cannot predict which RV lack homeometric reserve.

3. Right ventricular reserve correlates with exercise capacity, while resting RV function does not.

4. MPA average velocity does not increase on exercise in patients with PAH, while it does in healthy volunteers. This could be a novel parameter on CMR to assess pulmonary vascular distensibility and warrants further investigation.

Chapter 8 - Future Directions: An Exercise CMR Study in patients with Inoperable Chronic Thromboembolic Pulmonary Hypertension

8.1 Introduction

We are now planning to progress our work to study patients with inoperable CTEPH, before and after treatment with Riociguat. CTEPH, defined as a mean pulmonary artery pressure (mPAP) >25mmHg with a pulmonary capillary wedge pressure (PCWP) <15mmHg and at least one segmental perfusion defect following three months of adequate anticoagulation, is an important, treatable cause of persistent pulmonary hypertension (133, 134). In selected cases with centrally located anatomic obstruction in one or both branch pulmonary arteries, surgical pulmonary thromboarterectomy (PEA) can be performed often, but not always, with excellent clinical outcomes. A subset of patients has predominantly small vessel arteriopathy and are not surgical candidates with medical therapy being the standard of care for these patients. This disease is often progressive with poor outcomes. With a positive clinical trial of Riociguat in inoperable CTEPH (283), the ability to determine the extent of response early would be clinically relevant and might guide decisions to initiate more intensive therapy in these patients.

The nitric oxide (NO) pathway is impaired in patients with PAH and Sildenafil and Tadalafil increase cycle guanosine monophosphate (cGMP) by inhibiting phosphodiesterase type-5 (PDE-5). However, this is not effective in all patients, possibly because of impaired baseline NO production. Recently, a 4th class, the soluble guanylate cyclase (sGC) stimulator Riociguat, has been shown to be safe, tolerable, improve 6 minute walk distance (6MWD) and decrease mean pulmonary arterial pressure (mPAP) after 12 weeks of therapy in patients with CTEPH

and PAH (283-285). Specifically, in patients with inoperable CTEPH, Riociguat significantly improved 6MWD at 16 weeks while Bosentan did not (286).

Change in RV ejection fraction (EF) 1 year after medical therapy has been shown to be prognostic in patients with PAH (75). As we have also demonstrated in our study, RV remodeling has been shown to occur post operatively in patients with operable CTEPH (287-289), but its prognostic impact has not been assessed and the use of resting imaging and pre-operative haemodynamic evaluation does not necessarily predict exercise capacity (82, 83). We have also demonstrated these points in our studies that have been outlined in this thesis.

More recently, Blumberg et al demonstrated in a group of PAH and inoperable CTEPH subjects that peak VO_2 was the strongest predictor of survival and amongst haemodynamic variables, only exercise cardiac index and the slope of the pressure flow relationship were significant prognostic indictors. This suggests that RV reserve on exercise is an important determinant of exercise capacity, predicts prognosis and hence could potentially be used in the clinical assessment of these patients (94).

Claessen et al studied 14 CTEPH patients with exercise CMR with concurrent invasive haemodynamic monitoring, before and after acute administration of Sildenafil. They demonstrated that Sildenafil decreased RVESVi during resting and exercise, increased LVEF and RVEF at rest and exercise and increased SVi that was greater during peak exercise than at rest. Furthermore, resting RV and LV parameters did not correlate with CPET but RVEF reserve correlated moderately with peak VO_2, VE/VCO_2 and $PETCO_2$. They also found that the reduction in total PVR during peak exercise correlated highly with the increase in peak exercise SVi and RVEF after Sildenafil (161).

Surie et al similarly studied 18 patients and demonstrated, using exercise CMR, an improvement in exercise SVi post pulmonary endarterectomy in 14 patients while resting SVi, HR and cardiac index were unchanged (162). The studies, together, demonstrate how assessment of the RV and LV function during exercise may add important clinical and potentially prognostic information. Furthermore, our studies outlined in this thesis show that our approach is reproducible and feasible in patients, and that we are able to assess pathophysiological changes, which are otherwise, not present at rest.

We believe that the use of CMR in the assessment of RV function at rest and during exercise, before and after treatment, will provide better and more accurate appraisal. We hypothesize that treatment with Riociguat will improve RVEF, reduce RVH and increase CO predominantly on exercise, as assessed by CMR. Given the particular impact of Riociguat on cardiac output, evaluation of the impact of therapy on this at rest and during exercise would be useful.

8.2 Aims

To determine the impact of Riociguat on right and left ventricular (RV and LV) function at rest and on exercise using cardiac magnetic resonance imaging (CMR) in patients with non-operable Chronic Thromboembolic Pulmonary Hypertension (CTEPH).

8.2.1 Primary Study Objective

To assess the impact of treatment with Riociguat on exercise cardiac function using CMR after 12 weeks of optimal dose Riociguat therapy. The primary outcome variable at 12-20 weeks will be change in exercise right ventricular reserve, as measured by CMR from baseline.

8.2.3 Secondary Study Objective

To assess the impact of treatment with Riociguat on cardiac function at rest using CMR, 6MWD, NYHA functional class, CPET and BNP at 12 weeks. Secondary outcome variables at 12-20 weeks will be change in exercise RVEF, RVSVI and LVSVI, and change in resting biventricular parameters.

8.3 Proposed Study Design

8.3.1 Study Organisation

The PH service at Hammersmith hospital is part of the designated national pulmonary hypertension service for England. We have a programme of clinical and basic science research in pulmonary hypertension and exercise physiology. Diagnosis is made according to current European guidelines. (186). In 2014 the service saw 1162 patients; 361 were new referrals of whom 40 had CTEPH.

8.3.2 Study Population

Inclusion Criteria

35 patients undergoing routine assessment and treatment by the Pulmonary Hypertension team at Hammersmith Hospital will be recruited. All patients will undergo cardiopulmonary exercise testing, 6MWD, echocardiography, computed tomography of the pulmonary arteries, ventilation perfusion scanning and lung function tests and right heart catheterization. Inclusion

criteria will include: Age ≥18 with a diagnosis of inoperable or operable CTEPH. Investigation and treatment follow the current European guidelines (186).

Exclusion Criteria

Exclusion criteria will include contraindication to CMR such as implanted ferrous devices, pregnancy, claustrophobia, PAH that is unstable and deteriorating and any joint condition limiting exercise capacity.

8.3.3 Test Treatment

Riociguat with increments at 2 week intervals of 0.5mg, from a starting dose of 1mg to a maximum of 2.5mg tds.(286)

8.3.4 CMR Protocol:

Imaging will be carried out using a 1.5T Siemens Aera with a 60 cardiac channel coil. This is a newly acquired research CMR machine in our department in the Robert-Steiner Unit. Continuous heart rate and oxygen saturations will be monitored. We will use a resting and exercise protocol to acquire the following data for analysis and validation.

RV and LV structure and function: Real time cine acquisitions of a stack of contiguous short axis cines to allow calculation of RV and LV end systolic/diastolic volumes (ESV/EDV), myocardial wall thickness and systolic interventricular septal curvature will be acquired. Image acquisition will be performed during free breathing. Cardiac output, stroke volumes, left and right ventricular mass can be accurately and reproducibly calculated from these values and indexed to body surface area (193).

Pulmonary vascular haemodynamics: Real time flow quantification will be performed using high temporal resolution phase contrast imaging. Pulmonary arterial (PA) cross sectional area between diastole and systole using cross sectional imaging with high-resolution rapid frame acquisition will be acquired.   Mean and peak velocities in the PA, net PA blood flow, acceleration time and ejection time will be derived from the flow curves. Pulse wave velocity will be derived using the flow-area method. Using both right heart catheterization (RHC) and CMR data, PVR, PA fractional area change, compliance, capacitance and distensibility will be calculated (139).

Strain: Analysis of LV and RV strain will be analysed using TomTec software, of the resting and exercise cine images.

Supine Exercise Bicycle Protocol

Exercise will be performed with an MR-compatible bicycle ergometer (MRI cardiac ergometer Bicycle, Lode, Groningen, Netherlands) in the MRI machine. An exercise protocol will be tailored for subjects according to their CPET results, set at 40% of the watts achieved. A Cardiologist will supervise the test and exercise will be terminated either at completion of the protocol, by the subject, or if any concern is raised during the procedure.   During exercise CMR, continuous heart rate and oxygen saturations will be monitored.

8.3.4 Follow up period and Visit Schedule

Baseline exercise CMR will be performed at diagnosis, prior to treatment. Subjects will be treated with Riociguat with routine follow up at 12 weeks after optimal therapy with repeat resting and exercise CMR. Exercise CMR will be separated from other routine tests, such as CPET and 6MWD, by at least 4 hours. Drug titration will be carried out by the Pulmonary

Hypertension service or the referring physician at 2 weekly intervals. Exercise CMR will be carried out once the patient has been on 12 weeks of optimal dose therapy. Clinical outcomes will be assessed at 1, 2 and 5 years.

8.3.5 Statistical and Analytical Plan and Methodology

Descriptive data will be expressed as mean ± standard deviation. The analysis of the data requires Linear Mixed Models applied to longitudinal data. Longitudinal data require special statistical methods because observations made on each subject are correlated. This correlation must be taken into account to draw valid statistical inferences. Longitudinal analysis allows to estimate the marginal effect of the main intervention and other subject's characteristics as well to assess changes over time (e.g. before and after the intervention.) A two tailed p-value <0.05 will be considered statistically significant. An interim analysis will be carried out after recruitment of half of the subjects.

Power Calculation:

The sample size (N) was calculated for both groups (rest and exercise). The power and level of significance used were, respectively, 80% and 5 %. Because measurements before and after are correlated, the methodology used was a paired T-Test which requires the input of the SD of the difference between before and after. To detect a 3% increase in resting RVEF and a 5% increase in exercise RVEF, a sample size of 35 subjects will be required.

8.4 Discussion

We have demonstrated that assessment of dynamic biventricular function using CMR during submaximal, steady state exercise is reproducible, feasible in patients, and can detect subtle

pathophysiological changes that are otherwise not apparent at rest. In particular, assessment of right ventricular reserve may add important clinical information in addition to the current available tests, which could influence treatment decisions. A key challenge to this study is recruitment. We are currently liaising with the exercise CMR group in Leuven, with a potential to collaborate with them on this study.

This study in patients with inoperable CTEPH, carried out before and after treatment with Riociguat, offers the opportunity to study the impact of treatment on the change of right ventricular reserve at early follow up, and furthermore, follow up on the clinical outcomes. If we were demonstrate that change in right ventricular reserve at early follow up after treatment could predict a positive clinical response at longer term follow up, this could have an important impact on how we view end-points in clinical trials in the treatment of subjects with pulmonary hypertension.

Chapter 9 – Overview of Thesis

The right ventricle is anatomically and structurally different as compared to the left ventricle and has traditionally been difficult to assess functionally. Hence the gold standard of measuring ventricular-vascular coupling has been through invasive haemodynamics, with manipulation of preload or more recently, through exercise haemodynamics. However, developments in non-invasive imaging techniques are safer and potentially more clinically and prognostically relevant, and CMR is now the gold standard for measuring resting RV function and is superior technically to echocardiography. Demonstrating and developing the ability to assess RV and biventricular changes in response to changes in afterload, could potentially offer new insight and detect subclinical ventricular-vascular uncoupling, which is otherwise not present at rest.

In Chapter 3, we aimed to develop a feasible and reproducible approach to exercise CMR. Exercise CMR comes with several, unique challenges. These include the type of exercise, the timing of image acquisition, the analysis of images particularly in relation to the respiratory cycle and ensuring the correct balance between temporal and spatial resolution. We demonstrated that our approach is not only feasible, but shows intra-observer, inter-observer, inter-study and inter-test reproducibility. There are important differences in stroke volume between flow and cine acquisitions, as well as the left and right ventricle, which have technical and physiological explanations. Further work includes developing software that can incorporate respiratory bellow information so that flow analysis can be carried out during expiration, rather than being an average of 5 heart-beats.

In Chapter 4, we demonstrated the ability of CMR to detect RV remodeling in response to a decrease in afterload, in patients with operable CTEPH, before and after PEA. We also showed

that biventricular interactions, expressed in a composite RVEDV to LVEDV ratio, correlated with exercise capacity while parameters of right and left ventricular function alone did not. Left ventricular under-filling as a consequence of elevated RV pressure, was thought to be the predominant mechanism of increased RV size as compared to LV size, given that left atrial size correlated with LVEDVI.

We went on to demonstrate dynamic biventricular function and interactions using exercise CMR in Chapter 5, establishing a set of normal parameters and describing normal supine exercise physiology. LVEDVI increased on exercise, demonstrating that LV filling as well as increases in contractility contributed to an increase in LV SVI. Furthermore, we also demonstrated that the normal heart remodels in response to the amount of exercise per week, with an increase in biventricular size, and that biventricular size correlates with a higher VO2 peak. It was important to establish normal parameters, and the normal biventricular response to exercise before studying the effects of acute and chronic pulmonary hypertension.

In Chapter 6, we showed that acute pulmonary hypertension induced by acute normobaric hypoxia, leads to a reduction in LV size at rest, with no changes in RV function. However, on exercise, there was evidence of a reduction in RV forward flow, blunting of the rise in RVEF and a reduction in RVEDVI. This lead to LV under-filling and a consequent reduction in LVSVI. These changes were not captured, when imaging was performed immediately after exercise, showing the importance of continuous, steady state acquisitions during exercise.

Finally, we went on to demonstrate important feasibility of exercise CMR in patients with pulmonary arterial hypertension, and describe important pathophysiological changes that were otherwise not present at rest. In Chapter 7, we showed exercise CMR could detect an

impairment in right ventricular reserve, in subjects with otherwise normal resting RVEF. This was characterized by a reduction in RV forward flow, but contrasting to the healthy hearts in Chapter 6, there was an increase in RVEDVI and no rise in RVEF, with LV underfilling and no rise in LVSVI. Cardiac output increased driven by an increase in heart rate. Importantly, we were able to show that some patients increased while others decreased RVEF on exercise, but there were no discriminating factors at rest to predict this. It is this information that could be clinically and prognostically important.

This work is leading on to a project in patients with inoperable CTEPH, before and after treatment, to test our hypothesis that change in right ventricular reserve as measured by exercise CMR will be more clinically relevant, and linked to outcomes, over and above traditional parameters such as 6MWD or those measured on exercise testing, echocardiography or invasive haemodynamics. Our research and the research of other groups could potentially have a significant impact on how we assess response to treatment in PAH, as well lead to a review of the end-points we use in clinical trials.

References

1. Voelkel NF, Schranz D. The Right Ventricle in Health and Disease. Rounds SIS, editor: Humana Press; 2015.

2. Haddad F, Hunt SA, Rosenthal DN, Murphy DJ. Right ventricular function in cardiovascular disease, part I: Anatomy, physiology, aging, and functional assessment of the right ventricle. Circulation. 2008;117(11):1436-48.

3. Fuster V, Walsh R, Harrington R, Hunt SA, King S, Nash I, et al. Hurst's The Heart. 13th ed: The McGraw-Hill Companies; 2011.

4. Voelkel NF, Quaife RA, Leinwand LA, Barst RJ, McGoon MD, Meldrum DR, et al. Right ventricular function and failure: report of a National Heart, Lung, and Blood Institute working group on cellular and molecular mechanisms of right heart failure. Circulation. 2006;114(17):1883-91.

5. Leather HA, Ama R, Missant C, Rex S, Rademakers FE, Wouters PF. Longitudinal but not circumferential deformation reflects global contractile function in the right ventricle with open pericardium. Am J Physiol Heart Circ Physiol. 2006;290:H2369-H75.

6. Carlsson M, Ugander M, Heiberg E, Arheden H. The quantitative relationship between longitudinal and radial function in left, right and total heart pumping in humans. Am J Physiol Heart Circ Physiol. 2007;293:H636-44.

7. Hamdan A, Thouet T, Kelle S, Paetsch I, Gebker R, Wellnhofer E, et al. Regional right ventricular function and timing of contraction in healthy volunteers evaluated by strain-encoded MRI. Journal of magnetic resonance imaging : JMRI. 2008;28(6):1379-85.

8. Feneley MP, Gavaghan TP, Baron DW, Branson JA, Roy PR, Morgan JJ. Contribution of left ventricular contraction to the generation of right ventricular systolic pressure in the human heart. Circulation. 1985;71(3):473-80.

9. Bove AA, Santamore WP. Ventricular Interdependence. Prog Cardiovasc Dis. 1981;23:365-88.

10. Klima U, Guerrero JL, Vlahakes GJ. Contribution of the interventricular septum to maximal right ventricular function. European Journal of Cardio-thoracic surgery. 1998;14:250-5.

11. Gurudevan SV, Malouf PJ, Auger WR, Waltman TJ, Madani M, Raisinghani AB, et al. Abnormal left ventricular diastolic filling in chronic thromboembolic pulmonary hypertension: true diastolic dysfunction or left ventricular underfilling? Journal of the American College of Cardiology. 2007;49(12):1334-9.

12. Gan CT, Lankhaar JW, Marcus JT, Westerhof N, Marques KM, Bronzwaer JG, et al. Impaired left ventricular filling due to right-to-left ventricular interaction in patients with pulmonary arterial hypertension. Am J Physiol Heart Circ Physiol. 2006;290:H1528-H33.

13. Belenkie I, Horne G, Dani R, Smith ER, Tyberg JV. Effect of Aortic Constriction During Experimental Acute Right Ventricular Pressure Loading. Circulation. 1995;95:546-54.

14. Levick JR. An Introduction to Cardiovascular Physiology. Great Britain: Hodder Arnold; 2003.

15. Braunwald's Heart Disease. Libby P, Bonow RO, Mann DL, Zipes DP, Braunwald E, editors. United States of America: Saunders Elsevier; 2008.

16. Rodeheffer RJ, Gerstenblith G, Becker LC, Fleg JL, Weisfledt ML, Lakatta EG. Exercise cardiac output is maintained with advancing age in healthy human subjects:

cardiac dilatation and increased stroke voulme compensate for a dimished heart rate. Circulation. 1984;69:203-13.

17.   Kelbaek H, Gjorup T, Christensen NJ, B. V, Godtfredsen J. Cardiac function and plasma catecholamines during upright exercise in healthy young adults. Int J Cardiol. 1986;10(3):223-35.

18.   Roberts PA, Cowan BR, Liu Y, Lin AC, Nielsen PM, Taberner AJ, et al. Real-time aortic pulse wave velocity measurement during exercise stress testing. Journal of cardiovascular magnetic resonance : official journal of the Society for Cardiovascular Magnetic Resonance. 2015;17:86.

19.   Stratton JR, Levy WC, Cerquerira MD, Schwartz RS, Abrass IB. Cardiovascular Response to Exercise: Effects of Aging and Exercise Training in Healthy Men. Circulation. 1994;89:1648-55.

20.   Ginzton LE, Conant R, Brizendine M, Laks MM. Effect of Long-Term High Intensity Aerobic Training on Left Ventricular Volume During Maximal Upright Exercise. Journal of the American College of Cardiology. 1989;14(2):364-71.

21.   Aksut SV, Johnson PS, Walter JD, DiMarzio D, Cave V, Cassel D, et al. Comparison of left ventricular performance in healthy young women and men during exercise. J Nucl Cardiol. 1996;3(5):415-21.

22.   Kitzman DW, Higginbotham MB, Cobb FR, Sheikh KH, Sullivan MJ. Exercise intolerance in patients with Heart Failure and Preserved Left Ventricular Systolic Function: Failure of the Frank Starling Mechanism. Journal of the American College of Cardiology. 1991;17(5):1065-72.

23.   Steingart RM, Wexler J, Salgle S, Scheuer J. Radionuclide ventriculographic responses to graded supine and upright exercise: critical role of the Frank-Starling mechanism at submaximal exercise. Am J Cardiol. 1984;53(11):1671-7.

24.   Higginbotham MB, Morris KG, Coleman E, Cobb FR. Sex-related differences in the normal cardiac response to upright exercise. Circulation. 1984;70(3):357-66.

25.   Manyari DE, Kostuk WJ. Left and Right Ventricular Function at Rest and During Bicycle Exercise in the Supine and Sitting Positions in Normal Subjects and Patients with Coronary Artery Disease. Am J Cardiol. 1983;51.

26.   Roest AAW, Kunz P, Lamb H, Helbing WA, van der Wall E, de Roos A. Biventricular Response to Supine Physicla Exercise in Young Adults Assessed with Ultrafast Magnetic Resonance Imaging. Am J Cardiol. 2001;87:601-5.

27.   von Knobelsdorff-Brenkenhoff F, Dieringer MA, Fuchs K, Hezel F, Niendorf T, Schulz-Menger J. Isometric handgrip exercise during cardiovascular magnetic resonance imaging: set-up and cardiovascular effects. Journal of magnetic resonance imaging : JMRI. 2013;37(6):1342-50.

28.   Mortensen KH, Jones A, Steeden JA, Taylor AM, Muthurangu V. Isometric stress in cardiovascular magnetic resonance-a simple and easily replicable method of assessing cardiovascular differences not apparent at rest. European radiology. 2016;26(4):1009-17.

29.   Alegret JM, Beltran-Debon R, La Gerche A, Franco-Bonafonte L, Rubio-Perez F, Calvo N, et al. Acute effect of static exercise on the cardiovascular system: assessment by cardiovascular magnetic resonance. European journal of applied physiology. 2015;115(6):1195-203.

30.   Steding-Ehrenborg K, Jablonowski R, Arvidsson PM, Carlsson M, Saltin B, Arheden H. Moderate intensity supine exercise causes decreased cardiac volumes and increased outer volume variations: a cardiovascular magnetic resonance study. Journal of Cardiovascular Magnetic Resonance. 2013;15(96).

31.   Poliner LR, Dehmer GJ, Lewis SE, Parkey RW, Blomqvist CG, Willerson JT. Left Ventricular Performance in Normal Subjects: A Comparison of the Reponses to Exercise in the Upright and Supine Positions. Circulation. 1980;62(3):528-34.

32.   Higginbotham MB, Morris KG, Williams RS, McHale PA, Coleman E, Cobb FR. Regulation of Stroke Volume during Submaximal and Maximal Upright Exercise in Normal Man. Circ Res. 1986;58:281-91.

33.   Boutcher SJ, Mclaren PF, Cotton Y, Boutcher Y. Stroke volume response to incremental submaximal exercise in aerobically trained active and sedentary men. Can J Appl Physiol. 2003;28(1):12-26.

34.   Warburton DE, Haykowsky MJ, Quinney HA, Blackmore D, Teo KK, Humen DP. Myocardiacl response to incremental exercise in endurance-trained athletes influence heart rate, contractility and the Frank-Starling effect. Exp Physiol. 2002;87(5):613-22.

35.   Hanley PC, Zinsmeister AR, Clements IP, Bove AA, Brown ML, Gibbons RJ. Gender-Related Differences in Cardiac Response to Supine Exercise Assessed by Radionuclide Angiography. Journal of the American College of Cardiology. 1989;13(3):624-9.

36.   Mols P, Huynh CH, Naije N, Ham HR. Volumetric response of the right ventricle during progressive supine exercise in men. Am J Physiol. 1991;261:751-4.

37.   La Gerche A, Claessen G, Van de Bruaene A, Pattyn N, Van Cleemput J, Gewillig M, et al. Cardiac MRI: a new gold standard for ventricular volume quantification during high-intensity exercise. Circulation Cardiovascular imaging. 2013;6(2):329-38.

38.   Roest AAW. Cardiovascular response to physical exercise in adult patients after atrial correction for transposition of the great arteries assessed with magnetic resonance imaging. Heart. 2004;90(6):678-84.

39.   Roest AAW, Helbing WA, Kunz P, van den Aardweg J, Lamb H, Vliegan H, et al. Exercise MR Imaging in the Assessment of Pulmonary Regurgitation and Biventricular Function in Patients after Tetralogy of Fallot Repair. Radiology. 2002;223:204-11.

40.   Holverda S, Tji-Joong Gan C, Marcus JT, Postmus PE, Boonstra A, Vonk Noordegraaf A. Impaired Stroke Volume Response to Exercise in Pulmonary Arterial Hypertension. JACC. 2006;47(8):1724-38.

41.   Plehn G, Vormbrock J, Perings S, Plehn A, Meissner A, Butz T, et al. Comparison of right ventricular functional response to exercise in hypertrophic versus idiopathic dilated cardiomyopathy. Am J Cardiol. 2010;105(1):116-21.

42.   Holverda S, Rietema H, Westerhof N, Marcus JT, Gan CT, Postmus PE, et al. Stroke volume increase to exercise in chronic obstructive pulmonary disease is limited by increased pulmonary artery pressure. Heart. 2009;95(2):137-41.

43.   Argiento P, Chesler N, Mule M, D'Alto M, Bossone E, Unger P, et al. Exercise stress echocardiography for the study of the pulmonary circulation. The European respiratory journal : official journal of the European Society for Clinical Respiratory Physiology. 2010;35(6):1273-8.

44.   Reeves JT, Dempsey JA, RF. G. Pulmonary circulation during exercise. Pulmonary Vascular Physiology and Physiopathology. New York:: Marcel Dekker. p. 107-33,.

45.   Chesler NC, Roldan A, Vanderpool RR, Naeije R. How to measure pulmonary vascular and right ventricular function. Conference proceedings : Annual International Conference of the IEEE Engineering in Medicine and Biology Society IEEE Engineering in Medicine and Biology Society Conference. 2009;2009:177-80.

46.   Brimioulle S, Wauthy P, Ewalenko P, Rondelet B, Vermeulen F, Kerbaul F, et al. Single-beat estimation of right ventricular end-systolic pressure-volume relationship. Am J Physiol Heart Circ Physiol. 2003;284(5):H1625-30.

47.   Elizinga G, Westerhof N. The Effect of An Increase in Inotropic State and End-Diastolic Volume on the Pumping Ability of the Feline left heart. Circ Res. 1978;42:620-8.

48.   Overbeek MJ, Lankhaar JW, Westerhof N, Voskuyl AE, Boonstra A, Bronzwaer JG, et al. Right ventricular contractility in systemic sclerosis-associated and idiopathic pulmonary arterial hypertension. The European respiratory journal : official journal of the European Society for Clinical Respiratory Physiology. 2008;31(6):1160-6.

49.   Trip P, Kind T, van de Veerdonk MC, Marcus JT, de Man FS, Westerhof N, et al. Accurate assessment of load-independent right ventricular systolic function in patients with pulmonary hypertension. The Journal of heart and lung transplantation : the official publication of the International Society for Heart Transplantation. 2013;32(1):50-5.

50.   Kuehne T, Yilmaz S, Steendijk P, Moore P, Groenink M, Saaed M, et al. Magnetic resonance imaging analysis of right ventricular pressure-volume loops: in vivo validation and clinical application in patients with pulmonary hypertension. Circulation. 2004;110(14):2010-6.

51.   Lankhaar JW, Westerhof N, Faes TJC, Gan CT, Marques KM, Boonstra A, et al. Pulmonary vascular resistance and compliance stay inversely related during treatment of pulmonary hypertension. Eur Heart J. 2008;29:1688-95.

52.   Karunanithi MK, Michniewicz J, Copeland SE, Feneley MP. Right Ventricular Preload Recruitable Stroke Work, End-Systolic Pressure-Volume and dP/dtmax-End Diastolic Volume Relations Compared as Indexes of Right Ventricular Contractile Performance in Conscious Dogs. Circ Res. 1992;70:1169-79.

53.   Dwyer N, Yong AC, Kilpatrick D. Variable open-end wave reflection in the pulmonary arteries of anesthetized sheep. The journal of physiological sciences : JPS. 2012;62(1):21-8.

54.   McCabe C, White PA, Hooker SP, Axell RG, Priest AN, Gopalan D, et al. Right ventricular dysfunction in chronic thromboembolic obstruction of the pulmonary artery: a pressure-volume study using the conductance catheter. J Appl Physiol. 2014;116:355-63.

55.   Brewis MJ, Bellofiore A, Vanderpool RR, Chesler NC, Johnson MK, Naeije R, et al. Imaging right ventricular function to predict outcome in pulmonary arterial hypertension. Int J Cardiol. 2016;218:206-11.

56.   Vanderpool RR, Pinsky MR, Naeije R, Deible C, Kosaraju V, Bunner C, et al. RV-pulmonary arterial coupling predicts outcome in patients referred for pulmonary hypertension. Heart. 2015;101(1):37-43.

57.   Sanz J, Garcia-Alvarez A, Fernandez-Friera L, Nair A, Mirelis JG, Sawit ST, et al. Right ventriculo-arterial coupling in pulmonary hypertension: a magnetic resonance study. Heart. 2012;98(3):238-43.

58.   Anavekar NS, Gerson D, Skali H, Kwong RY, Yucel EK, Solomon SD. Two-dimensional assessment of right ventricular function: an echocardiographic-MRI correlative study. Echocardiography. 2007;24(5):452-6.

59.   Lang RM, Bierig M, Devereux RB, Flachskampf FA, Foster E, Pellikka PA, et al. Recommendations for chamber quantification: a report from the American Society of Echocardiography's Guidelines and Standards Committee and the Chamber Quantification Writing Group, developed in conjunction with the European Association of Echocardiography, a branch of the European Society of Cardiology. Journal of the American Society of Echocardiography : official publication of the American Society of Echocardiography. 2005;18(12):1440-63.

60.   van der Zwaan HB, Geleijnse ML, McGhie JS, Boersma E, Helbing WA, Meijboom FJ, et al. Right ventricular quantification in clinical practice: two-dimensional vs. three-

dimensional echocardiography compared with cardiac magnetic resonance imaging. European journal of echocardiography : the journal of the Working Group on Echocardiography of the European Society of Cardiology. 2011;12(9):656-64.

61.   Sato T, Tsujino I, Ohira H, Oyama-Manabe N, Yamada A, Ito YM, et al. Validation study on the accuracy of echocardiographic measurements of right ventricular systolic function in pulmonary hypertension. Journal of the American Society of Echocardiography : official publication of the American Society of Echocardiography. 2012;25(3):280-6.

62.   Vogel M. Validation of Myocardial Acceleration During Isovolumic Contraction as a Novel Noninvasive Index of Right Ventricular Contractility: Comparison With Ventricular Pressure-Volume Relations in an Animal Model. Circulation. 2002;105(14):1693-9.

63.   Ernande L, Cottin V, Leroux PY, Girerd N, Huez S, Mulliez A, et al. Right isovolumic contraction velocity predicts survival in pulmonary hypertension. Journal of the American Society of Echocardiography : official publication of the American Society of Echocardiography. 2013;26(3):297-306.

64.   Ogihara Y, Yamada N, Dohi K, Matsuda A, Tsuji A, Ota S, et al. Utility of right ventricular Tei-index for assessing disease severity and determining response to treatment in patients with pulmonary arterial hypertension. Journal of cardiology. 2014;63(2):149-53.

65.   Leong DP, Grover S, Molaee P, Chakrabarty A, Shirazi M, Cheng YH, et al. Nonvolumetric echocardiographic indices of right ventricular systolic function: validation with cardiovascular magnetic resonance and relationship with functional capacity. Echocardiography. 2012;29(4):455-63.

66.   Fine N, Chen L, Bastiansen P, Frantz RP, Pellikka PA, Jae OK, et al. Outcome Prediction by Quantitative Right Ventricular Function Assessment in 575 Subjects Evaluated for Pulmonary Hypertension. Circulation Cardiovascular imaging. 2013;6:711-21.

67.   Giusca S, Jurcut R, Coman IM, Ghiorghiu I, Catrina D, Popescu BA, et al. Right ventricular function predicts clinical response to specific vasodilator therapy in patients with pulmonary hypertension. Echocardiography. 2013;30(1):17-26.

68.   Raymond RJ, Hinderliter AL, Willis PW, Ralph D, Caldwell EJ, Williams W, et al. Echocardiographic Predictors of Adverse Outcomes in Primary Pulmonary Hypertension. Journal of the American College of Cardiology. 2002;39:1214-9.

69.   Grapsa J, Dawson D, Nihoyannopoulos P. Assessment of right ventricular structure and function in pulmonary hypertension. Journal of cardiovascular ultrasound. 2011;19(3):115-25.

70.   Buechel ERV, Mertens LL. Imaging the right heart: the use of integrated multimodality imaging. European Heart Journal. 2012;33:949-60.

71.   Benza R, Biederman R, Murali S, Gupta H. Role of Cardiac Magnetic Resonance Imaging in the Management of Patients with Pulmonary Arterial Hypertension. 2008. 2008;52:1683-92.

72.   Grothues F, Smith G, Moon JC, Bellenger NG, Collins P, Klein H, et al. Comparison of Interstudy Reproducibility of Cardiovascular Magnetic Resonance With Two Dimensional Echocardiography in Normal Subjects and in Patients wtih Heart Failure or Left Ventricular Hypertrophy. Am J Cardiol. 2002;90:29-34.

73.   Rajaram S, Swift AJ, Capener D, Elliot CA, Condliffe R, Davies C, et al. Comparison of the diagnostic utility of cardiac magnetic resonance imaging, computed tomography, and echocardiography in assessment of suspected pulmonary arterial hypertension in

patients with connective tissue disease. The Journal of rheumatology. 2012;39(6):1265-74.

74.   Yamada Y, Okuda S, Kataoka M, Tanimoto A, Tamura Y, Abe T, et al. Prognostic Value of Cardiac Magnetic Resonance Imaging for Idiopathic Pulmonary Arterial Hypertension Before Initiating Intravenous Prostacyclin Therapy. Circulation Journal. 2012;76(7):1737-43.

75.   van de Veerdonk MC, Kind T, Marcus JT, Mauritz GJ, Heymans MW, Bogaard HJ, et al. Progressive right ventricular dysfunction in patients with pulmonary arterial hypertension responding to therapy. Journal of the American College of Cardiology. 2011;58(24):2511-9.

76.   Morrison DA, Lancaster L, Henry R, Goldman S. Right Ventricular Function at Rest and During Exercise in Aortic and Mitral Valve Disease. Journal of the American College of Cardiology. 1985;5:21-8.

77.   Flox Camacho A, Escribano Subias P, Jimenez Lopez Guarch C, Fernandez Vaqueo A, Martin-Rios D, de la Calzada CS. Factors Affecting the Response to Exercise in Patients with Severe Pulmonary Arterial Hypertension. Arch Bronconeumol. 2011;47:10-6.

78.   Raeside D, Smith A, Brown A, Patel K, Madhok R, Cleland J, et al. Pulmonary artery pressure measurement during exercise testing in patients with suspected pulmonary hypertension. The European respiratory journal : official journal of the European Society for Clinical Respiratory Physiology. 2000;16:282-7.

79.   Riley MS, Porszasz J, Engelen MPKJ, Shapiro SM, Brundage BH, Wasserman K. Responses to Constant Work Rate Bicycle Ergometry Exercise in Primary Pulmonary Hypertension: The Effect of Inhaled Nitric Oxide. Journal of the American College of Cardiology. 2000;36:547-56.

80.   Bonderman D, Martischnig AM, Vonbank K, Nikfardjam M, Meyer B, Heinz G, et al. Right ventricular load at exercise is a cause of persistent exercise limitation in patients with normal resting pulmonary vascular resistance after pulmonary endarterectomy. Chest. 2011;139(1):122-7.

81.   McCullagh B, Girgis RE. Exercise as an end-point in pulmonary hypertension trials. International journal of clinical practice Supplement. 2010(165):4-6.

82.   Stevens G, Lala A, Sanz J, Garcia MJ, Fuster V, Pinney S. Exercise Performance in Patients with Pulmonary Hypertension Linked to Cardiac Magnetic Resonance Measures. The Journal of heart and lung transplantation : the official publication of the International Society for Heart Transplantation. 2009;28:899-905.

83.   Roest A, Lamb H, van der Wall E, Vliegen H, van den Aardweg J, Kunz P, et al. Cardiovascular response to physical exercise in adult patients after atrial correction for transposition of the great arteries assessed with magnetic resonance imaging. Heart. 2004;90:678-84.

84.   Stevens GR, Garcia-Alvarez A, Sahni S, Garcia MJ, Fuster V, Sanz J. RV dysfunction in pulmonary hypertension is independently related to pulmonary artery stiffness. JACC Cardiovascular imaging. 2012;5(4):378-87.

85.   Chia EM, Lau EM, Xuan W, Celermajer DS, Thomas L. Exercise testing can unmask right ventricular dysfunction in systemic sclerosis patients with normal resting pulmonary artery pressure. Int J Cardiol. 2016;204:179-86.

86.   Sharma T, Lau EM, Choudhary P, Torzillo PJ, Munoz PA, Simmons LR, et al. Dobutamine stress for evaluation of right ventricular reserve in pulmonary arterial hypertension. The European respiratory journal : official journal of the European Society for Clinical Respiratory Physiology. 2015;45(3):700-8.

87.   Hsu S, Houston BA, Tampakakis E, Bacher AC, Rhodes PS, Mathai SC, et al. Right Ventricular Functional Reserve in Pulmonary Arterial Hypertension. Circulation. 2016;133(24):2413-22.

88.   Domingo E, Grignola JC, Aguilar R, Arredondo C, Bouteldja N, Messeguer ML, et al. Impairment of pulmonary vascular reserve and right ventricular systolic reserve in pulmonary arterial hypertension. BMC Pulmonary Medicine. 2014;14(69).

89.   Borlaug BA, Kane GC, Melenovsky V, Olson TP. Abnormal right ventricular-pulmonary artery coupling with exercise in heart failure with preserved ejection fraction. Eur Heart J. 2016.

90.   Morrison DA, Adcock K, Collins M, Goldman S, Caldwell JH, Schwarz MI. Right Ventricular Dysfunction and the Exercise Limitation of Chronic Obstructive Pulmonary Disease. Journal of the American College of Cardiology. 1987;9:1219-29.

91.   Haddad F, Vrtovec B, Ashley EA, Deschamps A, Haddad H, Denault AY. The concept of ventricular reserve in heart failure and pulmonary hypertension: an old metric that brings us one step closer in our quest for prediction. Current opinion in cardiology. 2011;26(2):123-31.

92.   Di Salvo TG, Mathier MA, Semigran MJ, William Dec G. Preserved Right Ventricular Ejection Fraction Predicts Exercise Capacity and Survival in Advanced Heart Failure. Journal of the American College of Cardiology. 1995;25:1143-53.

93.   Kusunose K, Popovic ZB, Motoki H, Marwick TH. Prognostic significance of exercise-induced right ventricular dysfunction in asymptomatic degenerative mitral regurgitation. Circulation Cardiovascular imaging. 2013;6(2):167-76.

94.   Blumberg FC, Artz M, Lange T, Schroll S, Pfeifer M, Wensel R. Impact of right ventricular reserve on exercise capacity and survival in patients with pulmonary hypertension. European Journal of Heart Failure. 2013;15:771-5.

95.   Cotrim C, Simoes O, Loureiro M, Cordeiro P, Lopes L, Almeida S, et al. Stress echocardiography in the evaluation of exercise physiology in patients with severe arterial pulmonary hypertension. Rev Port Cardiol. 2005;24(12):1451-60.

96.   Oosterhof T, Tulevski I, Roest AAW, Steendijk P, Vliegan H, van der Wall E, et al. Disparity between dobutamine stress and physicial exercise magnatic resonance imaging in patients with an intra-atrial correction for transposition of the great arteries. Journal of cardiovascular magnetic resonance : official journal of the Society for Cardiovascular Magnetic Resonance. 2005;7(2):383-9.

97.   Cnota JF, Mays WA, Knecht SK, Kopser S, Michelfelder EC, Knilans TK, et al. Cardiovascular physiology during supine cycle ergometry and dobutamine stress. Medicine and science in sports and exercise. 2003;35(9):1503-10.

98.   Claessen G, La Gerche A, Voigt JU, Dymarkowski S, Schnell F, Petit T, et al. Accuracy of Echocardiography to Evaluate Pulmonary Vascular and RV Function during Exercise. JACC Cardiovascular imaging. 2015;9(5):532-43.

99.   Grunig E, Weissmann S, Ehlken N, Fijalkowska A, Fischer C, Fourme T, et al. Stress Doppler echocardiography in relatives of patients with idiopathic and familial pulmonary arterial hypertension: results of a multicenter European analysis of pulmonary artery pressure response to exercise and hypoxia. Circulation. 2009;119(13):1747-57.

100.   Arcasoy SM, Christie JD, Ferrari VA, Sutton MS, Zisman DA, Blumenthal NP, et al. Echocardiographic assessment of pulmonary hypertension in patients with advanced lung disease. American journal of respiratory and critical care medicine. 2003;167(5):735-40.

101.   Fisher MR, Forfia PR, Chamera E, Housten-Harris T, Champion HC, Girgis RE, et al. Accuracy of Doppler echocardiography in the hemodynamic assessment of pulmonary

hypertension. American journal of respiratory and critical care medicine. 2009;179(7):615-21.

102.   La Gerche A, Claessen G, Dymarkowski S, Voigt JU, De Buck F, Vanhees L, et al. Exercise-induced right ventricular dysfunction is associated with ventricular arrhythmias in endurance athletes. Eur Heart J. 2015;36(30):1998-2010.

103.   Vachiery JL, Pavelescu A. Exercise echocardiography in pulmonary hypertension. European Heart Journal Supplements. 2007;9(Suppl H):H48-H53.

104.   Baptista R, Serra S, Martins R, Teixeira R, Castro G, Salvador MJ, et al. Exercise echocardiography for the assessment of pulmonary hypertension in systemic sclerosis: a systematic review. Arthritis research & therapy. 2016;18(1):153.

105.   Huonker M, Konig D, Keul J. Assessment of Left Ventricular Dimensions and Functions in Athletes and Sedentary Subjects at Rest and During Exercise Using Echocardiography. International Journal of sports medicine. 1996;17:S173-S9.

106.   Hardziyenka M, Campian ME, Reesink HJ, Surie S, Bouma BJ, Groenink M, et al. Right ventricular failure following chronic pressure overload is associated with reduction in left ventricular mass evidence for atrophic remodeling. Journal of the American College of Cardiology. 2011;57(8):921-8.

107.   Marcus JT, Vonk Noordegraaf A, Roeleveld RJ, Postmus PE, Heethar R, van Rossum A, et al. Impaired left ventricular filling due to right ventricular pressure overload in primary pulmonary hypertension: noninvasive monitoring using MRI. Chest. 2001;119(6):1761-5.

108.   Hardegree EL, Sachdev A, Fenstad ER, Villarraga HR, Frantz RP, McGoon MD, et al. Impaired left ventricular mechanics in pulmonary arterial hypertension: identification of a cohort at high risk. Circulation Heart failure. 2013;6(4):748-55.

109.   Hardziyenka M, Campian ME, Verkerk AO, Surie S, van Ginneken AC, Hakim S, et al. Electrophysiologic remodeling of the left ventricle in pressure overload-induced right ventricular failure. Journal of the American College of Cardiology. 2012;59(24):2193-202.

110.   Wauthy P, Pagnamenta A, Vassalli F, Naeije R, Brimioulle S. Right ventricular adaptation to pulmonary hypertension: an interspecies comparison. Am J Physiol Heart Circ Physiol. 2004;286(4):H1441-7.

111.   Naeije R, Chesler N. Pulmonary Circulation at Exercise. Comprehensive Physiology. 2012;2(1):711-41.

112.   Naeije R, Dedobbeleer C. Pulmonary hypertension and the right ventricle in hypoxia. Exp Physiol. 2013;98(8):1247-56.

113.   Morrell N, Nijran KS, Biggs T, Seed WA. Magnitude and time course of hypoxic pulmonary vasoconstriction in man. Respiration Physiology. 1995;100:271-81.

114.   Fishman AP, Fritts HW, Cournand A. Effects of Acute Hypoxia and Exercise on the Pulmonary Circulation. Circulation. 1960;22(2):204-15.

115.   Reichenberger F, Kohstall MG, Seeger T, Olschewski H, Grimminger F, Seeger W, et al. Effect of sildenafil on hypoxia-induced changes in pulmonary circulation and right ventricular function. Respiratory physiology & neurobiology. 2007;159(2):196-201.

116.   Naeije R. Physiological adaptation of the cardiovascular system to high altitude. Prog Cardiovasc Dis. 2010;52(6):456-66.

117.   Huez S, Retailleau K, Unger P, Pavelescu A, Vachiery JL, Derumeaux G, et al. Right and left ventricular adaptation to hypoxia: a tissue Doppler imaging study. Am J Physiol Heart Circ Physiol. 2005;289(4):H1391-8.

118.   Goebel B, Handrick V, Lauten A, Fritzenwanger M, Schutze J, Otto S, et al. Impact of acute normobaric hypoxia on regional and global myocardial function: a speckle tracking

echocardiography study. The international journal of cardiovascular imaging. 2013;29(3):561-70.

119. Kullmer T, Kneissl G, Katova T, Kronenberger H, Urhausen A, Kindermann W, et al. Experimental acute hypoxia in healthy subjects: evaluation of systolic and diastolic function of the left ventricle at rest and during exercise using echocardiography. Eur J Appl Physiol Occup Physiol. 1995;70:169-74.

120. Boussuges A, Molenat F, Burnet H, Cauchy E, Gardette B, Sainty J, et al. Operation Everest III (Comex '97): Modifications of Cardiac Function Secondary to Altitude-induced Hypoxia. American journal of respiratory and critical care medicine. 2000;161:264-70.

121. Pavelescu A, Naeije R. Effects of epoprostenol and sildenafil on right ventricular function in hypoxic volunteers: a tissue Doppler imaging study. European journal of applied physiology. 2012;112(4):1285-94.

122. Netzer NC, Strohl KP, Hogel J, Gatterer H, Schilz R. Right ventricle dimensions and function in response to acute hypoxia in healthy human subjects. Acta physiologica. 2016.

123. Oliver RM, Peacock A, Challenor VF, Fleming JS, Waller DG. The effect of acute hypoxia on right ventricular function in healthy adults. International Journal of Cardiology. 1991;31:235-42.

124. Peltonen JE, Tikkanen HO, Rusko HK. Cardiorespiratory responses to exercise in acute hypoxia, hyperoxia and normoxia. European journal of applied physiology. 2001;85(1-2):82-8.

125. Naeije R, Huez S, Lamotte M, Retailleau K, Neupane S, Abramowicz D, et al. Pulmonary artery pressure limits exercise capacity at high altitude. The European respiratory journal : official journal of the European Society for Clinical Respiratory Physiology. 2010;36(5):1049-55.

126. Kjaergaard J, Snyder EM, Hassager C, Olson TP, Oh JK, Johnson BD, et al. Right ventricular function with hypoxic exercise: effects of sildenafil. European journal of applied physiology. 2007;102(1):87-95.

127. Yan B, Hu Y, Ji H, Bao D. The effect of acute hypoxia on left ventricular function during exercise. European journal of applied physiology. 2007;100(3):261-5.

128. Fukada T, Maegawa W, Komatsu Y, Nakajina T, Nagai R, Kawahara T. Effects of acute hypoxia at moderate altitude on stroke volume and cardiac output during exercise. Int Heart J. 2010;51(3):170-5.

129. Galie N, Humbert M, Vachiery JL, Gibbs S, Lang I, Torbicki A, et al. 2015 ESC/ERS Guidelines for the diagnosis and treatment of pulmonary hypertension: The Joint Task Force for the Diagnosis and Treatment of Pulmonary Hypertension of the European Society of Cardiology (ESC) and the European Respiratory Society (ERS): Endorsed by: Association for European Paediatric and Congenital Cardiology (AEPC), International Society for Heart and Lung Transplantation (ISHLT). Eur Heart J. 2016;37(1):67-119.

130. Mayer E, Jenkins D, Lindner J, D'Armini A, Kloek J, Meyns B, et al. Surgical management and outcome of patients with chronic thromboembolic pulmonary hypertension: results from an international prospective registry. The Journal of thoracic and cardiovascular surgery. 2011;141(3):702-10.

131. Benza RL, Miller DP, Barst RJ, Badesch DB, Frost AE, McGoon MD. An evaluation of long-term survival from time of diagnosis in pulmonary arterial hypertension from the REVEAL Registry. Chest. 2012;142(2):448-56.

132. Members ATF. Guidelines for the diagnosis and treatment of pulmonary hypertension: The Task Force for the Diagnosis and Treatment of Pulmonary Hypertension of the European Society of Cardiology (ESC) and the European Respiratory

Society (ERS) endorsed by the International Society of Heart and Lung Transplantation (ISHFL). European Heart Journal. 2009;30:2493-537.

133.   Lang IM, Pesavento R, Bonderman D, Yuan J. Risk factors and basic mechanisms of CTEPH - a current understanding. The European respiratory journal : official journal of the European Society for Clinical Respiratory Physiology. 2012.

134.   Delcroix M, Vonk-Noordegraaf A, Fadel E, Lang IM, Simonneau G, Naeije R. Vascular and right ventricular remodeling in chronic thromboembolic pulmonary hypertension. The European respiratory journal : official journal of the European Society for Clinical Respiratory Physiology. 2012.

135.   de Perrot M, McRae K, Shargall Y, Thengannat J, Moric J, Mak S, et al. Early Postoperative Pulmonary Vascular Compliance Predicts Outcome After Pulmonary Endarterectomy for Chronic Thromboembolic Pulmonary Hypertension. Chest. 2011;140(1):34-41.

136.   Voelkel N, Quaife RA, Leinwand LA, Barst RJ, McGoon MD, Meldrum DR, et al. Right Ventricular Function and Failure: Report of a National Heart, Lung and Blood Institute Working Group on Cellular and Molecular Mechanisms of Right Heart Failure. Circulation. 2006;114:1883-91.

137.   Voelkel N, Natarajan R, Drake J, Bogaard H. Right Ventricle in Pulmonary Hypertension. Comprehensive Physiology. 2011;1(525-540).

138.   Masci PG, Francone M, Desmet W, Ganame J, Todiere G, Donate R, et al. Right Ventricular Ischaemia Injury in Patients with Acute ST Segment Elevation Myocardial Infarction: Characterisation with Cardiovascular Magnetic Resonance. Circulation. 2010;122:1405-12.

139.   Sanz J, Kariisa M, Dellegrottaglie S, Prat-Gonzalez S, Garcia MJ, Fuster V, et al. Evaluation of Pulmonary Artery Stiffness in Pulmonary Hypertension with Cardiac Magenetic Resonance. JACC: Cardiovascular Imaging. 2009;2:286-95.

140.   Stevens G, Garcia-Alvarez A, Sahni S, Garcia MJ, Fuster V, Sanz J. RV Dysfunction in Pulmonary Hypertension is Independently Related to Pulmonary Artery Stiffness. JACC: Cardiovascular Imaging. 2012;5:378-87.

141.   Mahapatra S, Nishimura RA, Sorajja P, Cha S, McGoon MD. Relationship of Pulmonary Arterial Capacitance and Mortality in Idiopathic Pulmonary Arterial Hypertension. Journal of the American College of Cardiology. 2006;47:799-803.

142.   Bonderman D, Martischnig AM, Nikfardjam M, Meyer B, Heinz B, Klepetko W, et al. Right Ventricular Load at Exercise Is a Cause of Persistent Exercise Limitation in Patients with Normal Resting Pulmonary Vascular Resistance after Pulmonary Endarterectomy. Chest. 2011;139:122-7.

143.   Swiston JR, Johnson SR, Granton JT. Factors that prognosticate mortality in idiopathic pulmonary arterial hypertension: a systematic review of the literature. Respiratory medicine. 2010;104(11):1588-607.

144.   Benza R, Miller DP, Gomberg-Maitland M, Frantaz RP, Foreman A, Coffey C, et al. Predicting Survival in Pulmonary Arterial Hypertension: Insights from the Registry to Evaluate Early and Long Term Pulmonary Arterial Hypertension Disease Management (REVEAL). Circulation. 2010;122:164-72.

145.   Humbert M, Sitbon O, Chaouat A, Bertocchi M, Habib G, Gressin V, et al. Survival in Patients with Idiopathic, Familial and Anorexigen-Associated Pulmonary Arterial Hypertension in the Modern Management Era. Circulation. 2010;122:156-63.

146.   Humbert M, Sitbon O, Chaouat A, Bertocchi M, Habib G, Gressin V, et al. Survival in patients with idiopathic, familial, and anorexigen-associated pulmonary arterial hypertension in the modern management era. Circulation. 2010;122(2):156-63.

147.   Condliffe R, Kiely DG, Gibbs JS, Corris PA, Peacock AJ, Jenkins DP, et al. Prognostic and aetiological factors in chronic thromboembolic pulmonary hypertension. The European respiratory journal : official journal of the European Society for Clinical Respiratory Physiology. 2009;33(2):332-8.

148.   van de Veerdonk M, Kind T, Marcus JT, Mauritz G-J, Heymans MW, Bogaard H, et al. Progressive Right Ventricular Dysfunction in Patients with Pulmonary Arterial Hypertension Responding to Therapy. Journal of the American College of Cardiology. 2011;58:2511-19.

149.   Kawut SM, Al-Naamani N, Agerstrand C, Rosenzweig EB, Rowan C, Barst RJ, et al. Determinants of right ventricular ejection fraction in pulmonary arterial hypertension. Chest. 2009;135(3):752-9.

150.   Swift AJ, Rajaram S, Campbell MJ, Hurdman J, Thomas S, Capener D, et al. Prognostic value of cardiovascular magnetic resonance imaging measurements corrected for age and sex in idiopathic pulmonary arterial hypertension. Circulation Cardiovascular imaging. 2014;7(1):100-6.

151.   Baggen VJ, Leiner T, Post MC, van Dijk AP, Roos-Hesselink JW, Boersma E, et al. Cardiac magnetic resonance findings predicting mortality in patients with pulmonary arterial hypertension: a systematic review and meta-analysis. European radiology. 2016.

152.   Girgis RE. Predicting long-term survival in pulmonary arterial hypertension: more than just pulmonary vascular resistance. Journal of the American College of Cardiology. 2011;58(24):2520-1.

153.   Courand PY, Jomir GP, Khouatra C, Scheiber C, Turquier S, Glerant JC, et al. Prognostic value of right ventricular ejection fraction in pulmonary arterial hypertension. The European respiratory journal : official journal of the European Society for Clinical Respiratory Physiology. 2015;45:139-49.

154.   van de Veerdonk MC, Marcus JT, Westerhof N, de Man FS, Boonstra A, Heymans MW, et al. Signs of right ventricular deterioration in clinically stable patients with pulmonary arterial hypertension. Chest. 2015;147(4):1063-71.

155.   Fritz JS, Blair C, Oudiz RJ, Dufton C, Olschewski H, Despain D, et al. Baseline and follow-up 6-min walk distance and brain natriuretic peptide predict 2-year mortality in pulmonary arterial hypertension. Chest. 2013;143(2):315-23.

156.   Barst RJ, Chung L, Zamanian RT, Turner M, McGoon MD. Functional class improvement and 3-year survival outcomes in patients with pulmonary arterial hypertension in the REVEAL Registry. Chest. 2013;144(1):160-8.

157.   Savarese G, Paolillo S, Costanzo P, D'Amore C, Cecere M, Losco T, et al. Do changes of 6-minute walk distance predict clinical events in patients with pulmonary arterial hypertension? A meta-analysis of 22 randomized trials. Journal of the American College of Cardiology. 2012;60(13):1192-201.

158.   Savarese G, Paolillo S, Costanzo P, D'Amore C, Cecere M, Losco T, et al. Do Changes of 6-Minute Walk Distance Predict Clinical Events in Patients with Pulmonary Arterial Hypertension. Journal of the American College of Cardiology. 2012;60:1192-201.

159.   Groepenhoff H, Vonk-Noordegraaf A, Boonstra A, Spreeuwenberg MD, Postmus PE, Bogaard HJ. Exercise testing to estimate survival in pulmonary hypertension. Medicine and science in sports and exercise. 2008;40(10):1725-32.

160.   Miyamoto S, Nagaya N, Satoh T, Kyotani S, Sakamaki F, Fujita M, et al. Clinical Correlates and Prognostic Significance of Six-Minute walk test in Patients with Primary Pulmonary Hypertension. American journal of respiratory and critical care medicine. 2000;161:487-92.

161. Claessen G, La Gerche A, Wielandts JY, Bogaert J, Van Cleemput J, Wuyts W, et al. Exercise pathophysiology and sildenafil effects in chronic thromboembolic pulmonary hypertension. Heart. 2015.

162. Surie S, van der Plas MN, Marcus JT, Kind T, Kloek JJ, Vonk-Noordegraaf A, et al. Effect of pulmonary endarterectomy for chronic thromboembolic pulmonary hypertension on stroke volume response to exercise. Am J Cardiol. 2014;114(1):136-40.

163. Dandel M, Knosalla C, Kemper D, Stein J, Hetzer R. Assessment of right ventricular adaptability to loading conditions can improve the timing of listing to transplantation in patients with pulmonary arterial hypertension. The Journal of heart and lung transplantation : the official publication of the International Society for Heart Transplantation. 2015;34(3):319-28.

164. Grunig E, Tiede H, Enyimayew EO, Ehlken N, Seyfarth HJ, Bossone E, et al. Assessment and prognostic relevance of right ventricular contractile reserve in patients with severe pulmonary hypertension. Circulation. 2013;128(18):2005-15.

165. Chaouat A, Sitbon O, Mercy M, Poncot-Mongars R, Provencher S, Guillaumot A, et al. Prognostic value of exercise pulmonary haemodynamics in pulmonary arterial hypertension. The European respiratory journal : official journal of the European Society for Clinical Respiratory Physiology. 2014;44(3):704-13.

166. Beygui F, Furber A, Delepine S, GHelft G, Metzger J, Geslin P, et al. Routine breath-hold gradient echo MRI-derived right ventricular mass, volumes and function: accuracy, reproducibility and coherence study. The international journal of cardiovascular imaging. 2004;20(6):509-16.

167. Grouthes F, Smith GC, Moon JCC, Bellenger NG, Collins P, Klein HU, et al. Comparison of Interstudy Reproducibility of Cardiovascular Magnetic Resonance with Two-Dimenstional Echocardiography in Normal Subjects and in Patients with Heart Failure or Left Ventricular Hypertrophy. Am J Cardiol. 2002;90:29-34.

168. Ridgway JP. Cardiovascular magnetic resonance physics for clinicians: part I. Journal of cardiovascular magnetic resonance : official journal of the Society for Cardiovascular Magnetic Resonance. 2010;12:71.

169. Varghese A, Pennell DJ. Cardiovascular Magnetic Resonance Imaging Made Easy: Churchill Livingstone; 2008.

170. Slavin GS, Bluemke DA. Spatial and Temporal Resolution in Cardiovascular MR Imaging: Review and Recommendations. Radiology. 2004;234:330-38.

171. Radiology ACo. ACR-NASCI-SPR Practice Guidelines for the Performance and Interpretation of Cardiac Magnetic Resonance Imaging. Pratice Guidelines.

172. Gatehouse PD, Keegan J, Crowe LA, Masood S, Mohiaddin RH, Kreitner KF, et al. Applications of phase-contrast flow and velocity imaging in cardiovascular MRI. European radiology. 2005;15(10):2172-84.

173. Lotz J, Meier C, Leppert A, Galanski M. Cardiovascular Flow Measurement with Phase-Contrast MR Imaging: Basic Facts and Implementation. RadioGraphics. 2002;22:651-71.

174. Tsao J, Kozerke S. MRI temporal acceleration techniques. Journal of magnetic resonance imaging : JMRI. 2012;36(3):543-60.

175. Axel L, Otazo R. Accelerated MRI for the assessment of cardiac function. The British journal of radiology. 2016;89(1063):20150655.

176. Wright KL, Hamilton JI, Griswold MA, Gulani V, Seiberlich N. Non-Cartesian parallel imaging reconstruction. Journal of magnetic resonance imaging : JMRI. 2014;40(5):1022-40.

177.   Steeden JA, Atkinson D, Taylor AM, Muthurangu V. Assessing vascular response to exercise using a combination of real-time spiral phase contrast MR and noninvasive blood pressure measurements. Journal of magnetic resonance imaging : JMRI. 2010;31(4):997-1003.

178.   Lurz P, Muthurangu V, Schievano S, Nordmeyer J, Bonhoeffer P, Taylor AM, et al. Feasibility and reproducibility of biventricular volumetric assessment of cardiac function during exercise using real-time radial k-t SENSE magnetic resonance imaging. Journal of magnetic resonance imaging : JMRI. 2009;29(5):1062-70.

179.   Lurz P, Muthurangu V, Schuler PK, Giardini A, Schievano S, Nordmeyer J, et al. Impact of reduction in right ventricular pressure and/or volume overload by percutaneous pulmonary valve implantation on biventricular response to exercise: an exercise stress real-time CMR study. Eur Heart J. 2012;33(19):2434-41.

180.   Pflugi S, Roujol S, Akcakaya M, Kawaji K, Foppa M, Heydari B, et al. Accelerated cardiac MR stress perfusion with radial sampling after physical exercise with an MR-compatible supine bicycle ergometer. Magnetic resonance in medicine. 2015;74(2):384-95.

181.   Gusso S, Salvador C, Hofman P, Cutfield W, Baldi JC, Taberner A, et al. Design and testing of an MRI-compatible cycle ergometer for non-invasive cardiac assessments during exercise. Biomedical engineering online. 2012;11:13.

182.   Lafountain RA, da Silveira JS, Varghese J, Mihai G, Scandling D, Craft J, et al. Cardiopulmonary exercise testing in the MRI environment. Physiological measurement. 2016;37(4):N11-25.

183.   Forouzan O, Warczytowa J, Wieben O, Francois CJ, Chesler NC. Non-invasive measurement using cardiovascular magnetic resonance of changes in pulmonary artery stiffness with exercise. Journal of cardiovascular magnetic resonance : official journal of the Society for Cardiovascular Magnetic Resonance. 2015;17:109.

184.   Claessen G, La Gerche A, Petit T, Gillijns H, Bogaert J, Claeys M, et al. Right ventricular and pulmonary vascular reserve in asymptomatic BMPR2 mutation carriers. The Journal of heart and lung transplantation : the official publication of the International Society for Heart Transplantation. 2016.

185.   Padang R, Ganigara M, O'Meagher S, Grieve SM, Bannon PG, Celermajer DS, et al. Feasibility of using real-time CMR imaging to evaluate acute thoracic aortic response to exercise. Int J Cardiol. 2015;197:306-8.

186.   ISHLT TTFftDaToPHotEaEebt. Guidelines for the diagnosis and treatment of pulmonary hypertension. The European respiratory journal : official journal of the European Society for Clinical Respiratory Physiology. 2009;34:1219-63.

187.   American Thoracic Society I. ATS Statement: Guidelines for the Six-Minute Walk Test. American journal of respiratory and critical care medicine. 2002;166:111-7.

188.   Howard L. CPX Standard Operating Procedure, Version 1. In: Trust ICH, editor. 2015.

189.   Standardization of cardiac tomographic imaging: From the Committee on Advanced Cardiac Imaging and Technology, Council on Clinical Cardiology, American Heart Association; Cardiovacsular Imaging Committee, American College of Crdiology; and Board of Directors, Cardiovascular Council, Society of Nuclear Medicine. Circulation.86(1):338-9.

190.   Miller CA, Jordan P, Borg A, Argyle R, Clark D, Pearce K, et al. Quantification of left ventricular indices from SSFP cine imaging: impact of real-world variability in analysis methodology and utility of geometric modeling. Journal of magnetic resonance imaging : JMRI. 2013;37(5):1213-22.

191.   Weinsaft JW, Cham MD, Janik M, Min JK, Henschke CI, Yankelevitz DF, et al. Left ventricular papillary muscles and trabeculae are significant determinants of cardiac MRI volumetric measurements: effects on clinical standards in patients with advanced systolic dysfunction. Int J Cardiol. 2008;126(3):359-65.

192.   Marcus JT, Gotte MJ, DeWaal L, Stam M, Van der Geest R, Heethar R, et al. The influence of through-plane motion of left ventricular volumes measured by magnetic resonance imaging: implications for image acquisition and analysis. Journal of cardiovascular magnetic resonance : official journal of the Society for Cardiovascular Magnetic Resonance. 1999;1(1):1-6.

193.   La Gerche A, Claessen G, Van de Bruaene A, Pattyn N, Van Cleemput J, Gewillig M, et al. Cardiac Magnetic Resonance Imaging: A New Gold Standard for Ventricular Volume Quantification During High-Intensity Exercise. Circulation: Cardiovasvular Imaging. 2012.

194.   Pedersen EM, Stenbog E, Frund T, Houlind K, Kromann O, Sorensen K, et al. Flow during exercise in the total cavopulmonary connection measured by magnetic resonance velocity mapping. Heart. 2002;87:554-8.

195.   Cheng CP, Herfkens RJ, Taylor CA, Feinstein JA. Proximal pulmonary artery blood flow characteristics in healthy subjects measured in an upright posture using MRI: the effects of exercise and age. Journal of magnetic resonance imaging : JMRI. 2005;21(6):752-8.

196.   Raman SV, Dickerson JA, Jekic M, Foster EL, Pennell ML, McCarthy B, et al. Real-time cine and myocardial perfusion with treadmill exercise stress cardiovascular magnetic resonance in patients referred for stress SPECT. Journal of cardiovascular magnetic resonance : official journal of the Society for Cardiovascular Magnetic Resonance. 2010;12:41.

197.   Foster EL, Arnold JW, Jekic M, Bender JA, Balasubramanian V, Thavendiranathan P, et al. MR-compatible treadmill for exercise stress cardiac magnetic resonance imaging. Magnetic resonance in medicine. 2012;67(3):880-9.

198.   Holverda S, Tji-Joong Gan C, Marcus JT, Postmus PE, Boonstra A, Vonk-Noordegraaf A. Impaired Stroke Volume Response to Exercise in Pulmonary Arterial Hypertension. Journal of the American College of Cardiology. 2006;47(8):1732-33.

199.   Roest A, Kunz P, Lamb H, Helbing WA, van der Wall E, de Roos A. Biventricular Response to Supine Physical Exercise in Young Adults Assessed with Ultrafast Magnetic Resonance Imaging. Am J Cardiol. 2001;87:601-5.

200.   Leyk D, Ebfeld D, Hoffman W, Wunderlich H, Baum K, Stegemann. Postural effect on cardiac output, oxygen uptake and lactate during cycle exercise of varying intensity. Eur J Appl Physiol and Occ Physiol. 1994;68:30/5.

201.   Toska K, Eriksen M. Respiration-Synchronous Fluctuations in Stroke Volume, Heart Rate and Arterial Pressure in Humans. Journal of Physiology. 1993;472:501-12.

202.   Williams AH, Gropper AL. Interrelationships of Cardiac Output, Blood Pressure, and Peripheral Resistance during Normal Respiration in Normotensive and Hypertensive Individuals. Circulation. 1951;4(2):278-87.

203.   Elstad M. Respiratory variations in pulmonary and systemic blood flow in healthy humans. Acta physiologica. 2012;205(3):341-8.

204.   Sakuma H, Kawada N, Kubo H, Nishide Y, Takano K, Kato N, et al. Effect of Breath Holding on Blood Flow Measurement Using Fast Velocity Encoded Cine MRI. Magnetic resonance in medicine. 2001;45:346-8.

205.   Guz A, Innes JA, Murphy K. Respiratory modulation of Left Ventricular Stroke Volume in Man Measured Using Pulsed Doppler Ultrasound. J Physiol. 1987;393(499-512).

206.   van den Hout RJ, Lamb H, van den Aardweg J, Schot R, Steendijk P, van der Wall E, et al. Real-Time MR Imaging of Aortic Flow: Influence of Breathing on Left Ventricular Stroke Volume in Chronic Obstructive Pulmonary Disease. Radiology. 2003;229:513-9.

207.   Joseph A, Kowallick JT, Merboldt KD, Voit D, Schaetz S, Zhang S, et al. Real-time flow MRI of the aorta at a resolution of 40 msec. Journal of magnetic resonance imaging : JMRI. 2014;40(1):206-13.

208.   Bolen MA, Setser RM, Gabriel RS, Renapurkar RD, Tandon Y, Lieber ML, et al. Effect of protocol choice on phase contrast cardiac magnetic resonance flow measurement in the ascending aorta: breath-hold and non-breath-hold. The international journal of cardiovascular imaging. 2013;29(1):113-20.

209.   Hori Y, Yamada N, Higashi M, Hirai N, Nakatani S. Rapid Evaluation Of Right And Left Ventricular Function And Mass Using Real-time True-fisp Cine Mr Imaging Without Breath-hold: Comparison With Segmented True-fisp Cine Mr Imaging With Breath-hold. Journal of Cardiovascular Magnetic Resonance. 2003;5(3):439-50.

210.   Reiter U, Reiter G, Fuchsjager M. MR phase-contrast imaging in pulmonary hypertension. The British journal of radiology. 2016;89(1063):20150995.

211.   Untenberger M, Hullebrand M, Tautz L, Joseph AA, Voit D, Merboldt KD, et al. Spatiotemporal phase unwrapping for real-time phase-contrast flow MRI. Magnetic resonance in medicine. 2015;74(4):964-70.

212.   Nayak KS, Nielsen JF, Bernstein MA, Markl M, P DG, R MB, et al. Cardiovascular magnetic resonance phase contrast imaging. Journal of cardiovascular magnetic resonance : official journal of the Society for Cardiovascular Magnetic Resonance. 2015;17:71.

213.   Gatehouse PD, Rolf MP, Graves MJ, Hofman MB, Totman J, Werner B, et al. Flow measurement by cardiovascular magnetic resonance: a multi-centre multi-vendor study of background phase offset errors that can compromise the accuracy of derived regurgitant or shunt flow measurements. Journal of cardiovascular magnetic resonance : official journal of the Society for Cardiovascular Magnetic Resonance. 2010;12:5.

214.   Chernobelsky A, Shubayev O, Comeau CR, Wolff SD. Baseline correction of phase contrast images improves quantification of blood flow in the great vessels. Journal of cardiovascular magnetic resonance : official journal of the Society for Cardiovascular Magnetic Resonance. 2007;9(4):681-5.

215.   Rigsby CK, Hilpipre N, McNeal GR, Zhang G, Boylan EE, Popescu AR, et al. Analysis of an automated background correction method for cardiovascular MR phase contrast imaging in children and young adults. Pediatric radiology. 2014;44(3):265-73.

216.   Nayak KS, Hu BS. The Future of Real-Time Cardiac Magnetic Resonance Imaging. Current Cardiology Reports. 2005;7:45-51.

217.   Zhang S, Joseph AA, Voit D, Schaetz S, Merboldt KD, Unterberg-Buchwald C, et al. Real-time magnetic resonance imaging of cardiac function and flow-recent progress. Quantitative imaging in medicine and surgery. 2014;4(5):313-29.

218.   Kaji S, Yang P, Kerr AB, Tang WH, Meyer C, Macovski A, et al. Rapid Evaluation of Left Ventricular Volume and Mass Without Breath-Holding Using Real-Time Interactive Cardiac Magnetic Resonance Imaging Systemq. Journal of the American College of Cardiology. 2001;38:527-33.

219.   Plein S, Smith W, Ridgway JP, Kassner A, Beacock DJ, Bloomer TN, et al. Measurements of left ventricular dimensions using real-time acquisition in cardiac

magnetic resonance imaging: comparison with conventional gradient echo imaging. Magnetic Resonance Materials in Physics, Biology and Medicine. 2001;13:101-8.

220. Appleton CP, Hatle LK, Popp RL. Relation of transmitral flow velocity patterns to left ventricular diastolic function: New insights from a combined hemodynamic and Doppler echocardiographic study. Journal of the American College of Cardiology. 1988;12(2):426-40.

221. Spirito P, Maron BJ, Verter I, Merrill JS. Reproducibility of Doppler echocardiographic measurements of left ventricular diastolic function. European Heart Journal. 1988;9:879-86.

222. Biering-Sorensen T, Mogelvang R, de Knegt MC, Olsen FJ, Galatius S, Jensen JS. Cardiac Time Intervals by Tissue Doppler Imaging M-Mode: Normal Values and Association with Established Echocardiographic and Invasive Measures of Systolic and Diastolic Function. PloS one. 2016;11(4):e0153636.

223. Marcus JT, Vonk Noordegraaf A, De Vries PM, van Rossum A, Roseboom B, Heethar R, et al. MRI evaluation of right ventricular pressure overload in chronic obstructive pulmonary disease. Journal of magnetic resonance imaging : JMRI. 1998;8(5):999-1005.

224. Claessen G, Claus P, Delcroix M, Bogaert J, La Gerche A, Heidbuchel H. Interaction between respiration and right versus left ventricular volumes at rest and during exercise: a real-time cardiac magnetic resonance study. Am J Physiol Heart Circ Physiol. 2014;206:H816-H24.

225. Evans AJ, Iwai F, Grist TA, Sostman HD, Hedlund LW, Spritzer CE, et al. Magnetic resonance imaging of blood flow with a phase subtraction technique. In vitro and in vivo validation. Invest Radiol. 1993;28(2):109-15.

226. Kondo C, G.R. C, Semelka R, Foster E, Shimakawa A, Higgins CB. Right and left ventricular stroke volume measurements with velocity encoded cine MR imaging: in vitro and in vivo validation. AJR Am J Roentgenol. 1991;157(1):9-16.

227. Ley S, Fink C, Puderbach M, Zaporozhan J, Plathow C, Eichinger M, et al. MRI Measurement of the Hemodynamics of the Pulmonary and Systemic Arterial Circulation: Influence of Breathing Maneuvers. American Journal of Roentgenology. 2006;187(2):439-44.

228. Johansson B, Baby-Narayan SV, Kilner PJ. The effects of breath-holding on pulmonary regurgitation measured by cardiovascular magnetic resonance velocity mapping. Journal of Cardiovascular Magnetic Resonance. 2009;11:1-6.

229. Lovering AT, Duke JW, Elliott JE. Intrapulmonary arteriovenous anastomoses in humans--response to exercise and the environment. The Journal of physiology. 2015;593(3):507-20.

230. Eldridge MW, Dempsey JA, Haverkamp HC, Lovering AT, Hokanson JS. Exercise-induced intrapulmonary arteriovenous shunting in healthy humans. J Appl Physiol. 2004;97:797-805.

231. Stickland MK, Welsh RC, Haykowsky MJ, Petersen SR, Anderson WD, Taylor DA, et al. Intra-pulmonary shunt and pulmonary gas exchange during exercise in humans. The Journal of physiology. 2004;561(Pt 1):321-9.

232. Lalande S, Yerly P, Faoro V, Naeije R. Pulmonary vascular distensibility predicts aerobic capacity in healthy individuals. The Journal of physiology. 2012;590(Pt 17):4279-88.

233. Ehsani AA, Biello DR, Schultz J, Soebel VE, Holloszy JO. Improvements of left ventricular contractile function by exercise training in patients with coronary artery disease. Circulation. 1986;2:250-8.

234.   Spence AL, Naylor LH, Carter HH, Buck CL, Dembo L, Murray CP, et al. A prospective randomised longitudinal MRI study of left ventricular adaptation to endurance and resistance exercise training in humans. The Journal of physiology. 2011;589(Pt 22):5443-52.
235.   Wolfe LA, Martin RP, Watson DD, Lasley RD, Bruns DE. Chronic exercise and left ventricular structure and function in healthy human subjects. Journal of Applied Physiology. 1985;58:409-15.
236.   Levine BD, Lane LD, Buckey JC, Friedman DB, Blomqvist CG. Left Ventricular Pressure-Volume and Frank-Starling Relations in Endurance Athletes. Circulation. 1991;84:1016-23.
237.   Brynjolf I, Kelbaek H, Munck O, Godtfredsen J, Larsen S, Eriksen M. Right and left ventricular ejection fraction and left ventricular volume changes at rest and during exercise in normal subjects. Eur Heart J. 1984;5(9):756-61.
238.   Mahler DA, Richard AM, Snyder PE, Pytlik L, Zaret BL, Loke J. Volumetric responses of right and left ventricles during upright exercise in normal subjects. J Appl Physiol. 1985;58(6):1818-22.
239.   Stein RA, Michelli D, Diamond J, Horwitz B, Krasnow N. The Cardiac Response to Exercise Training: Echocardiographic Analysis at Rest and During Exercise. The American Journal of Cardiology. 1980;46:219-25.
240.   Heiskanen MA, Leskinen T, Heinonen I, Loyttyniemi E, Eskelinen JJ, Virtanen K, et al. Right ventricular metabolic adaptations to high-intensity interval and moderate-intensity continuous training in healthy middle-aged men. Am J Physiol Heart Circ Physiol. 2016:ajpheart 00399 2016.
241.   Horwitz LD, Atkins JM, Dubar SA. Left ventricular dynamics during recovery from exercise. J Appl Physiol. 1975;39(3):449-52.
242.   Stein RA, Michelli D, Fox EL, Krasnow N. Continuous Ventricular Dimensions in Man During Supine Exercise and Recovery. The American Journal of Cardiology. 1978;41:655-60.
243.   Takahashi T, Saitoh T, Miyamoto S. Difference in human cardiovascular response between upright and supine recovery from upright cycle exercise. European journal of applied physiology. 2000;81:233-9.
244.   Johnson EC, Hudson TL, Greene ER. Left ventricular haemodynamics during exercise recovery. J Appl Physiol. 1985;69(1):104-11.
245.   Kilgour RD, Mansi JA, Williams PA. Cardiodynamic responses during seated and supine recovery from supramaximal exercise. Can J Appl Physiol. 1995;20(1):52-64.
246.   Plotnick FD, Becker LC, Fisher ML. Changes in left ventricular function during recovery from upright bicycle exercise in normal persons and patients with coronary artery disease. Am J Cardiol. 1986;58(3):247-51.
247.   Roeleveld RJ, Marcus JT, Boonstra A, Postmus PE, Marques KM, Bronzwaer JG, et al. A comparison of noninvasive MRI-based methods of estimating pulmonary artery pressure in pulmonary hypertension. Journal of magnetic resonance imaging : JMRI. 2005;22(1):67-72.
248.   Sanz J, Kariisa M, Dellegrottaglie S, Prat-Gonzalez S, Garcia MJ, Fuster V, et al. Evaluation of pulmonary artery stiffness in pulmonary hypertension with cardiac magnetic resonance. JACC Cardiovascular imaging. 2009;2(3):286-95.
249.   Gan CT, Lankhaar JW, Westerhof N, Marcus JT, Becker A, Twisk JW, et al. Noninvasively assessed pulmonary artery stiffness predicts mortality in pulmonary arterial hypertension. Chest. 2007;132(6):1906-12.

250.	Garcia-Alvarez A, Fernandez-Friera L, Mirelis JG, Sawit S, Nair A, Kallman J, et al. Non-invasive estimation of pulmonary vascular resistance with cardiac magnetic resonance. Eur Heart J. 2011;32(19):2438-45.

251.	Alfakih K, Plein S, Thiele H, Jones T, Ridgway JP, Sivananthan MU. Normal human left and right ventricular dimensions for MRI as assessed by turbo gradient echo and steady-state free precession imaging sequences. Journal of magnetic resonance imaging : JMRI. 2003;17(3):323-9.

252.	Stembridge M, Ainslie PN, Hughes MG, Stohr EJ, Cotter JD, Tymko MM, et al. Impaired myocardial function does not explain reduced left ventricular filling and stroke volume at rest or during exercise at high altitude. J Appl Physiol. 2015;119:1219-23.

253.	Allemann Y, Stuber M, de Marchi SF, Rexhaj E, Sartori C, Scherrer U, et al. Pulmonary artery pressure and cardiac function in children and adolescents after rapid ascent to 3,450m. Am J Physiol Heart Circ Physiol. 2012;302:H2646-H53.

254.	Calbet JAL, Boushel R, Radegran G, Sondergaard H, Wagner PD, Saltin B. Determinants of maximal oxygen uptake in severe acute hypoxia. Am J Physiol Regul Integr Comp Physiol. 2003;284:R291-R303.

255.	Saito M, Mano T, Iwase S, Koga K, Abe H, Yamazaki Y. Responses in muscle sympathetic activity to acute hypoxia in humans. J Appl Physiol. 1988;65:1548-52.

256.	Olsen NV, Kanstrup IL, Richalet J, Hansen MS, Plazen G, Galen FX. Effects of acute hypoxia on renal and endocrine function at rest and during graded exercise in hydrated subjects. J Appl Physiol. 1992;73(5):2036-43.

257.	Burwash IG, Morgan DE, Koilpillair CJ, Blackmore GL, Johnstone DE, Armour JA. Sympathetic stimulation alters left ventricular relaxation and chamber size. Am J Physiol. 1993;264:R1-7.

258.	Faoro V, Boldingh S, Moreels M, Martinez S, Lamotte M, Unger P, et al. Bosentan decreases pulmonary vascular resistance and improves exercise capacity in acute hypoxia. Chest. 2009;135(5):1215-22.

259.	Ghofrani A, Reichenberger F, Kohstall MG. Sildenafil increased exercise capacity during hypoxia at low altitudes and at Mount Everest base camp. ACC Curent Journal Review. 2004;13(11):13-4.

260.	Hsu AR, Barnholt KE, Grundmann NK, Lin JH, McCallum SW, Friedlander AI. Sildenafil improves cardiac output and exercise performance during acute hypoxia, but not normoxia. J Appl Physiol. 2006;100:2031-40.

261.	La Gerche A, Heidbuchel H, Burns AT, Mooney DJ, Taylor AM, Pfluger HB, et al. Disproportionate Exercise Load and Remodeling of the Athlete's Right Ventricle. Med Sci Sports Exerc. 2011;43(6):974-81.

262.	Utomi V, Oxborough D, Ashley E, Lord R, Fletcher S, Stembridge M, et al. The impact of chronic endurance and resistance training upon the right ventricular phenotype in male athletes. European journal of applied physiology. 2015;115(8):1673-82.

263.	D'Ascenzi F, Pelliccia A, Corrado D, Cameli M, Curci V, Alvino F, et al. Right ventricular remodelling induced by exercise training in competitive athletes. European heart journal cardiovascular Imaging. 2016;17(3):301-7.

264.	Aaron CP, Tandri H, Barr RG, Johnson WC, Bagiella E, Chahal H, et al. Physical activity and right ventricular structure and function. The MESA-Right Ventricle Study. American journal of respiratory and critical care medicine. 2011;183(3):396-404.

265.	Stembridge M, Ainslie PN, Hugher MG, Seohr EJ, Cotter JD, Nio AQX, et al. Ventricular structure, function and mechanics at high altitude: chronic remodeling in Sherpa vs short-term lowlander adaptation. J Appl Physiol. 2014;117:334-43.

266.   Reeves J, Groves B, Sutton J, Wagner PD, Cymerman A, Malconian M, et al. Operation Everest II: preservation of cardiac function at extreme altitude. J Appl Physiol. 1987;63(2):631-539.

267.   De Vroomen M, Cardozo RHL, Steendijk P, Van Bel F, Baan J. Improved contractile performance of right ventricle in response to increased RV afterload in newborn lamb. Am J Physiol. 2000;278:H100-5.

268.   De Vroomen M, Steendijk P, Cardozo RHL, Brouwers HHA, Van Bel F, Baan J. Enhanced systolic function of the right ventricle during respiratory distress syndrome in newborn lambs. Am J Physiol Heart Circ Physiol. 2001;280:H392-H400.

269.   Faber MJ, Dalinghaus M, Lankhuizen IM, Steendijk P, Hop WC, Schoemaker RG, et al. Right and left ventricular function after chronic pulmonary artery banding assessed with biventricular pressure-volume loops. Am J Physiol Heart Circ Physiol. 2006;291:H1580-H6.

270.   Schwartz GG, Steinman S, Garcia JE, Greyson C, Massie B, Weiner MW. Energetics of Acute Pressure Overload of the Porcine Right Ventricle. J Clin Invest. 1992;89:909-18.

271.   Ghuysen A, Lambermont B, Kolh P, Tchana-Sato V, Magis D, Gerard P, et al. Alteration of right ventricular-pulmonary vascular coupling in a porcine model of progressive pressure overloading. Shock. 2008;29(2):197-204.

272.   Ricart A, Maristany J, Fort N, Leal C, Pages T, Viscor G. Effect of Sildenafil on the Human Response to Acute Hypoxia and Exercise. High Altitude Medicine and Biology. 2005;6:43-9.

273.   Bartsch P, Gibbs JS. Effect of altitude on the heart and the lungs. Circulation. 2007;116(19):2191-202.

274.   Harris P, Segel N, Green I, Housley E. The Influence of the Airways Resistance and Alveolar Pressure on the Pulmonary Vascular Resistance in Chronic Bronchitis. Cardiovascular Research. 1968;2:84-92.

275.   Wyss CA, Koepfli P, Fretz G, Seebauer M, Schirlo C, Kaufmann PA. Influence of altitude exposure on coronary flow reserve. Circulation. 2003;108(10):1202-7.

276.   Malconian M, Rock P, Hutgreen H, Donner H, Cymerman A, Groves B, et al. The Electrocardiogram at Rest and Exercise During a Simulated Ascent of Mt Everest (Operation Everest II). Am J Cardiol. 1990;65:1475-80.

277.   Kaijser L, Grubbstrom J, Berglund B. Coronary circulation in acute hypoxia. Clinical Physiology. 1990;10:259-63.

278.   Friedmann B, Bauer T, Menold E, Bartsch P. Exercise wtih the intensity of the individual anaerobic threshold in acute hypoxia. Medicine and science in sports and exercise. 2004;36(10):1737-42.

279.   Nootens M, Wolfkiel CJ, Chomka EV, Rich S. Understanding Right and Left Ventricular Systolic Function and Interactions at Rest and With Exercise in Primary Pulmonary Hypertension. Am J Cardiol. 1995;75:374-7.

280.   Provencher S, Herve P, Sitbon O, Humbert M, Simonneau G, Chemla D. Changes in exercise haemodynamics during treatment in pulmonary arterial hypertension. The European respiratory journal : official journal of the European Society for Clinical Respiratory Physiology. 2008;32(2):393-8.

281.   Sharma T, Lau EMT, Choudhary P, Torzillo PJ, Munoz PA, Simmons LR, et al. Dobutamine stress for evaluation of right ventricular reserve in pulmonary arterial hypertension. European Respiratory Journal. 2015;45(3):700-8.

282.   Claessen G, La Gerche A, Voigt JU, Dymarkowski S, Schnell F, Petit T, et al. Accuracy of Echocardiography to Evaluate Pulmonary Vascular and RV Function During Exercise. JACC Cardiovascular imaging. 2016;9(5):532-43.

283.   Ghorfrani A, Grimminger F, Hoeper MM. Riociguat For the Treatment Of Inoperable Chronic Thromboembolic Pulmonary Hypertension: A Randomised, Double-Blind, Placebo Controlled Study (CHEST-1). Chest. 2012;142(4_MeetingAbstracts):1023A-A.

284.   Ghorfrani A, Hoeper MM, Halank M, Meyer FJ, Staehler G, Behr J, et al. Riociguat for chronic thromboembolic pulmonary hypertension and pulmonary arterial hypertension: a phase II study. The European respiratory journal : official journal of the European Society for Clinical Respiratory Physiology. 2010;36:792-9.

285.   Ghorfrani A, Galie N, Grimminger F. Riociguat For the Treatment of Pulmonary Arterial Hypertension: A Randomised, Double-Blind, Placebo Controlled Study (PATENT-1). Chest. 2012;142(4_MeetingAbstracts):1027A-A.

286.   Ghofrani HA, Hoeper MM, Halank M, Meyer FJ, Staehler G, Behr J, et al. Riociguat for chronic thromboembolic pulmonary hypertension and pulmonary arterial hypertension: a phase II study. The European respiratory journal : official journal of the European Society for Clinical Respiratory Physiology. 2010;36(4):792-9.

287.   Surie S, Bouma BJ, Bruin-Bon RA, Hardziyenka M, Kloek JJ, Van der Plas MN, et al. Time course of restoration of systolic and diastolic right ventricular function after pulmonary endarterectomy for chronic thromboembolic pulmonary hypertension. Am Heart J. 2011;161(6):1046-52.

288.   Menzel T. Pathophysiology of Impaired Right and Left Ventricular Function in Chronic Embolic Pulmonary Hypertension<xref rid="AFF1">[*]</xref><subtitle>Changes After Pulmonary Thromboendarterectomy</subtitle>. CHEST Journal. 2000;118(4):897.

289.   Kreitner KFJ, Ley S, Hans-Ulrich K, Mayer E, Kramm R, Pitton MB, et al. Chronic Thromboembolic Pulmonary Hypertension: Pre and Post operative Assessment with Breath-hold MR Imaging Techniques. Radiology. 2004;232:535-43.